

Synthesis, characterization and application of smart materials based on low-molecular-weight compounds and polymers

Dissertation

Zur Erlangung des Doktorgrades

Dr. rer. nat.

**an der Fakultät für Chemie und Pharmazie
der Universität Regensburg**



vorgelegt von

Judith Mayr

aus Holzhausen am Ammersee

Regensburg 2017

Die Arbeit wurde angeleitet von: Prof. Dr. David Díaz Díaz

Promotionsgesuch eingereicht am: 05.05.2017

Promotionskolloquium am: 02.06.2017

Prüfungsausschuss: Vorsitz: Prof. Dr. Joachim Wegener

1. Gutachter: Prof. Dr. David Díaz Díaz

2. Gutachter: Prof. Dr. Ramón Eritja

3. Prüfer: Prof. Dr. Jens Schlossmann

Der experimentelle Teil der vorliegenden Arbeit wurde in der Zeit von Januar 2014 bis Januar 2017 unter der Gesamtleitung von Prof. Dr. David Díaz Díaz am Lehrstuhl für Organische Chemie der Universität Regensburg angefertigt. Zusätzliche Betreuer waren von Juli 2016 bis August 2016 Prof. Jens Schlossmann und von September 2016 bis Oktober 2016 Prof. Ramón Eritja und Dr. Santiago Grijalvo am CSIC-IQAC in Barcelona (Spanien).

Table of Contents

A	Introduction	1
1.	Gels.....	1
1.1	Supramolecular Gels.....	3
1.2	Application of Gels in Drug Release.....	5
B	Gels based low molecular weight compounds	6
1.	Isosteric replacement for tuning self-assembly and incorporating new functions into soft supramolecular materials.....	6
1.1	Introduction.....	6
1.2	Results and Discussion	8
1.2.1	Gelation properties	8
1.2.2	Drug release experiments	12
1.2.3	Antimicrobial studies	15
1.3	Experimental Part.....	17
1.3.1	Synthesis of glutamic acid derived gelators.....	17
1.3.2	Gelation time and T_{gel} vs. concentration.....	20
1.3.3	Stimuli response test	21
1.3.4	Drug release.....	21
1.3.5	Antimicrobial studies	21
1.4	Conclusions.....	22
2.	Release of camptothecin, oxytetracycline and mitoxantrone from glycyrrhizic acid derived water/ethanol gels into several buffered solutions	24
2.1	Introduction.....	24
2.2	Results and Discussion	25
2.2.1	Drug Release	25
2.2.2	Response to buffer solutions	29
2.3	Experimental Part.....	30
2.4	Conclusions.....	30

Contents

2.5 Additional Graphics	31
3. Improvement of gelation properties of a formamidine based gelator by ultrasonication	33
3.1 Introduction.....	33
3.2 Results and discussion.....	34
3.3 Experimental Part.....	39
3.3.1 Synthesis.....	39
3.3.2 Gel-formation.....	41
3.3.3 Temperature controlled NMR	42
3.3.4 UV-Vis	42
3.3.5 Polarized Light.....	42
3.3.6 PXRD	42
3.4 Conclusions.....	42
C Ionenes	44
1. Antimicrobial and Hemolytic Studies of a Series of Polycations Bearing Quaternary Ammonium Moieties: Structural and Topological Effects.....	44
1.1 Introduction.....	44
1.2 Results and Discussion	45
1.3 Experimental Section	49
1.3.1 Materials.....	49
1.3.2 Synthesis of Ionenes	50
1.3.3 Antimicrobial assay	52
1.3.4 Hemolysis testing	52
1.3.5 Contact angle measurements.....	53
1.4 Conclusions.....	53

Contents

2. Transfection of Antisense Oligonucleotides Mediated by Cationic Vesicles Based on Non-Ionic Surfactant and Polycations Bearing Quaternary Ammonium Moieties.....	54
2.1 Introduction.....	54
2.2 Results and Discussion	56
2.2.1 Size and Zeta-Potential Measurements	56
2.2.2 SAXS Measurements	57
2.2.3 Cytotoxicity Assay	59
2.2.4 Transfection.....	60
2.3 Materials and Methods	62
2.3.1 Materials.....	62
2.3.2 Preparation of Polyplexes.....	63
2.3.3 Zeta-Potential.....	63
2.3.4 Size Measurements.....	64
2.3.5 Small-Angle X-Ray Scattering (SAXS) Measurements of Ionene Polyplexes	64
2.3.6 cryo-Scanning Electron Microscopy (cryo-SEM)	64
2.3.7 Cytotoxicity Assay	65
2.3.8 Gene Transfection and Antisense Technology Studies.....	65
2.4 Conclusions.....	66
3. Aromatic ionene topology and counterion-tuned gelation of acidic aqueous solutions.....	68
3.1 Introduction.....	68
3.2 Results and Discussion	70
3.2.1 Gelation properties in aqueous acidic and salt solutions.....	70
3.2.2 Computer Simulations	75
3.2.3 HCl gas adsorption.....	76
3.3. Experimental Part.....	77

Contents

3.3.1 Gelation of aqueous acidic solutions	77
3.3.2 HCl gas adsorption.....	77
3.4 Conclusions.....	77
D Summary.....	79
E Literature	83
F Annexes	94
1. Amidine-Glu.....	94
1.1 Aim	94
1.2 Results.....	94
1.3 Experimental Part.....	95
2. X-bi(phenylalanine-diglycol)-benzene	97
2.1 Aim	97
2.2 Results	97
2.3 Experimental Part.....	98
3. New Ionenes	104
3.1 Aim	104
3.2 Results	104
3.3 Experimental Part.....	105
G NMR Spectra and PXRD	108
H List of Abbreviations.....	131
I Curriculum Vitae	132
J Acknowledgements.....	136
K Declaration	138

A Introduction

1. Gels

Nature has ever since been an inspiration and many engineers and scientists have tried to mimic numerous of its features. One of these is self-assembly which is found in a variety of natural systems such as proteins,¹⁻³ DNA/RNA,¹⁻⁴ cell membranes⁵ and viruses^{2,3} but also biomineralization in e.g. bones or mollusc shells.⁶⁻⁸ Another example, where the phenomenon of self-assembly occurs is gel formation.

Gels surround us in our daily life as they are used in manifold fields such as agriculture, food and cosmetic industry, pharmaceutical and biomedical applications or electronic devices.⁹⁻¹¹

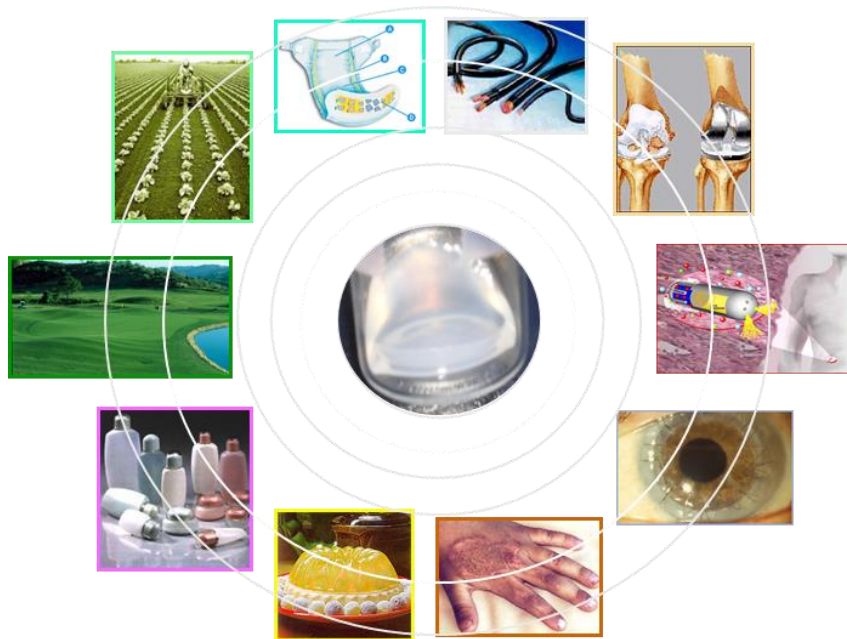


Fig. 1 Variety of application fields of gels.

The term “gel” is not easy to define, as Dorothy Jordon Lloyd recognized in 1926 “the gel, is one which is easier to recognize than to define”.¹² Graham coined the term already in 1864 as being materials that seem to constitute an intermediate state between solids and liquids.¹³ However, over the time many different definitions have been made. One of the most comprehensive definitions was presented by Paul Flory in 1974.¹⁴ According to him, a gel 1) has a permanent continuous structure with macroscopic dimensions and 2) in terms of rheology shows a solid like behaviour. In general, gels always consist of at least two parts: a solid phase, which is the gelator and a liquid phase, which is the solvent, where the latter is the major ingredient. The gelator builds up one-dimensional (1D) polymeric structures by either covalent

(conventional polymers) or non-covalent forces (supramolecular polymers) which then entangle to a three-dimensional (3D) network by physical and/or chemical forces and, in this process, includes the solvent molecules mainly through surface tension and capillary forces (**Fig. 2**).^{15–23}

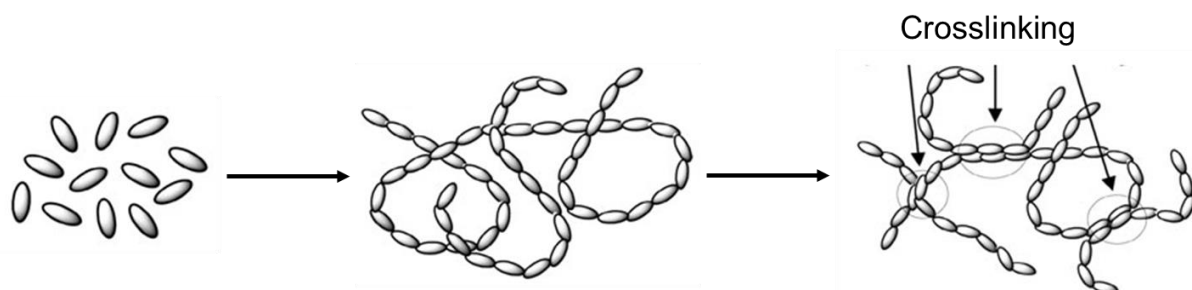


Fig. 2 The formation of supramolecular and conventional polymers. Adapted from Ref. 24 with the permission of Royal Society of Chemistry.

For a better understanding of the hierarchical self-assembly process, the polymeric structure of gels can be classified into primary, secondary and tertiary structure (**Fig. 3**).²¹ The primary structure (Å – nm) is defined by the recognition of molecules that cause preferably 1D aggregates. The secondary structure (nm - μm) depicts the morphology of these aggregates that can be e.g. micelles, vesicles, fibres, ribbons, or sheets. Finally, the tertiary structure (μm – mm) comprises interaction of individual aggregates and is the final criterion if a stable gel is formed.

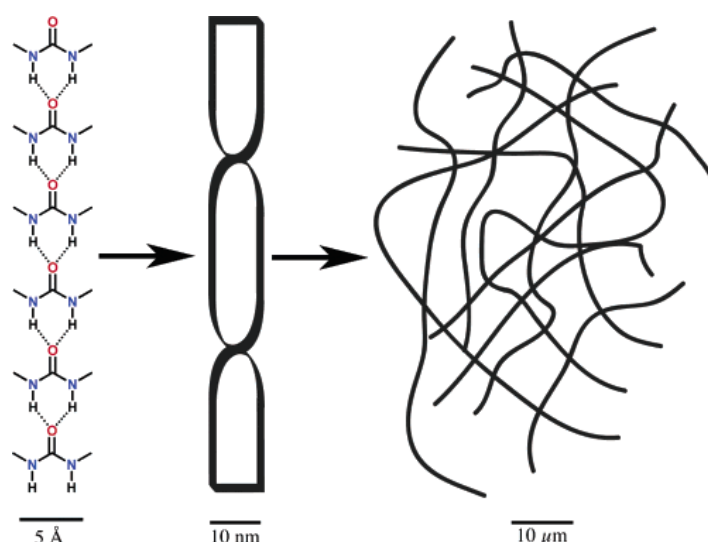


Fig. 3 The primary, secondary, and tertiary structure. Reprinted from Ref. 21 with the permission of American Chemical Society

Gels can be classified according to different criteria: 1) medium, 2) source, 3) constitution or 4) crosslinking (see **Fig. 4**).¹⁷ The medium can vary from organic

solvents (organogels), water (hydrogel), or air (aero- or xerogel). Gelators can derive from both artificial and natural sources which are mostly polymers (e.g. agarose, alginate, chitosan, gelatin, etc.). The constitution describes the nature of the one-dimensional polymers, which can be macromolecular (covalent linked monomers) or supramolecular. Last but not least, gels can be sorted by the type of interaction, which is responsible for the three-dimensional network formation which can be again covalent (chemical) gel or non-covalent (physical gel).

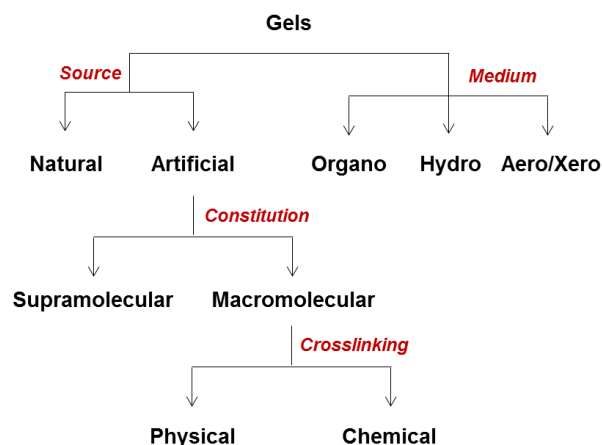


Fig. 4 Classification of gels. Reprinted from Ref. 17 with the permission of Royal Society of Chemistry.

1.1 Supramolecular Gels

The first low-molecular-weight gelator (LMWG) was already discovered in the early 19th century,²⁵ however as the knowledge of aggregation was very poor, it took until the 20th century for these type of gelator to gain more interest of the scientific community.¹⁷ In the early times, supramolecular gelators have been found by serendipity, often during a failed crystallization attempt.¹⁷ However in the last 20 years, as the knowledge of aggregation increased, researchers became able to design gelators in a rational way, which allows to create material with tailor-made properties. As described above, supramolecular gels base on weak, non-covalent interactions and typically they are prepared by forcing the gelator into solution by heat followed by spontaneous cooling of the isotropic solution to room temperature (**Fig. 5**).¹⁷ But gelation can be also induced by various other stimuli, such as ultrasonication,^{26,27} building a pH-gradient^{28,29} or enzymatically.³⁰

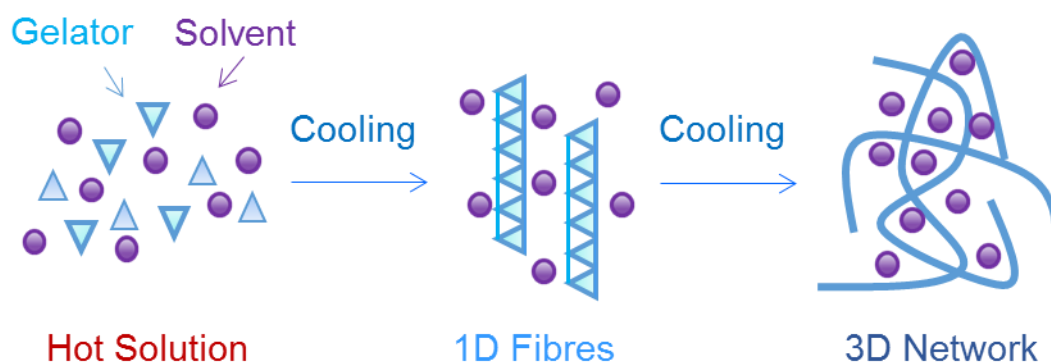


Fig. 5 Formation of a supramolecular gel by heating-cooling process.

During the cooling process, the gelator molecules start to assemble based on forces such as hydrogen-bonding, solvophobic forces, π - π stacking, donor-acceptor interaction, metal-coordination, etc. to 1D strands which entangle themselves to finally build up a 3D network that entrapped the solvent molecules.^{24,17,22,31–33}

In most of the cases, gelators can only form gels in organic solvents or aqueous solutions, although some exceptions exist.^{34–37} Responsible for this are the different types of interactions that cause the self-assembly. The main driving force for the formation of organogels are dipolar interactions, hydrogen bonding or metal coordination which in sum must overcome the loss of translational and rotational freedom (free energy).^{20,22,24,38} In contrast to this, hydrogelation is dominated mainly by solvophobic interactions and therefore control over hydrophobic interactions is essential.^{21,23,39}

Within the last three decades, gels based on LMW-compounds ($M < 3000 \text{ gmol}^{-1}$) have outnumbered scientific interest of their macromolecular analogues due to a variety of reasons:^{17,21–23,38,39} a) a huge diversity of gelator-structures is accessible by standard synthetic methods, b) there are many naturally occurring LMWG which have good chances of being biocompatible and biodegradable as their network is solely formed by non-covalent forces, which makes them easier biodegradable than polymeric gel-systems); c) their thermo-reversible property d) very low minimum gelation concentrations are possible and e) their high tolerance towards salts and other additives.^{17,40} All these features make LMW-compound derived gels very interesting materials as they can react to a variety of external stimuli and can hence be used in a great range of applications.

1.2 Application of Gels in Drug Release

The number of drugs with a low solubility in water with less than 1 g mL^{-1} represents a high percentage.^{41,42} The disadvantages derived from low solubility in water are poor dissolution and membrane permeability, low bioavailability and therefore bad efficiency.^{41–43} Important for an optimal drug action is the presence at the site of action, a sufficient concentration for a long enough time period.^{44,45} In order to overcome solubility problems, different strategies have been developed including complexation, solid dispersion, micronization, use of co-solvents, colloidal particulates (e.g. microemulsions, self-emulsifying drug delivery systems, liposomes, niosomes and solid lipid nanoparticles) and nanosizing (nanoemulsions, nanosuspensions, nanoparticles, nanocrystals).^{41–43,46,47} From administration to the target site drugs may follow a long route on which they can cause severe side effects, especially in case of anti-cancer medicaments.^{44,45} Therefore parenteral drug delivery systems have been studied extensively over the past few decades. In this field formulations including for example surgical implants,⁴⁸ PEGylated nanoparticles⁴⁹ and biodegradable microspheres⁵⁰ have been developed. Unfortunately those formulations suffer from several drawbacks. Polymeric implants require a surgical intervention and microspheres are very costly.⁵¹ An alternative formulation for a huge field of medicaments are gels which can protect their payload from enzymes or low stomach pH. Gels have been studied already more than a century ago. However, the research interest in this field rocketed around three decades ago.⁵² More than 95% of publications of the last 60 years were published after 1989.⁵³ The largest part of these dealt with hydrogels derived from cross-linked polymers and there are numerous publications on drug release from gels derived from covalent crosslinking. However these carrier systems comprise several disadvantages including a costly synthesis, the need of non-biocompatible organic solvents, poor mechanics and slow self-healing.^{51,54} As these gels are formed by a self-assembly process based on non-covalent forces they have several advantages as they are often injectable and can respond to several bio-medically relevant stimuli such as temperature, pH, and the presence of enzymes or ions.^{55,56}

B Gels based low molecular weight compounds

1. Isosteric replacement for tuning self-assembly and incorporating new functions into soft supramolecular materials¹

1.1 Introduction

Bioisosteric replacement is one of the most important tools in medicinal chemistry for the rational design of new drugs.^{57,58} The origins of isosterism can be traced back to the early twentieth century to the pioneering work of Langmuir in which he coined this concept to define atoms or molecules which possess the same number and/or arrangement of electrons.⁵⁹ Thereafter, Grimm's hydride displacement law⁶⁰ and Erlenmeyer's work⁶¹ paved the way to the definition of bioisosteres, largely spread by Friedman⁶² and Thornber⁶³ and later broadened by Burger⁶⁴ as "compounds or groups that possess near-equal molecular shapes and volumes, approximately the same distribution of electrons, and which exhibit similar physical properties ...". Nowadays, bioisosteric replacement of amide bonds represents a key strategy in modern research due to its implications in peptide chemistry.^{65–67} Within this context, many promising approaches introducing acyclic esters, thioamides, ureas, carbamates, oxadiazoles and diazoles have been successfully applied to improve the activity of known drugs or to create new bioactive compounds and materials.^{58,68} Among these examples, disubstituted 1,2,3-triazoles have been considered as powerful non-classical isosteres of amides as they can mimic either a trans- or a cis-configuration of the amide bond depending on the substitution pattern of the triazole (1,4- or 1,5-, respectively).^{69,70} Their planar structure exhibits the ability of H-bonding due to the presence of both donor and acceptor groups with similar relative positions. Although the distance R¹-R² in trans-amides is about 1 Å shorter than that in 1,4-disubstituted triazoles, the overall dipolar moment of the latter (about 5.0 D) is slightly larger than that of secondary amides (about 3.5–4.0 D).

¹ Adapted from Ref. 37 with permission from The American Society of Chemistry. Gelation experiments on C₁₈-Glu and click-Glu were performed by J. Bachl. Gelation experiments on sulfo-Glu were performed by J. V. Alegre-Requena apart from stimuli-response tests and Gelation time and T_{gel} vs. concentration experiments, which were conducted by J. Mayr. Synthesis was performed by J. Bachl, J. V. Alegre-Requena and J. Mayr. Drug release and antimicrobial experiments were performed by J. Mayr.

Isosteric replacement for tuning self-assembly and incorporating new functions into soft supramolecular materials

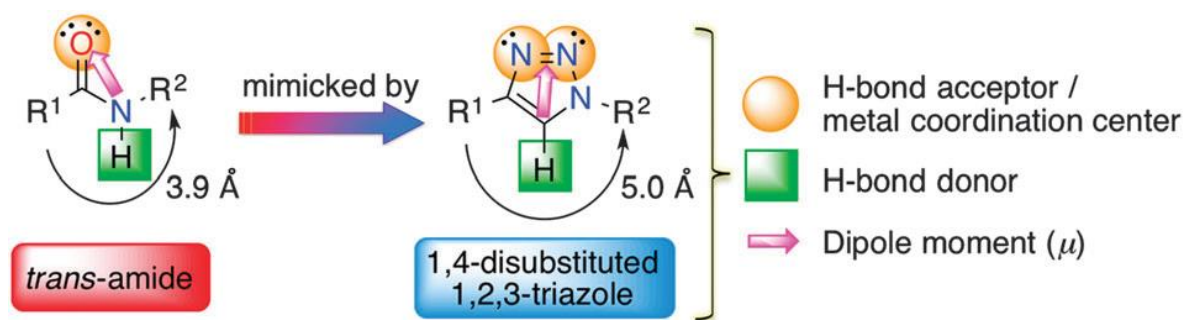


Fig. 6 Main structural features of disubstituted *trans*-amides and 1,2,3-triazoles for their consideration as bioisosteres. Reproduced from Ref. 37 with permission from The Royal Society of Chemistry.

Moreover, the H-bonding abilities (oxygen lone pair electrons = acceptor; N–H amide bond = donor) can be mimicked by the N-2/N-3 lone pairs (acceptor) and the triazole C–H bond (donor) (**Fig. 6**). Calculations in the gas phase have also suggested that the lone pair on N-3 may be a better H-bond acceptor and metal coordination center than N-2. In addition, the potential β -turn geometry of 1,4-disubstituted triazoles has been supported by computational studies.⁷¹ A similar analysis can be done between *cis*-amides and 1,5-disubstituted 1,2,3-triazoles. Another important isostere of amides is the sulfonamide which is the basis of several groups of drugs. Although there are only very few sulfonamides found in nature,^{72,73} they are a very popular motif in pharmacy and agriculture.⁷⁴ Sulfanilamide, the first sulfonamide was synthesized already in 1908 by Gelmo⁷⁵ followed by the first chemotherapeutic agent with the brand name Prontosil® which was synthesized in 1934 by Mietzsch and Klarer⁷⁶ and its antibacterial efficacy was demonstrated 1935 by Domagk.⁷⁷ Nowadays sulfonamides are not only used as antibiotics but also as diuretics⁷⁸ and they depict a very important class of antiepileptics.⁷⁹

Bioisosterism proved to be one of the most important tools in the rational design of new drug molecules but we aimed to use it for the development of new gel materials. *N*-stearoyl-L-glutamic acid (**C₁₈-Glu**) is an amphiphilic compound that has been reported to self-assemble into nanofibers in chloroform and nanodisc-like structures in 1 : 1 mixed EtOH– water.³⁶ We envisioned that this molecule could also undergo self-assembly in many other solvents at suitable concentrations. In addition, it provided us with a unique opportunity to assess the transplantation of the isosteric replacement paradigm from medicinal chemistry to soft materials.

1.2 Results and Discussion

1.2.1 Gelation properties

Our group presented in 2014 the replacement of the amide moiety in **C₁₈-Glu** by a 1,4-disubstituted 1,2,3-triazole unit, in which the total number of C atoms has formally been kept intact. This new compound, **click-Glu**, was readily synthesized by the copper(I)-catalysed azide–alkyne cycloaddition, also known as click reaction.⁸⁰

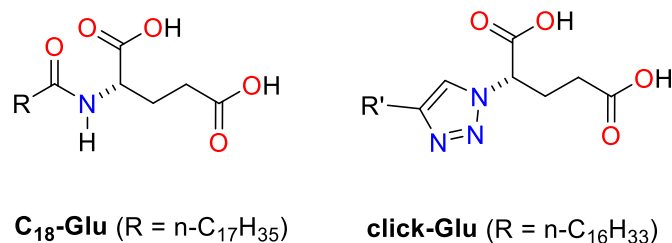


Fig. 7 Gelators **C₁₈-Glu** and **click-Glu** derived from L-glutamic.

The gelation ability of **C₁₈-Glu** and **click-Glu** was systematically investigated by applying a heating–cooling cycle in water and several organic solvents (including non-polar, polar protic and polar aprotic solvents). Materials that did not exhibit gravitational flow upon turning the vial upside-down were preliminary classified as stable gels. No visible changes were observed in model examples upon one year of aging, and their gel nature was further confirmed by dynamic rheological measurements. Eleven different gels could be obtained with both gelators in oxygenated, hydrocarbon (including aromatic and aliphatic) and halogenated solvents. Despite the fact that many solvents could be gelled by either **C₁₈-Glu** or **click-Glu**, the critical gelation concentration (CGC), thermal stability and gelation kinetics were different in each case. **Click-Glu** generally exhibited about 25–55% lower CGC values than **C₁₈-Glu** when polar protic and polar aprotic solvents were used (e.g., water, MeOH, glycerol, and MeCN). On the other hand, an opposite behavior (around 10–75% higher CGC) was usually observed in non-polar solvents (e.g., Et₂O, DCM, n-hexane, and toluene). Although most gels were obtained within minutes regardless of the gelator structure, the gelation kinetics was found to be significantly slower in polar solvents. Independent of the nature of the solvent or the gelator, all gels exhibited full thermo-reversibility with gel-to-sol transition temperatures (T_{gel}) in the range of about 40–70 °C as indicated by DSC among other techniques. Remarkably, some T_{gel} values exceeded the boiling points of the corresponding solvents. Similar to the trends observed for CGC-values, materials

derived from **click-Glu** generally exhibited, at comparable concentrations, higher T_{gel} values in polar solvents than those obtained from **C₁₈-Glu**, which were superior in non-polar solvents.

Electron microscopy imaging was used in order to gain visual insight into the morphologies of model gels prepared in water and CHCl_3 , respectively.

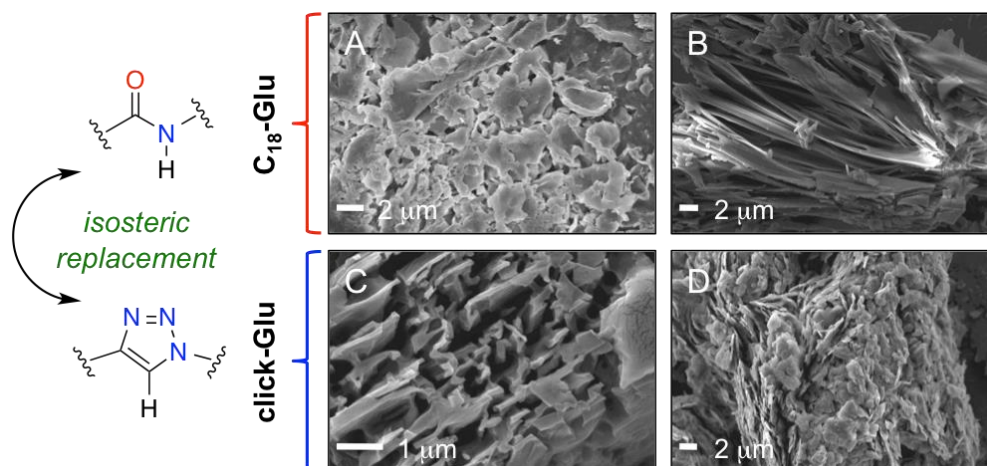
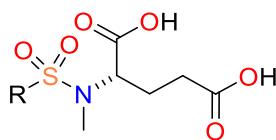


Fig. 8 FESEM images of xerogels **A)** **C₁₈-Glu** in water (25 g L⁻¹); **B)** **C₁₈-Glu** in CHCl_3 (100 g L⁻¹); **C)** **click-Glu** in water (25 g L⁻¹); **D)** **click-Glu** in CHCl_3 (100 g L⁻¹).

In good agreement with previous observations,³⁶ FESEM images of the xerogels based on **C₁₈-Glu** in a polar-protic environment revealed the formation of nano-almond-like structures, whereas layered lamellar assemblies were observed in CHCl_3 . A practically opposite behavior was observed for materials based on the isosteric **click-Glu**. Thus, wrinkled lamellar structures were observed in water, whereas almond crunch-like structures were revealed in CHCl_3 . In general, dense fibrillar networks of high aspect ratios were also observed by TEM imaging. When **click-Glu** was used as the gelator, the density of the fibrillary bundles was much higher than observed in the case of **C₁₈-Glu**.

As the isosteric replacement of the amide function in *N*-stearoyl L-glutamic acid by a 1,4-disubstituted 1,2,3-triazole could be successfully transmitted to the tuning of soft materials, we decided to investigate another isostere of an amide function which is the sulfonamide. This **sulfo-Glu** gelator was synthesized via substitution of 1-octadecyne sulfonyl chloride by a double tert-butyl protected L-glutamic acid and subsequent deprotection. The new compound was tested for its gelation ability of the same solvents as described above.



sulfo-Glu (R = n-C₁₇H₃₅)

Fig. 9 Structure of sulfonamide based gelator **sulfo-Glu** derived from isosteric replacement.

In general **sulfo-Glu** was found to show lower CGCs than the other two gelators in non-polar halogenated and aromatic solvents (e.g. DCM, CHCl₃, xylene, benzene, and toluene) as well as in the polar, aprotic solvents glycerol and MeCN. In contrast to **click-Glu** and **C₁₈-Glu**, it was able to gel AcOEt, chlorobenzene and benzonitrile. However, **sulfo-Glu** revealed the highest CGC for water and polar protic solvents such as MeOH, EtOH, ⁱPrOH. Additionally DMSO, Et₂O and n-hexane could not be gelled in contrast to **click-Glu** and **C₁₈-Glu** which could gel these solvents.

In the following the influence of gelator concentration on T_{gel} and gelation time was investigated for gels in water and CHCl₃ derived from **C₁₈-Glu** and **click-Glu** (see Ref. ³⁷ Fig S9) as well for hydrogels derived from **sulfo-Glu** (**Fig. 10**). As expected, T_{gel} increased with the increasing gelator concentration regardless of the solvent or the gelator, which is in agreement with the gradual formation of denser packed supramolecular networks.

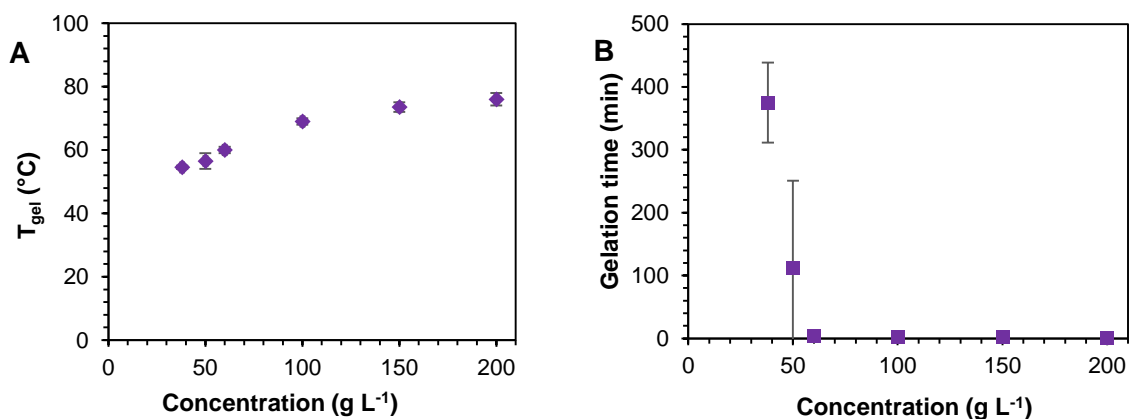


Fig. 10 A) Evolution of T_{gel} with increasing gelator concentration. **B)** Gelation kinetics of **sulfo-Glu**.

For each gelator obvious plateau regions were reached at around 100 g L⁻¹ indicating the thermal stability cannot be increased infinitely. The time necessary to form stable gels drops extremely with increasing concentration which again indicates a denser packaging.

Isosteric replacement for tuning self-assembly and incorporating new functions into soft supramolecular materials

Additionally the stimuli response behavior of gels derived from **C₁₈-Glu**, **click-Glu** and **sulfo-Glu** was investigated.

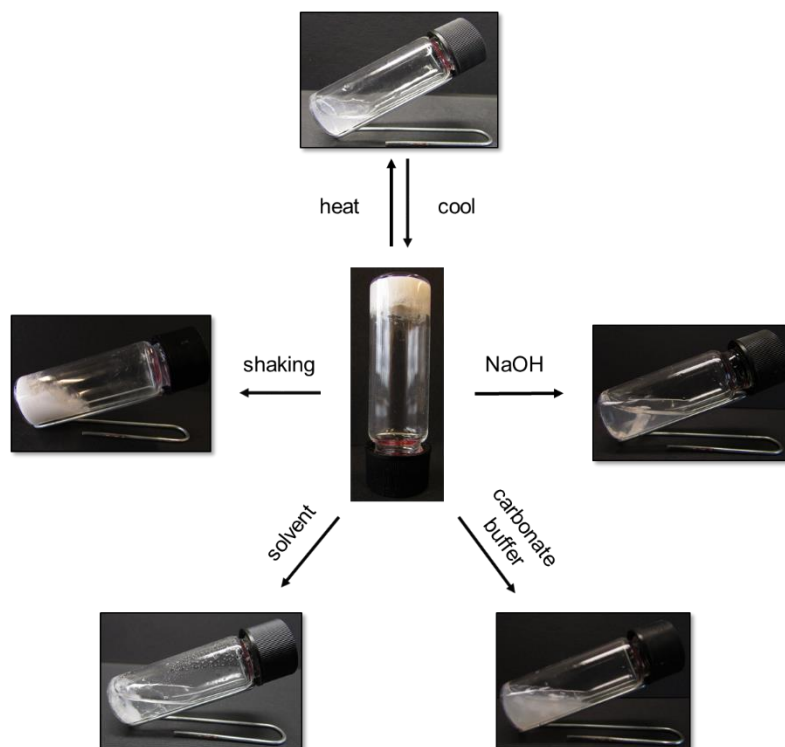


Fig. 11 Multistimuli response of a gel derived from **sulfo-Glu** in water (38 g L⁻¹).

Generally all gel-materials showed full thermo-reversible behaviour, regardless of gelator and nature of the solvent, without any remarkable changes in T_{gel} -values even after several cycles of heating and cooling. Irreversible gel-to-sol phase transitions could be observed by mechanical agitation and addition of certain chemical substances. Gel-materials were dissolved in the presence of NaOH and basic buffered solutions (borate buffer pH = 9.2) while being stable towards neutral and acidic conditions. Only **click-Glu** dissolved slowly upon addition of phosphate buffer saline (PBS; pH = 7.4) while **C₁₈-Glu** and **sulfo-Glu** remained stable. Treatment with several organic solvents led to multifaceted results. While **C₁₈-Glu** and **click-Glu** were stable against addition of most organic solvents, **sulfo-Glu** underwent phase transition in the presence of EtOAc and n-hexane. Response towards other organic solvents (i.e. MeOH, acetone and DCM), as well as to metal-ions (i.e., Ag⁺, Cu²⁺ and Fe³⁺), halides (TBAF), could not be observed regardless of the gelator. In general the response towards external stimuli was quite fast being in a range between 30–240 min resulting in complete dissolution or collapse of the gel phases.

1.2.2 Drug release experiments

Hydrogels prepared from **C₁₈-Glu** and **click-Glu** were for the first time evaluated as carriers for tuning the kinetics of drug release. Vancomycin, a useful glycopeptidic antibiotic for the treatment of infections mostly caused by Gram-positive bacteria, was selected in the first instance as hydrophilic model drug.⁸¹ Stable hydrogels towards a PBS buffer could be obtained using a gelator concentration of 60 g L⁻¹.

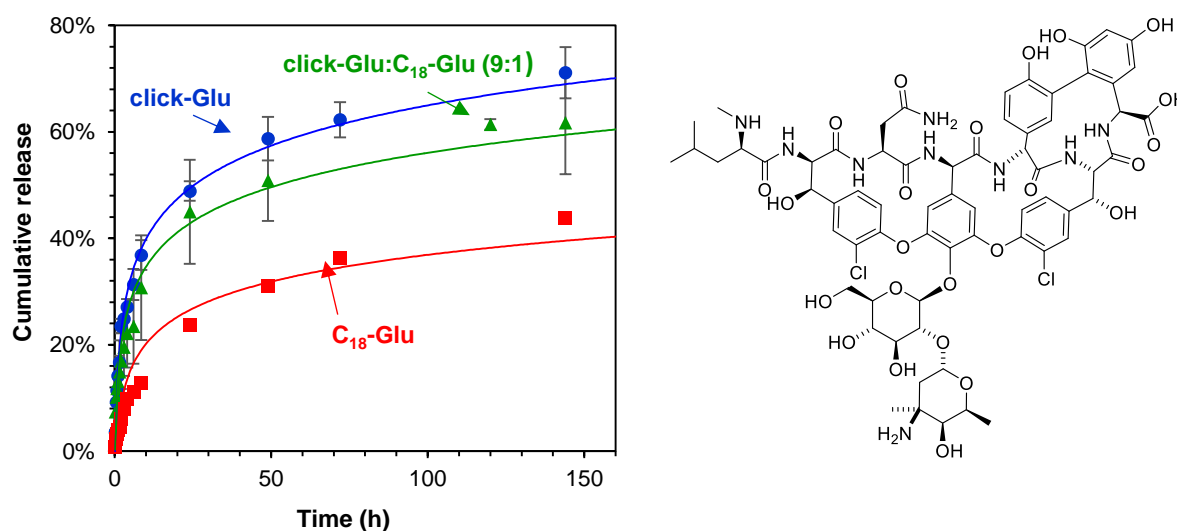


Fig. 12 Left: Release profile of vancomycin in PBS from hydrogels based on **click-Glu**, **C₁₈-Glu** and co-assembled **click-Glu:C₁₈-Glu** (9:1, w/w). **Right:** Chemical structure of vancomycin.

Thus, we used these conditions for preliminary studies of the release kinetics of entrapped vancomycin (initial drug concentration in the gel phase = 1.38×10^{-3} M). Up to 90% drug release was observed within 13 days in the case of **click-Glu**, whereas **C₁₈-Glu** showed much slower kinetics (around 56% within the same period). In general, release kinetics obeyed a first-order integrated rate law reasonably well (k_{obs} [**C₁₈-Glu**] = $1.5 \pm 0.2 \times 10^{-2}$ h⁻¹; k_{obs} [**click-Glu**] = $4.3 \pm 0.3 \times 10^{-2}$ h⁻¹). These results can be associated with different diffusion properties of the drug through hydrogels with diverse nano-morphologies, which are ultimately governed by the isosteric gelator structure (obviously, the interaction patterns between solvent–gelator, gelator–gelator and gelator/fibril–drug molecules play a key role in such a complex scenario). As expected, a faster release rate was also observed upon decreasing the gelator concentration due to the decrease of the crosslink density of the network (**Fig. 13A**) Remarkably, the complementary structure of the isosteric gelators allowed the preparation of stable hydrogels via co-assembly of both gelators

at different ratios, offering an alternative tuning option for fine-tuning the drug release (Fig. 12).

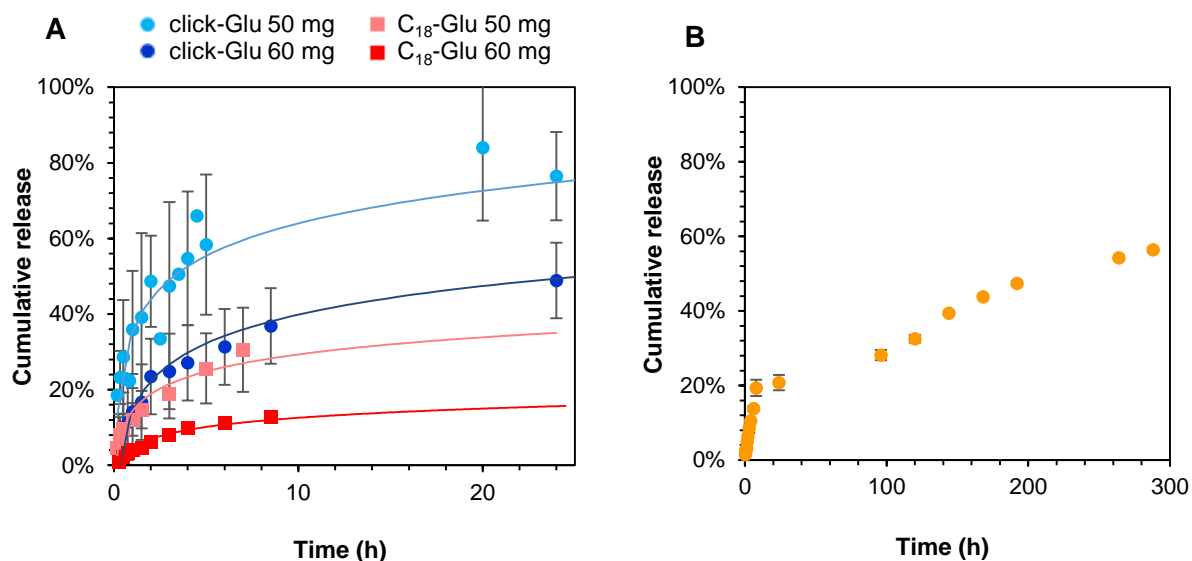


Fig. 13 A) Effect of the gelator concentration on the release of vancomycin from hydrogels made of **click-Glu** and **C₁₈-Glu**. **B)** Release of vancomycin from a hydrogel prepared using **click-Glu:C₁₈-Glu** (1:1, w/w).

However, the change in the kinetics upon co-assembly was not proportional to the molar ratio of the gelator (Fig. 13B) suggesting the formation of complex interpenetrated networks and release kinetics.

Not only vancomycin was used as model drug in this study. Also, the release of methotrexate hydrate, which is a non-water-soluble anti-cancer agent, was investigated (initial drug concentration in the gel phase = 0.66×10^{-3} M). Gels were prepared for this purpose in a stock solution of methotrexate in water/EtOH 1:1 mixture with **C₁₈-Glu** and **click-Glu**. In this case, a gelator concentration of 50 g L^{-1} was sufficient to form stable gels in contrast to 60 g L^{-1} for vancomycin release, which is eventually due to the presence of EtOH. However, this is surprisingly, since **C₁₈-Glu** did not show the ability to gel pure EtOH. The stability of gels derived from both gelators towards addition of PBS turned out to be similar which is in good agreement with the great similarity in the release profiles (k_{obs} [**C₁₈-Glu**] = $2.9 \times 10^{-2} \text{ h}^{-1}$; k_{obs} [**click-Glu**] = $3.3 \times 10^{-2} \text{ h}^{-1}$) of methotrexate from **C₁₈-Glu** and **click-Glu** derived gels (Fig. 14). Also in the water /EtOH 1:1 mixture a co-assembly of both gelators at different ratio was possible. However, again the change in the kinetics upon co-assembly was not proportional to the molar ratio of the gelator.

Isosteric replacement for tuning self-assembly and incorporating new functions into soft supramolecular materials

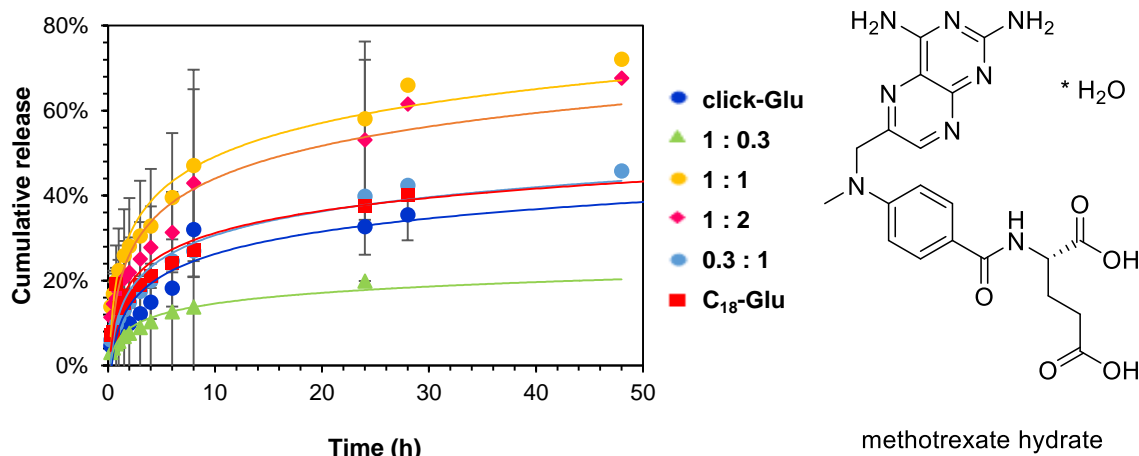


Fig. 14 Left: Release profile of methotrexate- water in PBS from hydrogels based on **click-Glu**, **C₁₈-Glu** and co-assemblies of both gelators at different **click-Glu:C₁₈-Glu** (w/w) ratios. Right: Chemical structure of methotrexate·H₂O.

In order to compare the influence of drug hydrophilicity on their release rate, preliminary release tests with flutamide and camptothecin, which are anti-cancer agents, as well were performed (**Fig. 15A** and **B**). The three anti-cancer drugs exhibit a molecular weight in the same range but differ in their hydrophilicity (flutamide: $\log P = 3.35$ ⁸², camptothecin: $\log P = 1.74$ ⁸³, methotrexate: $\log P = -1.85$ ⁸³) were methotrexate inherits the greatest hydrophilicity and flutamide the greatest hydrophobicity.

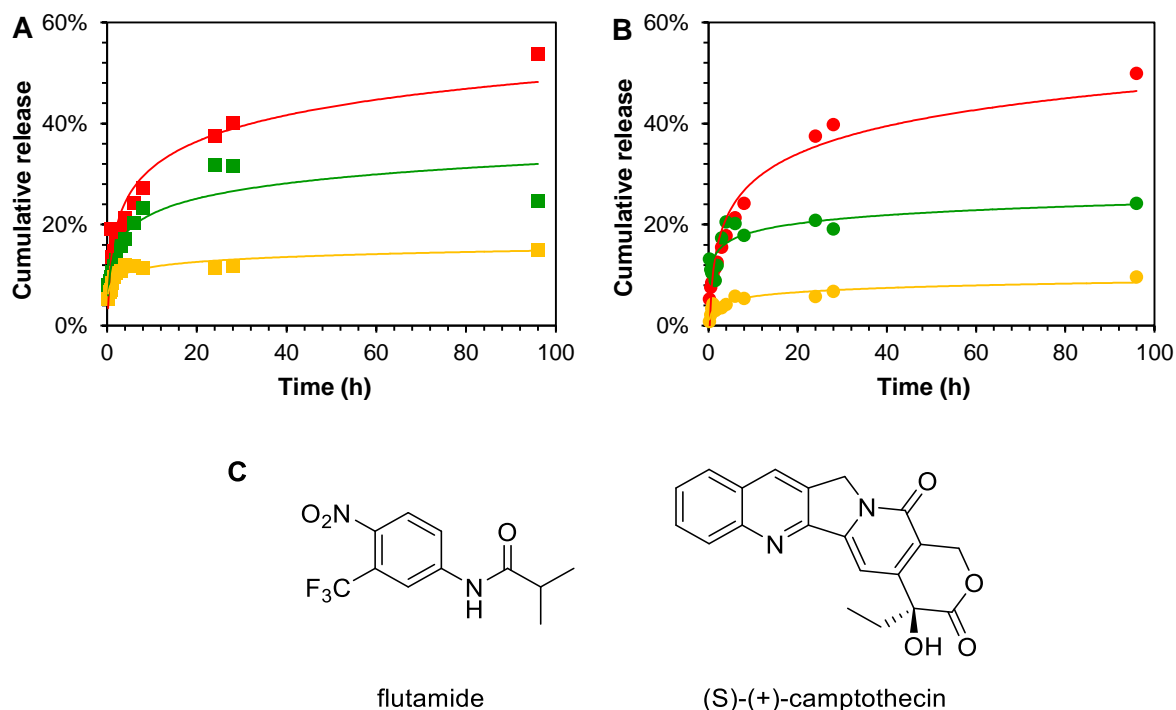


Fig. 15 Release profile of methotrexate-H₂O (■,●), camptothecin (■,●) and flutamide (■,●) in PBS from hydrogels based on **A)** **C₁₈-Glu** and **B)** **click-Glu**. **C)** Chemical structures of flutamide and camptothecin.

A clear relation between hydrophilicity and diffusion of the drugs into the surrounding release medium was found. This can be explained by the environmental conditions in the gel, which are more hydrophobic in comparison to the release buffer. Therefore, hydrophobic molecules tend to be more retained in the gel medium which comprises the favorable environment. More hydrophilic molecules experience a higher repulsion by the gel fibers and a higher attraction by the release medium which leads to a faster diffusion into the release medium.

Finally, also a hydrogel derived from **sulfo-Glu** was used as a drug carrier for vancomycin. Again the drug release followed a first-order integrated rate law ($k_{\text{obs}} [\text{sulfo-Glu}] = 1.3 \pm 0.1 \times 10^{-2} \text{ h}^{-1}$). Within 13 days around 58% of the initial drug amount was released into the surrounding medium whereat the release profile showed a remarkable similarity to that from **C₁₈-Glu** derived hydrogel ($k_{\text{obs}} [\text{C}_{18}\text{-Glu}] = 1.5 \pm 0.2 \times 10^{-2} \text{ h}^{-1}$; 56% release in 13 days).

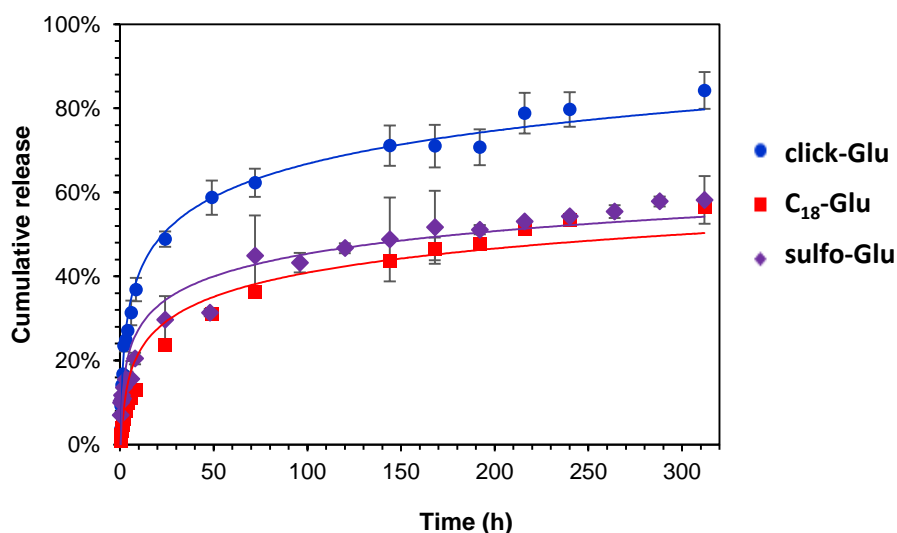


Fig. 16 Release profile of vancomycin in a PBS buffer from hydrogels based on **click-Glu**, **C₁₈-Glu** and **sulfo-Glu**.

1.2.3 Antimicrobial studies

The antimicrobial activities of the hydrogels with and without vancomycin against the Gram-positive bacteria *Staphylococcus aureus* were evaluated using the Kirby–Bauer test (**Fig. 17**, left).

Isosteric replacement for tuning self-assembly and incorporating new functions into soft supramolecular materials

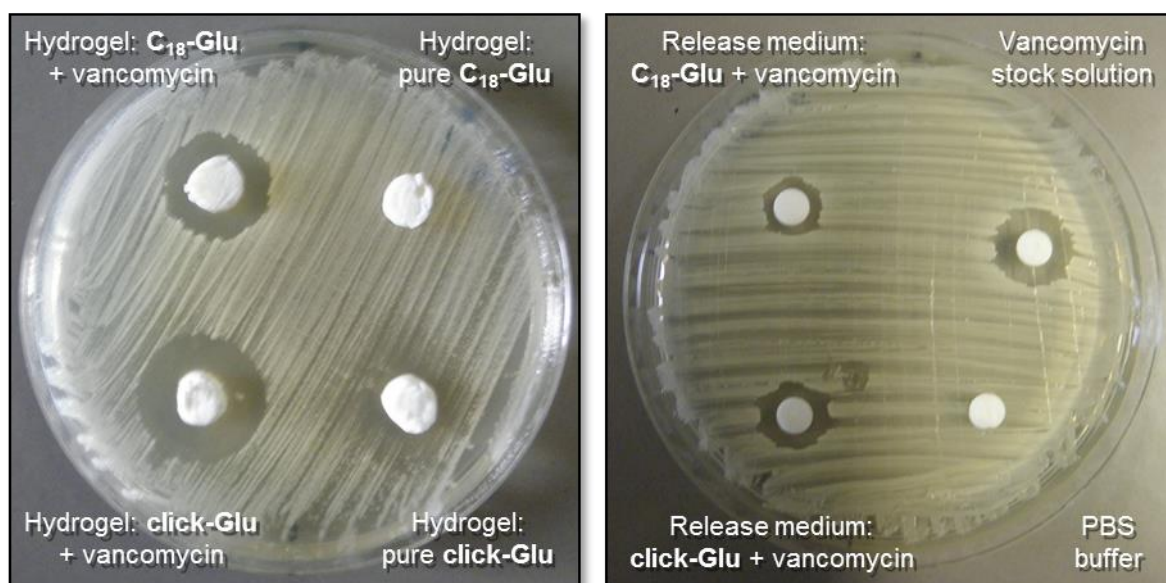


Fig. 17 The zone of inhibition test against *Staphylococcus aureus*. **Left**) for vancomycin containing hydrogels derived from **C₁₈-Glu** and **click-Glu** and their corresponding controls **right**) for release medium (on filter paper) after 24 h of vancomycin release from hydrogels.

Large inhibition zones (21.5 mm and 18 mm for drug loaded **click-Glu** and **C₁₈-Glu**, respectively) were observed. The results were in good agreement with the faster release kinetics of **click-Glu** hydrogels vs. **C₁₈-Glu**. No inhibition zones were evident with control gel samples. Maintenance of antimicrobial activity of the released drug was also confirmed (**Fig. 17**, right).

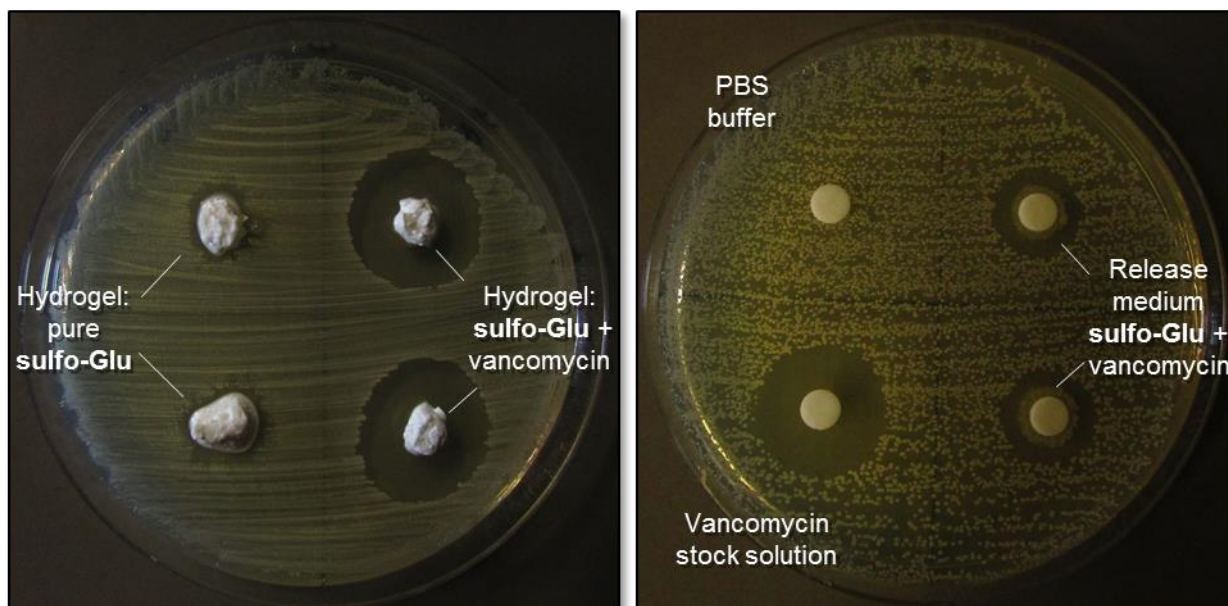


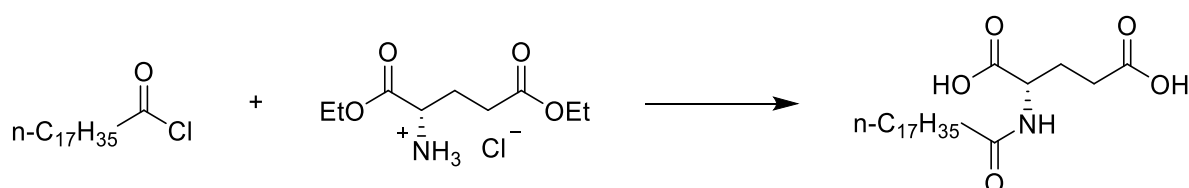
Fig. 18 The zone of inhibition test against *Staphylococcus aureus* **Left**) for vancomycin containing hydrogels derived from **sulfo-Glu** and their corresponding controls **right**) for release medium (on filter paper) after 24 h of vancomycin release from hydrogels.

Also **sulfo-Glu** derived hydrogels were tested in the Kirby-Bauer test (**Fig. 18**). Large inhibition zones ($\varnothing = 22.5 \pm 0.5$ mm) were formed around the hydrogel samples containing the drug, whereas the bacteria grew almost to the edge of the pure hydrogels. Even though the conditions for the zone of inhibition test were the same as for **click-Glu** and **C₁₈-Glu** the sizes of the inhibition zones cannot be compared since the test was not performed on the same agar plate. Testing the buffer medium of the drug release experiment after 24 h showed that the antimicrobial activity maintained (zone $\varnothing = 14.5 \pm 0.5$ mm). A positive control (aq. vancomycin solution 2 g L^{-1} , zone $\varnothing = 20$ mm) and a negative control (pure PBS buffer) illustrates, in good agreement with the drug release experiment, that within the first 24 h only parts of the drug diffused from the gel.

1.3 Experimental Part

1.3.1 Synthesis of glutamic acid derived gelators

Synthesis of *N*-stearoyl-L-glutamic acid **C₁₈-Glu**



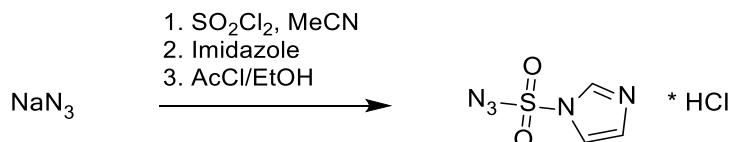
To a stirred solution of L-glutamic acid diethyl ester hydrochloride (1.72 g, 7.2 mmol) and NEt_3 (3.0 mL, 21.5 mmol) in dry methylene chloride (150 mL) at 0°C , a solution of stearoyl chloride (2.47 g, 8.2 mmol) in dry methylene chloride (20 mL) was added slowly over a period of 1 h. The mixture was allowed to warm to RT and stirred for additional 3 h, after which time water (50 mL) was added. The organic layer was separated, washed with water (4×50 mL), dried over Na_2SO_4 , filtered and the solvent was removed under reduced pressure. The obtained residue was dissolved in a 1:1 mixture of MeOH/water (150 mL) and KOH (1.18 g, 21.6 mmol) was added. The obtained suspension was stirred at RT for 18 h. MeOH was removed under reduced pressure and the aqueous phase was acidified with 2 M HCl to pH = 2. The formed precipitate was filtered off, thoroughly washed with water, dried and recrystallized from acetone affording the title compound as white solid.

Yield: 1.23 g (36%); $\text{C}_{23}\text{H}_{43}\text{NO}_5$ (413.60);

Isosteric replacement for tuning self-assembly and incorporating new functions into soft supramolecular materials

¹H NMR (300 MHz, DMSO-d₆) δ (ppm) 8.03 (d, 1H), 4.21–4.14 (m, 1H), 2.26 (t, 2H), 2.09 (t, 2H), 2.00–1.88 (m, 1H), 1.80–1.67 (m, 1H), 1.49–1.41 (m, 2H), 1.23 (s, 28H), 0.85 (t, 3H)

Synthesis of 1H-imidazole-1-sulfonyl azide

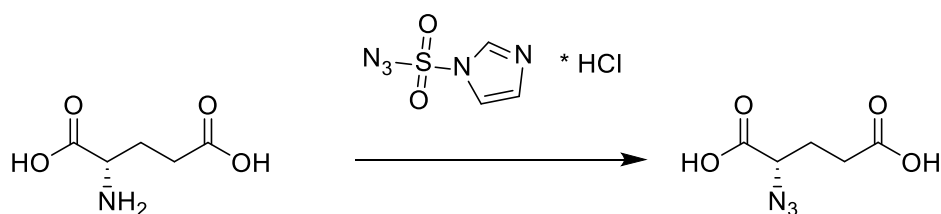


Sodium azide (7.5 g, 115 mmol) was suspended in dry MeCN (100 mL) followed by cooling this mixture to 0 °C, then thionyl chloride (8.1 mL, 100 mmol) was added dropwise over a period of 30 min. After stirring at room temperature for 20 h imidazole (13.0 g, 190 mmol) was added in portions and the slurry was stirred at room temperature for further 3 h. Subsequently EtOAc (200 mL) was added and the mixture was washed with water (3 x 100 mL) and sat. NaHCO₃ (3 x 100 mL). The organic layer was dried over Na₂SO₄, filtered and cooled to 0 °C. To this solution acetyl chloride (10.7 mL, 150 mmol) was added dropwise over a period of 30 min. The slurry was allowed to chill at 0 °C for 1.5 h while precipitation occurred which was then filtered and washed with ice cold EtOAc (25 mL) and dried in vacuum to give the product as pure white crystalline solid.

Yield: 11.0 g (52%), C₃H₃N₅O₂S·HCl (209.61 g mol⁻¹)

¹H NMR (300 MHz, D₂O) δ (ppm) 9.24 – 9.19 (m, 1H); 7.87 – 7.86 (m, 1H); 7.46 – 7.44 (m, 1H)

Synthesis of (S)-2-azidopentanedioic acid



1H-Imidazole-1-sulfonyl azide hydrochloride (6.23 g, 36 mmol), was added to a suspension of L-glutamic acid (4.41 g, 30 mmol), anhydrous potassium carbonate (15.34 g, 111 mmol) and copper(II) sulfate pentahydrate (75 mg, 0.30 mmol) in methanol (75 mL). The reaction mixture was stirred overnight at room temperature. Then, the solvent was removed and the resulting residue was diluted with water

Isosteric replacement for tuning self-assembly and incorporating new functions into soft supramolecular materials

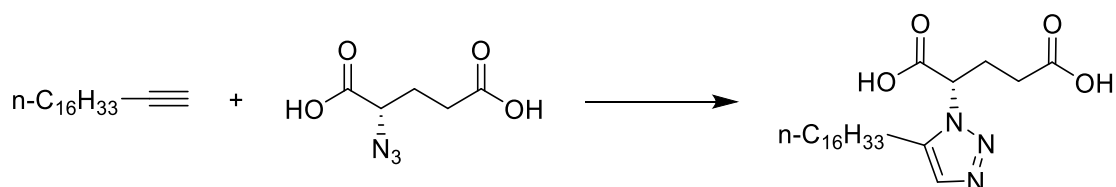
(40 mL), acidified with conc. HCl to give pH 2 and extracted with EtOAc (3 × 100 mL). The combined organic layers were dried over Na₂SO₄, filtered and concentrated. The resulting residue was purified by column chromatography (eluent: EtOAc) affording the desired product as colourless oil.

C₅H₇N₃O₄ (173.13 g mol⁻¹)

For safety reasons the solvent was not evaporated completely so no yield was determined.

¹H NMR (300 MHz, DMSO-d₆) δ (ppm) 12.75 (brs, 2H), 4.11 (dd, 1H), 2.39–2.22 (m, 2H), 2.05–1.98 (m, 1H), 1.88–1.73 (m, 1H)

Synthesis of (S)-2-(5-hexadecyl-1H-1,2,3-triazol-1-yl)pentanedioic acid **click-Glu**

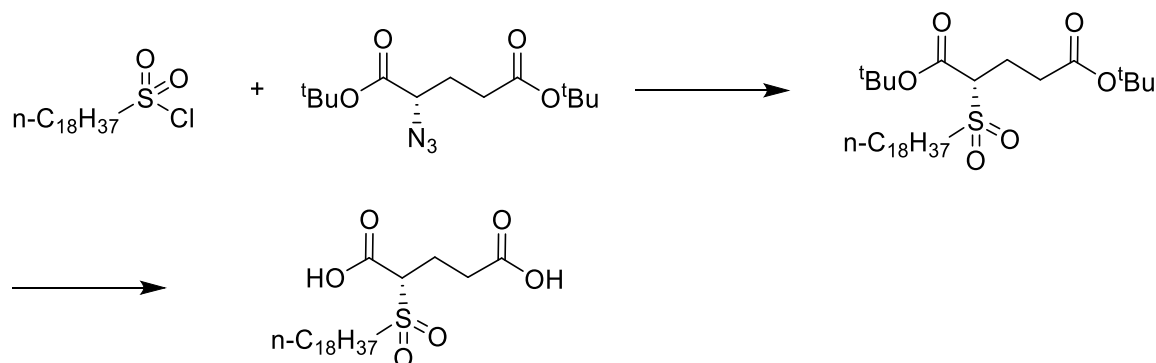


To a stirred solution of octadec-1-yne (1.20 g, 4.80 mmol) and (S)-2-azidopentanedioic acid (1.25 g, 4.80 mmol) in a 1:2 (v/v) mixture of DMSO/ water (5 mL) at RT CuSO₄·5H₂O (120 mg, 0.48 mmol) and sodium ascorbate (380 mg, 1.92 mmol) were added. Due to a clear increase of viscosity after a short period of time, the total solvent volume was further increased to 10 mL. After stirring for 72 h, the solvent mixture was removed by lyophilization. The obtained residue was redissolved in a 1:1 (v/v) mixture of EtOAc/THF (50 mL) and washed with brine containing 0.1 M EDTA·Na₂ (2 × 50 mL), brine (2 × 25 mL) and water (3 × 25 mL) in order to remove most of organic and inorganic impurities. The organic layer was dried over Na₂SO₄, filtered and concentrated under reduced pressure. The obtained residue was recrystallized from acetone affording the title compound as a white solid.

Yield: 1.01 g (50%), C₂₃H₄₁N₃O₄ (423.60g mol⁻¹)

¹H NMR (300 MHz, DMSO-d₆) δ (ppm) 7.95 (s, 1H), 5.35 (dd, 1H), 2.60 (t, 2H), 2.46–2.37 (m, 1H), 2.35–2.22 (m, 1H), 2.17–1.96 (m, 2H), 1.58 (t, 2H), 1.23 (s, 26H), 0.85 (t, 3H)

Synthesis of (octadecylsulfonyl)-L-glutamic acid **sulfo-Glu**



1-octadecyne sulfonyl chloride (1.44 g, 4.1 mmol) was dissolved in dry DCM (40 mL) under N₂-atmosphere at 0 °C. NEt₃ (1.71 mL, 12.3 mmol) and L-Glutamic acid di-tert-butyl ester-HCl (1.21 g, 4.1 mmol) were added. The reaction mixture was stirred at 0 °C for 1 h and subsequently for 3 days at room temperature. The solvent was evaporated and the resulting residue was purified by column chromatography (eluent hexanes/EtOAc 5:1 to 1:5). The intermediate was redissolved in DCM (18 mL) and TFA (3 mL) and was stirred at room temperature for 18 h. The solvent was evaporated and crude product was washed with ice cold DCM (20 mL) to give the desired product as a white solid.

Yield: 1.06 g (56%); C₂₃H₄₅NO₆S (463.67);

¹H NMR (300 MHz, DMSO-d₆) δ (ppm) 7.57 (m, 1H); 3.83 (m, 1H); 2.94 (m, 2H); 2.33 (m, 2H); 1.92 (m, 1H); 1.67 (m, 3H); 1.23 (s, 30H); 0.85 (t, 3H)

1.3.2 Gelation time and T_{gel} vs. concentration

Gelator and milli-Q water (500 μL) were placed in screw capped vials (final concentrations 38, 50, 60, 100, 150 and 200 g L⁻¹). The samples were heated until turbid solutions were formed. The time that was necessary for gel formation was measured by turning the vials upside down and the point where no flow occurred was considered as being the gelation time. After resting for 19 h, the samples were heated in a custom-made heating block at a rate of about 2 °C / 5 min. Melting points were measured by inverse flow method.

1.3.3 Stimuli response test

A weighted amount of the corresponding gelator and milli-Q water (500 μL) were placed in a screw capped vial (final concentrations: **C₁₈-Glu** 25 g L⁻¹, **click-Glu** 17 g L⁻¹ and **sulfo-Glu** 38 g L⁻¹, respectively). The samples were tempered in a custom made heating block at 100 °C for 1 h whereat homogeneous, turbid solutions were formed. Subsequently the samples were allowed to cool slowly to room temperature. After 19 h stable gels were obtained which were overlaid with each 500 μl of different solvents or solutions (0.1 M). The samples were stored at room temperature and observed for 24 h.

1.3.4 Drug release

A weighted amount of the corresponding gelator (50 – 60 mg), and 1 mL of a drug stock solution (vancomycin: 2 g L⁻¹ in water, methotrexate hydrate: 0.3 g L⁻¹ in water/EtOH 1:1; camptothecin: 0.1 g L⁻¹ in water/EtOH 9:1; flutamide: 0.8 g L⁻¹ in water/EtOH 9:1) were placed in a screw-capped glass vial and gently heated until all solid materials were completely dissolved. The obtained isotropic solution was allowed to cool down to RT resulting in gel formation with a physically incorporated drug.

Obtained gel materials were overlaid with phosphate buffered saline (PBS, 1 mL, pH = 7.4) 16 h after their formation, which was considered as the starting point for the experiments. At selected points of time aliquots (100 μL) were removed and diluted with PBS to 1 mL. Then fresh PBS (100 μL) was added over the gel to maintain infinite sink conditions. Drug concentration in the aliquots was determined during the experiments using UV-spectroscopy after proper calibration using the maximum absorbance of drugs in aqueous media (vancomycin: 280 nm; methotrexate hydrate 303 nm; camptothecin: 371 nm; flutamide: 303 nm). Samples were centrifuged (EBA 12 Hettich Zentrifugen) at 4000 rpm for 5 min before measurements. It was verified that degraded gel materials exhibited a minimum absorbance in the region of drug detection.

1.3.5 Antimicrobial studies

The Zone of Inhibition Test, also called Kirby-Bauer Test, is used clinically to qualitatively measure antibiotic resistance and industrially to test the ability of specimens to inhibit microbial growth.

Preparation of agar plates: A solution of 1% peptone, 0.5% yeast, 0.2% glucose and 1.5% of agar-agar (w/v) in milli-Q water was autoclaved at 120 °C for 20 min and then shaken. After cooling down to 95 °C, a Petri dish (8.5 cm diameter) was filled to half of the volume (about 25 mL). The dishes were shaken circularly on the bench to bring air bubbles to the edge. After cooling to room temperature, the plates were placed upside down to avoid condensed water to drop on the medium and stored in the refrigerator at 2-8 °C.

Hydrogels preparation: An aqueous vancomycin solution (1 mL from a 2 M solution) was added to a screw-capped vial containing either **C₁₈-Glu**, **click-Glu** or **sulfo-Glu** (60 mg). The mixture was heated until complete dissolution of the material, transferred to a 2 mL syringe with cut cap and rested over night to obtain the corresponding stable hydrogels.

Antimicrobial tests with hydrogel pieces: *S. aureus* was seeded out evenly with a cotton bud on agar medium. Cylindrical gel pieces of approximately 4 mm length and 9 mm diameter (0.25 mL) were placed on the bacteria plates. The plates were stored at 37 °C for 17 h.

Release of vancomycin from the hydrogels: An aqueous vancomycin solution (1 mL from a 2 M solution) was added to a screw-capped vial containing either **C₁₈-Glu**, **click-Glu** or **sulfo-Glu** (60 mg). The mixture was heated until complete dissolution of the material and rested over night to obtain the corresponding hydrogels. The loaded-hydrogels were overlaid with PBS buffer (1 mL) and rested for additional 24 h.

Antimicrobial tests with drug release supernatants: *S. aureus* was seeded out evenly with a cotton bud on agar medium. Three samples of filter papers were soaked separately in 20 µL of (a) supernatant obtained from the drug release experiment, (b) pure PBS and (c) aqueous vancomycin solution (2 M). The specimens were placed on the plates and stored at 37 °C for 17 h.

1.4 Conclusions

In conclusion, the isosteric replacement paradigm from medicinal chemistry can be successfully applied to the synthesis of novel soft functional materials. As a proof-of-concept, isosteric gelators **C₁₈-Glu**, **click-Glu** and **sulfo-Glu** afforded the preparation of a variety of physical hydrogels and organogels with different thermal, mechanical, morphological and diffusional properties. In general, **click-Glu** revealed superior features with respect to the CGC, T_{gel} and mechanical stabilities in polar protic solvents, whereas **sulfo-Glu** exhibited improved properties in non-polar solvents and

C₁₈-Glu showed in average values between those of **click-Glu** and **sulfo-Glu**. Additionally the three isosteres proofed to be applicable for the *in vitro* delivery of drugs with different sizes and hydrophilicities. A sustained release over several days up to two weeks could be achieved, where diffusion from **click-Glu** derived hydrogels was faster than from **C₁₈-Glu** and **sulfo-Glu**, which exhibited similar release profiles. Moreover, the co-assembly of **C₁₈-Glu** and **click-Glu** was successfully applied for fine-tuning the release of the antibiotic vancomycin and the anti-cancer agent methotrexate. The antibiotic activity of vancomycin loaded hydrogels against the Gram-positive *Staphylococcus aureus*, as well as maintenance of efficacy of the released drug was also confirmed. Overall, these results open up many exciting opportunities for the development of new functional materials with unique properties for different applications beyond the field of gels.

2. Release of camptothecin, oxytetracycline and mitoxantrone from glycyrrhizic acid derived water/ethanol gels into several buffered solutions

2.1 Introduction

Glycyrrhizic acid (GA) or glycyrrhizin is a natural occurring saponin, which can be extracted from the licorice (liquorice) root (*Glycyrrhiza glabra*) in the form of its potassium, calcium and magnesium salts. It is the ingredient which is mainly responsible for the sweet taste of this root. The chemical structure consists of a lipophilic pentacyclic triterpenoid and a hydrophilic part which are two β (1 \rightarrow 2) linked glucuronic acid units (**Fig. 19**) Due to this amphiphilic structure it is able to form micelles in water and water/alcoholic solutions. Its ability to form stable hydrogels was already described in 1879 by Habermann.⁸⁴

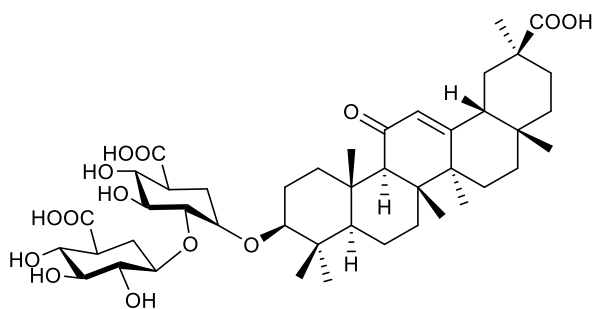


Fig. 19 Structure of Glycyrrhizic acid

X-ray crystallography has shown that GA can self-assemble into a supramolecular interdigitated network, with alternating hydrophilic and hydrophobic areas.^{85,86} The diglucuronic acid units build up hydrophilic platforms via H-bonding (**Fig. 20**) while the hydrophobic areas, deriving from terpenoid structures, exhibit channels which can be filled with solvent or guest molecules. Remarkably chemical differences between GA and its mono- and dibasic salts practically have no impact on the supramolecular organization. This isomorphism is due to a specific structure of hydrophilic bilayers assembled from zigzag chains of neutral, mono-anionic, or di-anionic diglucuronic acid units. Counter ions like ammonium, potassium, or cesium were found to be able to replace hydrogen-bonded water molecules in the hydrophilic sugar platform.

Release of camptothecin, oxytetracycline and mitoxantrone from glycyrrhizic acid derived water/ethanol gels into several buffered solutions

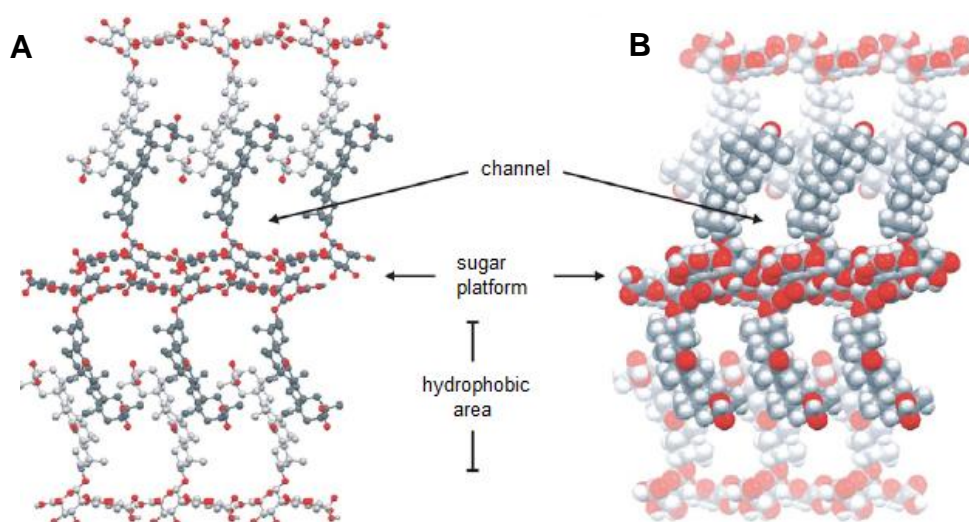


Fig. 20 Self-assembly of glycyrrhizic acid. **A)** Ball and stick and **B)** space filling representation. Reprinted from Ref. 86 with permission from American Chemical Society.

The applications of GA are manifold, e.g. as emulsifier and sweetener in food industry. Apart from that, the *Glycyrrhiza glabra* has been used as medical plant for more than 100 years. Glycyrrhizic acid has many pharmaceutical application it has been found to have anti-hepatotoxic,^{87,88} anti-ulcerogenic,⁸⁹ anti-allergenic⁹⁰ and anti-inflammatory activities⁹¹ as well as inhibitory activities in the replication of several DNA and RNA viruses in vitro.⁹² Indeed GA has been also used as an adjuvant for drug delivery due to its ability to solubilize poorly water soluble drugs which was first described in 1963.⁹³ The first time glycyrrhizin was used as a drug carrier itself, was presented by Segal et. al in 1986, where the authors entrapped several bioactive compounds in hydrogels derived from GA for the treatment of mucosal lesions due to herpes.⁹⁴

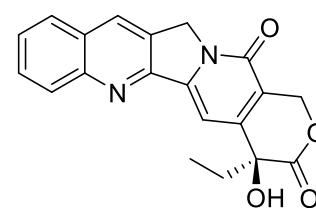
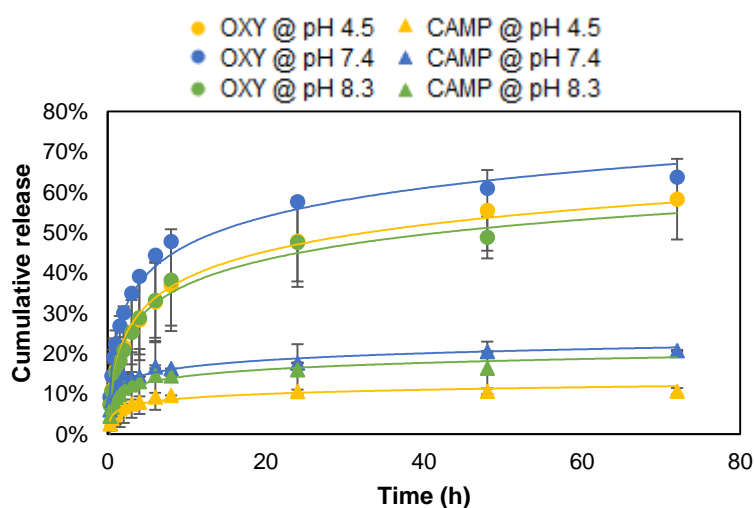
2.2 Results and Discussion

2.2.1 Drug Release

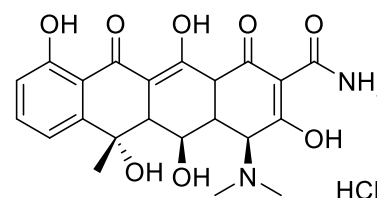
Glycyrrhizic acid ammonium salt is also a good hydrogelator with excellent biocompatibility whose hydrogels additionally are able to tolerate up to 25 wt% ethanol. Therefore, it is an interesting candidate for the physical entrapment and subsequent release of hydrophilic as well as hydrophobic drug molecules. For the purpose of studying the drug release from glycyrrhizic acid ammonium salt derived gels, in the first instance, two drug molecules with different hydrophilicity, namely camptothecin (CAMP) ($\log P = 1.74$ ⁸³) and oxytetracycline hydrochloride (OXY) ($\log P = -0.90$ ⁹⁵) were used as model drugs. Stable hydrogels containing the drug molecules could be

Release of camptothecin, oxytetracycline and mitoxantrone from glycyrrhizic acid derived water/ethanol gels into several buffered solutions

obtained using a gelator concentration of 20 g L^{-1} . After 16 h of equilibration time the samples were overlaid with several buffered solutions. In the first instance the release of camptothecin and oxytetracycline into acetate buffer pH 4.5, phosphate buffered saline (PBS) pH 7.4 and borate buffer pH 8.3 was investigated (**Fig. 21**). Clean release curves were achieved which could be fitted reasonably well by Weibull's equation (see **Fig. 27**). In good agreement with results described in chapter B, the more hydrophilic OXY was released considerably faster and in a clearly greater amount (around 4 fold) than the less water soluble camptothecin. As mentioned before, due to the more hydrophobic environment of the gel material in comparison to the release buffer the more hydrophobic drug experiences a greater retention than a more hydrophilic compound. Hydrophobic molecules experience a greater retention from the gel medium in contrast to more hydrophilic molecules which are more repelled by the gel fibers and have a higher attraction to the release medium and hence diffuse faster.



(S)-(+)-Camptothecin



Oxytetracycline hydrochloride

Fig. 21 Left: Release profile of oxytetracycline-HCl and camptothecin from hydrogels based on glycyrrhizic acid ammonium salt into several buffered solutions at different pH values. pH 4.5: acetate buffer, pH 7.4: phosphate buffered saline and pH 8.3: borate buffer. Error bars are calculated as standard deviation from at least two independent experiments. **Right:** Chemical structures of oxytetracycline-HCl and camptothecin.

We expected a clear trend in the release rate depending on the pH of the release medium. However, no such trend was observable. The order of release rate of oxy into the buffer solutions was $\text{PBS} > \text{acetate buffer} \geq \text{borate buffer}$ whereas for camp it was $\text{PBS} \geq \text{borate buffer} > \text{acetate buffer}$. Interestingly the two drugs did not show the same buffer dependency in their release behavior. One factor could be the diffusion of buffer salts into the gel medium which can cause different responses like shrinkage, swelling or erosion. But also the attraction between drug and release

Release of camptothecin, oxytetracycline and mitoxantrone from glycyrrhizic acid derived water/ethanol gels into several buffered solutions

medium might play an important role. As these results did not provide us with clear answers we decided to run quick tests with three further buffer solutions for the release of camp, namely 2-(*N*-morpholino)ethanesulfonic acid (MES) buffer at pH 3.7 and pH 5.5 as well as carbonate buffer at pH 9.2.

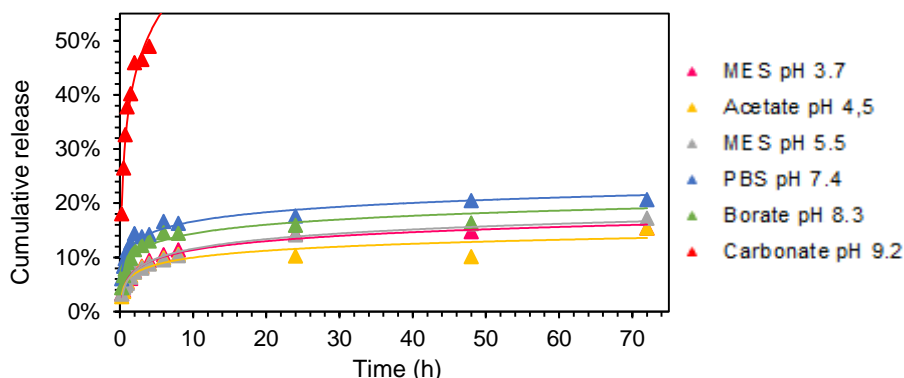


Fig. 22 Release profile of camp from hydrogels based on glycyrrhizic acid ammonium salt into several buffered solutions at different pH values. pH 3.7: MES, pH 4.5: acetate buffer, pH 5.5: MES, pH 7.4: phosphate buffered saline, pH 8.3: borate buffer and pH 9,2 carbonate buffer.

However, still no explicit influence of environmental pH on release rate could be drawn (**Fig. 22**). Nonetheless some interesting results were found. The release of camptothecin into carbonate buffer at pH 9.2 was extremely rapid and finished at a value of around 50% after only 4 hours which is clearly due to the rapid dissolution of the gel material. The next fastest release rates were exhibited with PBS pH 7.4 and borate buffer pH 8.3 which are close to neutral pH. The diffusion into those buffers reached values of around 25% and 21%, respectively after 3 days. Interestingly, release profiles into MES buffers at two different pH values did not show any difference, which indicates, the nature of the buffer system might have a stronger influence than pH. The release into acetate buffer was the slowest with a level of around 13%. It seems that an acidic environment stabilizes the gel material and hence leads to a slower release of embedded drugs than more basic environments.

In order to check the long term delivery of drugs, the release of camptothecin into PBS was monitored for 13 days where the release still did not reach a plateau level, which gives good expectancies that glycyrrhizic acid ammonium salt derived gels can act as a depot with long term delivery of more than two weeks of camptothecin. Unfortunately such test could not be performed with OXY as this drug degraded over time in an aqueous environment, indicated by an orange discoloration of the originally clear gel as well as a shift of the absorbance maximum after around 48 h (**Fig. 23**).

Release of camptothecin, oxytetracycline and mitoxantrone from glycyrrhizic acid derived water/ethanol gels into several buffered solutions

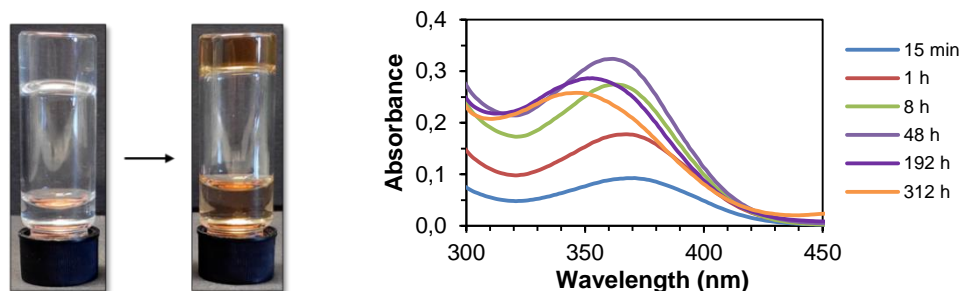


Fig. 23 Left: Discoloration of oxy containing gel after around 1 week. **Right:** shift of absorbance maximum of oxy over time.

As the stability of OXY caused problems, we decided to look for a new hydrophilic model drug. Mitoxantrone hydrate (MITOX) which is a good water soluble ($\log P = -2.9$ ⁹⁶) anti-cancer drug, with an absorption maximum of 661 nm was chosen. Again the release into those buffer solutions mentioned above was performed, where carbonate buffer was omitted as it caused a rapid dissolution of the gel.

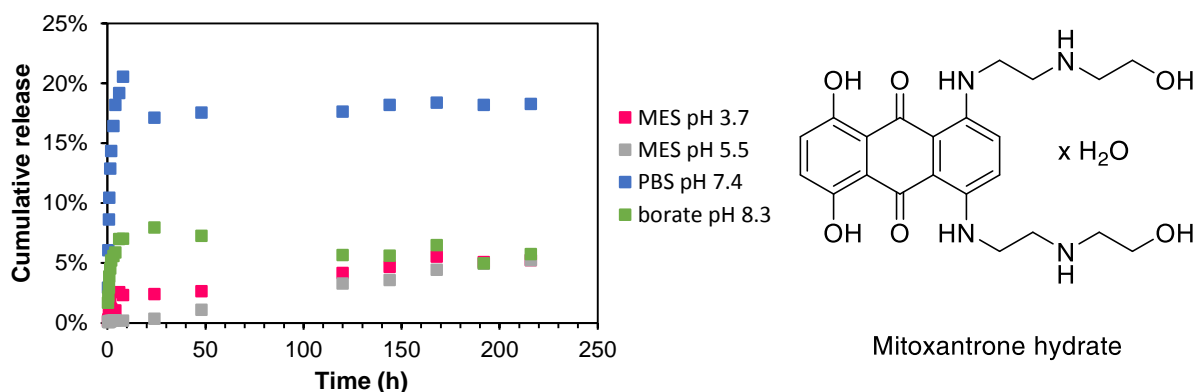


Fig. 24 Left: Release profile of MITOX from hydrogels based on glycyrrhizic acid ammonium salt into several buffered solutions at different pH values. pH 3.7: MES, pH 5.5: MES, pH 7.4: phosphate buffered saline and pH 8.3: borate buffer. **Right:** Chemical structure of MITOX.

Surprisingly no signal of MITOX release into acetate buffer, even after 9 days, could be observed (see also **Fig. 26**). In good agreement with camptothecin release, also the release of MITOX into the two different MES buffers was very similar. However, the diffusion into the more acidic MES buffer was slightly faster (~ 6% after 7 days) than that into the more basic one (~6% after 9 days). The next faster release was found to occur in the presence of borate buffer with reaching a maximum of around 8% within 24 h. In agreement with CAMP and OXY, the diffusion into PBS buffer was the fastest (excluded carbonate buffer). In general MITOX release curves did not follow any typical diffusion models – in contrast to CAMP and OXY - which suggests a coexistence of diffusion and erosion phenomena. This, the generally very slow diffusion of MITOX as well as the nonappearance of release in the presence of

acetate buffer indicates a strong interaction between MITOX and the gelator molecules and presumably a destabilization of the gel fibres. The latter would need to be proven by rheological measurements.

2.2.2 Response to buffer solutions

One reason for the non-concrete dependence of drug release rate on the environmental pH could be the varying reactions of the gel material towards the different buffer systems (see **Fig. 25**). A complete gel-sol transition was observed upon addition of highly basic (pH 9.2) carbonate within around 8 h. This process was also observed in still basic (pH 8.3) borate buffer and neutral (pH 7.4) PBS, whereas degradation was much slower. Around half of the gel material dissolved within 3 days. Additionally in case of PBS the, at first transparent, gel turned translucent over time which indicates a formation of particles bigger than the wavelength of visible light (350–750 nm). In general the presence of an acidic environment did not affect the gel stability as no degradation was observed. However, MES buffer which is the only buffer system which is not based on inorganic but on organic salts, led to a swelling of the gel material accompanied by a phase separation. This may be inferred that MES diffuses into the gel and thereby introduce additional solvent.

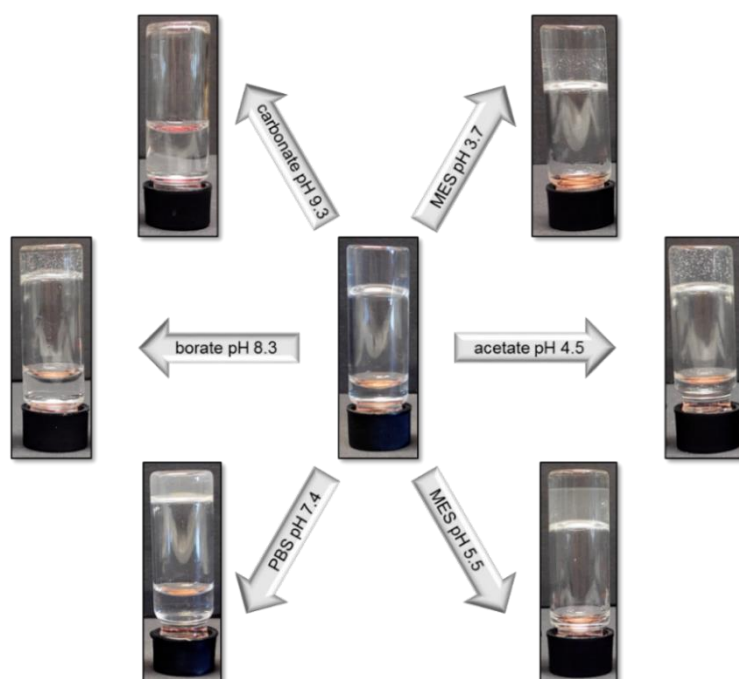


Fig. 25 Response of glycyrrhizic acid ammonium salt derived gels in water/EtOH 9:1 (20 g L⁻¹) with physically entrapped CAMP (0.1 g L⁻¹).

2.3 Experimental Part

Glycyrrhizic acid ammonium salt from glycyrrhiza root (licorice) and oxytetracycline hydrochloride were purchased from Sigma Aldrich. (S)-(+)-camptothecin was purchased from TCI.

A weighted amount of the corresponding gelator (20 mg), and 1 mL of a drug stock solution (MITOX: 0.6 g L⁻¹ in water; OXY: 0.08 g L⁻¹ in water; CAMP: 0.1 g L⁻¹ in water/EtOH 9:1) were placed in a screw-capped glass vial and gently heated until all solid materials were completely dissolved. The obtained isotropic solution was allowed to cool down to RT resulting in the formation of a transparent gel with physically incorporated drug.

Obtained gel materials were overlaid with 1 mL buffer solution (MES pH = 3.7; acetate buffer pH = 4.5; MES pH = 5.5; PBS pH = 7.4; borate buffer pH = 8.3 or carbonate buffer pH = 9.2) 16 h after their formation, which was considered as the starting point for the experiments. At selected points of time aliquots (100 µL) were removed and diluted with the corresponding buffer to 1 mL. Then fresh buffer (100 µL) was added over the gel to maintain infinite sink conditions. Drug concentration in the aliquots was determined during the experiments using UV-spectroscopy after proper calibration using the maximum absorbance of drugs in aqueous media (MITOX hydrate: 661 nm; OXY: 357 nm; CAMP: 371 nm). It was verified that degraded gel materials exhibited a minimum absorbance in the region of drug detection.

2.4 Conclusions

Glycyrrhizic acid ammonium salt, a natural product derived from the licorice root, was used to gel water and water/ethanol solutions. Three different bioactive agents, namely camptothecin, oxytetracycline hydrochloride and mitoxantrone hydrate were selected as model drugs for the physical entrapment into these gels and the subsequent release into several buffered solutions namely MES pH 3.7, acetate pH 4.5, MES pH 5.5, PBS pH 7.4, borate pH 8.3 and carbonate buffer pH 9.2. In good agreement with previous results, comparison between the relatively hydrophobic CAMP and the more hydrophilic OXY revealed much faster release rates for the latter over the prior as the gel material depicts a more hydrophobic environment than the surrounding release medium and therefore exhibits a greater retention for more hydrophobic drugs. Interestingly the even more hydrophilic MITOX showed in average the slowest release rates. This and the observation, that MITOX loaded gels

Release of camptothecin, oxytetracycline and mitoxantrone from glycyrrhizic acid derived water/ethanol gels into several buffered solutions

suffer from a greater erosion suggests a strong interaction between this drug and the gelator molecule which can cause a destabilization of the gel fibers. These results demonstrate clearly the difficulty of predicting the release behavior from matrix type drug formulations.

In addition, the dependence of drug delivery on the environmental pH was aimed to investigate. In general it was observed that acidic environment led to a slower release of embedded drugs than more basic environments as GA ammonium salt derived gels were sensitive towards basic solutions. However, the nature of the buffer system also had a strong impact on release rates. This exposes the limitations of *in vitro* drug delivery experiments. Nevertheless those kind of investigations play an important role in gaining preliminary insights into the potential application of gel materials as drug carriers before *in vivo* experiments can be considered.

2.5 Additional Graphics

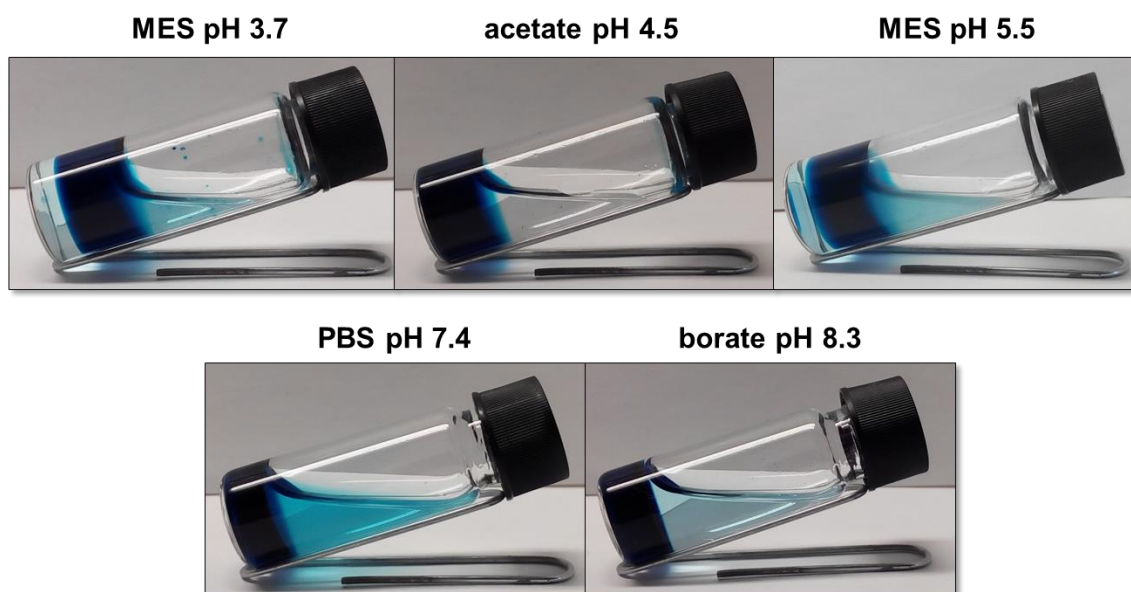


Fig. 26 Photographs of GA ammonium salt derived hydrogels with physically entrapped MITOX, overlaid with different buffer solutions.

Release of camptothecin, oxytetracycline and mitoxantrone from glycyrrhizic acid derived water/ethanol gels into several buffered solutions

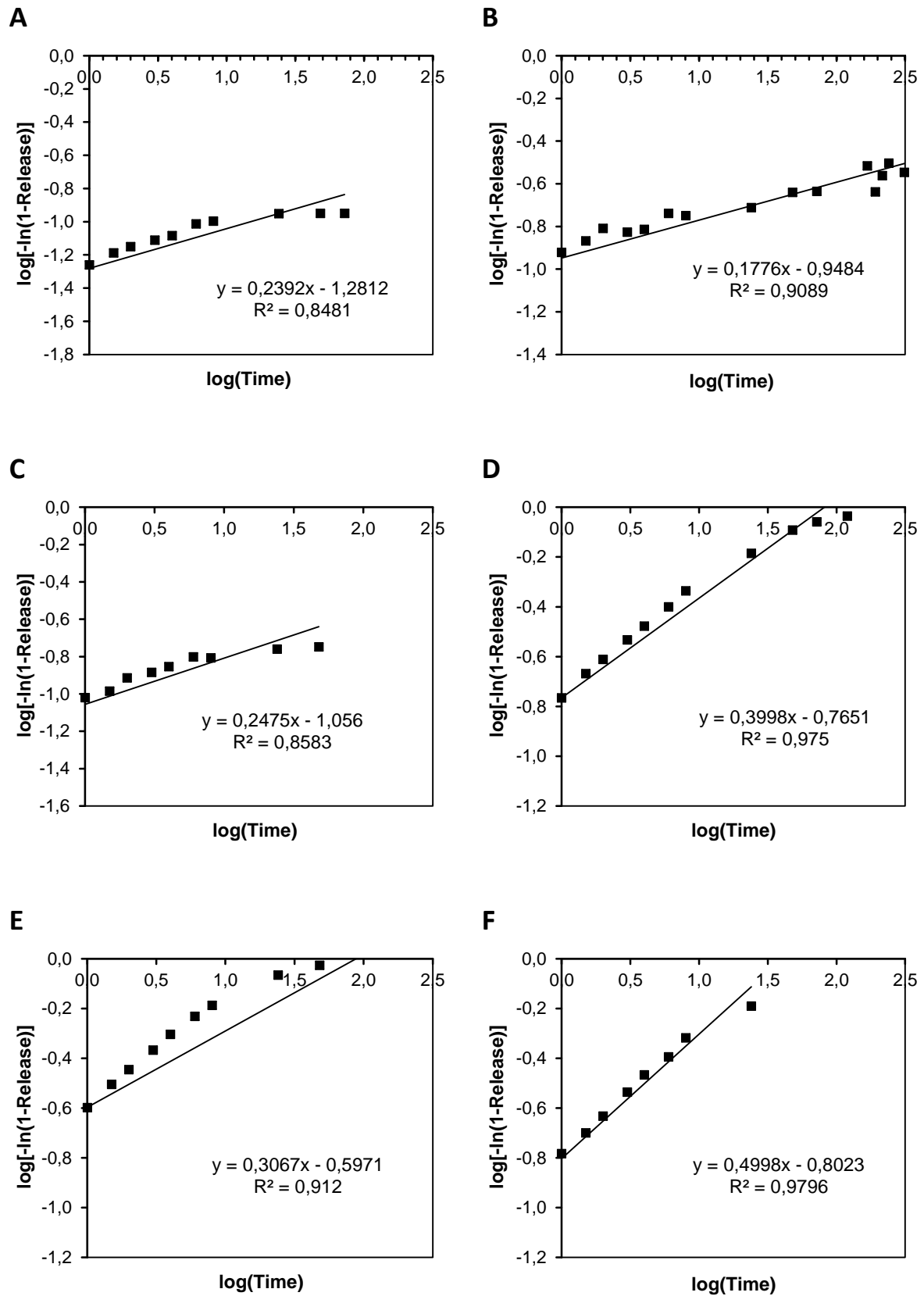


Fig. 27 Log(-ln) – log plot showing the monomial relationship between drug release and time. Release of CAMP into **A)** acetate pH 3.7 **B)** PBS pH 7.4 **C)** borate pH 8.3 and release of OXY into **D)** acetate pH 3.7 **E)** PBS pH 7.4 **F)** borate pH 8.3.

3. Improvement of gelation properties of a formamidine based gelator by ultrasonication²

3.1 Introduction

During the last decades formamidines received great attention. They have been described to be easily synthesized and have a high potential for biological and pharmacological applications.^{97–103} Formamidines such as chlordimeform^{104–106} and amitraz^{106,107} have been used as insecticides already since the late 1960s in a large industrial scale, however later have been proven to inherit potentially carcinogenic activity. Another field where formamidines are popular is in the design of new drug molecules as they have been found to increase bioactivity in comparison to parent drugs.¹⁰⁸ Also in the field of organo-metallics, formamidines are applied as complexing agents for metals in catalysis as they offer high structural variety and diversity of binding modes.^{109–112} But so far they have not been used in materials sciences. However in 2014 when Díaz and Finn attempted to find new synthetic approaches towards multi-substituted formamidines, their amphiphilic compounds turned out to be able to gel protic organic solvents.⁹⁸

Supramolecular gels with viscoelastic properties are stimuli-responsive materials which were intensively studied during the last decades as they found to have applications in a great variety of fields such as food, agriculture, catalysis, sensing, cosmetics and biomedicine.^{9–11} According to Flory a gel has a permanent continuous structure with macroscopic dimensions and in terms of rheology shows a solid-like behavior.¹⁴ Gels can be e.g. divided into organogels and hydrogels according to the nature of the solvent. Other classifications are chemical¹¹³ or physical¹¹⁴ gels depending on the types of interactions (covalent or non-covalent, respectively) which are responsible for the network formation.

In the case of low-molecular-weight gelators (LMWG), the gel formation is based on the self-assembly of LMWG molecules into one-dimensional strands and the entanglement of the latter, which can be typically achieved by cooling hot isotropic solutions to room temperature.^{114,115}

Besides the classical heating-cooling protocol for gel-formation, some compounds are also known to form gels upon application of ultrasound.^{116–118} This is remarkable

² In this chapter gelation experiments were performed by J. Bachl. Remaining experiments were performed by J. Mayr.

as previously it was assumed that ultrasonic waves would disrupt self-assembly in solution.¹¹⁹ Here we report a novel amphiphilic gelator molecule bearing a formamidine unit, which shows enhanced gelation properties upon ultrasonication treatment in comparison to a standard heating-cooling protocol.

3.2 Results and discussion

A new formamidine based, amphiphilic gelator compound (FAG) (**Fig. 28**), consisting of a long carbon chain (C₁₆) and acetyl L-phenyl alanine connected via a formamidine function was synthesized in four steps.

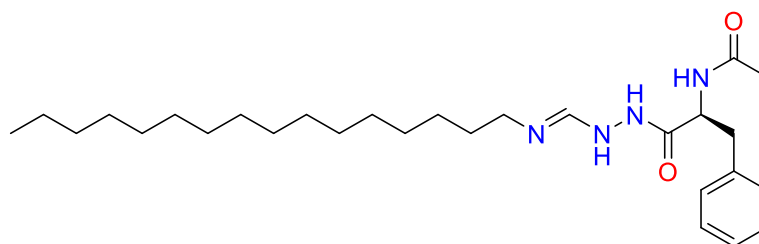


Fig. 28 Formamidine based, amphiphilic gelator compound.

Briefly, first protection of C-terminus of L-phenylalanine as methyl ester, followed by protection of N-terminus by an acetate. Next step was the transformation of the methyl ester into a hydrazine ester. Last but not least hexadecyl-dimethylformimidamide was formed, where subsequently dimethylamine was substituted by the acetyl-L-phenylalanine hydrazine ester to give the final gelator molecule.

The gelation ability of the FAG was investigated for 30 organic solvents of different nature (apolar, polar aprotic or polar protic) by applying a classical heating-cooling cycle. Materials that did not exhibit gravitational flow according to the “stable-to-inversion” method were preliminarily classified as gels and their solid-like appearance was further confirmed using dynamic rheological measurements. The FAG was not able to form gels with DMF, THF and chlorinated solvents like DCM, CHCl₃ or 1,2-dichloroethane as its solubility in these solvents was too high, while gelation of glycerine failed due to insolubility. Partial gels at maximum concentrations of 200 g L⁻¹ have been formed in alcoholic solvents like MeOH, EtOH, i-PrOH, 2-butanol, 1-hexanol. Nineteen other solvents, including two room temperature ionic liquids, aromatic and several oil-based solvents, were able to produce stable gels in a concentration range varying from about 15-150 g L⁻¹ for most samples, which opens the door for potential applications in removal of oil spills and fabrication of conducting materials. During investigations concerning other approaches towards the formation

of stable gels different to the classical heating-cooling cycle, it was found that ultrasound-treatment of isotropic solutions of FAG and an appropriate organic solvent had a remarkably positive effect. Not only could the range of solvents gelled be extended by the 5 alcoholic solvents mentioned above. But also gel properties themselves could be enhanced drastically. The critical gelation concentration (CGC) could be reduced by at least 23% and up to 82%, gelation kinetics were up to 99% faster and thermal stability increased up to 33% (at same gelation concentration). Last but not least rheological measurements of gels in MeCN and toluene revealed enhanced mechanical stability (with respect to the absolute value of G' , the $\tan \delta$ and the maximum % strain at break) of those gels prepared with ultrasound-treatment in comparison to the classical heating-cooling cycle. Due to this demonstrative superiority of ultrasound-formed gels, this gelation method was used for all further experiments.

In order to study the driving forces for molecular aggregation, temperature-dependent $^1\text{H-NMR}$ spectra of a gel in MeCN- d_3 were recorded in a range of 35 to 65 °C in steps of 5 °C. Three different regions were selected to show which protons are involved in the gelation process. First an N-H signal in the field of 8.08 to 8.00 ppm was picked (**Fig. 29A**), that revealed a small downfield shift of the signal by around 0.027 ppm. Another downfield shift could be observed for the phenyl protons (**Fig. 29B**). In this case the shift was much smaller, around 0.008 ppm. The biggest shift was observed for the major C-H signal of the long carbon chain with 0.062 ppm (**Fig. 29C**). According to these results H-bonding, π - π -stacking, as well as van-der-Waals interactions are responsible for the gelation process, although their impact seems to be of varying importance.

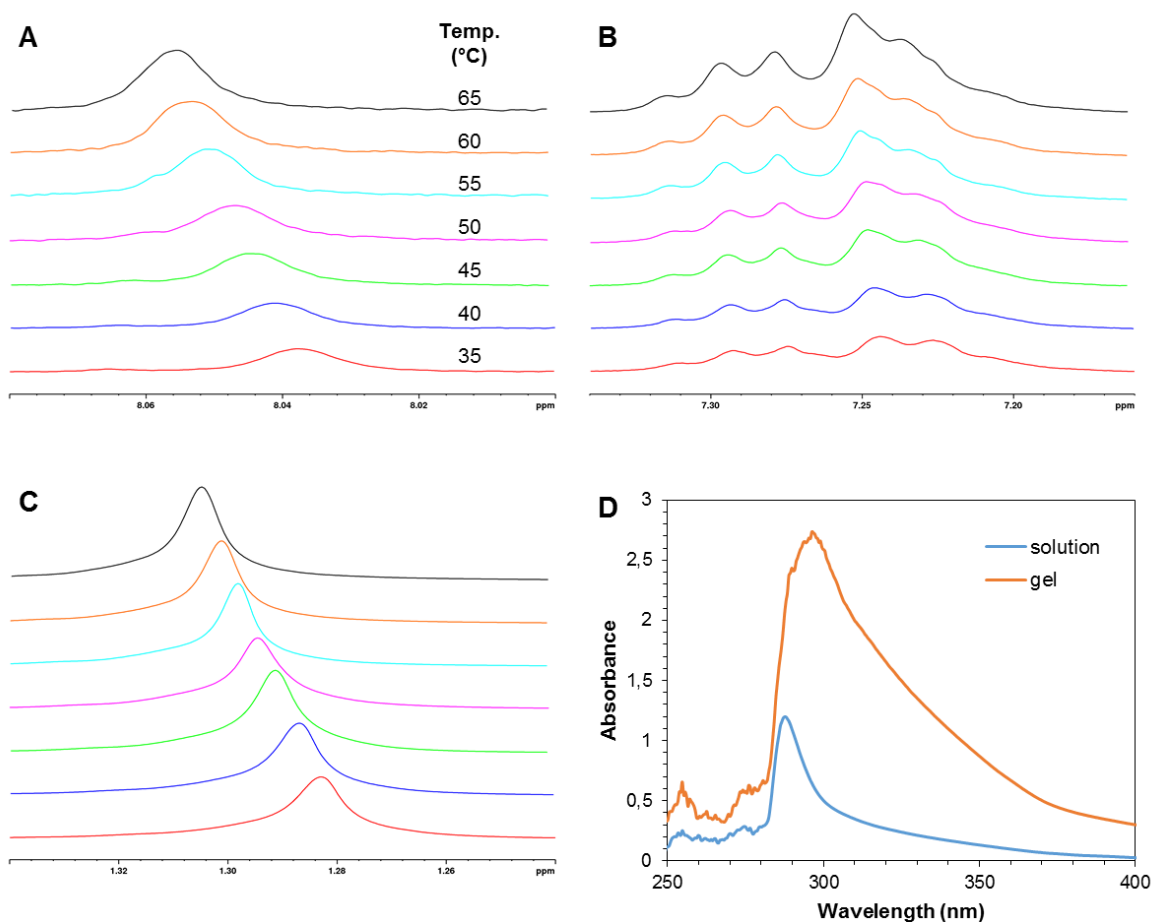


Fig. 29 A-C) Shift of proton signals in $^1\text{H-NMR}$ spectra with rising temperature. **A)** N-H (8.08 - 8.00 ppm), **B)** phenyl C-H (7.34 - 7.16 ppm and **C)** C-H from carbon chain (1.34 - 1.24 ppm). **D)** UV-Vis of FAG in MeCN as gel at CGC and in solution.

In good agreement with the results derived from temperature-dependent $^1\text{H-NMR}$, UV-Vis analysis showed a shift of the absorption maximum from 288 nm in solution to 296 nm in the gel phase (**Fig. 29D**), suggesting that the aggregation mode of the FAG in solution differs from that in the gel phase.

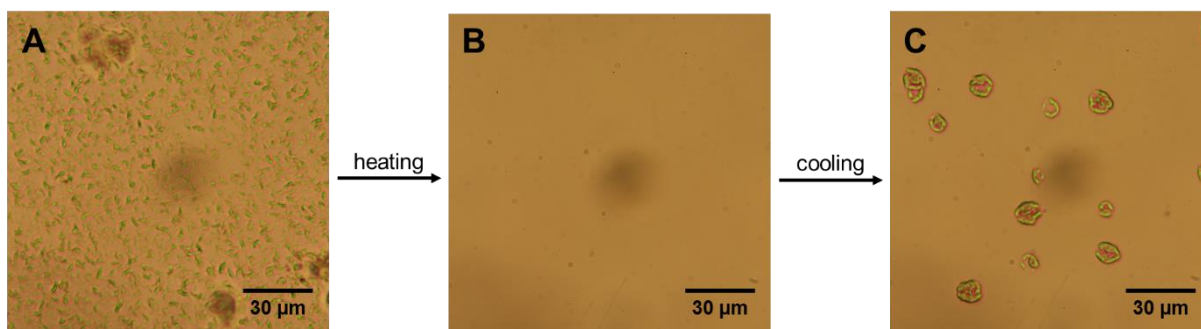


Fig. 30 Optical microscope images at 500 x magnification of **A)** an organogel in MeCN at CGC, **B)** gel-sol transition upon heating and **C)** a few seconds of cooling.

Additionally, thermo-reversible features of gels in MeCN were shown under optical microscopes in **Fig. 30** at 500 x magnification and **Fig. 31A+B** at 43.75 x magnification and under polarized light. Also the anisotropic behaviour was demonstrated under polarized light (**Fig. 31C+D**). In **Fig. 31A+B** the ability of organogels for turning on/off their birefringence in a temperature-dependent manner is depicted. The ability to control the refractive index of soft materials constitutes an important property for applications in optical devices.

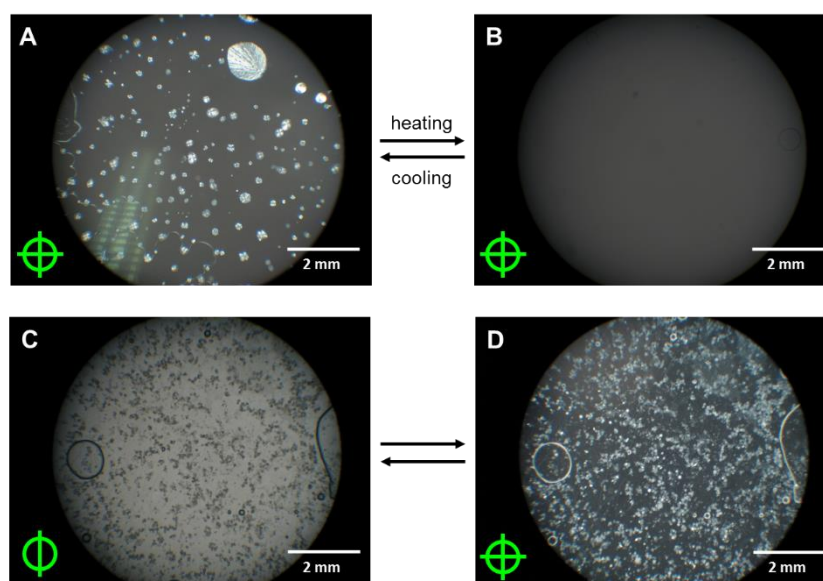


Fig. 31 Polarized light microscope images (at 43.75 x magnification) of **A, C, D**) organogel in MeCN at CGC and **B**) solution upon gel-to-sol thermal transition. **A, B, D**) with and **C**) without crossed polarizers.

Powder X-ray diffractograms (PXRD) of FAG as powder (as derived from synthesis) and xerogels derived from a MeCN organogel and a hydrogel were recorded. Interestingly the original powder showed crystalline behavior as seen in the relatively sharp reflexes from $2\theta = 21 - 42$ (see **Fig. 32**). The reflexes at $2\theta = 3$ and 6 imply a short range order which could derive from early self-assembly processes during synthesis/isolation. Xerogel from hydrogel did not show any crystalline behaviour anymore. However signals at $2\theta = 3$ and 6 were still present which implies a persistence of the short range order (sharp reflexes derive from NaCl, a left-over of the hydrogelation process). Surprisingly these reflexes were not observable in the xerogel which was derived from MeCN organogels indicating that crystal growth is more likely in hydrogels, rather than in organogels.

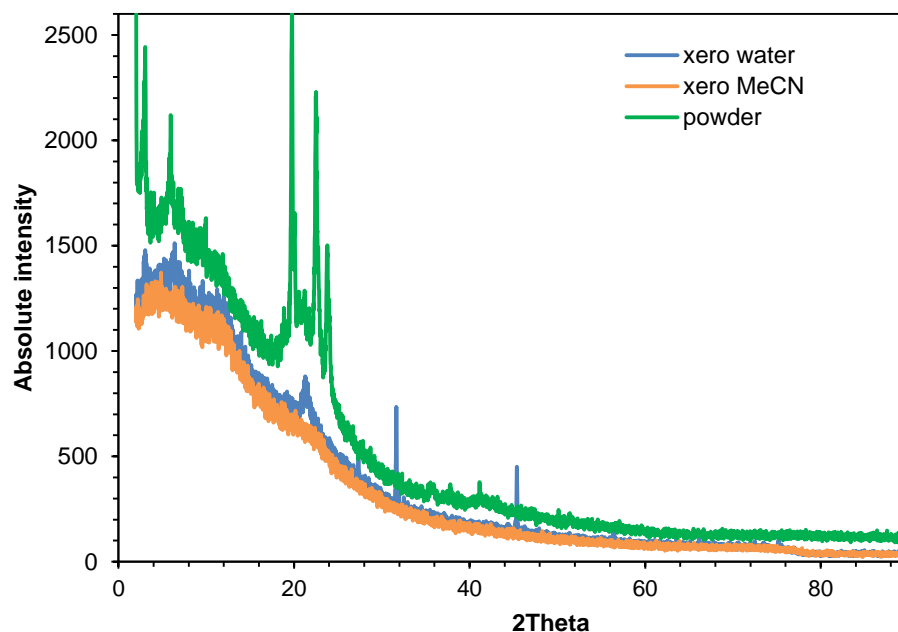


Fig. 32 PXRD of FAG as powder and xerogels derived from MeCN organogel and hydrogel. For a more detailed vision see annex.

Lattice spacing d was calculated according to Bragg's equation

$$d = \frac{n\lambda}{2 \sin\theta}$$

where n is the diffraction order and λ the wavelength of the $\text{CuK}\alpha 1$ radiator (1.54 Å).

Table 1 Calculation of lattice spacing in FAG powder and xerogel derived from a FAG hydrogel according to Bragg's equation.

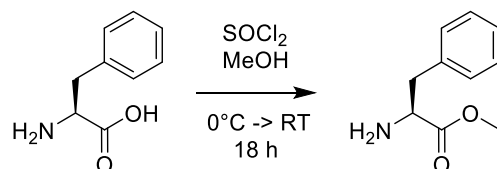
powder			xerogel water		
2θ (°)	n	d (Å)	2θ (°)	n	d (Å)
3.07	1	28.83	3.05	1	28.97
5.95	2	29.71	6.40	2	27.64
19.8	1	4.44	21.3	1	4.16
22.5	1	3.95			
23.8	1	3.74			

Unfortunately, an MTT assay of FAG revealed a toxic behaviour of both the gelator itself as well as FAG derived hydrogels, which led to an exclusion of biomedical applications.

3.3 Experimental Part

3.3.1 Synthesis

Synthesis of (S)-methyl L-phenylalaninate

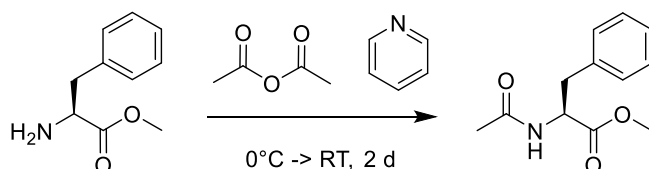


(L)-Phenylalanine (5.00 g, 42.0 mmol) was added carefully in portions to a cooled solution of thionyl chloride (15.30 mL, 210.0 mmol) in MeOH (50 mL) at 0 °C. After stirring for 1 h, the solution was allowed to warm to RT and stirred for additional 18 h. The solvent was removed under reduced pressure and the resulting residue was co-evaporated with MeOH (5 x 30 mL) to give the title compound as white solid without need of purification.

Yield: 6.45 g (99%); C₁₀H₁₃NO₂; (179.22)

¹H-NMR (300 MHz, MeOD): δ (ppm) = 7.42 – 7.32 (m, 3H), 7.29 – 7.24 (m, 2H), 4.33 (dd, 1H), 3.81 (s, 3H), 3.29 – 3.13 (m, 2H).

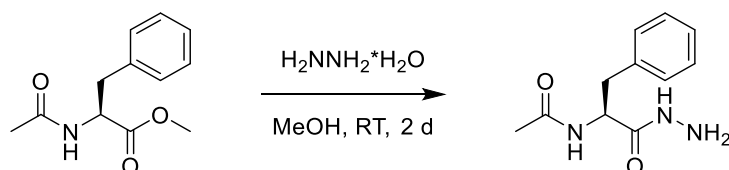
Synthesis of methyl acetyl-L-phenylalaninate



(S)-methyl L-phenylalaninate (5.00 g, 27.9 mmol) was added in one portion to a cooled solution of acetic anhydride (11.0 mL, 116.4 mmol) in pyridine (9.5 mL, 117.7 mmol) at 0 °C. After stirring for 0.5 h, the solution was allowed to warm to RT and stirred for 2 days. After addition of ice-water (50 mL), the aqueous mixture was extracted with DCM (4 x 25 mL) and the combined organic layers were washed with sat. NH₄Cl (3 x 25 mL), 0.1 M HCl (3 x 25 mL) and water (3 x 25 mL). The organic layer was dried over Na₂SO₄, filtered and the solvent removed under reduced pressure to give the title compound as light brown solid.

Yield: 4.62 g (75%); C₁₂H₁₅NO₃; (221.26)

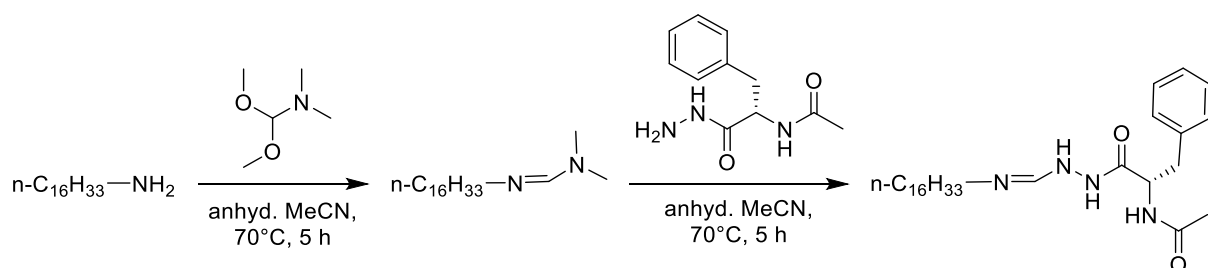
¹H-NMR (300 MHz, CDCl₃): δ (ppm) = 7.31 – 7.20 (m, 3H), 7.11 – 7.05 (m, 2H), 5.98 (s, 1H), 4.88 (dt, 1H), 3.71 (s, 3H), 3.18 – 3.03 (m, 2H), 1.97 (s, 3H).

Synthesis of (S)-N-(1-hydrazineyl-1-oxo-3-phenylpropan-2-yl)acetamide

To a stirred solution of methyl acetyl-L-phenylalaninate (4.14 g, 18.8 mmol) in MeOH (125 mL) was added carefully hydrazine*H₂O (2.0 mL, 41.2 mmol) and the mixture was stirred at RT for 2 days. The solvent was removed under reduced pressure to give the title compound as white solid.

Yield: 4.06 g (97%); C₁₁H₁₅N₃O₂ (221.26)

¹H-NMR (300 MHz, MeOD): δ (ppm) = 7.31 – 7.16 (m, 5H), 4.55 (dd, 1H), 3.08 (dd, 1H), 2.87 (dd, 1H), 1.89 (s, 3H).

Synthesis of FAG

A solution of hexadecylamine (1.00 g, 4.1 mmol) and 1,1-dimethoxy-*N,N*-dimethylmethanamine (0.30 mL, 6.2 mmol) was stirred in dry MeCN (100 mL) under N₂-atmosphere for 5 h at 70 °C until TLC-analysis showed full consumption of the amine starting material. The solvent was removed under reduced pressure using a rotary evaporator and trace amounts of the acetal were removed by co-evaporation with toluene (3 x 20 mL). The resulting residue was redissolved in dry MeCN (60 mL) under a N₂-atmosphere. At 70 °C (S)-*N*-(1-hydrazineyl-1-oxo-3-phenylpropan-2-yl)acetamide (0.92 g, 4.1 mmol) was added in one portion. After stirring for 18 h at 70 °C the reaction solution was allowed to cool down to RT resulting in the formation of a precipitate, which was filtered off, washed with MeCN (3 x 20 mL) and recrystallized from acetone twice to yield the desired product as a white solid.

Yield: 0.91 g (37%); C₂₈H₄₈N₄O₂ (472.72)

¹H-NMR (300 MHz, MeOD): δ (ppm) = 7.44 – 6.90 (m, 6H), 4.54 (s, 1H), 3.21 – 3.05 (m, 3H), 3.02 – 2.80 (m, 1H), 1.91 (s, 3H), 1.88 (s, 1H), 1.51 (s, 2H), 1.29 (s, 28H), 0.90 (t, 3H).

3.3.2 Gel-formation

Preparation of organogels via a heating-cooling cycle

A weighted amount of the formamidine-based gelator and an appropriate organic solvent (0.5 mL) were placed into a screw-capped glass vial (4 cm length \pm 1 cm diameter) and gently heated with a heat gun until the solid material was completely dissolved. In some cases ultrasonication of the samples before heating could facilitate the dissolution of the compound. The resulting isotropic solution was then spontaneously cooled down to RT. No control over temperature rate during the heating-cooling process was applied. The material was preliminary classified as “gel” if it did not exhibit gravitational flow upon turning the vial upside-down at RT. The state was further confirmed by rheological measurements.

Preparation of organogels via ultrasound treatment

An isotropic solution consisting of the formamidine compound and an appropriate solvent obtained by gentle heating was treated with ultrasound while still be warm using a VWR™ ultrasonic cleaner (USC200TH, 45 kHz, 120 Watt) keeping a constant temperature of 23 ± 2 °C. During sonication stable gels were formed in situ during time intervals varying from a few seconds to several minutes, which were defined as the time necessary to promote gelation. Sole ultrasound treatment without applying heat did not facilitate gelation due to simple solubility issues of formamidine based gelator in most organic solvents.

Preparation of hydrogels

Hydrogelation of the formamidine compound could be achieved by building a pH gradient in aqueous solution. The procedure of formation of hydrogels at optimized conditions is given as following: A certain amount of the formamidine (35 mg) is placed in a screw-capped glass vial when water (0.4 mL) was added. A minimum amount of 1 M HCl (0.05 mL) is added to the mixture in order to dissolve the compound by gentle heating. Thereto 1 M NaOH is added in portions of 0.01 mL (in total 0.04 mL) during treatment with ultrasound until a translucent gel-material at a final concentration of 71 ± 8 g L⁻¹ was formed in situ.

3.3.3 Temperature controlled NMR

A gel of formamidine in MeCN-d₃ was prepared at CGC following ultrasonication-protocol. After chilling overnight at room temperature, ¹H-NMR were recorded on a 400 MHz Bruker Avance spectrometer from 35 to 65 °C in steps of 5 °C. Before each measurement the gel was tempered for 20 min.

3.3.4 UV-Vis

UV-Vis spectra of a formamidine gel in xylene at CGC and a solution in xylene at around 4 g L⁻¹ was recorded on an Ocean Optics, Flame Spectrometer with a DH-2000-BAL light source.

3.3.5 Polarized Light

The birefringence of the gels under polarized light was monitored using a Wild Makroskop M420 optical microscope equipped with a Canon Power shot A640 digital camera.

3.3.6 PXRD

Powder X-ray diffraction (PXRD) patterns were collected on a STOE STADI P powder diffractometer (Start Fragment Transmission mode, flat samples, Dectris MYTHEN 1k microstrip solid-state detector) with CuK α 1 radiation operated at 40 kV and 40 mA. Conditions: Start Fragment 0.0151°, time 60 s per step, 2 theta range 2–90°.

3.4 Conclusions

In conclusion the effective gelation of various organic solvents by an amphiphilic formamidine-based gelator molecule was described. Interestingly ultrasound treatment of isotropic solutions resulted in an enhancement of typical physical properties of gel materials in all tested cases. For example, CGC could be reduced by at least 23% and up to 82%, gelation kinetics were up to 99% faster and thermal stability increased up to 33%. Additionally an enhancement of mechanical stability of those gels prepared with ultrasound treatment in comparison to the classical heating-cooling cycle was shown by rheological measurements of gels in MeCN and toluene. Also hydrogels could effectively be prepared by building a pH-gradient in aqueous media from acidic to more basic conditions. Temperature dependent ¹H-NMR spectra depicted that H-bonding, π - π -stacking, as well as van-der-Waals interactions are responsible for the gelation process. Also in UV-Vis spectra a shift of absorption

maximum revealed a different aggregation of FAG in solution than in the gel-phase. Polarized light microscopy revealed the ability of a FAG derived gel in MeCN to turn on/off the birefringence in a temperature-dependent manner which is an important property for potential applications in optical devices. Interestingly PXRD showed crystallinity of FAG powder but only short range order in xerogels derived from a hydrogel and signals in xerogels derived from a MeCN organogel, indicating that crystal growth is more likely in hydrogels, rather than in organogels. Last but not least an MTT assay of FAG was performed revealing a toxic behaviour of both the gelator itself as well as FAG derived hydrogels, which leads to an exclusion of biomedical applications.

C Ionenenes

1. Antimicrobial and Hemolytic Studies of a Series of Polycations Bearing Quaternary Ammonium Moieties: Structural and Topological Effects³

1.1 Introduction

Around one fourth of the global deaths annually are caused by infections.^{120–122} The unjustifiable use of antibiotics and disinfectants has caused a huge rise in the occurrence of resistant strains.^{123–126} Only in USA over 2 million people are infected with these strains and more than 23000 die yearly for this reason.¹²⁷ In Europe more than 150000 patients are affected by methicillin-resistant *Staphylococcus aureus* (MRSA) infections, which leads to costs of 380 million euros per year.^{128,129} Hence, the demand for new antibiotics to combat resistant strains is currently very high. Low molecular weight compounds like antimicrobial peptides have been found to be effective against a wide spectrum of bacteria.^{130,131} However, they often comprise disadvantages such as the need for a multistep synthesis or biocidal diffusion, which can cause toxicity and may lead to a fast resistance.^{132,133} An alternative and versatile approach is the use of antimicrobial active polymers, whose physical, chemical and biological activities can be fine-tuned by simple modifications of the corresponding monomers. Among different antimicrobial polymers^{134–137}, ionenes are synthetic polycations with quaternary ammonium functions, which are distributed along the backbone.^{138,139} In general, the synthesis of ionenes can be performed by a) self-polyaddition of aminoalkyl halides, b) Menshutkin reaction between bis-tertiary amines and activated dihalide compounds or c) via cationic functionalization of precursor polymers.^{140,141} In 1935, Domagk reported for the first time the antibiotic activity of quaternary ammonium salts (QAS).¹⁴² Since then different QAS have been extensively investigated as disinfectants.^{143–147} Recently, Xiao and co-workers have reported a comprehensive overview of the synthetic methods and antimicrobial action of polymers with quaternary ammonium/phosphonium salts.¹⁴⁸ The long review demonstrates the high relevance of such materials for the search for new antimicrobial compounds. Related to the type of ionenes that we describe in this paper, Mathias and coworkers reported bis-quaternary ammonium carboxylate

³ Reproduced from Ref. 185 with permission from MDPI. Synthesis of ionenes was carried out by J. Mayr and J. Bachl. All other experiments were performed by J. Mayr.

polymers based on 1,4-diazabicyclo-[2.2.2]-octane (DABCO) with good activities against *Staphylococcus aureus* and *Escherichia coli*.¹⁴⁹ In addition, Melkonian and her group functionalized cotton to give an antimicrobial material where DABCO was also used to introduce the quaternary ammonium function by attaching different aliphatic chains.¹⁵⁰ Most of these polymers were active against a range of Gram-negative and Gram-positive bacteria.

Herein, we report the antimicrobial properties of different ionene polymers based on *N,N'*-(*p*-phenylene)dibenzamide and α,ω -tertiary diamines, whose self-assembly properties have been previously described by us¹⁵¹ and others¹⁵². The antimicrobial activity against the Gram-negative bacterium *Escherichia coli* has been determined for a library of 13 ionenes with different topologies and diamine linkers (Fig. 33).

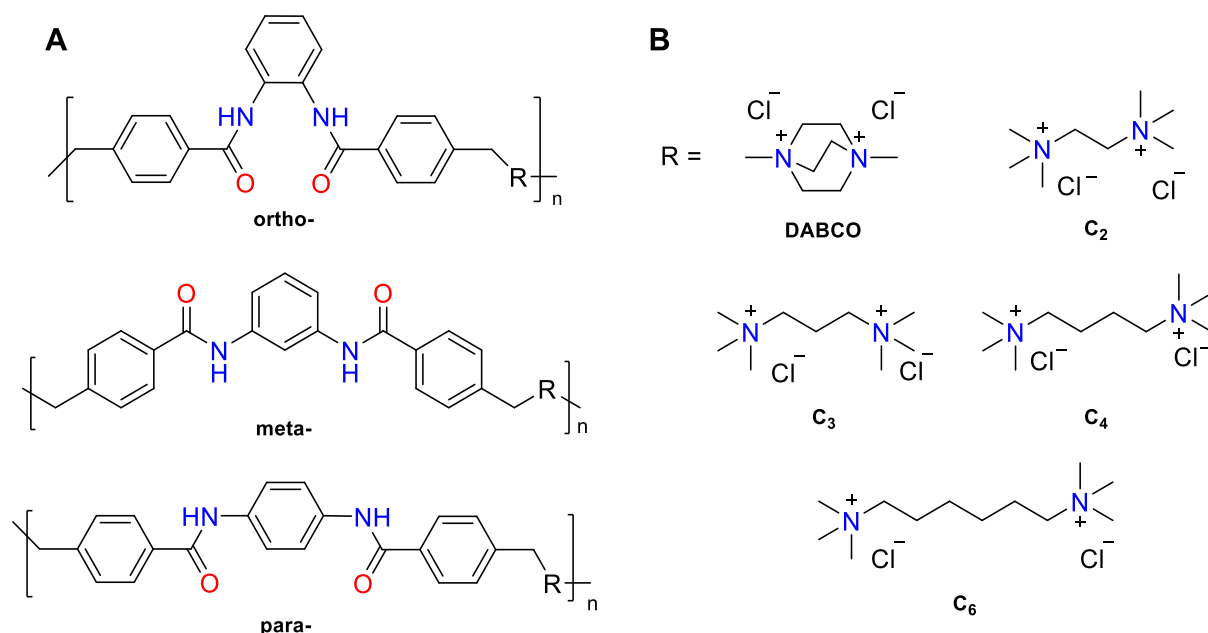


Fig. 33 A) General structures of ionene polymers used in this study and B) charged diammonium moieties with different structures and chain length. The combinations investigated in this work were *o*-DABCO, *o*-C₂, *o*-C₃, *o*-C₆, *m*-DABCO, *m*-C₂, *m*-C₃, *m*-C₄, *m*-C₆, *p*-DABCO, *p*-C₂, *p*-C₃ and *p*-C₄. Note: *o*- = ortho-; *m*- = meta-; *p*- = para-.

1.2 Results and Discussion

Ionene polymers were synthesized via a two steps process as previously reported.^{151–153} Briefly, first step involves the amidation of *o*-, *m*- and *p*-phenylenediamine with 4-(chloromethyl)benzoyl chloride in the presence of Et₃N in DCM to afford the corresponding bis-benzamides in good yields (75–98%) upon recrystallization. Subsequent copolymerization of the obtained bis-benzamides with

the desired α,ω -diamine linker under equimolar conditions in DMF at 80 °C afforded the desired pure polymers (**Fig. 33**) within 2–6 days in modest yields (43–80%) after a simple filtration, washing and drying protocol^{151–153} In order to achieve adequate solubility and mobility of the polymers for GPC analysis, it was necessary to carry out counteranion exchange of chloride by bis(trifluoromethanesulfonyl)amide (TFSA) anions using LiTFSA in hot water as previously described.^{151–153} As expected for many step-growth polymers, these ionenes·TFSA are generally characterized by low degree of polymerizations ($n = 7–34$) and high dispersity values ($\mathcal{D} = 2.1–6.5$).^{151–153}

The resulting ionenes were tested for antimicrobial activity and the minimum inhibitory concentration (MIC) was investigated in a range of 0.125 to 2 mmol L⁻¹, respectively (**Fig. 34**). The lowest MIC was found for **m-C6** and **p-C3** with values of 0.2 mmol L⁻¹ followed by **m-C3** and **p-C2** with MICs of 0.5 mmol L⁻¹ and **p-C4** of 1.2 mmol L⁻¹. Interestingly, compounds containing DABCO instead of linear linkers showed quite high MICs (i.e., 1.4, 1.6 and 1.8 mmol L⁻¹, respectively), similarly to **o-C6** and **m-C4** that revealed MICs of 2 mmol L⁻¹. Surprisingly, ionenes **o-C2** and **m-C2** did not show any antimicrobial activity within the measured range. Overall, these results suggested a synergistic role, at least to some extent, between the polymer topology and the nature of the tertiary diamine linker.

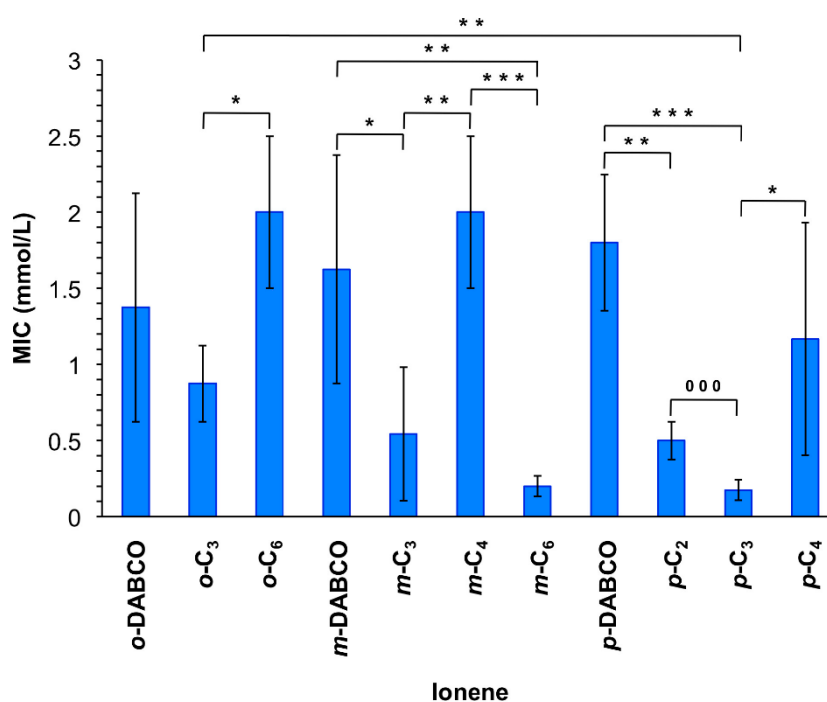


Fig. 34 Minimum inhibitory concentrations (MIC) of ionene suspensions for inhibition of bacterial growth. Each value represents the mean of MIC from at least three replicates with standard deviation (SD) and analysis of variances (ANOVA) with (*) Bonferroni comparison or (0) unpaired t-test. * Indicates $p < 0.05$; ** indicates $p < 0.01$; ***/000 indicates $p < 0.001$.

Despite the difficulty to draw correlations between the structural moieties and efficiency in bacterial toxicity, **DABCO**-containing compounds always showed comparably high MIC values (1.4–1.8 mmol L⁻¹), only exceeded by **o-C₆** and **m-C₄** within the experimental error. Interestingly, **o**- and **m**-ionenes bearing the **C₂**-linker did not show any antimicrobial activity (not depicted). This phenomenon could be explained by a judicious degree of flexibility in the polymer chain. Moreover, **o**-substituted polymers also revealed comparably higher MICs (0.8–2.0 mmol L⁻¹). The high tendency of these polymers to form coils, which was described in a previous publication¹⁵¹, could hinder the efficient interaction of these polymers with the cell membrane. Ionenes with the **C₃**-linker revealed comparably low or the lowest MICs (0.9, 0.5 and 0.2 mmol L⁻¹ for the corresponding **o**-, **m**-, and **p**-topomers, respectively). Apparently, a medium sized chain length (**C₃**) of the linker in these polymers has the optimal effect on the antimicrobial activity. In contrast, in the case of **m**-topomers, the ionene with the longest chain showed the strongest activity (0.2 mmol L⁻¹). It seems evident that a proper balance between flexibility and topological features of these polymers is needed for optimal effects. In comparison to other antimicrobial polymers, our compounds lie in a good middle field. As representative examples, Tew and co-workers described quaternary pyridinium functionalized polynorbornenes with MICs ranging from 4–200 µg mL⁻¹ (7.2×10^{-3} – 0.40 mmol L⁻¹)¹²²; Lecomte's group described a poly(oxepan-2-one) with quaternary ammonium with a very high MIC of 12.6 g L⁻¹ (23 mmol L⁻¹)¹³⁴ and Mathias and coworkers reported bis-quaternary ammonium methacrylate polymers with MICs ranging from 62.5 to 250 µg mL⁻¹ (0.095 – 0.40 mmol L⁻¹)¹⁴⁹.

Since antimicrobial agents should be ideally not harmful to mammalian cells, the hemolytic activity of these polymers was also tested at similar concentration as for the antimicrobial assay. Thus, the polymer solutions were measured at 2 mmol L⁻¹, which was the limit for antimicrobial studies, and 1 mmol L⁻¹ for comparison (**Fig. 35**). The results showed that these ionenes are not or only slightly hemolytic, judged by very low levels of released hemoglobin in most cases. However, release of hemoglobin increased with increasing polymer concentration. In general, **DABCO**-containing polymers revealed the highest hemoglobin levels, being **m-DABCO** the ionene of this class with the lowest values (15% and 8% for 2 mmol L⁻¹ and 1 mmol L⁻¹, respectively). About 10% reduction of hemoglobin release was observed for **m-DABCO** compared to **o-DABCO** and **p-DABCO** at both concentrations.

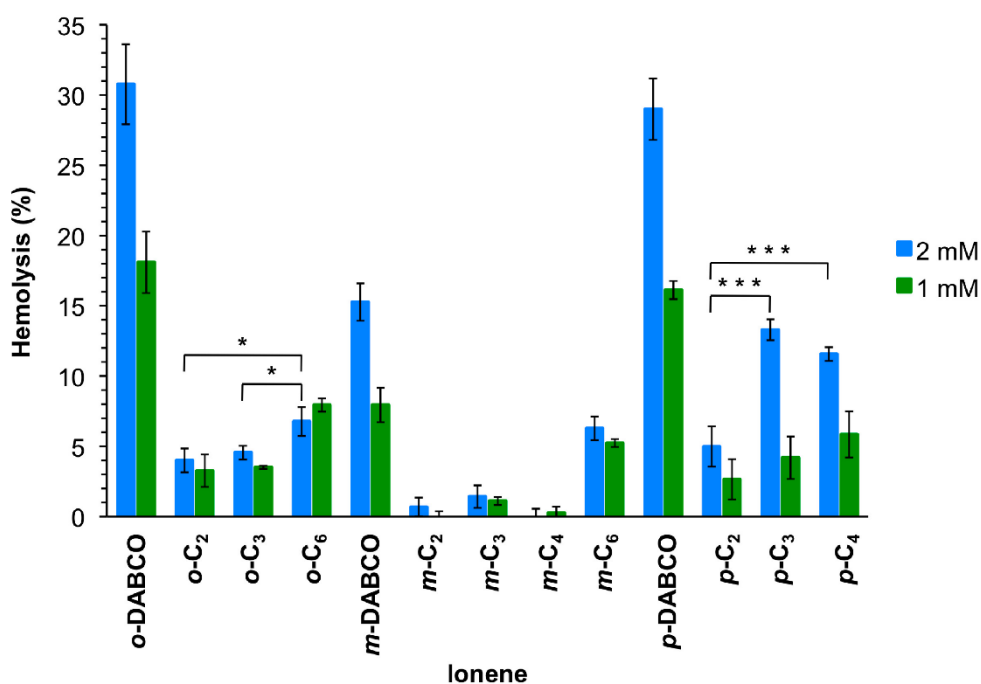


Fig. 35 Mean values of hemolysis from at least three replicates with SD and ANOVA with Bonferroni comparison. For the sake of clarity, only comparisons within one topomeric set (ortho-, meta-, para-) at 2 mmol L⁻¹ are shown in this plot. All DABCO-containing compounds showed higher hemolysis (***, omitted for clarity) in comparison to their set members. * Indicates $p < 0.05$; *** indicates $p < 0.001$.

The remaining polymers showed hemoglobin release ranging between 13% for **p-C₃** 2 mmol L⁻¹ and 1% for **m-C₃** at both concentrations. In general, the length of the linear linker within the same series of topomers showed an irregular effect on the hemolytic properties. Thus, the lowest hemolysis was observed for **p**- and **o**-topomers with a **C₂**-linker (5% and 4%, respectively) at 2 mmol L⁻¹, whereas the same the **C₄**-linker provided the lowest hemoglobin release for the **m**-series (0.25%). On the other hand, the topology of the polymers seemed to be a more important factor at higher concentration (2 mmol L⁻¹) within the series bearing the same linker, albeit again without a regular trend. Thus, **m**-topomers displayed lower hemoglobin release than the corresponding **o**- and **p**-topomers with a **C₂**-linker (4% vs 1% and 5%, respectively). The same was found for **C₃**-, **C₄**- and **DABCO**-linkers, whereas no significant differences were found for the series based on **C₆**-linkers. With respect to the concentration effect, the most pronounced differences between the two concentrations were found for the **p**-series. For comparison, hemolysis obtained with other polycations such as poly(diallyl-dimethyl-ammonium chloride) and poly(vinyl pyridinium bromide) were found to be 2.6% and 9.4%, respectively,¹⁵⁴ within the same range of concentration as we used for this investigation.

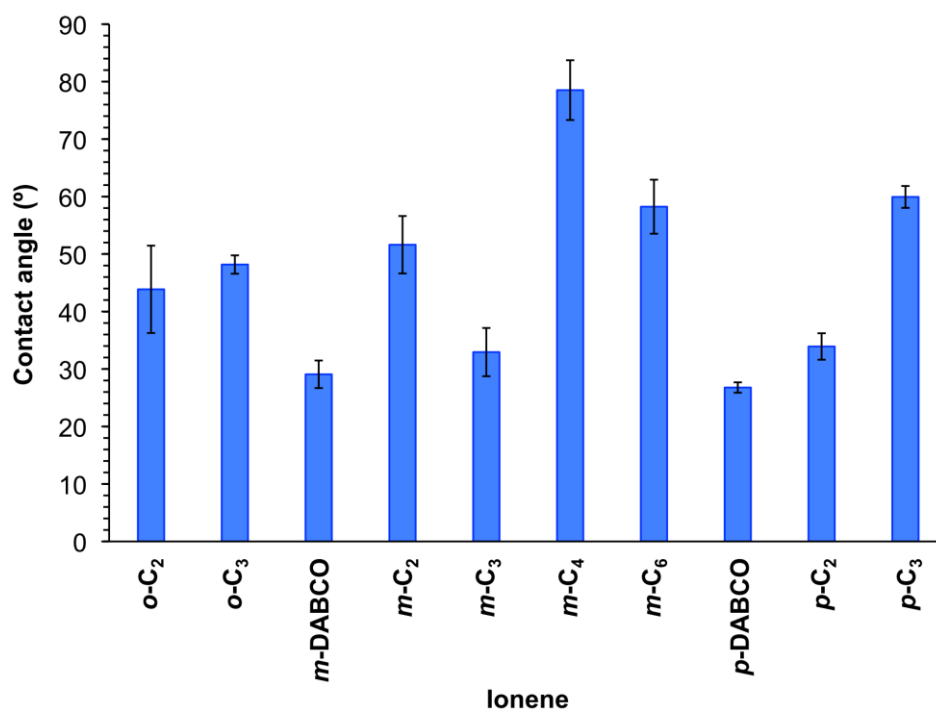


Fig. 36 Static contact angle for films prepared with the different ionenes as described in the Experimental Section. Reliable measurements were not obtained for samples prepared with **o-DABCO** (too hydrophilic), **p-C₄** (too hydrophilic) and **o-C₆** (inhomogeneous film).

In contrast to other polycations,¹⁵⁵ contact angle measurements of films prepared with the different ionenes revealed no obvious correlations between the antimicrobial or hemolytic activity and the surface wettability of the polymers (**Fig. 36**). Although **DABCO**-containing polymers displayed in general higher MIC, hemolytic activity and higher hydrophilic character (i.e., contact angle < 30°) compared to the ionenes bearing linear linkers, other significant correlations among the different linkers and topological features of the polymers were not found.

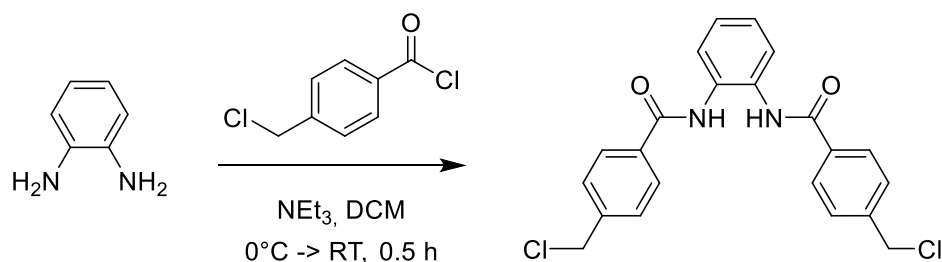
1.3 Experimental Section

1.3.1 Materials

Starting materials for polymer synthesis were purchased from Sigma Aldrich or TCI. TGYE-medium ingredients were from Becton, Dickinson and Company. Müller-Hinton-Broth was purchased from Merck. Hemolysis was measured on a sunrise tecan microplate reader.

1.3.2 Synthesis of Ionenes

Synthesis of *N,N'*-(1,2-phenylene)bis(4-(chloromethyl)benzamide) *ortho*-monomer

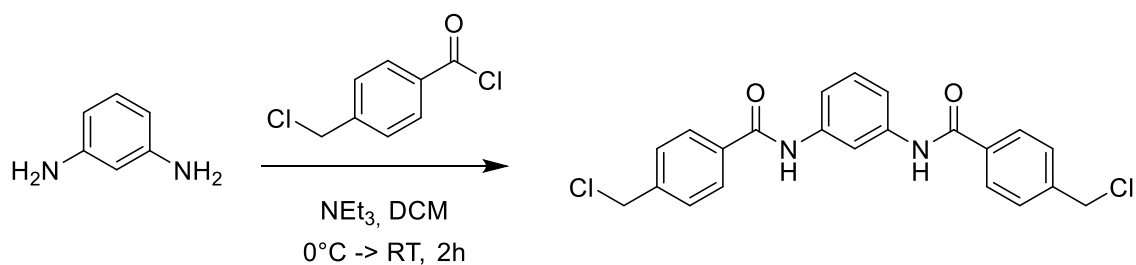


To a stirred solution of 1,2-diaminobenzene (1.62 g, 15.0 mmol) and Et_3N (5.23 mL, 37.5 mmol) in DCM (70 mL) at 0°C a solution of 4-(chloromethyl) benzoyl chloride (5.67 g, 30.0 mmol) in DCM (40 mL) was added dropwise via a pressure-compensated addition funnel. The reaction mixture was allowed to warm to RT and stirred for 0.5 h, until TLC analysis showed full conversion of the starting materials. The solvent was removed in vacuum and the resulting yellowish solid was used without further purification

Yield: 5.95 g (96%); $R_f = 0.9$ (DCM: MeOH 10:1); $\text{C}_{22}\text{H}_{18}\text{Cl}_2\text{N}_2\text{O}_2$ (413.30)

$^1\text{H NMR}$ (300 MHz, DMSO) δ (ppm) = 10.10 (s, 2H), 7.98 (d, 4H), 7.68 (d, 2H), 7.62 (d, 4H), 7.32 (d, 2H), 4.83 (s, 4H).

Synthesis of *N,N'*-(1,3-phenylene)bis(4-(chloromethyl)benzamide) *meta*-monomer

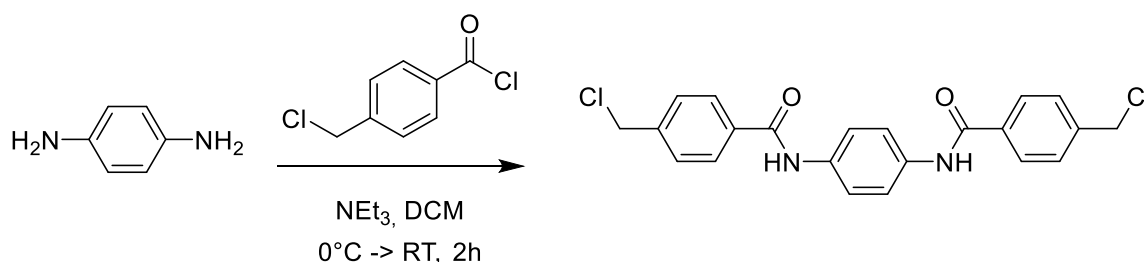


Synthesis was performed as described for *ortho*-monomer. However solvent was not evaporated but mixture was stored overnight at 4°C and resulting precipitate was filtered off, washed with ice cold DCM and dried to afford the product as white solid.

Yield: 5.44 g (88%); $R_f = 0.8$ (DCM: MeOH 10:1); $\text{C}_{22}\text{H}_{18}\text{Cl}_2\text{N}_2\text{O}_2$ (413.30)

$^1\text{H NMR}$ (300 MHz, DMSO) δ (ppm) = 10.36 (s, 2H), 8.38 (t, 1H), 7.98 (d, 4H), 7.62 (d, 4H), 7.52 (d, 2H), 7.42 (m, 1H), 4.88 (s, 4H).

Synthesis of *N,N'*-(1,4-phenylene)bis(4-(chloromethyl)benzamide) *para*-monomer

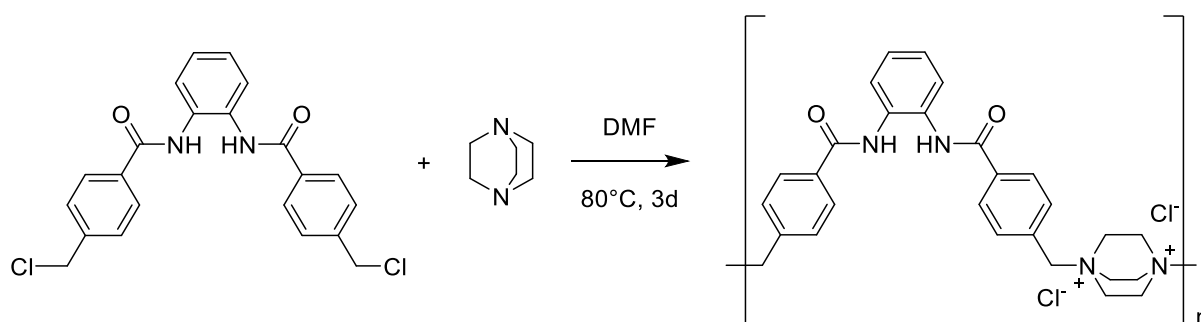


Synthesis was performed as described for *ortho*-monomer. The resulting precipitate was filtered off, washed with ice cold DCM and dried to afford the product was white solid.

Yield: 6.13 g (99%); $R_f = 0.7$ (DCM: MeOH 10:1); $\text{C}_{22}\text{H}_{18}\text{Cl}_2\text{N}_2\text{O}_2$ (413.30)

$^1\text{H NMR}$ (300 MHz, DMSO) δ (ppm) = 10.28 (s, 2H), 7.97 (d, 4H), 7.76 (s, 4H), 7.59 (d, 4H), 4.85 (s, 4H).

Representative preparation of polymers: *o*-DABCO



To a stirred solution of *ortho*-monomer (0.82 g, 2.00 mmol) in DMF (15 mL) at 80 °C 1,4-diazabicyclo[2.2.2]octane (DABCO) (0.22 g, 2.00 mmol) was added in one portion. The reaction mixture was stirred at 80 °C for 2 days, until TLC analysis showed full conversion of the starting materials. The mixture was cooled down to RT, stored at 4 °C overnight, filtered, washed subsequently with DMF, MeCN and DCM, and the final product was dried in vacuo.

General reaction duration: 2-6 days.

General yields: 70-95%

$^1\text{H NMR}$ see annex.

1.3.3 Antimicrobial assay

TGYE-medium (30 mL) was inoculated with one colony of *Escherichia coli*, incubated at 37 °C while orbital shaking at 150 rpm overnight. From this suspension a 1:100 dilution was prepared in Müller-Hinton-Broth (MHB) and 50 µL of this were added to 1 mL of solutions/dispersions of the polymers at different concentrations in MHB (i.e., 2, 1, 0.5 0.25 and 0.125 mM from serial dilution starting from 4 mM polymer in sodium chloride 9 g/L solution. The bacteria were incubated at 37 °C for 18 h. After this time 50 µL of sample were spread on TGYE agar plates, which were incubated at 37 °C for 22 h and bacterial growth was optically evaluated. MIC was determined as the lowest concentration of polymers at which no visible growth was observed.

1.3.4 Hemolysis testing

Blood from a healthy human volunteer was drawn into K2-EDTA coated vacutainer tubes and stored at 4 °C for 1 h. The blood was centrifuged at 1000 g for 10 min. The erythrocytes were washed with 2 mL PBS buffer and centrifuged again (3 times). The erythrocytes were resuspended in PBS buffer to give a 5% (v/v) suspension. Solutions/dispersions of polymers in sodium chloride 9 g/L solution (60 µL), erythrocyte suspensions (60 µL) and PBS buffer (60 µL) were mixed. As positive hemolysis control Triton-X100 1% (v/v) (60 µL) and as negative control PBS buffer (60 µL) was used. Samples were incubated at 37 °C and orbital shaking at 150 rpm for 2 h followed by centrifugation at 1000 g for 5 min. Sample solution (60 µL) and PBS buffer (60 µL) were filled into a 96 well plate and absorbance was measured at 540 nm. Hemolysis was calculated by following equation.

$$hemolysis = \left(\frac{S_{PBS} - S_{Poly}}{S_{TX} - S_{Poly}} \right) \cdot 100\%$$

where S_{PBS} is the value corresponding to the negative control, S_{TX} is the value corresponding to the positive control and S_{poly} is the value corresponding to the polymer sample.

1.3.5 Contact angle measurements

Polymer solutions/suspensions were prepared at a concentration of 50 g/L in DMSO/water (1:1, v/v). Menzel cover slips (18 × 18 mm) were washed with acetone and ethanol before usage. Samples (50 µL) were spread on the glass plates to cover as much as possible of the surface. The plates were left on air for 3 days to dry. The measurements were performed with a Dataphysics Contact Angle System OCA by dropping 3 µL on the surface and images were analyzed with the software SCA 20.

1.4 Conclusions

In summary, ionene polymers with different topologies derived from a disubstituted aromatic monomeric core and α,ω -ditertiary amines were prepared via step-growth polymerization. The polymers showed antimicrobial activity against the Gram-negative bacterium *Escherichia coli*, with MIC values affected by both the topology of the polymer and the nature of the diamine linker. In general, all ionenes containing **DABCO** (1.4–1.8 mmol L⁻¹), as well as **ortho**-compounds with other linkers (0.8 – 2.0 mmol L⁻¹), showed higher MICs. In contrast, medium chain length (**C**₃) showed best or comparably low MICs (0.9, 0.5 and 0.2 mmol L⁻¹ for **ortho**-, **meta**- and **para**-, respectively). In this assay, all **DABCO**-containing polymers showed a relatively high hemoglobin release (15–31%) whereas meta-compounds in general provided the lowest hemolysis (0–15%). In conclusion, **meta**-compounds with a flexible linker provided the best properties from both assays, and represent the most promising candidates for potential antimicrobial applications.

2. Transfection of Antisense Oligonucleotides Mediated by Cationic Vesicles Based on Non-Ionic Surfactant and Polycations Bearing Quaternary Ammonium Moieties⁴

2.1 Introduction

The last decades have been witness of a growing interest in the use of synthetic oligonucleotides for the inhibition of gene expression¹⁵⁶ as an alternative to classical small-molecule drugs to treat diseases. Examples for such oligonucleotides are antisense oligonucleotides, short interfering RNAs (siRNAs),¹⁵⁷ aptamers,¹⁵⁸ DNA/RNAzymes and antisense-induced exon-skipping.^{159,160} In order to achieve the desired inhibition some obstacles must be solved. The first problem to solve is the high sensitivity of oligonucleotides towards degradation by serum nucleases. This has been partially solved by the use of chemical modifications of the oligonucleotides at the sugar ring and/or at the phosphate back bone in order to increase their biostability.^{161,162} Cellular uptake of polyanionic oligonucleotides across the negatively charged cell membrane constitutes another problem. Although it has been shown that viral vectors are highly efficient for the transfection of plasmid DNA, there are still concerns about immunogenicity or recombination of oncogenes. Several alternatives for viral transfection methods have been developed including formulations, as a very fast and simple method.¹⁶³

In 1987, Felgner and co-workers reported the first transfection experiment. They used the cationic lipid *N*-[1-(2,3-dioleoyloxy)propyl]-*N,N,N*-trimethylammonium (DOTMA) for carrying out an efficient DNA-transfection protocol.¹⁶⁴ Since this, a huge variety of cationic lipids for formulation of oligonucleotides have been described.^{165,166} Even though they comprise promising tools for nucleic acid delivery there are several aspects to be considered. Cationic lipids have the tendency to interact with plasma proteins, which has a detrimental effect on transfection efficiency.¹⁶⁷ In addition, high positive net charge of the formulation can cause toxicity. Therefore a demand for new formulations is still present. One alternative to cationic lipids is the use of formulations based on cationic polymers and non-ionic surfactant agents to fine-tune the net charge. Cationic polymers are able to interact with DNA and RNA molecules with high efficiency and thus generate complexes with a relatively small size. This

⁴ Reproduced from Ref. 218 with permission from MDPI. J. Mayr and J. Bachl synthesized the polymers. J. Mayr and S. Grijalvo performed the rest of the experiments. R. Pons designed the SAXS experiments.

particularity makes cationic polymers as useful non-viral carriers for improving gene transfection efficiency.^{167,168} Although poly(ethylenimine) (PEI) and poly(L-lysine) (PLL) are the most well-known and used polymers for gene therapy, the synthesis and efficiency of novel cationic polymers to interact with nucleic acids in order to mediate cellular uptake have been recently reviewed.^{168,169}

Ionenes are synthetic polycations with quaternary ammonium functions, which are distributed along the backbone.^{138,139} In general, they can be synthesized by (a) self-polyaddition of aminoalkyl halides, (b) Menshutkin reaction between bis-tertiary amines and activated dihalide compounds or (c) via cationic functionalization of precursor polymers.^{140,170} Inspired by our results which described the self-assembly properties of 1,4-diazabicyclo[2.2.2]octane (DABCO) derived ionene¹⁵¹ as well as dye uptake¹⁵³ and phase-transfer catalysis,¹⁷¹ we decided to take advantage of the positively charged diammonium moieties present in ionene structures as cationic monomers to favor the electrostatic interaction process with nucleic acids.^{172–175} In this work we have prepared surfactant-ionene formulations with a series of ionenes made of *N,N'*-(*o*-phenylene) dibenzamide (**1**) and α,ω -tertiary diamines (**Fig. 37**) with the aim to further study the DNA complexation in terms of zeta potential, small-angle X-ray scattering (SAXS) and effect of transfection efficiency potency in antisense technology¹⁵⁶ by studying the ability of the polyplexes depending on the linker length and flexibility of the polymers to inhibit *Renilla* luciferase gene. As mentioned above the use of a non-ionic surfactant in the formulation (Tween 80) aims to avoid interactions with plasma proteins¹⁶⁷ and cell toxicity observed for cationic lipids. Our findings showed cationic ionene polymers formulated with a non-ionic surfactant were not toxic and were able to deliver antisense oligonucleotides into cells and thereby inhibited luciferase expression with promising efficiencies. These results open new insights on the design of novel ionene-based non-viral carriers for nucleic acids.

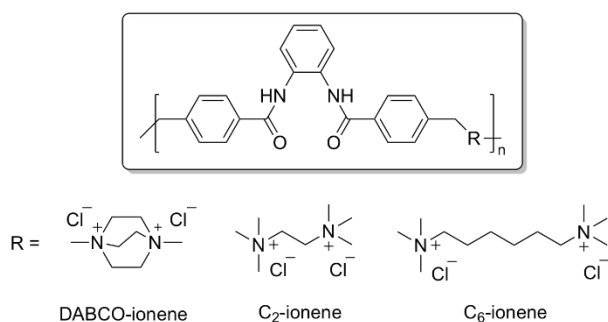


Fig. 37 Structures of ionene polymers used in this study with charged diammonium moieties with different structures and chain length.

2.2 Results and Discussion

2.2.1 Size and Zeta-Potential Measurements

Cationic vesicles containing the respective ionene polymer and polysorbate 80 as a non-ionic surfactant agent, were prepared by the thin-film hydration method in 20 mM HEPES (pH 7.4) buffer solution. A fixed amount of an antisense oligonucleotide (0.5 μ M, *Luc*) was used to obtain a series of polyplexes at several N/P ratios that ranged from 0.05 to 6. Finally, the surface charge was measured in order to determine the overall charge of the preformed ionene polyplexes in solution.

As depicted in **Fig. 38**, a transition from negative to positive values was clearly observed when the ionene concentration of the prepared cationic vesicle formulations was increased. This change suggested the evidence of electrostatic interactions among negatively charged oligonucleotides and positively charged vesicles, which led to the formation of the expected ionene-based polyplexes. Interestingly, we noticed that this transition was different depending on the formulation used. Thus, in case of **DABCO**-ionene the formulations reached a positive net charge at N/P ratios ≥ 1.5 ; whereas for **C₂**- and **C₆**-ionene was around ≥ 0.5 , 1 and 4, respectively. All formulations reached a *plateau* when compensated the surface charge density by increasing the number of cationic polymer chains in the three systems (N/P ratio of 2, 4 and 6).

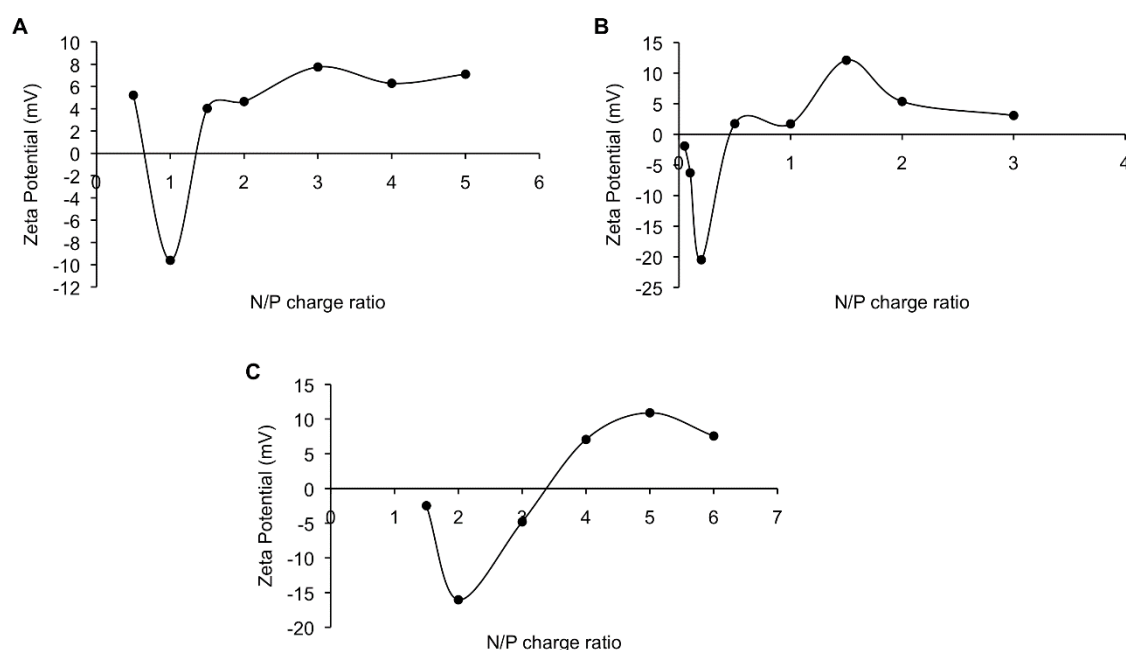


Fig. 38 Zeta potential of polyplexes at several N/P charge ratios derived from ionene polymers, antisense oligonucleotide and polysorbate 80. (A) **DABCO**-ionene, (B) **C₂**-ionene, (C) **C₆**-ionene.

Surprisingly, we observed similar trends in the behaviour of the systems when ionene formulations were added at lower N/P ratios. In particular, an initial decrease in the charge of the complexes was detected upon the addition of the cationic polymers, followed by a charge increase as described before. This initial decrease in the charge ratio was also observed and described with other family of cationic polymers like DNA-PEI complexes.¹⁷⁶ Similarly, the presence of initial amounts of cationic polymers in the three systems may result in varying the degree of folding of DNA molecules by decreasing the amount of free DNA and therefore leading to an increase in the concentration of the negative charge. This effect was primarily observed when the first ionene-based polymers were added to these three systems.

2.2.2 SAXS Measurements

To further investigate the structural information of our preformed ionene polyplexes, solutions of DNA salmon testes in 20 mM HEPES (pH 7.4) were put in contact with two representative ionene-based vesicle formulations (**C**₂- and **C**₆-ionene). The expected viscous complexes were formed, separated from the excess solution and washed with deionized water. The first attempts to visualize the scattered X-ray intensities were unsuccessful because the scattering signal was too weak for both complexes (data not shown). It is well known that DNA can be compacted by cationic surfactants forming lipoplexes, which in turn can co-precipitate at high concentrations forming gels having strong mechanical properties. When a drop of a concentrated DNA solution is placed in contact with a concentrated cationic surfactant solution, macroscopic films can be obtained that surround the droplet. Interestingly, these films are quite consistent as they can be cut and opened. Furthermore, films can be also dried and rehydrated preserving their main structural properties as observed by SAXS.¹⁷⁷ Thus, to get better resolution and enhance the signal spectra the resultant two complexes were further concentrated by evaporation. This process significantly showed the presence of one peak, which could be assigned to the pre-formed DNA complexes with **C**₂- and **C**₆-ionene, respectively.

As illustrated in **Fig. 39**, scattered X-ray intensities of the two ionene complexes showed the presence of single peaks in which their position did not differ too much among each other ($q = 2.402$ and 2.306 nm^{-1} for polyplexes based on **C**₂- and **C**₆-ionene, respectively).

Transfection of Antisense Oligonucleotides Mediated by Cationic Vesicles Based on Non-Ionic Surfactant and Polycations Bearing Quaternary Ammonium Moieties

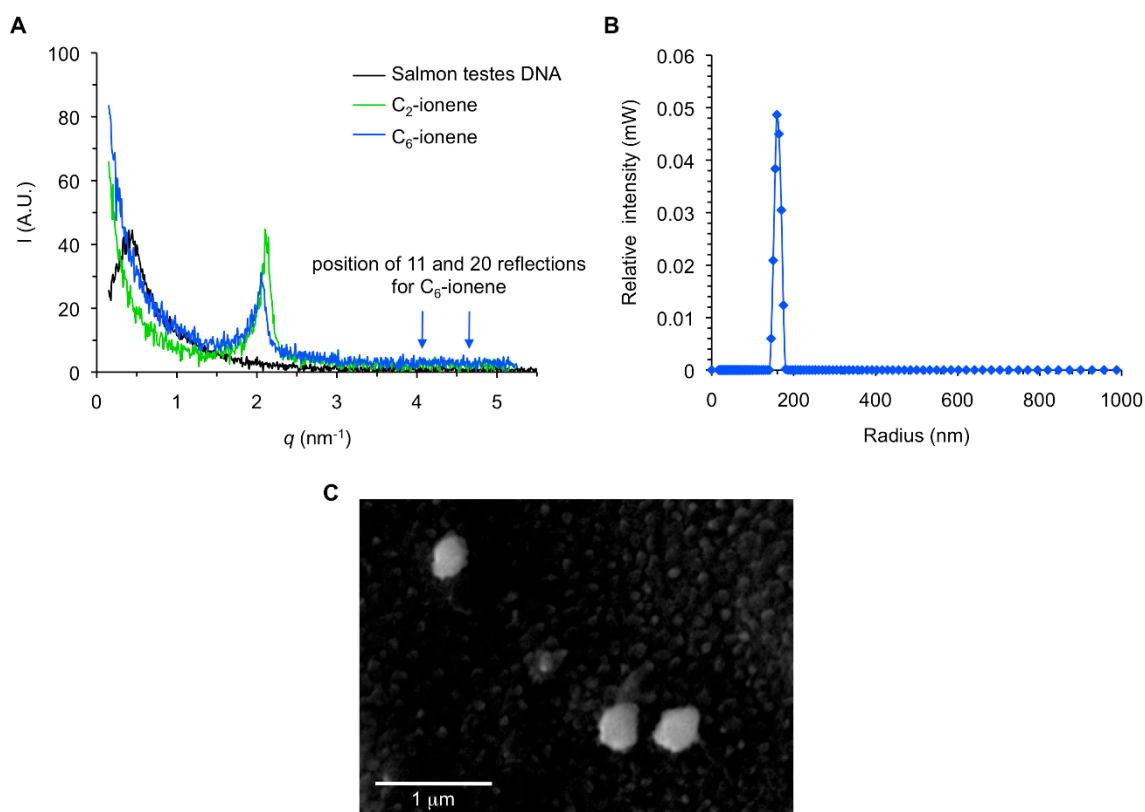


Fig. 39 **A)** Scattered X-ray intensity as a function of scattering vector q at 25 °C. The complex for C_2 -ionene (green) and C_6 -ionene (blue) are shown together. The scattering pattern produced by the Salmon testes DNA (black) is also included as a control. The expected positions of second and third reflections for hexagonal packing are shown for C_6 -ionene as arrows. **B)** Representative DLS measurement of polyplex made of C_6 :*Luc* oligonucleotide. **C)** Representative cryo-scanning electron microscopy image of polyplexes based on C_6 -ionene.

Disappointingly, we were not able to detect the presence of a second and third peak throughout the spectra, which might confirm a hexagonal packing of our pre-formed complexes. Additionally, the scattering pattern for DNA salmon testes without forming complexes was also included in the spectra for reference as a control. However, if we assume hexagonal symmetry as observed in lipoplexes,¹⁷⁸ the distance calculated between the centres of cylinders is 3.0 nm for C_2 -ionene and 3.1 nm for C_6 -ionene. By comparing these results with DNA complexes made using other kinds of surfactant agents, we see that both ionene complexes are much more compact (for example, the observed distances between cylinders was 4.2 ± 4.7 nm in the case of several lipo-amino acid derivatives whereas the distance for CTAB and MTAB were 6.5 and 5.68 nm, respectively).¹⁷⁹ If we tentatively compare these distances with the dimensions of a DNA double helix (diameter 2.2 ± 2.6 nm),¹⁸⁰ it seems that the structure of ionene-based complex might pack in a different way. Taking into consideration that DNA chains can form hexagonal structures intertwined with cationic lipid cylindrical micelles, the observed distances in the case of ionene

complexes suggest diameters of 1.2 and 1.4 nm for **C₂**- and **C₆**-ionene cylinders, respectively with a 2:1 hexagonal. These diameters seem reasonable for these molecules.

Finding that SAXS measurements showed polyplex structures formed by the formulation based on **C₂**- and **C₆**-ionene and DNA salmon testes were similar, the polyplex made of **C₆**:*Luc* oligonucleotide was chosen as a representative compound to carry out the corresponding dynamic light scattering (DLS) measurements. As illustrated in **Fig. 39B**, polyplexes were formed and showed an average diameter size of 320 ± 5 nm with good dispersity degree (0.3). Additionally, polyplexes based on **C₆**-ionene were characterized by cryo-scanning electron microscopy (cryo-SEM) (**Fig. 39C**). The cryo-SEM analysis revealed spherical morphologies of the particles with similar average sizes (340 nm) than those achieved through the use of DLS, as previously described. These results show the appropriateness of the use of **C₆**-ionene polymer as a non-viral vehicle for nucleic acids (e.g. phosphorothioate and siRNA oligonucleotides).

2.2.3 Cytotoxicity Assay

Prior to transfection experiments, the cytotoxicity of polyplexes (containing the antisense oligonucleotide, *Luc*) derived from the different ionenes were tested on HeLa cells. Three concentrations were evaluated (60, 120 and 300 nM) with respect to *Luc* oligonucleotide at N/P ratios of 2, 4 and 6, respectively. As a control, the effect on HeLa cells viability of the three cationic vesicle formulations (DABCO-ionene, **C₂**-ionene and **C₆**-ionene; *mock*) without forming complexes with *Luc* was also tested at 0.6, 1.20 and 3.0 μ M (concentrations that were used for the preparation of the polyplexes). Cells were incubated with the respective formulations at 37 °C for 24 h and normalized viabilities of treated cells with regard to untreated cells were measured by using a tetrazolium-based colorimetric (MTT) assay.¹⁸¹

As displayed in **Fig. 40**, vesicle formulations that did not contain *Luc* oligonucleotide showed no cytotoxicity at the three concentrations tested (cellular viabilities > 90%). Also polyplexes containing 60 nM of *Luc* proved to be harmless to HeLa cells at N/P ratios of 2, 4 and 6, respectively. At concentrations of 300 nM with respect to *Luc* those formulations derived from **DABCO**- and **C₂**-ionene still showed perfect nontoxic behavior. However, those derived from **C₆**-ionene based formulations showed a clear decrease in cell viability with rising N/P ratios (from N/P = 4: 78% to N/P = 6: 46%).

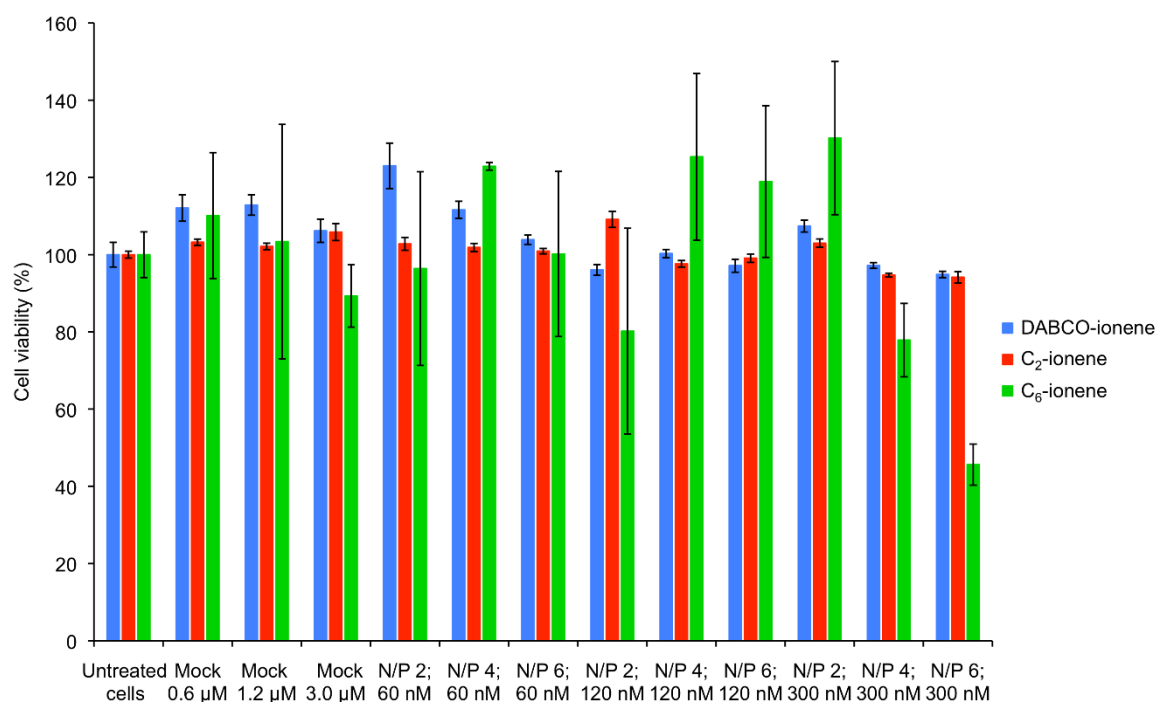


Fig. 40 Normalized cell viability of polyplexes derived from ionenes, antisense oligonucleotide and polysorbate 80. Toxicity of cationic vesicles without forming complexes was also tested. Polyplexes were tested at 60, 120 and 300 nM with N/P ratios of 2, 4 and 6. **DABCO**-ionene = blue colour, **C₂**-ionene = red colour, **C₆**-ionene = green colour. Each value represents the mean of at least 5 measurements.

2.2.4 Transfection

The described ionene-based formulations (**DABCO**-, **C₂**- and **C₆**-ionene) containing an antisense oligonucleotide (*Luc*), a 17-mer complementary to the mRNA *Renilla* luciferase gene, have been tested regarding their ability of silencing luciferase activity (**Fig. 41**). Generally, cationic particles are prone to interact with negatively charged proteins which may initiate aggregation processes leading to increasing particle sizes that may abolish the effectiveness of gene transfection.¹⁸² To avoid this undesirable effect, initial transfection experiments mediated by ionene formulations were evaluated in the absence of serum proteins (**Fig. 41A**). Thus, cationic polyplexes at concentrations of 120 nM with respect to *Luc* oligonucleotide at N/P ratios of 2 and 4 (N/P ratio of 6 was dismissed according to MTT data) were prepared.

Interestingly, two factors influenced the transfection process: the ionene structure and the relationship between ionene molar and charge ratio. According to **Fig. 41A**, the use of **DABCO** ionene-based formulation was detrimental in the transfection at the two N/P ratio tested probably due to the rigid linker which might have a detrimental effect on complex formation with oligonucleotides and therefore negative effect on mediating nucleic acid delivery. However, moderate gene silencing activities were obtained with cationic formulations at N/P ratio of 4 under serum-free conditions

at 120 nM with knockdown values of 40% and 27% for **C**₂- and **C**₆-ionene, respectively which inhibited luciferase production. This silencing activity, though modest, might come from the release and discharge of *Luc* oligonucleotide from endosomes probably by protonation mechanisms.¹⁸³

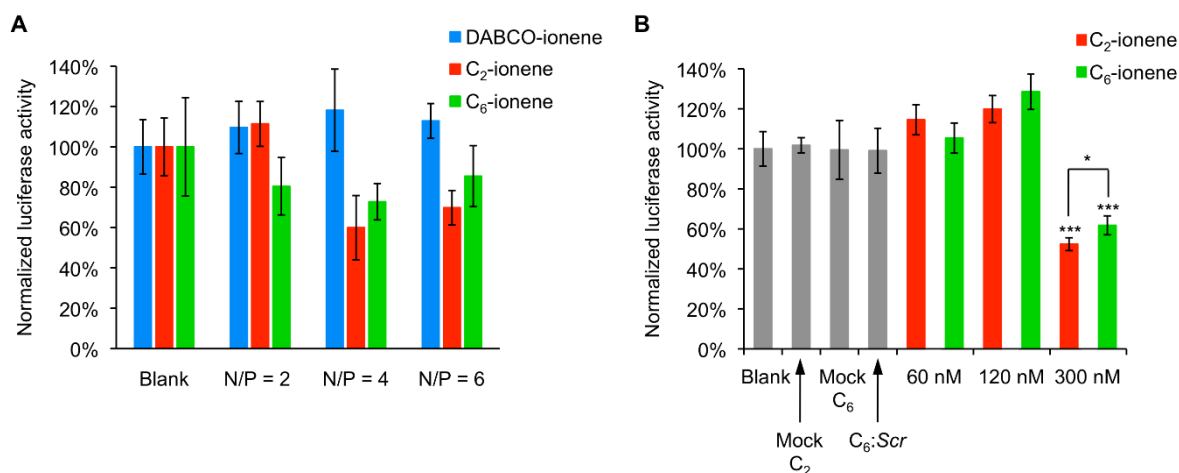


Fig. 41 Normalized gene-specific silencing activities targeting *Renilla* luciferase mRNA for polyplex formulations. (A) In the absence of FBS at different N/P ratios at 120 nM and (B) in the presence of FBS at concentrations of 60, 120 and 300 nM. Data are expressed as mean values of three replicates (\pm SD).

As **C**₂- and **C**₆-ionene formulations at N/P ratio of 4 showed the best transfection profile and low toxicity at 120 nM, they were used for investigating the gene silencing abilities in the presence of 10% fetal bovine serum (FBS) (**Fig. 41B**) and at concentrations of 60, 120 and 300 nM with respect to *Luc* oligonucleotide. According to the results, transfection efficiencies strongly depended upon the presence of serum, which eagerly tended to interact with our two cationic polyplexes. This interaction resulted in decreasing the transfection efficiency of the formulations. Thus, while **C**₂- and **C**₆-ionene polyplexes silenced *Renilla* luciferase 40 and 27% at 120 nM in the absence of FBS, the presence of FBS was detrimental on inhibiting luciferase at the same concentration. However, when the concentration of *Luc* oligonucleotide was increased up to 300 nM, both ionene formulations (**C**₂- and **C**₆-ionene) were able to promote gene delivery with similar and significant efficiencies (48 and 38% luciferase inhibition for **C**₂- and **C**₆-ionene, respectively). ($***p < 0.0001$). Interestingly, these silencing activities, though similar, were also found statistically significant in the case of **C**₂-ionene formulations when compared to **C**₆-ionene formulations ($*p < 0.05$). It seems that a medium sized chain length of the linker has a beneficial effect on the transfection ability. Probably the right balance between rigidity and flexibility of the polymers must be found for optimal effects.

Additionally, a scramble (*Scr*) oligonucleotide complexed with **C**₆-ionene formulation at the same N/P ratio of 4 together with **C**₂- and **C**₆-ionene formulations without forming polyplexes (mock) were used as controls and did not produce any effect on luciferase inhibition, as expected. Finally, to determine the specificity of the gene transfection process, *Luc* and *Scr* oligonucleotides were formulated into liposomes as controls (in the presence of lipofectamine) obtaining similar inhibition results as previously reported (data not shown).¹⁸⁴

2.3 Materials and Methods

2.3.1 Materials

Polysorbate 80 (Tween 80), 3-(4,5-dimethylthiazol-2-yl)-2,5-diphenyltetrazolium bromide (MTT reagent), sodium salt of DNA from salmon testes (polymerization average degree of 2000 base pairs) and antisense oligonucleotide of sequence (5'-CGT TTC CTT TGT TCT GGA-3'; *Luc*') were purchased from Sigma-Aldrich (St. Louis, Missouri, United States) and used as received. A scramble sequence (5'-CTG TCT GAC GTT CTT TGT-3'; *Scr*) was synthesized *in house* and purified by DMT *off*-based protocols. Lipofectamine 2000 was purchased from Invitrogen (Carlsbad, California, United States). PBS buffer and Dulbecco's Modified Eagle's Medium (DMEM), which was supplemented with a 10% heat-inactive fetal serum bovine (FBS) along with distilled water (DNase/RNase free) were purchased from Gibco (Waltham, Massachusetts, United States). Additional nuclease-free water was also prepared by using 0.1% of diethylpyrocarbonate (DEPC) to ensure the removal of RNase contamination, autoclaved and filtered before using. Luciferase assay kits were purchased from Promega (Madison, Wisconsin, United States). Qiagen Giga plasmid purification kit was purchased from Qiagen (Hilden, Germany). Starting materials for polymer synthesis were purchased from Sigma Aldrich (St. Louis, Missouri, United States) or TCI (Zwijndrecht, Belgium). Luminiscence values were measured in a Promega Glomax Multidetecion instrument (Madison, Wisconsin, United States). All ionene polymers were synthesized by step-growth polymerization following the two-step procedure previously described and showed the same spectroscopic data.^{151,153,171,185} In short, reaction of *o*-phenylenediamine with 4-(chloromethyl)benzoyl chloride in the presence of Et₃N in DCM afforded the corresponding bis-benzamides in good yields (75%–98%). Subsequent copolymerization with equimolar amounts of the desired α,ω -diamine in dimethylformamide (DMF) at 80 °C provided white precipitates within 2–6 days. The precipitates were

filtered, washed (with DMF, MeCN and DCM) and dried under vacuum to afford the ionenes in modest yields (43%–80%). Sufficient solubility for gel permeation chromatography (GPC) was achieved by exchanging the chloride anions by bis(trifluoromethanesulfonyl)amide (TFSA) anions using lithium bis(trifluoromethanesulfonyl)azanide (LiTFSA) in hot water. These ionenes-TFSA showed low degrees of polymerization ($n = 7-14$) and high dispersity values ($\mathcal{D} = 2.1-3.1$). Weight-average molecular weights, M_w (Da), for ionenes-TFSA: 8.1×10^3 (**DABCO**-ionene); 1.6×10^4 (**C₂**-ionene); 6.9×10^4 (**C₆**-ionene); number-average molecular weight, M_n (Da), for ionenes-TFSA: 3.9×10^3 (**DABCO**-ionene); 6.1×10^3 (**C₂**-ionene); 2.2×10^3 (**C₆**-ionene).

2.3.2 Preparation of Polyplexes

Cationic vesicles were prepared by mixing ionenes (1 – 2 mg) and polysorbate 80 in a 1:1 (n/n) molar ratio and dissolving/suspending those in MilliQ water (1 mL). Mixtures were dried in speed vacuum at 45 °C for 18 h. The resulting film was rehydrated in 1 mL of sterile HEPES buffer (20 mM, pH 7.4), incubated at 60 °C for 20 min, sonicated for 3 min and filtered through a 13 mm Nylon filter with 0.2 μm pore width. Polyplexes were obtained by adding an oligonucleotide stock solution to the cationic vesicle solutions to give N/P ratios ($[\text{cationic amino groups}]_{\text{ionene}}/[\text{anionic phosphate groups}]_{\text{nucleic acid}}$) between 0.05 and 8. The mixtures were vortexed, sonicated for 10 s and finally incubated at 37 °C for 30 min.

The synthesized ionene monomers each contain two terminal amine groups which will found positively charged at physiological pH conditions (7.4). The antisense oligonucleotide (*Luc* oligonucleotide) contains 17 negative charges and the N/P ratio can be calculated by using eq. 1, as described elsewhere.¹⁸⁶

$$\frac{N}{P} \text{ ratio} = \frac{\text{number of moles of ionene monomer} \times 2}{\text{number of moles of Luc oligonucleotide} \times 17} \quad (1)$$

2.3.3 Zeta-Potential

Zeta potential values were obtained by laser doppler velocimetry by using a Zetasizer Nano ZS (Malvern Instruments; Malvern, United Kingdom) equipped with a He–Ne red light laser ($\lambda = 633 \text{ nm}$). Polyplex solutions were measured at an oligonucleotide concentration of 0.5 μM and N/P ratios from 0.05 to 6 at 25 °C. Samples (50 μL) were diluted in 0.1 mM NaCl solution (950 μL) and introduced into folded capillary cells.

Smoluchowsky approximation was used to calculate zeta potential values. Measurements were run in triplicate.

2.3.4 Size Measurements

The hydrodynamic diameter of polyplexes (cationic ionene/DNA complexes) was determined by dynamic light scattering (DLS) spectrometer (LS Instruments, 3D-cross correlation multiple scattering) equipped with a He–Ne laser (632.8 nm). Measurements were carried out at a scattering angle of 90°, in triplicates at 25 °C without sonication. The particle radii were calculated by fitting the first cumulant parameter.

2.3.5 Small-Angle X-Ray Scattering (SAXS) Measurements of Ionene Polyplexes

Small-angle X-ray scattering measurements were recorded on S3-MICRO (Hecus X-ray system, GMBH Graz, Austria) which was coupled to a GENIX-Fox 3D X-ray source (Xenox, Grenoble) and coupled with a 3D focusing mirror that produces a detector-focused X-ray beam with $\lambda = 0.1542$ nm Cu K_{α} -line (greater than 97% purity and less than 0.3% of K_{α}). Transmitted scattering was measured by using a PSD 50 Hecus in the SAXS regime ($0.09 \text{ nm}^{-1} < q < 6 \text{ nm}^{-1}$) including Bragg peaks and diffuse scattering. Measurements were carried out at a constant temperature (25 °C) for 24 h. Detector counting was accumulated for 20 min intervals, if no temporal variation was observed, several runs were summed up to reduce the noise of background level. A stock concentration of DNA from salmon testes in 20 mM HEPES (pH 7.4) was properly mixed with a stock concentration of a surfactant-ionene formulation in 20 mM HEPES buffer at 37 °C for 30 min. The resultant polyplexes (DNA:ionene complexes) were isolated, dried and deposited in a glass capillary of 1 mm diameter with 10 μm wall thickness. SAXS scattering curves were plotted as a function of the scattering vector modulus (eq. 2) where θ is the scattering angle and λ the incident radiation wavelength is. A silver behenate sample was used in order to calibrate the system scattering vector.

$$q = \frac{4\pi}{\lambda} x \sin \frac{\theta}{2} \quad (2)$$

2.3.6 cryo-Scanning Electron Microscopy (cryo-SEM)

Polyplexes made of ionene- C_6 based formulation and Luc oligonucleotide were obtained at N/P ratio of 4. The resultant polyplexes were rapidly frozen in liquid

nitrogen and cut with an equipped cold knife. Polyplexes were sputtered with gold-palladium, observed and processed by using a Hitachi S-3500N (Hitachi High-Technologies Corp., Tokyo, Japan) scanning electron microscope operated at 5 kV.

2.3.7 Cytotoxicity Assay

The adherent cell line HeLa (human carcinoma) was plated at a density of 5×10^3 cells/well (50% confluency) on a 96-well plate in 200 μ L of Dulbecco's Modified Eagle's medium (DMEM) supplemented with 10% fetal bovine serum (FBS), in the absence of antibiotics. HeLa cells were incubated at 37 °C in a humidified atmosphere (5% CO₂) for 24 h to permit cell attachment. Then the medium was removed and replaced by fresh one to give a final concentration of 200 μ L. Polyplexes and cationic vesicles were prepared as described above and added to the wells to give concentrations of 60, 120 and 300 nM and N/P ratios of 2, 4 and 6. The mixture was incubated at 37 °C for 18 h and then medium was removed and the wells were washed with PBS (1 \times 200 μ L). Fresh DMEM was added (200 μ L) and cells were incubated again at 37 °C for 3 h. MTT solution (10 μ L, 5 g L⁻¹ in PBS buffer) was added to each well and plates were stored at 37 °C for further 2.5 h. Then medium was removed, DMSO (100 μ L) was added and absorbance was measured at 570 nm. Each measurement was performed with 6 replicates.

2.3.8 Gene Transfection and Antisense Technology Studies

In the Absence of FBS

HeLa cells were regularly passaged to maintain exponential growth. Cells were seeded the day before at a density of 10⁵ cells/well on a 24-well plate each well in DMEM supplemented with 10% FBS. Cells were incubated at 37 °C for 18 h in a humidified atmosphere (5% CO₂) to permit cell attachment. The medium was then replaced by fresh one (500 μ L). A solution containing firefly luciferase (pGL4) (30 μ L, 100 ng μ L⁻¹) and *Renilla* luciferase (30 μ L, 10 ng μ L⁻¹) in Opti-MEM™ (90 μ L) was combined to a solution containing Lipofectamine2000 (3.9 μ L, 1 g L⁻¹) in Opti-MEM™ (146.4 μ L). The resultant formulation was incubated 10 min at room temperature. To each well 100 μ L of this formulation was added and the cells were incubated at 37 °C for 6 h. Medium was removed, cells were washed with PBS (2 \times 400 μ L) and DMEM without FBS was added (500 μ L). Polyplexes were added (100 μ L) to give final oligonucleotide concentrations of 120 nM and N/P ratios of 2, 4 and 6 and cells were incubated at 37 °C for 24 h. Medium was removed, cells were washed with PBS

(1 × 500 µL) and cells were stored at –20 °C for 18 h. After thawing the cells 100 µL of lysis buffer were added to each well. The plate was shaken at 480 rpm at room temperature for 15 min. Lysates (25 µL) were transferred to a 96-well plate and luminescence was recorded after adding, alternatingly, Luciferase assay reagent (25 µL) and Stop&Glow reagent (25 µL). Inhibition results generated by polyplex-based ionenes were expressed as normalized ratios between the reported luciferase (*Renilla*) and control luciferase (Firefly). *Luc* and *Scr* oligonucleotides at 60 nM were formulated into liposomes (in the presence of lipofectamine) as positive and negative controls, respectively.

Statistical Analysis. Data were shown as mean ± standard deviation (SD) and are the result of an average of three replicates. Statistical differences were determined by using Student's t-test and were considered significant when **p* < 0.05 and ****p* < 0.001.

In the Presence of FBS

HeLa cells were regularly passaged to maintain exponential growth. Cells were seeded the day before at a density of 10⁵ cells/well on a 24-well plate each well in DMEM supplemented with 10% FBS. Cells were incubated at 37 °C for 18 h. *Renilla* and Firefly luciferases were transfected following the same procedure as described above. After 6 h incubation at 37 °C, medium was removed, cells were washed with PBS (2 × 400 µL) and DMEM supplemented with 10% FBS was added (500 µL). Polyplexes were added to give a final N/P ratio of 4 and oligonucleotide concentrations of 60, 120 and 300 nM. Cells were incubated at 37 °C for 24 h. Medium was removed, cells were washed with PBS (1 × 500 µL) and stored at –20 °C for 18 h. After thawing the cells, 100 µL of lysis buffer were added to each well. Luminescence was measured following the same protocol as described before. Inhibition results generated by polyplex-based ionenes were expressed as normalized ratios between the reported luciferase (*Renilla*) and control luciferase (Firefly).

2.4 Conclusions

Cationic vesicles derived from ionene polymers with alternating α,ω-tertiary diamine linker and the non-ionic surfactant polysorbate 80 were used to entrap oligonucleotide single strands which were complementary to *Renilla* luciferase mRNA. Zeta-potential of the vesicle formulations at different N/P ratios ([cationic amino groups]_{ionene}/[anionic phosphate groups]_{nucleic acid}) was measured to ensure a

positive charge of the system. MTT assay showed no toxicity for formulations derived from **DABCO**- and **C₂**-ionene at several concentrations and N/P ratios (2, 4 and 6) whereas **C₆**-ionene showed critical cell viabilities at 300 nM with a N/P ratio of 6 (46% of cell viability). Transfection experiments of all cationic vesicle formulation were investigated by performing a luciferase activity assay at 120 nM and N/P ratios of 2 and 4 in the absence of proteins. As a result, **DABCO**-ionene derived formulations showed no transfection ability at both N/P ratios tested. On the contrast for **C₂**- and **C₆**-ionene derived formulations showed perfect non-toxic behaviour, the luciferase activity was reduced by 48 and 38%, respectively at N/P ratio of 4 and *Luc* concentration of 300 nM. The use of this complete harmless formulation at higher concentrations might be an interesting alternative to current transfection agents and further structure-activity relationship need to be carried out in order to obtain optimized cationic ionene derivatives that are less susceptible to FBS proteins. Further studies to determine the effect of the polymer topology (positional isomers) on the transfection efficiency are currently undergoing in our laboratories and the results will be reported at due course.

3. Aromatic ionene topology and counterion-tuned gelation of acidic aqueous solutions⁵

3.1 Introduction

A large number of important biological macromolecules (e.g. nucleic acids, polypeptides and polysaccharides) and well-known synthetic macromolecules (e.g. polyacrylic acid and poly(styrene sulfonate)) are highly charged polymers, so-called polyelectrolytes, that have been object of abundant theoretical and experimental investigations during the last few decades.^{187–189} Commercial applications of these polymers range from colloidal stabilization to superabsorbent gels, where hydrophobic, charge transfer and long-ranged electrostatic interactions mediated by mobile ions and water molecules define the physical properties and, hence, the functionality of these systems.

Among different types of polyelectrolytes, polycations bearing quaternary ammonium in the backbone constitute a very interesting subgroup known as ionenes,^{138,190–195} which are usually prepared either by step polymerization via Menshutkin reaction or cationic functionalization of precursor polymers.^{140,141,196,197} These polymers have been widely used as antibacterial agents, building blocks for the preparation of chromatography stationary phases, simplexes or functional gels, among other applications.^{190,198,199} The charge distribution, the type of counterions, the molecular weight, structural flexibility and H-bonding capability are, among others, critical aspects that may influence the dynamics of the ionic chains that govern their properties.^{200–202} Unfortunately, a low control on some of these features as well as the lack of theoretical models developed at the atomistic level^{203–206} make it difficult to understand, predict and control their aggregation in different aqueous media.²⁰³ Within this context, we have recently reported¹⁵¹ a combined computational-experimental approach that led to the improvement of the hydrogelation ability of important 1,4-diazabicyclo[2.2.2]octane (**DABCO**)-based ionenes^{152,187–189,207} containing different structural isomers of phenylenediamine as molecular core (**Fig. 42**).

⁵ Adapted from Ref. 215 with permission from The Royal Society of Chemistry. Synthesis of ionenes was performed by J. Bachl and J. Mayr. Gelation vs. HCl conc. experiments, rheology and polarized light photos were made by J. Bachl. Gelation experiments in other acidic and salt solutions and HCl gas adsorption was performed by J. Mayr. Computer simulations were performed by O. Bertran.

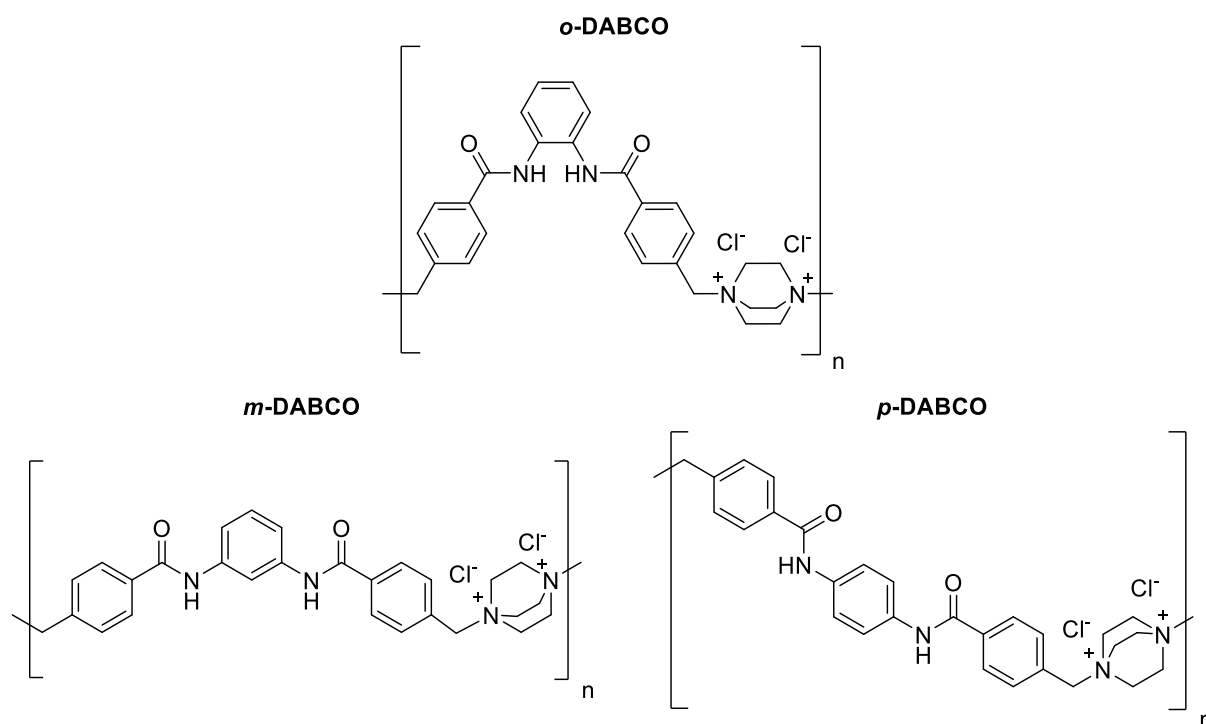


Fig. 42 Structures of topologically different water and acidic solutions gelling ionene polymers **ortho**-, **meta**- and **para**-DABCO.

Molecular dynamics simulations of these ionenes with explicit water molecules pointed out remarkable differences in the assembly of the polymeric chains in each case. Specifically, interchain regions with high degree of hydration (i.e. polymer ... water interactions) and regions dominated by polymer...polymer interactions were evident in the case of **o-DABCO** and **m-DABCO** isomeric ionenes, while domains governed by polymer ... polymer interactions were nearly inexistent in **p-DABCO**. This was experimentally correlated with the superior properties of the gels prepared from **o-DABCO**.¹⁵¹

Despite the potential interest of gelation of acidic solutions in areas such as safety and environmental remediation,^{208,209} this phenomenon is scarcely described in the literature and mainly associated to low molecular weight gelators.^{210–213} A reason behind this scenario may be the existence of labile structural moieties in many gelating agents and their potential cleavage and/or undesired protonation events in acidic media. Yoshida and co-workers¹⁵² reported that a polymer based on a *N,N'*-(*p*-phenylene) dibenzamide linkage bearing a C₆-flexible spacer was able to gel a 0.1 M HCl solution, although no further studies were carried out related to this observation. To our delight, we have found that the well-defined topology of ionenes^{187,189,190} not only govern their aggregation behaviour in pure water but also in a

variety of aqueous acidic solutions leading to the formation of a variety of stable acidic gels. Herein, we describe the details of this exceptional phenomenon and the understanding of the effects of the different polymer topologies through computational molecular dynamic simulations.

3.2 Results and Discussion

3.2.1 Gelation properties in aqueous acidic and salt solutions

During the study of the gelation ability of the ionenes we found that ***o*-DABCO** and ***p*-DABCO** efficiently gelled HCl solutions (0.1 M, pH = 1.0) at their corresponding CGC determined in pure water (25 g L⁻¹ and 48 g L⁻¹, respectively). In contrast, ***m*-DABCO** failed to gel these HCl solutions even at 2-fold higher gelator concentration (up to 200 g L⁻¹) than that in pure water.

Table 2 Effect of different aqueous environments containing various acids and inorganic Cl⁻ sources on the gelation properties of ionenes with respect to pure water^a

Aqueous medium ^b	<i>o</i>-DABCO			<i>m</i>-DABCO			<i>p</i>-DABCO		
	CGC (g L ⁻¹)	Gel-time (min)	T _{gel} (°C)	CGC (g L ⁻¹)	Gel-time (min)	T _{gel} (°C)	CGC (g L ⁻¹)	Gel-time (min)	T _{gel} (°C)
H ₂ O	25 ± 2	1080 ± 60	56 ± 1	100 ± 10	1260 ± 40	59 ± 1	48 ± 5	2640 ± 240	49 ± 1
HCl	22 ± 2	10 ± 2	60 ± 2	S	-	-	33 ± 3	50 ± 5	63 ± 1
HBr	56 ± 2	11 ± 5	44 ± 1	170 ± 30	1 ± 0.5	- ^d	58 ± 3	30 ± 10	34 ± 4
HI	68 ± 3	6 ± 1	41 ± 2	59 ± 9	420 ± 60	32 ± 2	I	-	-
H ₃ PO ₄	46 ± 4	20 ± 2	76 ± 1	S	-	-	105 ± 11	68 ± 8	55 ± 2
HNO ₃	46 ± 1	30 ± 5	35 ± 1	139 ± 29	4 ± 1	- ^d	88 ± 2	15 ± 1	- ^d
H ₂ SO ₄	S	-	-	S	-	-	S	-	-
CH ₃ COOH	48 ± 4	5 ± 1	61 ± 2	S	-	-	110 ± 10	30 ± 5	33 ± 2
HCOOH	45 ± 1	90 ± 20	57 ± 2	150 ± 50	3 ± 1	- ^d	68 ± 1	140 ± 20	67 ± 7
NaCl	92 ± 9	6 ± 1	54 ± 3	P	-	-	P	-	-
CsCl	97 ± 9	3 ± 1	53 ± 2	P	-	-	P	-	-
NH ₄ Cl	100 ± 10	4 ± 1	63 ± 2	P	-	-	P	-	-
CaCl ₂ ^c	89 ± 9	4 ± 1	36 ± 2	P	-	-	P	-	-

^a Experimental errors were determined from at least two randomized measurements. ^b Unless otherwise indicated, the concentration of aqueous solutions was adjusted to 0.1 M. ^c Concentration was adjusted to 0.05 M. ^d Gradual water loss of the material precluded an accurate determination of the T_{gel}. Abbreviations: I = insoluble, S = solution, P = precipitate.

As shown in **Table 2**, further investigations revealed that ***o*-DABCO** and ***p*-DABCO** were also able to promote effective gelation of 0.1 M HCl solutions not only at concentrations even lower than the CGC established in pure water, but also with much faster kinetics (about 100-times and 50-times shorter gelation times than in water for ***o*-DABCO** and ***p*-DABCO**, respectively). Motivated by these results, we

decided to explore the gelation ability of these systems in other acidic solutions. **O-DABCO** formed stable and homogeneous gels within 30 min in HBr, HI, H₃PO₄ and HNO₃ solutions (0.1 M, pH = 1.0 for HBr, HI, and HNO₃, pH = 1.62 H₃PO₄), whereas the gelation ability of **m-DABCO** and **p-DABCO** was rather limited and several of their gels were not homogeneous and underwent gradual water loss over time (**Table 2** and **Fig. 43**).

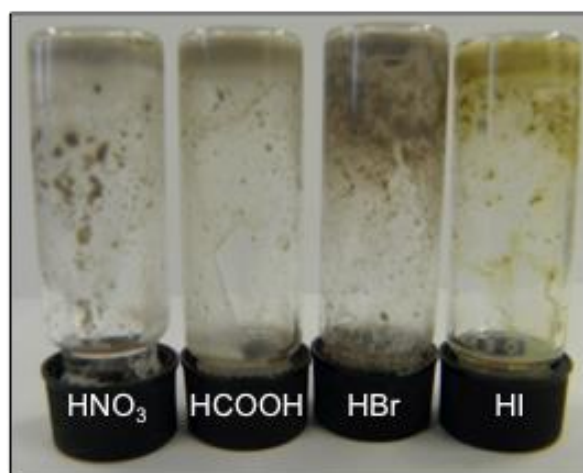


Fig. 43 Appearance of the inhomogeneous gels and undissolved solid material obtained **m-DABCO** in different acidic solutions.

No gelation was observed in H₂SO₄ (0.1 M, pH = 0.96) for any of the ionenes, which led to turbid solutions at concentrations ranging between 10 g L⁻¹ and 200 g L⁻¹. Remarkably, **o-DABCO** and **p-DABCO** also showed the capacity to form stable gels in solutions of organic acids such as acetic acid (CH₃COOH, 0.1 M, pH = 2.87) and formic acid (HCOOH, 0.1 M, pH = 2.37), being **o-DABCO** the most efficient gelator in terms of gelation concentration, kinetics and/or thermal stability of the gels. In terms of optical appearance, and in contrast to the hydrogel obtained from **o-DABCO** in water, all gels described in **Table 2** were opaque except the one made of **o-DABCO** in acetic acid, which was translucent. These appearances suggested the formation of aggregates in acidic solutions bigger than the wavelength of visible light (350 – 750 nm) causing its scattering. The acidic gels prepared from **o-DABCO** were stable for several months at room temperature without detriment of their consistency and visual appearance.

At this point we decided to take HCl solution as a model acidic medium to investigate and compare other properties of the obtained gels compared to those prepared in pure water. An important effect of the Cl⁻ counterion was revealed by the ability of **o-DABCO** to gel also solutions of different ionic strengths containing inorganic

chloride salts such as NaCl, CsCl, NH₄Cl (pH = 5.1) and CaCl₂, albeit the use of 3.5 – 4 fold excess in gelator concentration compared to the CGC in pure water was necessary to obtain the gels (**Table 2**). The superior gelation properties of ***o*-DABCO** were also evident in these solutions as neither ***m*-DABCO** nor ***p*-DABCO** were able to form gels at concentrations ranging from 10 g L⁻¹ and 200 g L⁻¹. These results suggest an apparent synergistic effect of both H⁺ and Cl⁻ ions to facilitate the gelation process using ***o*-DABCO**, thus lowering the CGC and increasing the stability of the resulting gel in comparison to pure water.

Additional positive effects of the HCl medium were obvious by comparing the gelation kinetics and the thermal stabilities of gels with those obtained in pure water at comparable ionene concentrations (**Fig. 44**). Thermal sol-to-gel transition temperatures (T_{gel}) of the gels prepared from ***o*-DABCO** and ***p*-DABCO** were found to be increased by 4 °C and 14 °C, respectively, with respect to those obtained in water (**Fig. 44A**). Furthermore, a remarkable decrease in the gelation time to about 20% of the value obtained in water was visible for both ***o*-DABCO** and ***p*-DABCO** in HCl solutions (**Fig. 44B**).

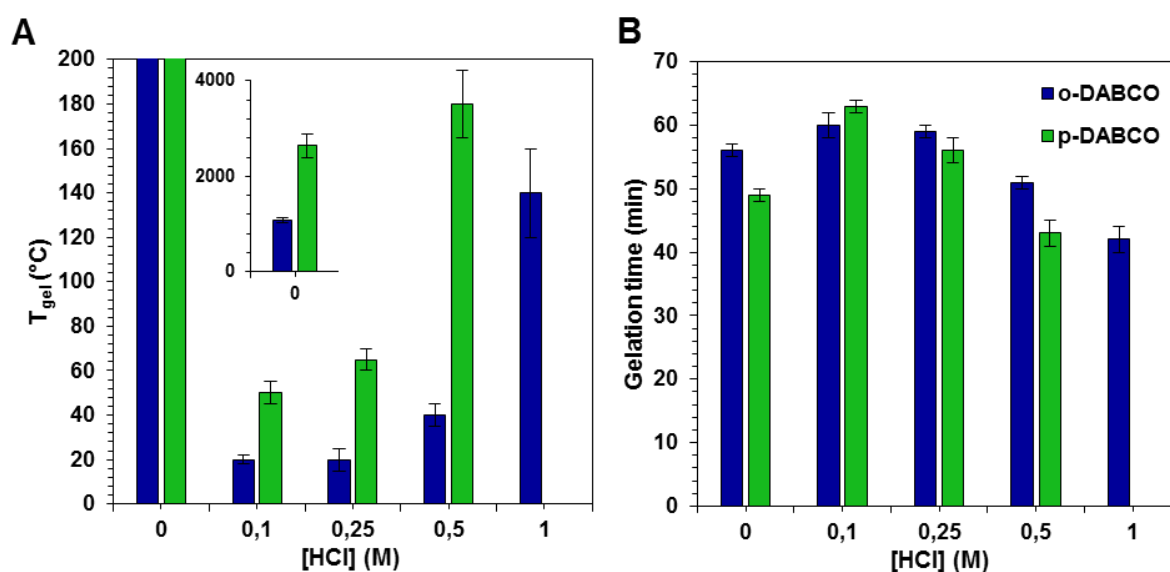


Fig. 44 Effect of HCl concentration on typical gelation properties **A)** T_{gel} ; **B)** gelation time of ionenes ***o*-DABCO** and ***p*-DABCO** at their CGC in water as indicated in

Table 3 Effect of the concentration of HCl on the gelation kinetics, T_{gel} and optical appearance of the gels made from ***o*-DABCO** and ***p*-DABCO** at their CGC in water as indicated in Table 1.^a

Concentration HCl (M)	Gelation time (min)		T_{gel} (°C)		Optical appearance	
	<i>o</i>-DABCO	<i>p</i>-DABCO	<i>o</i>-DABCO	<i>p</i>-DABCO	<i>o</i>-DABCO	<i>p</i>-DABCO
0.0	1080 ± 60	2640 ± 240	56 ± 1	49 ± 1	TG	OG
0.1	20 ± 2	50 ± 5	60 ± 2	63 ± 1	OG	OG
0.25	20 ± 5	65 ± 5	59 ± 1	56 ± 2	OG	OG
0.5	40 ± 5	180 ± 15	51 ± 1	43 ± 2	OG	OG
1.0	140 ± 20	S	42 ± 2	S	WG	S
2.0	S	S	S	S	S	S

^a Experimental errors were determined from at least two randomized measurements. Abbreviations: S = solution; TG = transparent gel; OG = opaque gel; WG = weak gel (i.e. exhibits gravitational flow after inverting a test tube within 30 min).

The optimum concentration of HCl in aqueous solution was determined by testing different concentrations at the CGC of the desired gelator in pure water, and comparing the effect on both the T_{gel} and the gelation kinetics. The results are summarized in **Table 3** and **Fig. 44** and indicate that a concentration of HCl of 0.1 M promotes the most effective gelation characterized by the highest T_{gel} and gelation kinetics for both ionenes. Gels made from ***o*-DABCO** and ***p*-DABCO** could also be prepared at acid concentrations of 1.0 M and 0.5 M, respectively, albeit with a detriment of the studied gels properties. Higher concentrations in each case lead to clear viscous solutions. In addition, and as also observed in pure water,¹⁵¹ both the thermal stability of the gels and the gelation kinetics in acidic medium were enhanced by increasing the ionene concentration (e.g. gel prepared from ***o*-DABCO** in 0.1 M HCl at its CGC displayed a T_{gel} of 60 ± 2 °C and a gelation time of 10 ± 2 min, whereas around 4-fold increase in the concentration of the ionene afforded an opaque gel within 4 ± 0.2 min and with a T_{gel} of 72 ± 1 °C) (**Table 3**).

Dynamic oscillatory rheology was conducted in order to confirm the viscoelastic gel nature of the materials and compare the overall mechanical stabilities towards external shear forces. Appropriate dynamic frequency sweep (DFS), dynamic strain sweep (DSS) and dynamic time sweep (DTS) experiments for the gels made of ***o*-DABCO** and ***p*-DABCO** both in water and in HCl solutions revealed a remarkable enhancement of the mechanical stabilities of the gels prepared in HCl, as indicated by higher storage modulus G_0 (one order of magnitude higher than in water) and lower $\tan \delta$ values. On the other hand, the materials derived from HCl seem to be more brittle in nature as indicated by the smaller maximum strain at break (γ) of the

gels. Furthermore, the macroscopic thixotropic behaviour of **o-DABCO** that we previously observed in water¹⁵¹ is also preserved in 0.1 M HCl solution and supported by a three-step loop test (i.e. >97% of the original moduli values was recovered after the second relaxation cycle) performed.

Optical microscopy images of the gels made of **o-DABCO** (25 g L⁻¹) in both 0.1 M HCl and pure water revealed the presence of distinctive domains of birefringence under crossed nicols dependent on the nature of the aqueous medium, indicating the formation of different anisotropic aggregates (**Fig. 45A–D**). FESEM images of the corresponding xerogels, obtained by the freeze-drying method,²¹⁴ confirmed the induction of different morphologies caused by the nature of the aqueous environment.

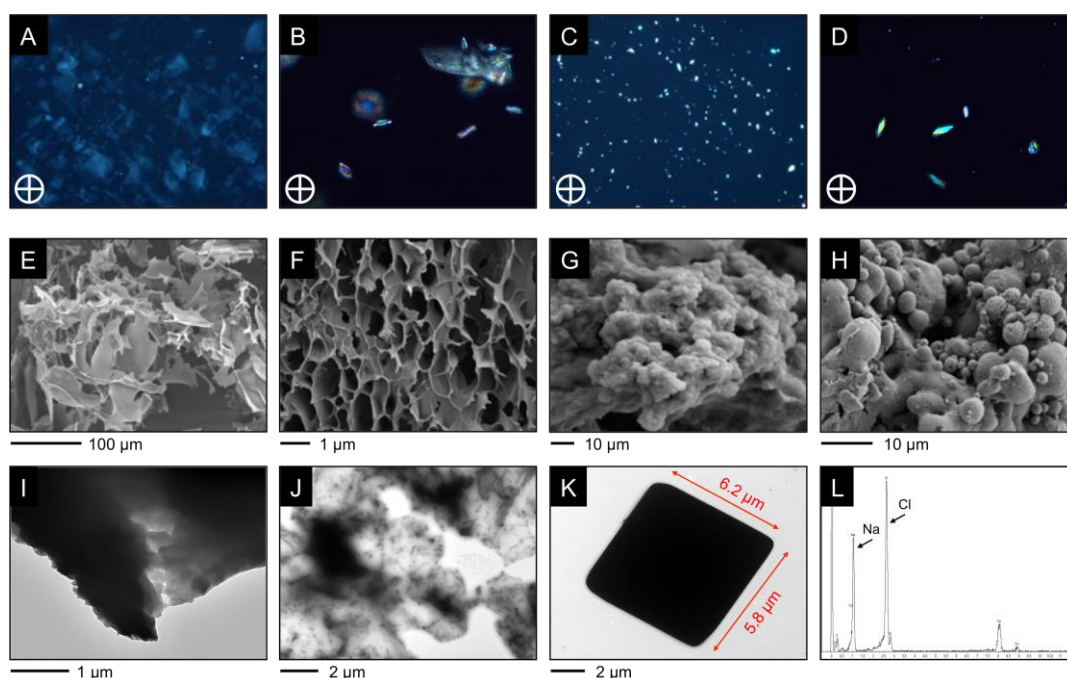


Fig. 45 Optical and morphological features of hydrogels prepared from **o-DABCO** and **p-DABCO** at their CGC in water. **A, B**) Optical images under crossed nicols of the gel film made from **o-DABCO** in water. Magnification: **A** = 10×; **B** = 50×. **C, D**) Optical images under crossed nicols of the gel film made from **o-DABCO** in 0.1 M HCl. Magnification: **C** = 10×; **D** = 50×. Note: Apparent higher birefringence density for gel-materials in acidic environment suggests the formation of more extended networks as compared to pure hydrogels, which is in agreement with their higher mechanical and thermal resistance. **E**) FESEM image of the xerogel derived from the gel made from **o-DABCO** in water. **F**) FESEM image of the xerogel derived from the gel made from **p-DABCO** in water. **G**) FESEM image of the xerogel derived from the gel made from **o-DABCO** in 0.1 M HCl. **H**) FESEM image of the xerogel derived from the gel made from **p-DABCO** in 0.1 M HCl. **I**) TEM image of the gel made from **o-DABCO** in water. **J**) TEM image of the xerogel derived from **o-DABCO** in 0.1 M HCl. **K-L**) TEM image and elemental analysis profile, respectively, of cubic structures (average edge lengths of around 5–15 μm) of NaCl obtained from compound **o-DABCO** (25 g L⁻¹) in 0.1 M HCl solution. Such NaCl crystals were presumably formed during the preparation process of the gels/xerogels or during an aging process involving traces of Na⁺ cations still present in the used purified water.

Specifically, dense and macroporous networks formed by connected leaf-like layers with interlamellar distances in a range of 5–10 nm were visualized for the xerogels of ***o*-DABCO** and ***p*-DABCO** in pure water (**Fig. 45E** and **F**). In sharp contrast, rougher and denser agglomerates could be observed for xerogels made of both ionenes in 0.1 M HCl (**Fig. 45G** and **H**). Agglomerates resembling pebble stones (average diameter for individual particles ~ 1–5 nm) were clearly characteristic for xerogels prepared from ionene ***p*-DABCO** (**Fig. 45H**). TEM images derived from compound ***o*-DABCO** in pure water revealed overlapped lamellar structures consisting of large and homogeneous sheets (**Fig. 45I**), in good agreement with the findings obtained by FESEM. On the other hand, TEM images of the materials derived from acidic environment showed the presence of very dense and non-layered structures (**Fig. 45J**).

3.2.2 Computer Simulations

Molecular dynamics (MD) simulations of ionenes were performed considering an aqueous solution containing 1000 $\text{H}_3\text{O}^+\text{-Cl}^-$ ion pairs to provide microscopic information about the relationships between the substitution pattern of the phenyl ring and the gelation capacity in acidic solutions. Visual inspection of the recorded snapshots reveals important differences between the three systems (**Fig. 46**).

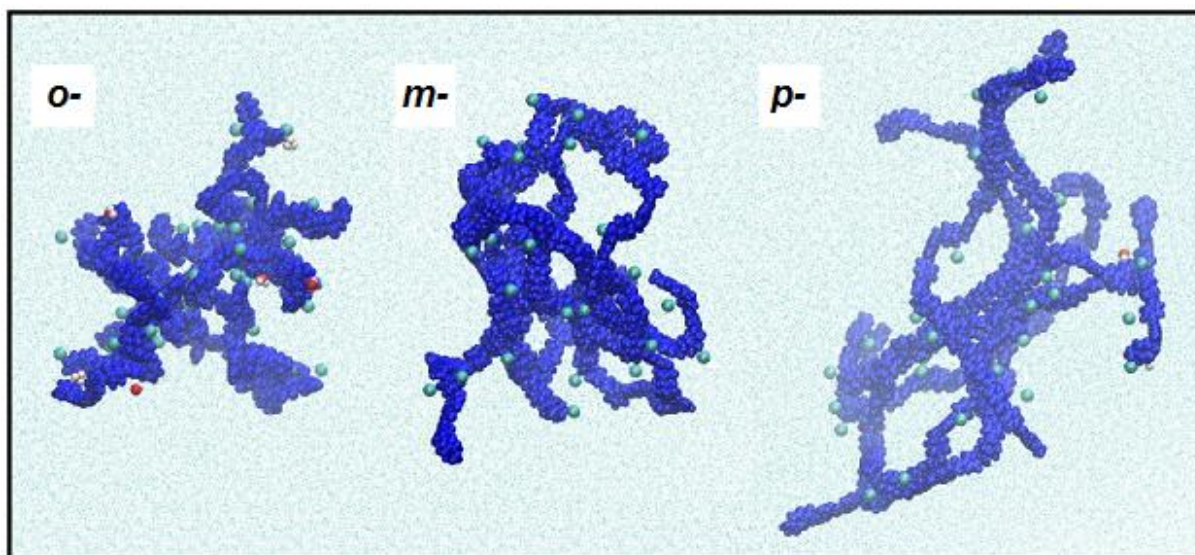


Fig. 46 Last snapshot of the MD simulations performed for ***o*-DABCO**, ***m*-DABCO** and ***p*-DABCO**.

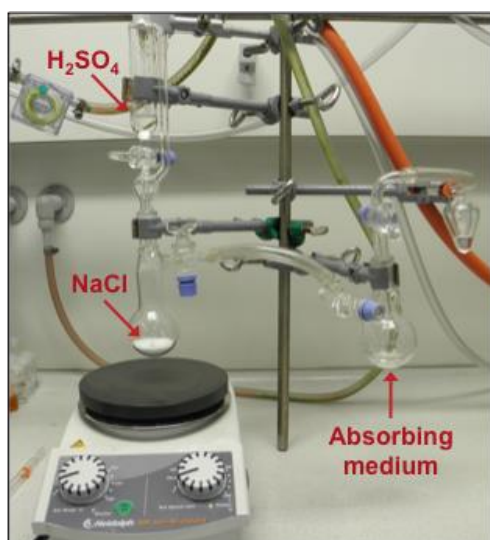
First, the degree of assembly among the polymer chains is different for the three ionenes. Thus, polymer ... polymer interactions dominate on ***o*-DABCO** while the dimensions of the internal hydration areas progressively increase for ***m*-DABCO** and,

especially, **p-DABCO**. Indeed, polymer ... polymer interactions are mainly localized at the central region for the latter. Thus, **o-DABCO** dominates with respect to the other two systems not only in terms of specific interactions (e.g. hydrogen bonds, N-H ... π and π - π), as proved below, but also in van der Waals forces (i.e. steric contacts among the polymer chains).

3.2.3 HCl gas adsorption

Furthermore we investigated the ability of hydrogels from **o-DABCO** to absorb acidic gases by leading a flow of in situ generated HCl over those hydrogels (**Fig. 47**). Comparison between the use of pure water or hydrogel as absorbing media (**Table 4** entry 1 and 2 or 3 and 4 respectively) shows the hydrogel reveals slightly lower absorption ability.

Table 4 Conditions for HCl adsorption experiments with hydrogels derived from **o-DABCO**.



Entry	NaCl [g]	H ₂ SO ₄ [mL]	Water [mL]	Gelator [mg]	Time [h]	Adsorption
1	1.18	1.1	5	-	0.5	5.6 % \equiv 7.6 g/L
2	1.18	1.1	5	225	0.5	3.7 % \equiv 5.3 g/L
3	4.68	4.3	5	-	1.5	15.2 % \equiv 89.4 g/L
4	4.68	4.3	5	500	1.5	12.6 % \equiv 73.7 g/L
5	4.68	4.3	5	225	1.5	12.9 % \equiv 75.2 g/L
6	4.68	4.3	-	500	1.5	7.35 % \equiv 203 mg

Fig. 47 Experimental setup for the determination of HCl absorption.

Increasing the amount of generated HCl by 4 and prolonging the time period of experiment by a factor of 3 leads (

Table 4 entry 1 and 3 or 2 and 4 respectively) leads to an increase of relative absorption by 9.6% and 8.9%, respectively. Varying the concentration of gelator did not lead to a significant difference in absorption. Additionally we could observe HCl absorption by the ionene powder itself which proves an interaction of polymer and HCl gas.

3.3. Experimental Part

3.3.1 Gelation of aqueous acidic solutions

CGC values were estimated by continuously adding aliquots of aqueous solution or water (0.02 - 0.1 mL), respectively into vials containing solid ionenes and performing a typical heating-cooling protocol for gel-formation until no gelation was observed. The starting point for CGC determinations was 200 g L⁻¹. The time that was necessary for gel formation was measured by turning the vials upside down and the point where no flow occurred was considered as being the gelation time. After resting overnight, the samples were heated in a custom made heating block at a rate of about 2 °C / 5 min. Melting points were measured by inverse flow method.

3.3.2 HCl gas adsorption

In a 50 mL Schlenk flask a hydrogel derived from **o-DABCO** (225 or 500 mg in 5 mL) was prepared by a classical heating-cooling protocol. After chilling for 90 min, in situ generated HCl gas was led over the gel. (HCl generation by addition of conc. H₂SO₄ to NaCl). After finishing the gas flow, the gel was transferred quantitatively, with the help of water, to a beaker and the absorbed amount of HCl was determined by titration against 0.1 M NaOH. As control, the same experiment was carried out with 5 mL of pure water.

3.4 Conclusions

The challenging gelation of acidic solutions was achieved using polycations bearing quaternary ammonium moieties. These ionene polymers were synthesized from a disubstituted phenylene dibenzamide core, which allows the construction of different topomers (i.e. **o-DABCO**, **m-DABCO** and **p-DABCO**). Remarkably, the topology of the polymers was found to play a crucial role on their aggregation behaviour both in pure water and in a variety of aqueous acidic solutions leading to the formation of uncommon acidic gels. In particular, **o-DABCO** showed superior gelation ability than the analogues **m-DABCO** and **p-DABCO** in solutions of different pH and ionic strengths. In terms of gel properties, lower critical gelation concentrations, higher gel-to-sol transition temperatures and faster gelation were routinely observed for **o-DABCO** topomer. Finally, atomistic MD simulations on huge models have allowed to conclude that the distinctive properties of **o-DABCO** are due to the formation of specific polymer ... polymer interactions (i.e. hydrogen bonds, N-H ... π and intramolecular π - π stacking), which are facilitated by the binder effect of Cl⁻ counterions.

Both the formation of intramolecular $\pi - \pi$ stacking networks and the role of the Cl^- in the stabilization of specific polymer ... polymer interactions are singular trends with respect to ***m*-DABCO** and ***p*-DABCO**. Thus, the ortho topology favours both the contact among polymer chains and, therefore, the formation of small internal hydration regions. This synergistic combination, which is not possible for the ***m*-DABCO** and ***p*-DABCO**, is responsible of the role played by Cl^- counterions in the superior gelation of the former. Finally, differences between the two latter ionenes have been attributed to the greater strength of intermolecular $\pi - \pi$ stacking in ***m*-DABCO**.

D Summary

In this dissertation the synthesis, characterization and application of smart materials based on low-molecular-weight compounds as well as polymers is described. The first half of this thesis (**chapter B**) deals with a selection of low molecular weight gelators with either synthetic or natural origin.

The first section (**chapter B1**) presents the transfer of a concept which is originally used for the design of new drug molecules, to the rational development of new gelator compounds, namely the isosteric replacement. Here the substitution of the amide function in *N*-stearoyl-L-glutamic acid (C_{18} -Glu) (see Fig. 48) – a compound which is known to be able to act as gelator for several solvents – was replaced by a 1,4-disubstituted 1,2,3-triazole unit (click-Glu) and a sulfonamide (sulfo-Glu), respectively. In both cases the total number of C atoms has formally been kept intact.

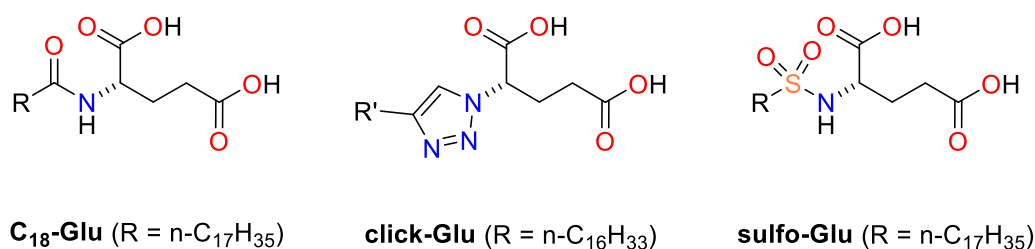


Fig. 48 L-glutamic acid derived gelator molecules described in **chapter B1**.

In terms of gelation of a range of different organic solvents, as well as water, it was found that click-Glu revealed superior features with respect to the CGC, T_{gel} and mechanical stability in polar protic solvents, whereas sulfo-Glu exhibited improved properties in non-polar solvents and C₁₈-Glu showed in average values between those of click-Glu and sulfo-Glu. But not only the characterization of the gel material itself was described but also the successful application of hydrogels derived from all three glutamic acid derivatives as carriers of several hydrophilic and hydrophobic drugs and the subsequent release over a period up to two weeks could be demonstrated which revealed the influence of the functional group in the respective gelator molecules on the release rate of the drugs.

Chapter B2 describes the application of hydrogels, derived from glycyrrhizic acid ammonium salt, as drug depot. Glycyrrhizic acid ammonium salt is a salt of glycyrrhizin, a natural compound which can be extracted from the licorice root.

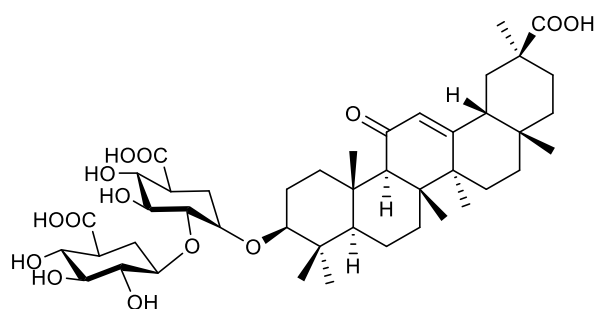


Fig. 49 Structure of glycyrrhizic acid.

It exhibits an excellent biocompatibility, which is why it was chosen for the formulation and drug release study of three anti-cancer agents of different hydrophilicity. The influence of drug inherent hydrophilicity as well as the pH and nature of the release medium on the drug diffusion rate was investigated. In good agreement with previous publications, more hydrophobic compounds were found to tend to a slower diffusion into the release medium as they experience a greater retention from the gel environment. In terms of pH of surrounding medium, the release into more basic solutions was found to be faster as high pH values seemed to destabilize the integrity of the gel network. However the nature of the release buffer (e.g. organic or inorganic) also played an important role, which makes a forecast of the release kinetics, depending on the pH difficult and therefore demonstrates the limitations of *in vitro* drug delivery experiments. Nevertheless, preliminary release studies provide important information necessary for the design of *in vivo* experiments.

A formamidine based low molecular weight compound and its gelation properties are presented in **chapter B3**. The amphiphilic molecule consists of a long chain containing 16 carbon atoms and an acetyl L-phenyl alanine connected via a formamidine group.

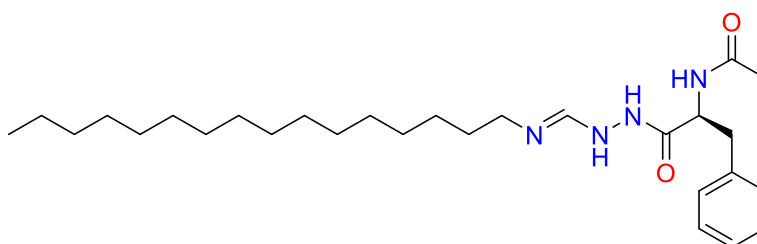


Fig. 50 Formamidine based, amphiphilic gelator compound.

This molecule is able to form gels in a variety of different organic solvents as well as two ionic liquids and water. It was found that ultrasonication of an isotropic solution of the gelator led to superior materials in comparison to gels prepared by the classical heating and spontaneous cooling of gelator solution. Furthermore temperature controlled $^1\text{H-NMR}$ revealed the participation of H-bonding, π - π -stacking, as well as van-der-Waals interactions in the gelation process. Moreover the temperature controlled turning on/off of birefringence of a gel in MeCN could be demonstrated, which constitutes an important property for potential applications in optical devices. Unfortunately this gelator, as well as its hydrogel was found to be toxic, which is why this material could not be used for drug delivery studies.

The second half, **chapter C** of this thesis describes the synthesis of different ionene polymers as well as various applications.

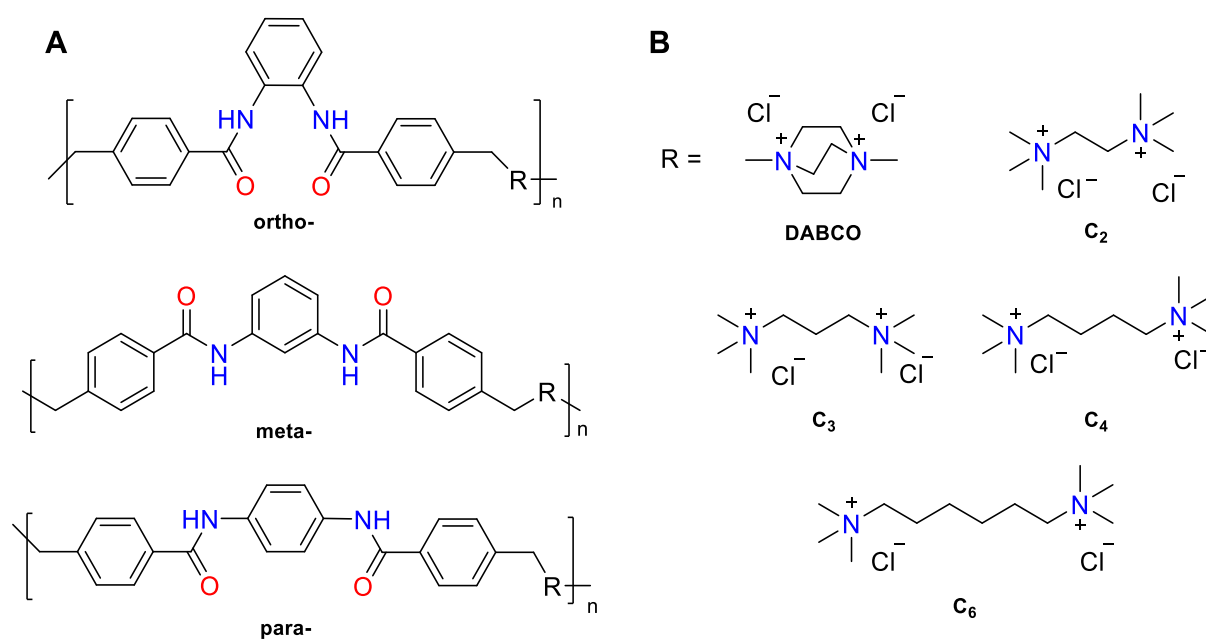


Fig. 51 A) General structures of ionene polymers and **B)** charged diammonium moieties with different structures and chain length.

In **chapter C1** the antimicrobial and hemolytic activity of ionenes (Fig. 51) was investigated. The majority of the polymers showed antimicrobial activity against the Gram-negative bacterium *Escherichia coli*, with minimum inhibition concentration values affected by both the topology of the polymer and the nature of the diamine linker. Most polymers revealed to be harmless towards red blood cells and therefore show a low hemolytic activity. In general, DABCO containing polymers exhibited the

lowest antimicrobial and the highest hemolytic activities. In contrast, meta-ionenes showed the best antimicrobial and lowest hemolytic activity, which makes them promising candidates for potential antimicrobial applications.

In **chapter C2** cationic vesicles derived from ionene polymers with alternating α,ω -tertiary diamine linker (ortho-DABCO, -C₂ and -C₆, see Fig. 51) and the non-ionic surfactant polysorbate 80 are presented. These vesicles were used in different formulations for the transfection of oligonucleotide single strands which are complementary to *Renilla* luciferase mRNA. Formulations based on ortho-DABCO and -C₂ were found to be non-toxic but those with ortho-C₆ showed critical cell viabilities at higher ionene concentrations. When testing the efficiencies of the cationic vesicles to silence the activity of *Renilla* luciferase, those formulations with DABCO-ionene showed no efficacy. On the contrast, C₂- and C₆-ionene derived formulations (at non-toxic ionene concentrations) could reduce the luciferase activity by 48 and 38%, respectively. The use of these formulations might be an interesting alternative to current transfection agents.

Last but not least in **chapter C3** ionenes with DABCO-linker were found to be able to gel water and acidic solutions. Here the topology, the substitution pattern (ortho-, meta- or para-) at the central benzene of the ionenes, was found to play a highly important role for the gelation properties. *Ortho*-DABCO showed superior gelation ability compared to the analogues *meta*-DABCO and *para*-DABCO in solutions of different pH and ionic strengths. Atomistic MD simulations have allowed to conclude that the distinctive properties of *ortho*-DABCO are due to the formation of specific polymer ... polymer interactions (i.e. hydrogen bonds, N-H ... π and intramolecular π - π stacking), which are facilitated by the binder effect of Cl⁻ counterions. Polymer ... polymer interactions are more abundant in *ortho*-DABCO than in *meta*-DABCO and *para*-DABCO which is responsible for the superior gelation of *ortho*-DABCO.

In the annex, projects which are still under investigation are presented.

E Literature

- (1) Zhang, S.; Marini, D. M.; Hwang, W.; Santoso, S. *Curr. Opin. Chem. Biol.* **2002**, *6*, 865–871.
- (2) Philp, D.; Stoddart, J. F. *Angew. Chemie Int. Ed. English* **1996**, *35*, 1154–1196.
- (3) Whitesides, G.; Mathias, J.; Seto, C. *Science* **1991**, *254*, 1312–1319.
- (4) Lin, C.; Liu, Y.; Yan, H. *Biochemistry* **2009**, *48*, 1663–1674.
- (5) Brizard, A. M.; van Esch, J. H. *Soft Matter* **2009**, *5*, 1320.
- (6) Fratzl, P. *J. R. Soc. Interface* **2007**, *4*, 637–642.
- (7) Mann, S. *Nature* **1988**, *332*, 119–124.
- (8) Ball, P. *Nanotechnology* **2002**, *13*, R15–R28.
- (9) Abdallah, D. J.; Weiss, R. G. *Langmuir* **2000**, *16*, 352–355.
- (10) de Loos, M.; van Esch, J.; Kellogg, R. M.; Feringa, B. L. *Angew. Chemie Int. Ed.* **2001**, *40*, 613–616.
- (11) Elemans, J. A. A. W.; Rowan, A. E.; Nolte, R. J. M. *J. Mater. Chem.* **2003**, *13*, 2661–2670.
- (12) Lloyd, D. J. *Colloid Chemistry*; Alexander, J., Ed.; 1st editio.; Chemical Catalogue Company: New York, USA, 1926.
- (13) Graham, T. *J. Chem. Soc.* **1864**, *17*, 318–327.
- (14) Flory, P. J. *Faraday Discuss. Chem. Soc.* **1974**, *57*, 7.
- (15) Ajayaghosh, A.; Praveen, V. K.; Vijayakumar, C. *Chem. Soc. Rev.* **2008**, *37*, 109–122.
- (16) Jung, J. H.; Park, M.; Shinkai, S. *Chem. Soc. Rev.* **2010**, *39*, 4286.
- (17) Sangeetha, N. M.; Maitra, U. *Chem. Soc. Rev.* **2005**, *34*, 821–836.
- (18) Hirst, A. R.; Escuder, B.; Miravet, J. F.; Smith, D. K. *Angew. Chemie - Int. Ed.* **2008**, *47*, 8002–8018.
- (19) Díaz Díaz, D.; Kühbeck, D.; Koopmans, R. J. *Chem. Soc. Rev.* **2011**, *40*, 427–448.
- (20) Abdallah, D. J.; Weiss, R. G. *Adv. Mater.* **2000**, *12*, 1237–1247.
- (21) Estroff, L. a; Hamilton, A. D. **2004**, *104*, 1201–1218.
- (22) Terech, P.; Weiss, R. G. *Chem. Rev.* **1997**, *97*, 3133–3160.
- (23) Dastidar, P. *Chem. Soc. Rev.* **2008**, *37*, 2699.
- (24) Suzuki, M.; Hanabusa, K. *Chem. Soc. Rev.* **2010**, *39*, 455–463.
- (25) von Lipowitz, A. *Justus Liebig's Ann. der Chemie* **1841**, *38*, 348–355.
- (26) Cravotto, G.; Cintas, P. *Chem. Soc. Rev.* **2009**, *38*, 2684.

- (27) Bardelang, D. *Soft Matter* **2009**, *5*, 1969.
- (28) Philippova, O. E.; Hourdet, D.; Audebert, R.; Khokhlov, A. R. *Macromolecules* **1997**, *30*, 8278–8285.
- (29) Nguyen, T. D.; Leung, K. C.-F.; Liong, M.; Pentecost, C. D.; Stoddart, J. F.; Zink, J. I. *Org. Lett.* **2006**, *8*, 3363–3366.
- (30) Yang, Z.; Xu, B. *Adv. Mater.* **2006**, *18*, 3043–3046.
- (31) van Esch, J. H.; Feringa, B. L. *Angew. Chemie Int. Ed.* **2000**, *39*, 2263–2266.
- (32) Gronwald, O.; Shinkai, S. *Chem. - A Eur. J.* **2001**, *7*, 4328–4334.
- (33) Yu, G.; Yan, X.; Han, C.; Huang, F. *Chem. Soc. Rev.* **2013**, *42*, 6697–6722.
- (34) Kumar Vemula, P.; Aslam, U.; Ajay Mallia, V.; John, G. *Chem. Mater.* **2007**, *19*, 138–140.
- (35) Boettcher, C.; Schade, B.; Fuhrhop, J.-H. *Langmuir* **2001**, *17*, 873–877.
- (36) Gao, P.; Zhan, C.; Liu, L.; Zhou, Y.; Liu, M. *Chem. Commun.* **2004**, 1174.
- (37) Bachl, J.; Mayr, J.; Sayago, F. J.; Cativiela, C.; Díaz Díaz, D. *Chem. Commun.* **2015**, *51*, 5294–5297.
- (38) George, M.; Weiss, R. G. *Acc. Chem. Res.* **2006**, *39*, 489–497.
- (39) De Loos, M.; Feringa, B. L.; Van Esch, J. H. *European J. Org. Chem.* **2005**, 3615–3631.
- (40) Nayak, S.; Lyon, L. A. *Angew. Chemie Int. Ed.* **2005**, *44*, 7686–7708.
- (41) Song, S.; Tian, B.; Chen, F.; Zhang, W.; Pan, Y.; Zhang, Q.; Yang, X.; Pan, W. *Drug Dev. Ind. Pharm.* **2015**, *41*, 51–62.
- (42) Ahmad, M. Z.; Mohammed, A. A.; Ibrahim, M. M. *Pharm. Dev. Technol.* **2016**, *7450*, 1–10.
- (43) Ahmad, M. Z.; Akhter, S.; Mohsin, N.; Abdel-Wahab, B. A.; Ahmad, J.; Warsi, M. H.; Rahman, M.; Mallick, N.; Ahmad, F. J. *Curr. Drug Discov. Technol.* **2014**, *11*, 197–213.
- (44) Hubbell, J. A.; Chilkoti, A. *Science* **2012**, *337*, 303–305.
- (45) Lin, R.; Cui, H. *Curr. Opin. Chem. Eng.* **2015**, *7*, 75–83.
- (46) Ahmad, M. Z.; Akhter, S.; Rahman, Z.; Akhter, S.; Anwar, M.; Mallik, N.; Ahmad, F. J. *J. Pharm. Pharmacol.* **2013**, *65*, 634–651.
- (47) Ahmad, M. Z.; Alkahtani, S. A.; Akhter, S.; Ahmad, F. J.; Ahmad, J.; Akhtar, M. S.; Mohsin, N.; Abdel-Wahab, B. A. *J. Drug Target.* **2016**, *24*, 273–293.
- (48) Renard, E.; Baldet, P.; Picot, M. C.; Jacques-Apostol, D.; Lauton, D.; Costalat, G.; Bringer, J.; Jaffiol, C. *Diabetes Care* **1995**, *18*, 300–306.

- (49) Ernsting, M. J.; Murakami, M.; Roy, A.; Li, S.-D. *J. Control. Release* **2013**, *172*, 782–794.
- (50) Shenderova, A.; Burke, T. G.; Schwendeman, S. P. *Pharm. Res.* **1997**, *14*, 1406–1414.
- (51) Xiang, N.; Zhou, X.; He, X.; Zhang, Y.; Zhang, J.; Zhang, Z. R.; Sun, X.; Gong, T.; Fu, Y. *J. Pharm. Sci.* **2016**, *105*, 1148–1155.
- (52) Hardy, W. B. *J. Phys. Chem.* **1900**, *4*, 254–273.
- (53) Xu, B. *Langmuir* **2009**, *25*, 8375–8377.
- (54) Appel, E. A.; Tibbitt, M. W.; Webber, M. J.; Mattix, B. A.; Veiseh, O.; Langer, R. *Nat. Commun.* **2015**, *6*, 6295.
- (55) Bae, Y. H. In *Controlled Drug Delivery: Challenge and Strategies*; Park, K., Ed.; American Chemical Society: Washington, 1997; pp. 147–160.
- (56) Hoffman, A. S. In *Controlled Drug Delivery: Challenge and Strategies*; Park, K., Ed.; American Chemical Society: Washington, 1997; pp. 485–497.
- (57) Langdon, S. R.; Ertl, P.; Brown, N. *Mol. Inform.* **2010**, *29*, 366–385.
- (58) *Bioisosteres in Medicinal Chemistry*; Brown, N., Ed.; 54th ed.; Wiley-VCH: Weinheim, 2012.
- (59) Langmuir, I. *J. Am. Chem. Soc.* **1919**, *41*, 1543–1559.
- (60) Grimm, H. G. *Naturwissenschaften* **1929**, *17*, 557–5564.
- (61) Erlenmeyer, H.; Leo, M. *Helv. Chim. Acta* **1932**, *15*, 1171–1186.
- (62) Friedman, H. L. *NASNRS* **1951**, *206*, 295–358.
- (63) Thornber, C. W. *Chem. Soc. Rev.* **1979**, *8*, 563.
- (64) Burger, A. *Prog. Drug Res.* **1991**, *37*, 287–371.
- (65) Angell, Y. L.; Burgess, K. *Chem. Soc. Rev.* **2007**, *36*, 1674.
- (66) Holub, J. M.; Kirshenbaum, K. *Chem. Soc. Rev.* **2010**, *39*, 1325.
- (67) Corredor, M.; Bujons, J.; Orzáez, M.; Sancho, M.; Pérez-Payá, E.; Alfonso, I.; Messeguer, A. *Eur. J. Med. Chem.* **2013**, *63*, 892–896.
- (68) Hamada, Y.; Kiso, Y. *Expert Opin. Drug Discov.* **2012**, *7*, 903–922.
- (69) Tron, G. C.; Pirali, T.; Billington, R. A.; Canonico, P. L.; Sorba, G.; Genazzani, A. A. *Med. Res. Rev.* **2008**, *28*, 278–308.
- (70) Chow, H.-F.; Lau, K.-N.; Ke, Z.; Liang, Y.; Lo, C.-M. *Chem. Commun.* **2010**, *46*, 3437.
- (71) Oh, K.; Guan, Z. *Chem. Commun.* **2006**, 3069–3071.
- (72) Mujumdar, P.; Poulsen, S.-A. *J. Nat. Prod.* **2015**, *78*, 1470–1477.

- (73) Mujumdar, P.; Teruya, K.; Tonissen, K. F.; Vullo, D.; Supuran, C. T.; Peat, T. S.; Poulsen, S.-A. *J. Med. Chem.* **2016**, *59*, 5462–5470.
- (74) Chinthakindi, P. K.; Naicker, T.; Thota, N.; Govender, T.; Kruger, H. G.; Arvidsson, P. I. *Angew. Chemie Int. Ed.* **2016**, *56*, 2–12.
- (75) Fieser, L. F.; Fieser, M. *Lehrbuch der organischen Chemie*; 3rd ed.; Verlag Chemie: Weinheim a. d. Bergstraße, 1957.
- (76) Török, E.; Moran, E.; Cooke, F. *Oxford Handbook of Infectious Diseases and Microbiolog*; OUP: Oxford, 2009.
- (77) Domagk, G. *Dtsch. Medizinische Wochenschrift* **1935**, *61*, 250–253.
- (78) Uday, K.; Amandeep, K. *Res. J. Pharm. Biol. Chem. Sci.* **2011**, *2*, 1116–1135.
- (79) Gupta, A.; Sharma, A.; Dhiman, N.; Mallikarjun, B. P. *World J. Pharm. Pharm. Sci.* **2016**, *5*, 328–338.
- (80) Rostovtsev, V. V.; Green, L. G.; Fokin, V. V.; Sharpless, K. B. *Angew. Chemie - Int. Ed.* **2002**, *41*, 2596–2599.
- (81) Overstreet, D. J.; Huynh, R.; Jarbo, K.; McLemore, R. Y.; Vernon, B. L. *J. Biomed. Mater. Res.* **2013**, *101*, 1437–1446.
- (82) Morris, J. J.; Hughes, L. R.; Glen, A. T.; Taylor, P. J. *J. Med. Chem.* **1991**, *34*, 447–455.
- (83) Hansch, C.; Hoekman, D.; Leo, A.; Zhang, L.; Li, P. *Toxicol. Lett.* **1995**, *79*, 45–53.
- (84) Habermann, J. *Justus Liebig's Ann. der Chemie* **1879**, *59*, 105–125.
- (85) Tykarska, E.; Sobiak, S.; Gdaniec, M. *Cryst. Growth Des.* **2012**, *12*, 2133–2137.
- (86) Tykarska, E.; Gdaniec, M. *Cryst. Growth Des.* **2013**, *13*, 1301–1308.
- (87) Kiso, Y.; Tohkin, M.; Hikino, H.; Hattori, M.; Sakamoto, T.; Namba, T. *Planta Med.* **1984**, *50*, 298–302.
- (88) van Rossum, T. G.; Vullo, A. G.; de Man, R. A.; Brouwer, J. T.; Schalm, S. W. *Aliment. Pharmacol. Ther.* **1998**, *12*, 199–205.
- (89) Yano, S.; Harada, M.; Watanabe, K.; Nakamaru, K.; Hatakeyama, Y.; Shibata, S.; Takahashi, K.; Mori, T.; Hirabayashi, K.; Takeda, M.; Nagata, N. *Chem. Pharm. Bull. (Tokyo)*. **1989**, *37*, 2500–2504.
- (90) Kuroyanagi, T.; Kurisu, A.; Sugiyama, H.; Saito, M. *Japanese J. Med. Prog.* **1962**, *49*, 458–465.
- (91) Finney, R. S. H.; Tárnoky, A. L. *J. Pharm. Pharmacol.* **1960**, *12*, 49–58.

- (92) Pompei, R.; Flore, O.; Marccialis, M. A.; Pani, A.; Loddo, B. *Nature* **1979**, *281*, 689–690.
- (93) Soltész, J.; Uri, J. *Naturwissenschaften* **1963**, *50*, 691.
- (94) Segal, R.; Pisanty, S.; Azaz, E. Topical pharmaceutical compositions containing glycyrrhizin. GB 2167296, 1986.
- (95) Stuer-Lauridsen, F.; Birkved, M.; Hansen, L. P.; Holten Lützhøft, H.-C.; Halling-Sørensen, B. *Chemosphere* **2000**, *40*, 783–793.
- (96) Raghunand, N.; Mahoney, B. P.; Gillies, R. J. *Biochem. Pharmacol.* **2003**, *66*, 1219–1229.
- (97) Díaz, D. D.; Finn, M. G. *Chem. - A Eur. J.* **2004**, *10*, 303–309.
- (98) Díaz, D. D.; Finn, M. G. *Chem. Commun. (Camb)*. **2004**, 2514–2516.
- (99) Billack, B.; Heck, D. E.; Porterfield, D. M.; Malchow, R. P.; Smith, P. J. S.; Gardner, C. R.; Laskin, D. L.; Laskin, J. D. *Biochem. Pharmacol.* **2001**, *61*, 1581–1586.
- (100) Hougaard, C.; Hammami, S.; Eriksen, B. L.; Sørensen, U. S.; Jensen, M. L.; Strøbæk, D.; Christophersen, P. *Mol. Pharmacol.* **2011**, *81*, 210–219.
- (101) Huang, J.; Hamasaki, T.; Ozoe, Y. *Arch. Insect Biochem. Physiol.* **2010**, *73*, 74–86.
- (102) Kim, E. J.; Shin, H. S.; Ryu, S. Y.; Lee, B. H.; Cho, S. H. *Arch. Pharm. Res.* **1995**, *18*, 1–7.
- (103) Chang, K.-M.; Knowles, C. O. *J. Agric. Food Chem.* **1977**, *25*, 493–501.
- (104) Matsumura, F.; Beeman, R. W. *Environ. Health Perspect.* **1976**, *14*, 71–82.
- (105) Lund, A. E.; Hollingworth, R. M.; Yim, G. K. W. *Neurotoxicol. Insectic. Pheromones, [Proc. Symp.]* **1979**, 119–137.
- (106) Hollingworth, R. M. *Environ. Health Perspect.* **1976**, *14*, 57–69.
- (107) Proudfoot, A. T. *Toxicol. Rev.* **2003**, *22*, 71–74.
- (108) Kik, K.; Studzian, Kazimierz Wasowska-Lukawska, M.; Oszczapowicz, Irena Szmigiero, L. *Acta Biochim. Pol.* **2003**, *56*, 135–142.
- (109) Chan, Z.-K.; Chen, T.-R.; Chen, J.-D.; Wang, J.-C.; Liu, C. W. *Dalt. Trans.* **2007**, 3450.
- (110) Junk, P. C.; Cole, M. L. *Chem. Commun.* **2007**, 1579.
- (111) Yang, P.-Y.; Chang, F.-C.; Suen, M.-C.; Chen, J.-D.; Keng, T.-C.; Wang, J.-C. *J. Organomet. Chem.* **2000**, *596*, 226–231.

- (112) Tortajada, J.; Leon, E.; Luna, A.; Mo, O.; Yanez, M. *J. Phys. Chem.* **1994**, *98*, 12919–12926.
- (113) Derossi, D.; Y, K.; Osada, Y. *Polymer Gels: Fundamentals and Biomedical Applications*; Plenum Press: New York, 1991.
- (114) Ilmain, F.; Tanaka, T.; Kokufuta, E. *Nature* **1991**, *349*, 400–401.
- (115) Osada, Y.; Khokhlov, A. R. *Polymer Gels and Networks*; Dekker, M., Ed.; CRC Press: New York, 2002.
- (116) Malicka, J. M.; Sandeep, A.; Monti, F.; Bandini, E.; Gazzano, M.; Ranjith, C.; Praveen, V. K.; Ajayaghosh, A.; Armaroli, N. *Chem. - A Eur. J.* **2013**, *19*, 12991–13001.
- (117) Naota, T.; Koori, H. *J. Am. Chem. Soc.* **2005**, *127*, 9324–9325.
- (118) Paulusse, J. M. J.; Sijbesma, R. P. *Angew. Chemie Int. Ed.* **2006**, *45*, 2334–2337.
- (119) Paulusse, J. M. J.; van Beek, D. J. M.; Sijbesma, R. P. *J. Am. Chem. Soc.* **2007**, *129*, 2392–2397.
- (120) Fauci, A. S.; Touchette, N. A.; Folkers, G. K. *Emerg. Infect. Dis.* **2005**, *11*, 519–525.
- (121) Fan, Z.; Senapati, D.; Khan, S. A.; Singh, A. K.; Hamme, A.; Yust, B.; Sardar, D.; Ray, P. C. *Chemistry* **2013**, *19*, 2839–2847.
- (122) Eren, T.; Som, A.; Rennie, J. R.; Nelson, C. F.; Urgina, Y.; Nüsslein, K.; Coughlin, E. B.; Tew, G. N. *Macromol. Chem. Phys.* **2008**, *209*, 516–524.
- (123) Gould, I. M. *J. Antimicrob. Chemother.* **1999**, *43*, 459–465.
- (124) Stone, A. *Nat. Rev. Drug Discov.* **2002**, *1*, 977–985.
- (125) Boucher, H. W.; Talbot, G. H.; Bradley, J. S.; Edwards, J. E.; Gilbert, D.; Rice, L. B.; Scheld, M.; Spellberg, B.; Bartlett, J. *Clin. Infect. Dis.* **2009**, *48*, 1–12.
- (126) Álvarez-Paino, M.; Muñoz-Bonilla, A.; López-Fabal, F.; Gómez-Garcés, J. L.; Heuts, J. P. A.; Fernández-García, M. *Biomacromolecules* **2015**, *16*, 295–303.
- (127) Talbot, G. H.; Bradley, J.; Edwards Jr., J. E.; Gilbert, D.; Scheld, M.; Bartlett, J. G. *Clin. Infect. Dis.* **2006**, *42*, 657–668.
- (128) Köck, R.; Becker, K.; Cookson, B.; van Gemert-Pijnen, J. E.; Harbarth, S.; Kluytmans, J.; Mielke, M.; Peters, G.; Skov, R. L.; Struelens, M. J.; Tacconelli, E.; Navarro Torné, A.; Witte, W.; Friedrich, A. W. *Euro Surveill.* **2010**, *15*, 19688.

- (129) Wong, E. H. H.; Khin, M. M.; Ravikumar, V.; Si, Z.; Rice, S. A.; Chan-Park, M. B. *Biomacromolecules* **2016**, *17*, 1170–1178.
- (130) Wenzel, M.; Chiriac, A. I.; Otto, A.; Zweytick, D.; May, C.; Schumacher, C.; Gust, R.; Albada, H. B.; Penkova, M.; Krämer, U.; Erdmann, R.; Metzler-Nolte, N.; Straus, S. K.; Bremer, E.; Becher, D.; Brötz-Oesterhelt, H.; Sahl, H.-G.; Bandow, J. E. *Proc. Natl. Acad. Sci. U. S. A.* **2014**, *111*, E1409-18.
- (131) Mohanram, H.; Bhattacharjya, S. *Antimicrob. Agents Chemother.* **2014**, *58*, 1987–1996.
- (132) Thomassin, J. M.; Lenoir, S.; Riga, J.; Jérôme, R.; Detrembleur, C. *Biomacromolecules* **2007**, *8*, 1171–1177.
- (133) Fuchs, A. D.; Tiller, J. C. *Angew. Chemie Int. Ed.* **2006**, *45*, 6759–6762.
- (134) Riva, R.; Lussis, P.; Lenoir, S.; Jérôme, C.; Jérôme, R.; Lecomte, P. *Polymer (Guildf)*. **2008**, *49*, 2023–2028.
- (135) Gabriel, G. J.; Som, A.; Madkour, A. E.; Eren, T.; Tew, G. N. *Mater. Sci. Eng. R. Rep.* **2007**, *57*, 28–64.
- (136) Lenoir, S.; Pagnouille, C.; Detrembleur, C.; Galleni, M.; Jérôme, R. *J. Polym. Sci. Part A Polym. Chem.* **2006**, *44*, 1214–1224.
- (137) Nonaka, T.; Hua, L.; Ogata, T.; Kurihara, S. *J. Appl. Polym. Sci.* **2003**, *87*, 386–393.
- (138) Punyani, S.; Singh, H. *J. Appl. Polym. Sci.* **2006**, *102*, 1038–1044.
- (139) Zelikin, A. N.; Putnam, D.; Shastri, P.; Langer, R.; Izumrudov, V. A. *Bioconjug. Chem.* **2002**, *13*, 548–553.
- (140) Laschewsky, A. *Curr. Opin. Colloid Interface Sci.* **2012**, *17*, 56–63.
- (141) Williams, Sharlene R.; Long, T. E. *Prog. Polym. Sci.* **2009**, *34*, 762–782.
- (142) Domagk, G. *Dtsch. Medizinische Wochenschrift* **1935**, *61*, 829–832.
- (143) Wilkoff, L. J.; Dixon, G. J.; Westbrook, L.; Happich, W. F. *Appl. Envir. Microbiol.* **1971**, *21*, 647–652.
- (144) Prickett, J. M.; Rawal, B. D. *Lab. Pract.* **1972**, *21*, 425–428.
- (145) Vesley, D.; Klapes, N. A.; Benzow, K.; Le, C. T. *Appl. Envir. Microbiol.* **1987**, *53*, 1042–1045.
- (146) Payne, J. B.; Kroger, E. C.; Watkins, S. E. *J. Appl. Poult. Res.* **2005**, *14*, 322–329.
- (147) Melin, V. E.; Melin, T. E.; Dessify, B. J.; Nguyen, C. T.; Shea, C. S.; Hrubec, T. C. *Reprod. Toxicol.* **2016**, *59*, 159–166.

- (148) Xue, Y.; Xiao, H.; Zhang, Y. *Int. J. Mol. Sci.* **2015**, *16*, 3626–3655.
- (149) Dizman, B.; Elasri, M. O.; Mathias, L. J. *J. Appl. Polym. Sci.* **2004**, *94*, 635–642.
- (150) Abel, T.; Cohen, J. I.; Engel, R.; Filshtinskaya, M.; Melkonian, A.; Melkonian, K. *Carbohydr. Res.* **2002**, *337*, 2495–2499.
- (151) Bachl, J.; Zanuy, D.; L6pez-P6rez, D. E.; Revilla-L6pez, G.; Cativiela, C.; Alem6n, C.; D6az, D. D. *Adv. Funct. Mater.* **2014**, *24*, 4893–4904.
- (152) Misawa, Y.; Koumura, N.; Matsumoto, H.; Tamaoki, N.; Yoshida, M. *Macromolecules* **2008**, *41*, 8841–8846.
- (153) Dragan, E. S.; Mayr, J.; H6ring, M.; Cocarta, A. I.; D6az, D. D. *ACS Appl. Mater. Interfaces* **2016**, *8*, 30908–30919.
- (154) Fischer, D.; Li, Y.; Ahlemeyer, B.; Krieglstein, J.; Kissel, T. *Biomaterials* **2003**, *24*, 1121–1131.
- (155) Sellenet, P. H.; Allison, B.; Applegate, B. M.; Youngblood, J. P. *Biomacromolecules* **2007**, *8*, 19–23.
- (156) Stephenson, M. L.; Zamecnik, P. C. *Proc. Natl. Acad. Sci.* **1978**, *75*, 285–288.
- (157) Watts, J.; Deleavey, G.; Damha, M. *Drug Discov. Today* **2008**, *13*, 842–855.
- (158) Keefe, A. D.; Pai, S.; Ellington, A. *Nat. Rev. Drug Discov.* **2010**, *9*, 537–550.
- (159) Mulhbachter, J.; St-Pierre, P.; Lafontaine, D. A. *Curr. Opin. Pharmacol.* **2010**, *10*, 551–556.
- (160) Niks, E. H.; Aartsma-Rus, A. *Expert Opin. Biol. Ther.* **2017**, *17*, 225–236.
- (161) Chiu, Y.-L. *RNA* **2003**, *9*, 1034–1048.
- (162) Terrazas, M.; Alagia, A.; Faustino, I.; Orozco, M.; Eritja, R. *ChemBioChem* **2013**, *14*, 510–520.
- (163) Geary, R.; Tillman, L.; Hardee, G. In *Antisense Drug Technology*; CRC Press, 2007; pp. 217–236.
- (164) Felgner, P. L.; Gadek, T. R.; Holm, M.; Roman, R.; Chan, H. W.; Wenz, M.; Northrop, J. P.; Ringold, G. M.; Danielsen, M. *Proc. Natl. Acad. Sci.* **1987**, *84*, 7413–7417.
- (165) Azzam, T.; Domb, A. *Curr. Drug Deliv.* **2004**, *1*, 165–193.
- (166) Grijalvo, S.; Alagia, A.; Puras, G.; Z6rate, J.; Pedraz, J. L.; Eritja, R. *Colloids Surfaces B Biointerfaces* **2014**, *119*, 30–37.
- (167) Audouy, S.; Molema, G.; de Leij, L.; Hoekstra, D. *J. Gene Med.* **2000**, *2*, 465–476.

- (168) Lv, H.; Zhang, S.; Wang, B.; Cui, S.; Yan, J. *J. Control. Release* **2006**, *114*, 100–109.
- (169) Zhang, P.; Wagner, E. *Top. Curr. Chem.* **2017**, *375*, 26.
- (170) Williams, S. R.; Long, T. E. *Prog. Polym. Sci.* **2009**, *34*, 762–782.
- (171) Tiffner, M.; Zielke, K.; Mayr, J.; Häring, M.; Díaz Díaz, D.; Waser, M. *ChemistrySelect* **2016**, *1*, 4030–4033.
- (172) Yudovin-Farber, I.; Yanay, C.; Azzam, T.; Linial, M.; Domb, A. J. *Bioconjug. Chem.* **2005**, *16*, 1196–1203.
- (173) San Juan, A.; Letourneur, D.; Izumrudov, V. A. **2007**, 922–928.
- (174) Reineke, T. M.; Davis, M. E. *Mater. Res. Soc. Symp. Proc.* **2002**, *724*, 209–214.
- (175) Wheeler, C. J. Complex cationic lipids having quaternary nitrogen therein. US8541628 B2, 2003.
- (176) Jorge, A. F.; Dias, R. S.; Pereira, J. C.; Pais, A. A. C. C. *Biomacromolecules* **2010**, *11*, 2399–2406.
- (177) Mezei, A.; Pons, R. *Colloids Surfaces B Biointerfaces* **2014**, *123*, 279–285.
- (178) Leal, C.; Wadsö, L.; Olofsson, G.; Miguel, M.; Wennerström, H. *J. Phys. Chem. B* **2004**, *108*, 3044–3050.
- (179) Mezei, A.; Pons, R.; Morán, M. C. *Colloids Surfaces B Biointerfaces* **2013**, *111*, 663–671.
- (180) Mandelkern, M.; Elias, J. G.; Eden, D.; Crothers, D. M. *J. Mol. Biol.* **1981**, *152*, 153–161.
- (181) Mosmann, T. *J. Immunol. Methods* **1983**, *65*, 55–63.
- (182) Xiong, F.; Mi, Z.; Gu, N. *Pharmazie* **2011**, *66*, 158–164.
- (183) Rehman, Z. ur; Hoekstra, D.; Zuhorn, I. S. *ACS Nano* **2013**, *7*, 3767–3777.
- (184) Grijalvo, S.; Eritja, R. *Mol. Divers.* **2012**, *16*, 307–317.
- (185) Mayr, J.; Bachl, J.; Schlossmann, J.; Díaz, D. *Int. J. Mol. Sci.* **2017**, *18*, 303.
- (186) Metwally, A. A.; Pourzand, C.; Blagbrough, I. S. *Pharmaceutics* **2011**, *3*, 125–140.
- (187) Netz, R. R.; Andelman, D. *Phys. Rep.* **2003**, *380*, 1–95.
- (188) Grosberg, A. Y.; Nguyen, T. T.; Shklovskii, B. I. *Rev. Mod. Phys.* **2002**, *74*, 329–345.
- (189) Poinsignon, C. *Mater. Sci. Eng. B* **1989**, *3*, 31–37.
- (190) Jaeger, W.; Bohrisch, J.; Laschewsky, A. *Prog. Polym. Sci.* **2010**, *35*, 511–577.

- (191) Werner, C. *Advances in Polymer Science: Polymers for Regenerative Medicine*; Springer: Dresden, 2006.
- (192) Kourai, H.; Yabuhara, T.; Shirai, A.; Maeda, T.; Nagamune, H. *Eur. J. Med. Chem.* **2006**, *41*, 437–444.
- (193) Zelikin, A. N.; Putnam, D.; Shastri, P.; Langer, R.; Izumrudov, V. A. *Bioconjug. Chem.* **2002**, *13*, 548–553.
- (194) Bortel, E.; Kochanowski, A.; Siniarska, B.; Wiek, E. *Polish J. Appl. Chem.* **2001**, *44*, 55–77.
- (195) Noguchi, H. *Polymeric materials encyclopedia*; Salomone, J. C., Ed.; CRC Press: Boca Raton, London, New York, Tokyo, 1996.
- (196) Littmann, E. R.; Marvel, C. S. *J. Am. Chem. Soc.* **1930**, *52*, 287–294.
- (197) Gibbs, C. F.; Littmann, E. R.; Marvel, C. S. *J. Am. Chem. Soc.* **1933**, *55*, 753–757.
- (198) Friedman, M. *J. Agric. Food Chem.* **2003**, *51*, 4504–4526.
- (199) Oh, J. K.; Drumright, R.; Siegwart, D. J.; Matyjaszewski, K. *Prog. Polym. Sci.* **2008**, *33*, 448–477.
- (200) Yoshida, M. *Synthesiology* **2012**, *5*, 181–189.
- (201) Schlick, S. *Ionomers: Characterization, Theory, and Applications*; CRC Press: Boca Raton, 1996.
- (202) Tant, M. R.; Mauritz, K. A.; Wilkes, G. L. *Ionomers: Synthesis, Structure, Properties, and Applications*; Blackie Academic and Professional: London, 1997.
- (203) Kovalenko, A.; Kobryn, A. E.; Gusarov, S.; Lyubimova, O.; Liu, X.; Blinov, N.; Yoshida, M. *Soft Matter* **2012**, *8*, 1508–1520.
- (204) He, Y.; Tsao, H.-K.; Jiang, S. *J. Phys. Chem. B* **2012**, *116*, 5766–5770.
- (205) Lee, S. G.; Brunello, G. F.; Jang, S. S.; Bucknall, D. G. *Biomaterials* **2009**, *30*, 6130–6141.
- (206) Jang, S. S.; Goddard, W. A.; Kalani, M. Y. S.; Myung, D.; Frank, C. W. *J. Phys. Chem. B* **2007**, *111*, 14440–14440.
- (207) Takewaki, T.; Beck, L. W.; Davis, M. E. *Microporous Mesoporous Mater.* **1999**, *33*, 197–207.
- (208) Omidian, H.; Rocca, J. G. Superporous hydrogels for heavy-duty applications, such as the low pH environment of the gastric fluid of the stomach. US20080089940 A1, 2008.

- (209) Xuan, J.-J.; Yan, Y.-D.; Oh, D. H.; Choi, Y. K.; Yong, C. S.; Choi, H.-G. *Drug Deliv.* **2011**, *18*, 305–311.
- (210) Suzuki, M.; Owa, S.; Yumoto, M.; Kimura, M.; Shirai, H.; Hanabusa, K. *Tetrahedron Lett.* **2004**, *45*, 5399–5402.
- (211) Suzuki, M.; Yumoto, M.; Kimura, M.; Shirai, H.; Hanabusa, K. *Tetrahedron Lett.* **2004**, *45*, 2947–2950.
- (212) Yamanaka, M.; Higashi, D. Substituted aromatic compound, its use as hydrogelation agent, hydrogel, and method for gelating aqueous sample in for examples coatings, plastics, and pharmaceutical fields. WO2012121394 A1, 2012.
- (213) Hwang, I.; Jeon, W. S.; Kim, H.-J.; Kim, D.; Kim, H.; Selvapalam, N.; Fujita, N.; Shinkai, S.; Kim, K. *Angew. Chemie Int. Ed.* **2007**, *46*, 210–213.
- (214) Eldridge, J. E.; Ferry, J. D. *J. Phys. Chem.* **1954**, *58*, 992–995.
- (215) Bachl, J.; Bertran, O.; Mayr, J.; Alemán, C.; Díaz Díaz, D. *Soft Matter* **2017**.
- (216) Nagasawa, J.; Matsumoto, H.; Yoshida, M. *ACS Macro Lett.* **2012**, *1*, 1108–1112.
- (217) Yoshida, M.; Koumura, N.; Misawa, Y.; Tamaoki, N.; Matsumoto, H.; Kawanami, H.; Kazaoui, S.; Minami, N. *J. Am. Chem. Soc.* **2007**, *129*, 11039–11041.
- (218) Mayr, J.; Grijalvo, S.; Bachl, J.; Rons, R.; Eritja, R.; Díaz Díaz, D. *Int. J. Mol. Sci.* **2017**.

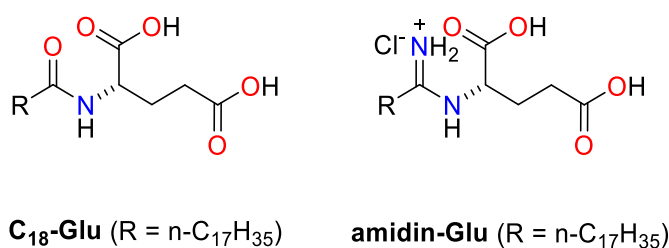
F Annexes

In this section, projects are presented which unfortunately did not deliver the desired results but still have the potential for other future applications.

1. Amidine-Glu

1.1 Aim

With the aim to create another gelator by isosteric replacement one further derivative of N-stearoyl-L-glutamic acid C₁₈-Glu was attempted to be synthesized. In this case we replaced the amide by an amidine function (**amidine-Glu**).



1.2 Results

Amidine-Glu was synthesized via a two-step reaction. Briefly, first an ice-cold solution of stearonitrile and EtOH in Et₂O was treated with a flow of *in-situ* generated HCl gas. The resulting precipitate and L-glutamic acid were dissolved in DMSO, heated mildly to obtain a clear solution which was then stirred for 4 days at room temperature. Both steps achieved only quite poor yields and reproduction was not trivial. Nevertheless preliminary gelation experiments were performed. According to the gelation behaviour of its predecessors **C₁₈**-, **click**- and **sulfo-Glu**, organic solvents were tested first. However, **amidine-Glu** did not show gelation ability in most of the tested organic solvents including polar protic MeOH, polar non-protic like MeCN or unpolar solvents like DCM or silicon oil (**Table 5A**). The only organic solvent that led to a stable gel with **amidine-Glu** was DMSO. Probably the ionic structure of amidine-Glu hinders a gel-formation in the majority of organic solvents. In contrast to this, several 1 M solutions of strong acids (HCl, HBr, HI, H₂SO₄, H₃PO₄ and HNO₃) could be gelled relatively well, whereas weak organic acids like acetic acid and formic acid failed to form gels. Additionally a 0.1 M NaOH solution could be gelled. This indicates, that the pH must be extreme to ensure a high enough ionisation state (either protonation of amine or deprotonation of carboxyl function) to ensure sufficient solubility in an aqueous solution.

Table 5 Gelation ability of **amidine-Glu** in several organic solvents and aqueous solutions. **B)** Influence of acid concentration on gelation ability.

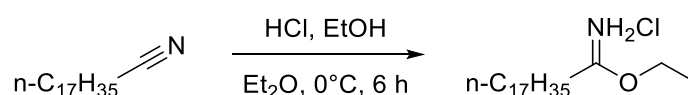
A					B	
Solvent	optical appearance	CGC (g L ⁻¹)	Gel- (min)	T _{gel} (°C)	acidic solution	CGC (g L ⁻¹)
EtOAc	I	-	-	-	0.01 M HCl	33.3
MeOH	I	-	-	-	0.1 M HCl	25
DCM	I	-	-	-	1 M HCl	33 ± 24
MeCN	I	-	-	-	2 M HCl	25
acetone	I	-	-	-	0.1 M H ₂ SO ₄	50
silicon oil	I	-	-	-	1 M H ₂ SO ₄	10 ± 3
DMSO	yellow TG	37.3	n.m.	n.m.	2 M H ₂ SO ₄	13 ± 2
HCl	white OG	33 ± 24	535	41		
H ₂ SO ₄	white OG	10 ± 3	5,5	30		
HNO ₃	white PG	75 ± 35	3	n.m.		
H ₃ PO ₄	white OG	16 ± 5	7	41		
HBr	white PG	32 ± 25	5	n.m.		
HI	red OG	25	-	-		
CH ₃ COOH	I	-	-	-		
HCOOH	I	-	-	-		
NaOH	white OG	50	2	n.m.		

TG = transparent gel; OG = opaque gel; PG = partial gel; I = insoluble; n.m. not measured. Values with error were measured twice. Acidic solutions in table A are at a concentration of 1 M, NaOH is 0.1 M.

In order to investigate the influence of acid concentration on the critical gelation concentration, the gelation of HCl and H₂SO₄ solutions at 4 and 3 different concentrations, respectively were tested (**Table 5B**). The gelation of HCl did not show any significant changes depending on acid concentration. In the contrast, with rising H₂SO₄ concentration from 0.1 to 1 M the CGC decreased around 5 fold. A further increase to 2 M H₂SO₄ concentration did not show relevant changes. However these are only preliminary results so for a clear conclusion further replications of these experiments would be necessary.

1.3 Experimental Part

Synthesis of ethyl stearamidate hydrochloride



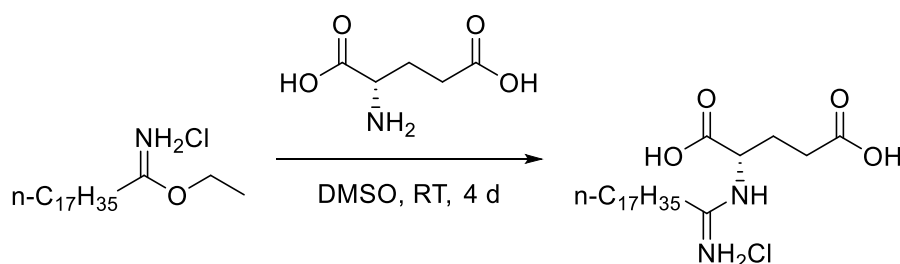
A solution of stearonitrile (5.0 g, 18.8 mmol) and EtOH abs. (1.13 mL, 19.3 mmol) in Et₂O (25 mL) was cooled to 0 °C in an ice bath. Through this solution a thin stream of *in-situ* generated HCl gas was led for 5 h and subsequently the mixture was stirred for 1 further hour and then stored at 4 °C overnight. The formed precipitate was

filtered off and washed with ice cold Et₂O (3 x 30 mL) to yield the desired product as white solid.

Yield: 1.86 g (28%); C₂₀H₄₁NO·HCl (347.96)

¹H NMR (300 MHz, DMSO-d₆) δ (ppm) = 7.32 - 6.98 (m, 2 H), 4.87 (dd, 1H), 4.03 (dd, 1H), 2.56 (t, 1H), 2.26 (t, 1H), 1.59 – 1.50 (m, 2H), 1.35 (t, 2H), 1.23 (ps, 28H), 1.16 (t, 2H), 0.85 (t, 3H).

Synthesis of (1-iminooctadecyl)-L-glutamic acid hydrochloride amidine Glu



Ethyl stearamidate hydrochloride (1.0 g, 2.87 mmol) and L-glutamic acid (634 mg, 4.31 mmol) were dissolved in DMSO (50 mL) by gentle heating. The solution was stirred at room temperature for 4 days when 200 mL of EtOAc were added. The organic layer was washed with water/brine 1:1 (3 x 200 mL) and dried over Na₂SO₄. Solvent was evaporated under reduced pressure to give the title compound as white solid.

Yield: 0.24 g (19%); C₂₃H₄₄N₂O₄·HCl (448.79)

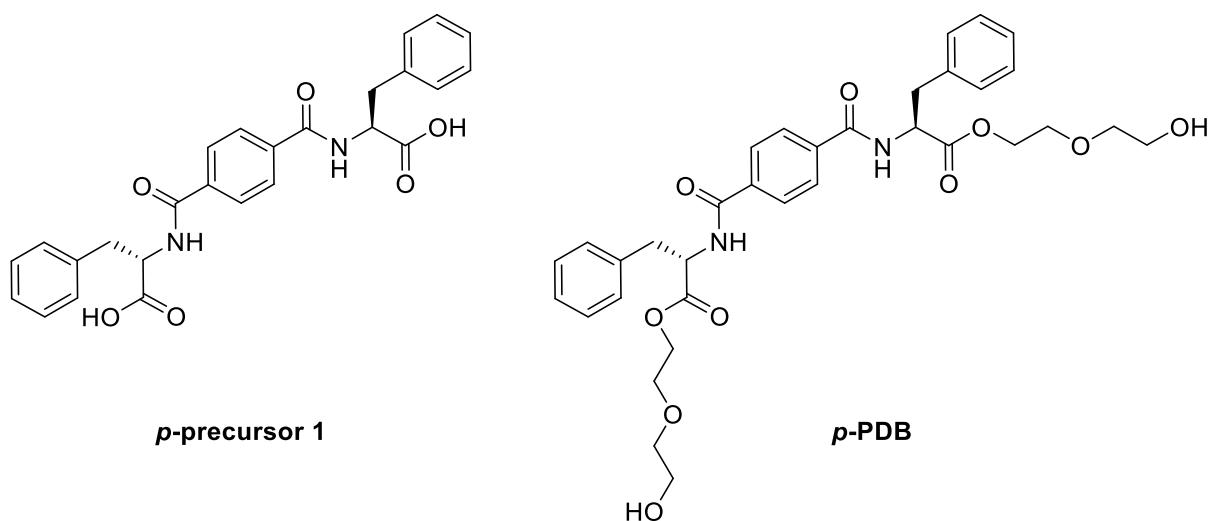
¹H NMR (300 MHz, DMSO-d₆) δ (ppm) = 9.11 – 8.76 (m, 2H), 3.88 (ps, 1H), 2.45 – 2.34 (m, 2H), 2.30 – 2.19 (m, 2H), 1.95 – 1.81 (m, 2H), 1.61 – 1.48 (m, 2H), 1.23 (ps, 28H), 0.85 (t, 3H).

MS (ESI): m/z (%) 413.34 (100) [M+H]⁺, calc. 413.34

2. X-bi(phenylalanine-diglycol)-benzene

2.1 Aim

The influence of topology on gelation abilities of ionenes was described in our group before,^{153,171,215} as well as in this thesis (**chapter C3**). But we wanted to test if the concept of topology can be transferred to low molecular weight gelators (LMWG), too. Two LMWG described by Feng et *para*-bi(phenylalanine-diglycol)-benzene (***p*-PDB**) bis(2-(2-hydroxyethoxy)ethyl) 2,2'-(terephthaloylbis (azanediyl))(2*S*,2'*S*)-bis(3-phenylpropanoate) and its precursor (2*S*,2'*S*)-2,2'-(terephthaloylbis(azanediyl)) bis(3-phenylpropanoic acid), which are able to gel water, were chosen as models.

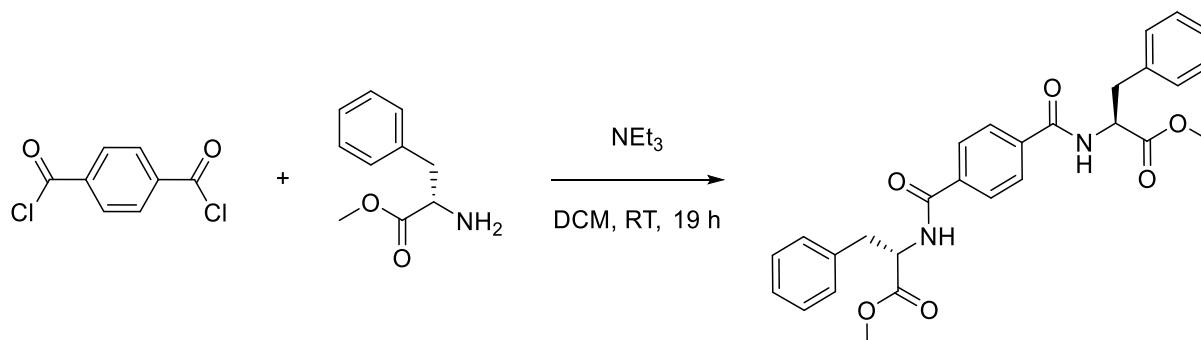


2.2 Results

The synthesis of **PDBs** comprised of three steps. First *x*-phthaloyl chloride was reacted with L-phenylalanine methyl ester hydrochloride in the presence of NEt_3 which afforded good to moderate yields. Next step was the deprotection of the amino acids which was quantitative for the ***para***-compound but resulted moderate (75%) and poor yields (36%) for ***meta***- and ***ortho***-compounds, respectively. Also the last step which was the esterification with two equivalents of diethylene glycol afforded quite poor yields (33%, 40% and 28% for ***para***-, ***meta***- and ***ortho***-, respectively). Gelation could be achieved with ***p*-PDB** and its direct precursor ***p*-precursor 1**, however ***m*-PDB**, ***o*-PDB** and ***o*-precursor 1** were not able to gel water. The direct precursor of ***m*-PDB** (***m*-precursor 1**) could form at least a partial hydrogel at a CGC of 29 g L^{-1} .

2.3 Experimental Part

Synthesis of dimethyl 2,2'-(terephthaloylbis(azanediy)))(2S,2'S)-bis(3-phenylpropanoate) **p**-precursor 2

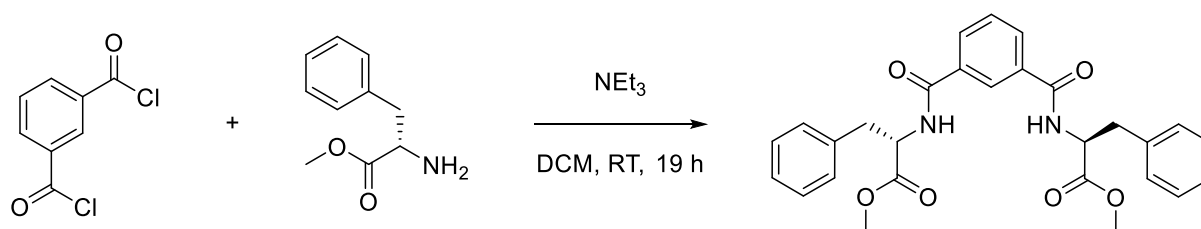


A solution of terephthaloyl chloride (2.6 g, 12.8 mmol) in dry DCM (20 mL) was added dropwise to an ice cold solution of L-phenylalanine methyl ester hydrochloride (6.0 g, 27.8 mmol) and NEt₃ (8.0 mL, 115 mmol) in dry DCM (100 mL). The mixture was stirred at room temperature for 19 h. Solvent was evaporated and the residue was washed with EtOAc (3 x 50 mL) to afford the product as a white solid.

Yield: 5.49 g (88%), C₂₈H₂₈N₂O₆ (488.54)

¹H-NMR (300 MHz, DMSO-d₆) δ (ppm) = 9.00 (pd, 2H), 7.86 (s, 4H), 7.32 – 7.24 (m, 8H), 7.22 – 7.19 (m, 2H), 4.72 – 4.64 (m, 2H), 3.64 (s, 6H), 3.22 – 3.06 (m, 4H).

Synthesis of dimethyl 2,2'-(isophthaloylbis(azanediy)))(2S,2'S)-bis(3-phenylpropanoate) **m**-precursor 2

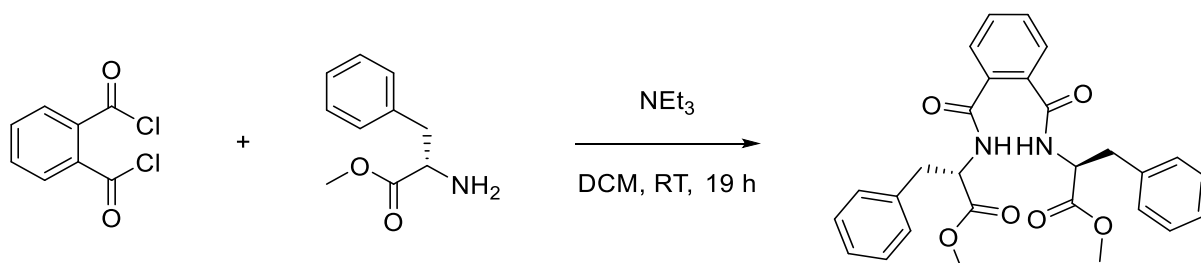


A solution of isophthaloyl chloride (2.6 g, 12.8 mmol) in dry DCM (20 mL) was added dropwise to an ice cold solution of L-phenylalanine methyl ester hydrochloride (6.0 g, 27.8 mmol) and NEt₃ (8.0 mL, 115 mmol) in dry DCM (100 mL). The mixture was stirred at room temperature for 24 h. Solvent was evaporated under reduced pressure and to afford the crude product as a white solid which was used for the next step without further purification.

Yield: 4.55 g (73%), C₂₈H₂₈N₂O₆ (488.54)

¹H-NMR (300 MHz, DMSO-d₆) δ (ppm) = 9.00 (pd, 2H), 7.86 (s, 4H), 7.32 – 7.24 (m, 8H), 7.22 – 7.19 (m, 2H), 4.72 – 4.64 (m, 2H), 3.64 (s, 6H), 3.22 – 3.06 (m, 4H).

Synthesis of dimethyl 2,2'-(phthaloylbis(azanediy)))(2S,2'S)-bis(3-phenylpropanoate) **o**-precursor 2

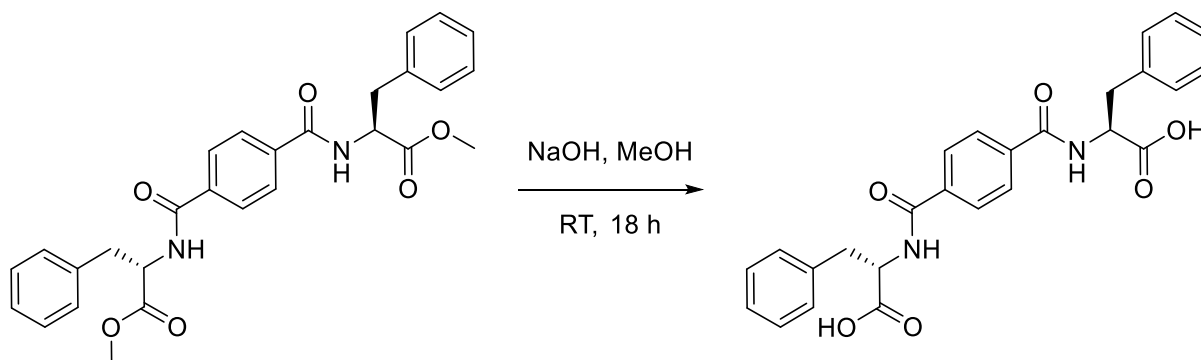


A solution of phthaloyl chloride (2.6 g, 12.8 mmol) in dry DCM (20 mL) was added dropwise to an ice cold solution of L-phenylalanine methyl ester hydrochloride (6.0 g, 27.8 mmol) and NEt₃ (8.0 mL, 115 mmol) in dry DCM (100 mL). The mixture was stirred at room temperature for 24 h. Solvent was evaporated under reduced pressure and to afford the crude product as a white solid which was used for the next step without further purification.

Yield: 4.55 g (73%), C₂₈H₂₈N₂O₆ (488.54)

¹H-NMR (300 MHz, DMSO-d₆) δ (ppm) = 9.00 (pd, 2H), 7.86 (s, 4H), 7.32 – 7.24 (m, 8H), 7.22 – 7.19 (m, 2H), 4.72 – 4.64 (m, 2H), 3.64 (s, 6H), 3.22 – 3.06 (m, 4H).

Synthesis of (2S,2'S)-2,2'-(isophthaloylbis(azanediy))bis(3-phenylpropanoic acid) **p**-precursor 1



p-precursor 2 (3.0 g, 6.1 mmol) was suspended in MeOH (20 mL) and cooled to 0 °C when a solution of NaOH (2 M, 10 mL) was added. The mixture was stirred at room temperature for 18 h when TLC showed full conversion of the starting material. The mixture was then acidified with 3M HCl and the resulting white precipitate was

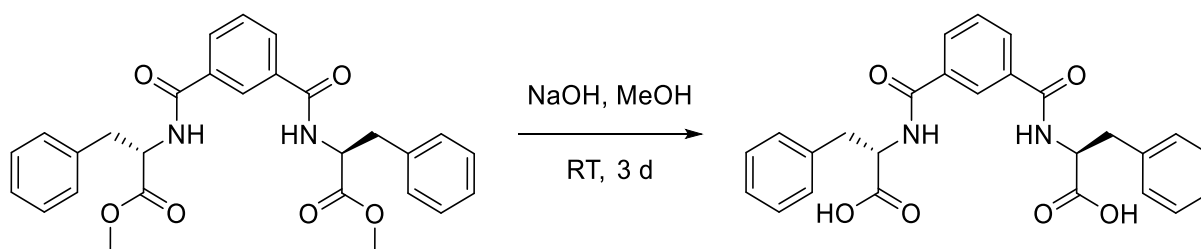
filtered off and washed until the washing water was almost neutral. The product was dried by lyophilization to afford the product as white powder.

Yield: 2.92 g (103%) C₂₆H₂₄N₂O₆ (460.49)

¹H-NMR (300 MHz, DMSO-d₆) δ (ppm) = 8.76 – 8.71 (m, 2H), 7.85 (s, 1H), 7.50 – 7.47 (m, 2H), 7.39 – 7.35 (m, 2H), 7.32 – 7.14 (m, 12H), 4.61 – 4.56 (m, 2H), 3.60 (s, 6H), 3.11 – 2.96 (m, 4H).

Synthesis of (2S,2'S)-2,2'-(isophthaloylbis(azanediyl))bis(3-phenylpropanoic acid)

m-precursor 1



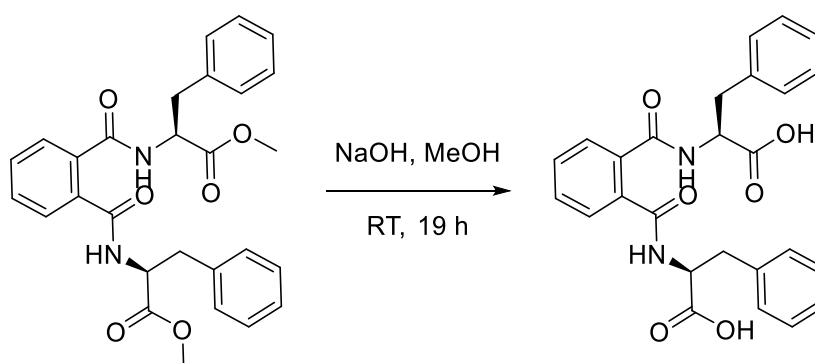
m-precursor 2 (4.0 g, 8.2 mmol) was suspended in MeOH (26 mL) and cooled to 0 °C when a solution of NaOH (2 M, 14 mL) was added. The mixture was stirred at room temperature for 18 h when TLC showed full conversion of the starting material. The mixture was then acidified with 3M HCl and the resulting white precipitate was filtered off and washed until the washing water was almost neutral. The product was dried by lyophilization to afford the product as white powder.

Yield: 2.81 g (75%) C₂₆H₂₄N₂O₆ (460.49)

¹H-NMR (300 MHz, DMSO-d₆) δ (ppm) = 8.74 (pd, 2H), 8.18 (s, 1H), 7.88 (dd, 2H), 7.52 (t, 2H), 7.30.-7.13 (m 9H) 4.62 – 4.53 (m, 2H), 3.64 (s, 6H), 3.22 – 3.02 (m, 4H).

Synthesis of (2S,2'S)-2,2'-(phthaloylbis(azanediyl))bis(3-phenylpropanoic acid)

o-precursor 1

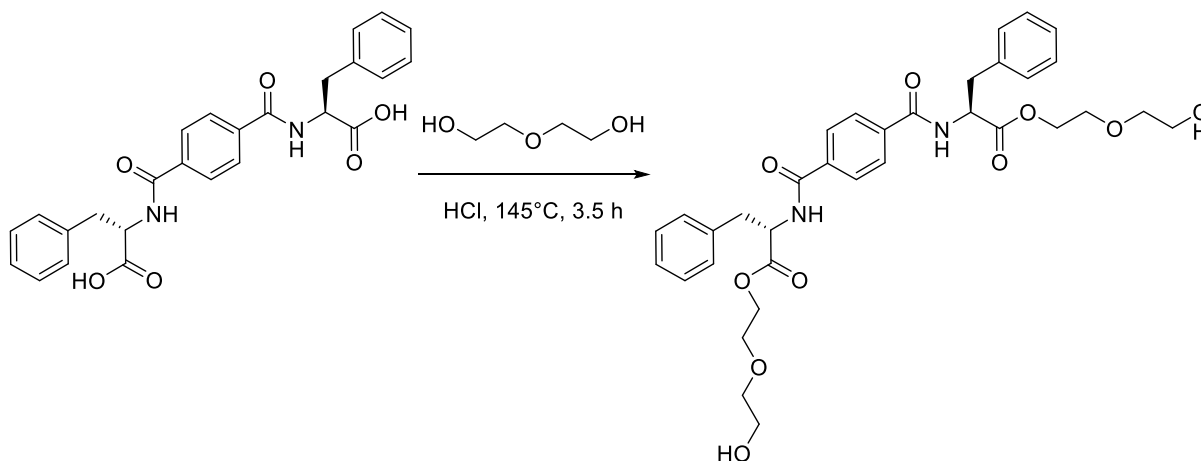


o-precursor 2 (3.0 g, 6.1 mmol) was suspended in MeOH (20 mL) and cooled to 0 °C when a solution of NaOH (2 M, 10 mL) was added. The mixture was stirred at room temperature for 19 h when TLC showed full conversion of the starting material. The mixture was then acidified with 3M HCl and the resulting white precipitate was filtered off and washed until the washing water was almost neutral. The product was dried by lyophilization to afford the product as white powder.

Yield: 1.03 g (36%) C₂₆H₂₄N₂O₆ (460.49)

¹H-NMR (300 MHz, DMSO-d₆) δ (ppm) = 8.59 – 8.52 (m, 2H), 7.51 – 7.45 (m, 2H), 7.39 – 7.35 (m, 2H), 7.29 – 7.18 (m, 10H), 4.57 – 4.48 (m, 2H), 3.16 – 2.92 (m, 4H).

Synthesis of bis(2-(2-hydroxyethoxy)ethyl) 2,2'-(terephthaloylbis(azanediy))((2S,2'S)-bis(3-phenylpropanoate) **p-PDB**



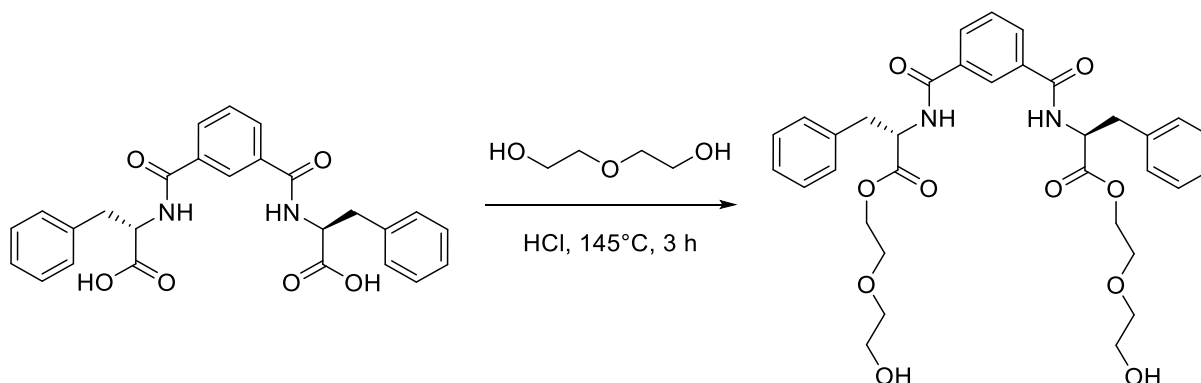
p-precursor 1 (2.8 g, 6.1 mmol) and conc. HCl (4 drops) were dissolved in diethylene glycol (80 mL, 843 mmol) and stirred at 145 °C for 3.5 h. The clear brown solution was poured on 350 mL ice water. The gel like precipitate was filtered off, dried by lyophilization and remaining diethylene glycol was removed by washing with water. The dried crude was purified by column chromatography (DCM:MeOH 10:1 to 5:1 (0.5% TFA)) to afford the title compound as brown solid.

Yield 0.92 g (33%), C₃₄H₄₀N₂O₁₀ (636.70)

¹H-NMR (300 MHz, DMSO-d₆) δ (ppm) = 9.01 – 8.84 (dd, 2H), 7.84 (s, 4H), 7.323–7.24 (m, 8H), 7.22 – 7.17 (m, 2H), 4.71 – 4.60 (m, 2H), 4.25 -4.12 (m, 3H) 3.63 – 3.36 (m, 16H), 3.23 – 3.02 (m, 4H).

MS (ESI): m/z (%) 637.28 (100) [M+H]⁺, 1273.5 (19) [2M+H]⁺, calc. 637.28

Synthesis of bis(2-(2-hydroxyethoxy)ethyl) 2,2'-(isophthaloylbis(azanediy)) (2S,2'S)-bis(3-phenylpropanoate) **m-PDB**



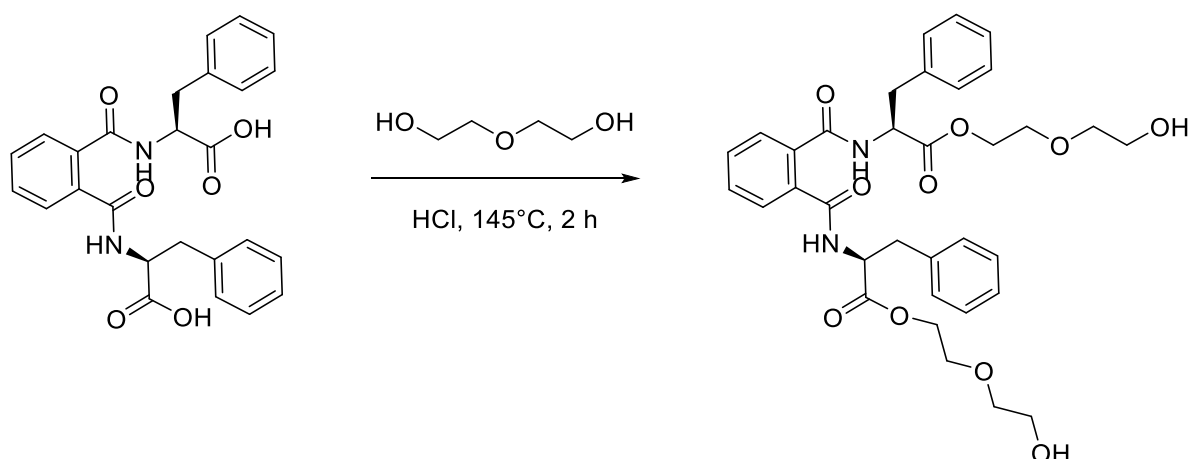
m-precursor 1 (1.0 g, 2.2 mmol) and conc. HCl (2 drops) were dissolved in diethylene glycol (80 mL, 843 mmol) and stirred at 145 °C for 3.5 h. EtOAc (150 mL) were added and diethylene glycol was removed by washing with water (3 x 150 mL). Remaining product in the collected aqueous layer was extracted with EtOAc (2 x 150 mL). Organic layer was dried over Na₂SO₄ and solvent was evaporated under reduced pressure. The crude product was purified by column chromatography (DCM:MeOH 10:1) to afford the title compound as brown solid.

Yield 0.40 g (40%), C₃₄H₄₀N₂O₁₀ (636.70)

¹H-NMR (300 MHz, DMSO-d₆) δ (ppm) = 9.02 (d, 2H), 8.23 (s, 1H), 7.93 (dd, 2H), 7.56 (t, 1H), 7.32–7.19 (m, 10H), 4.71 – 4.61 (m, 4H), 4.24 – 4.12 (m, 4H), 3.62 – 3.51 (m, 4H), 3.48 – 3.42 (m, 6H), 3.21 – 3.07 (m, 4H).

MS (ESI): m/z (%) 637.28 (100) [M+H]⁺, 1295.5 (14) [2M+Na]⁺, calc. 637.28

Synthesis of bis(2-(2-hydroxyethoxy)ethyl) 2,2'-(phthaloylbis(azanediy)) (2S,2'S)-bis(3-phenylpropanoate) **o-PDB**



o-precursor 1 (0.5 g, 1.1 mmol) and conc. HCl (1 drops) were dissolved in diethylene glycol (15 mL, 152 mmol) and stirred at 65 °C for 3 h. EtOAc (75 mL) were added and diethylene glycol was removed by washing with water (3 x 75 mL). Remaining product in the collected aqueous layer was extracted with EtOAc (3 x 75 mL). Organic layer was dried over Na₂SO₄ and solvent was evaporated under reduced pressure. The crude product was purified by column chromatography (DCM:MeOH 10:1) to afford the title compound as brown viscous oil.

Yield 0.14 g (28%), C₃₄H₄₀N₂O₁₀ (636.70)

¹H-NMR (300 MHz, DMSO-d₆) δ (ppm) = 8.76 – 8.84 (dd, 2H), 7.54 – 7.47 (m, 2H), 7.42 – 7.39 (m, 2H), 7.32– 7.19 (m, 10H), 4.65 – 4.55 (m, 4H), 4.20 -4.08 (m, 4H) 3.60 – 3.52 (m, 4H), 3.50 – 3.41 (m, 6H), 3.11 – 2.98 (m, 4H).

MS (ESI): m/z (%) 637.28 (100) [M+H]⁺, 659.5 (66) [M+Na]⁺, calc. 637.28

3. New Ionenenes

3.1 Aim

The influence of topology on gelation abilities of ionene polymers was described in our group before,^{153,171,215} as well as in this thesis (**chapter C3**). Therefore we wanted to test other ionene polymers for their potential enhancement of gelation by change of the topology. Two ionenes described by Yoshida et al (trans-cyclohexane-1,4-diyl) dibenzamide linked to *N,N,N',N'*-tetramethylhexane-1,6-diamine (**p-cyclohex**) and poly[pyridinium-1,4-diyliminocarbonyl-1,4-phenylene-methylene chloride] **p-polypyr** were chosen as models.^{216,217}

3.2 Results

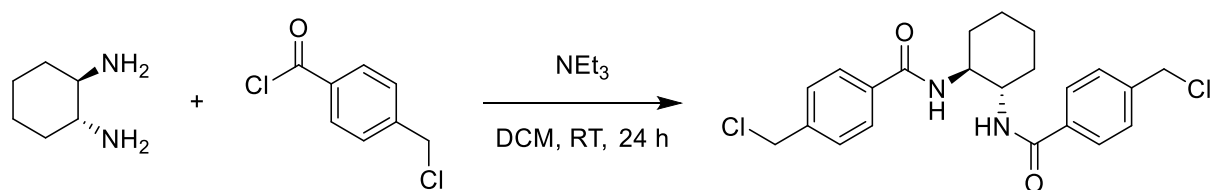
Synthesis of **cyclohex** ionenes was performed in two steps. Briefly, first step involves the amidation of *trans*-cyclohexanediamines with 4-(chloromethyl)benzoyl chloride in the presence of Et₃N in DCM, followed by step-growth copolymerization of the obtained bis-benzamides with the desired α,ω -diamine linker under equimolar conditions in DMF at 80 °C affording the desired polymers in good yields (80 and 96%). Synthesis of **m-cyclohex** was not performed as *trans*-1,3-cyclohexanediamine is too expensive. **Polypyr** ionenes were synthesized via copolymerization of aminopyridines again with 4-chloromethylbenzoylchloride affording moderate yields (77 and 73%). Synthesis of **o-polypyr** failed. The four obtained ionenes were investigated towards their hydrogelation behaviour (**Table 6**). Unfortunately, **o-cyclohex** was not able to form hydrogels in contrast to the already described **p-cyclohex**. **M-polypyr** was able to gel water, however the literature known *para*-topomer showed a lower and therefore better CGC.

Table 6 Critical gelation concentration of ionenes in water.

Gelator	CGC (g L ⁻¹)
<i>m</i> -polypyr	40
<i>p</i> -polypyr	80
<i>o</i> -cyclohex	solution
<i>p</i> -cyclohex	40

3.3 Experimental Part

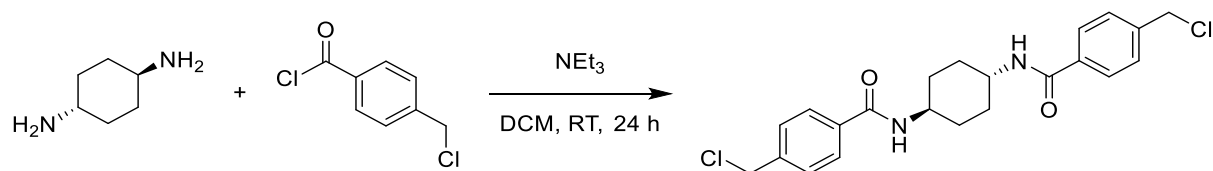
Synthesis of *N,N*-((trans)-cyclohexane-1,2-diyl)bis(4-(chloromethyl)benzamide) o-cyclohex monomer



To a stirred solution of trans-1,4-cyclohexanediamine (2.0 g, 17.5 mmol) and NEt₃ (4.87 mL, 35 mmol) in distilled DCM (150 mL) was added dropwise a solution of 4-chloromethylbenzoylchlorid (6.65 g, 35 mmol) in distilled DCM (60 mL). The mixture was stirred at room temperature overnight. The precipitate was filtered off and then washed three times with DCM to obtain the product as a white powder
Yield: 5.88 g (80%), C₂₂H₂₄Cl₂N₂O₂ (419.35)

¹H-NMR (300 MHz, DMSO-d₆) δ (ppm) = 8.32 – 8.34 (d, 2H), 7.82 – 7.85 (d, 4H), 7.49 – 7.52 (d, 4H), 4.80 (s, 4H), 3.78 (s, 2H), 1.90 (m, 4H), 1.45 (m, 4H)

Synthesis of *N,N*-((trans)-cyclohexane-1,4-diyl)bis(4-(chloromethyl)benzamide) p-cyclohex monomer

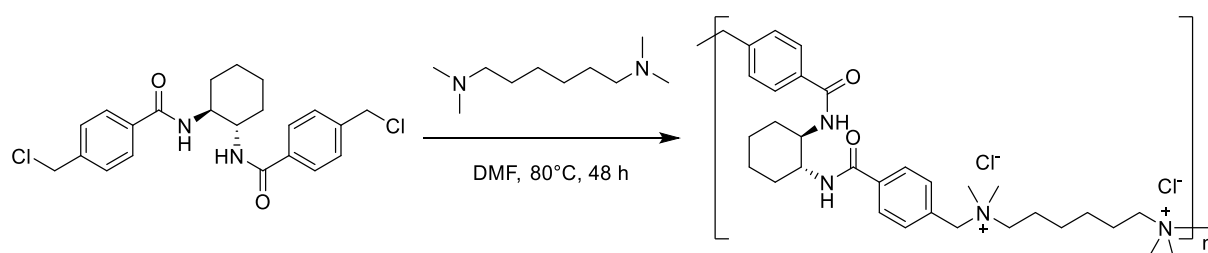


To a stirred solution of trans-1,2-cyclohexanediamine (2.0 g, 17.5 mmol) and NEt₃ (4.87 mL, 35 mmol) in distilled DCM (150 mL) was added dropwise a solution of 4-chloromethylbenzoylchlorid (6.65 g, 35 mmol) in distilled DCM (60 mL). The mixture was stirred at room temperature for 24 h. The precipitate was filtered off and then washed with DCM to obtain a white powder

Yield: 5.37 g (73%), C₂₂H₂₄Cl₂N₂O₂ (419.35)

¹H-NMR (300 MHz, DMSO-d₆) δ (ppm) = 8.31 – 8.28 (d, 2H), 7.68 – 7.70 (d, 4H), 7.43 – 7.45 (d, 4H), 4.75 (s, 4H), 3.92 (s, 2H), 1.72 – 1.85 (m, 4H), 1.28 – 1.52 (m, 4H).

Synthesis of poly[(dimethylamino)hexane-1,6-diyl(dimethyliminio)methylene-1,4-phenylenecarbonyliminio-trans-cyclohexane-1,2-diyliminocarbonyl-1,4-phenylene-methylene dichloride] **o-cyclohex**

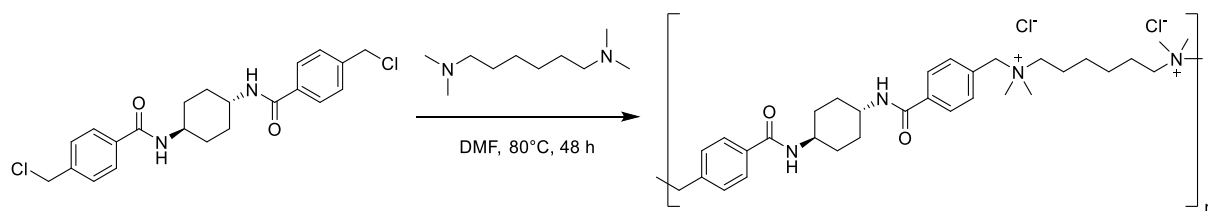


To a stirred suspension of **o-cyclohex monomer** (5.88 g, 14 mmol) in DMF (470 mL) at 80 °C was added dropwise a solution of *N,N,N',N'*-tetramethylhexane-1,6-diamine (2.42 g, 14 mmol) in DMF (95 mL). The mixture was stirred for 48 h. The precipitates were filtered off and washed two times with each DMF and acetone. Then it was dried under vacuum to obtain the product as a white powder.

Yield 8.0 g (96%)

¹H-NMR (300 MHz, D₂O) δ (ppm) = 7.82 – 7.88 (d, 4H), 7.60 – 7.62 (d, 4H), 4.50 (s, 4H), 3.83 (s, 2H), 3.30 (s, 4H), 3.00 (s, 12H), 1.87 – 2.03 (m, 8H), 1.40 – 1.51 (m, 8H)

Synthesis of poly[(dimethylamino)hexane-1,6-diyl(dimethyliminio)methylene-1,4-phenylenecarbonyliminio-trans-cyclohexane-1,4-diyliminocarbonyl-1,4-phenylene-methylene dichloride] **p-cyclohex**

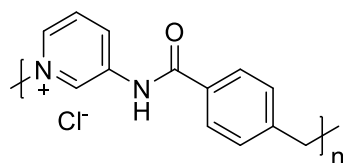


To a stirred suspension of **o-cyclohex monomer** (5.37 g, 12.8 mmol) in DMF (430 mL) at 80 °C was added dropwise a solution of *N,N,N',N'*-tetramethylhexane-1,6-diamine (2.12 g, 12.8 mmol) in DMF (85 mL). The mixture was stirred for 48 h. The mixture was cooled in the freezer and small crystals were dried under vacuum.

Yield: 1.5 g (20%)

¹H-NMR (300 MHz, D₂O) δ (ppm) = 7.56 – 7.59 (d, 4H), 7.43 – 7.47 (m, 4H), 4.36 (s, 4H), 3.88 (s, 2H), 3.15 (s, 4H), 2.87 (s, 12H), 1.72 – 1.90 (m, 8H), 1.28 – 1.43 (m, 8H).

Synthesis of poly[pyridinium-1,2-diyliminocarbonyl-1,4-phenylene-methylene chloride]
o-polypyr

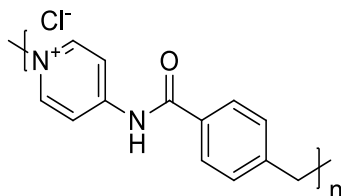


To a suspension of 3-aminopyridine (2.0 g, 21.2 mmol) in DCM (34 mL) and Et₃N (3.3 mL, 23.63 mmol) a solution of 4-chloromethylbenzoylchloride (4.02 g, 21.2 mmol) in DCM (16 mL) was added dropwise over 30 minutes. The reaction mixture was refluxed overnight at 50 °C, until TLC analysis showed full conversion of the starting materials. The mixture was cooled down to RT, filtered, washed with cold DCM (seven times), dried in vacuum. The product was obtained as light yellow powder.

Yield: 4.65g (77%), C₁₃H₁₁N₂OCl

¹H NMR (300 MHz, D₂O) δ (ppm) = 9.32 (s, 1 H), 8.58 (m, 1H), 8.31 (m, 1H), 7.62 – 7.90 (m, 1H, 2H), 7.50 (s, 2H), 5.70 (s, 2H).

Synthesis of poly[pyridinium-1,4-diyliminocarbonyl-1,4-phenylene-methylene chloride]
p-polypyr

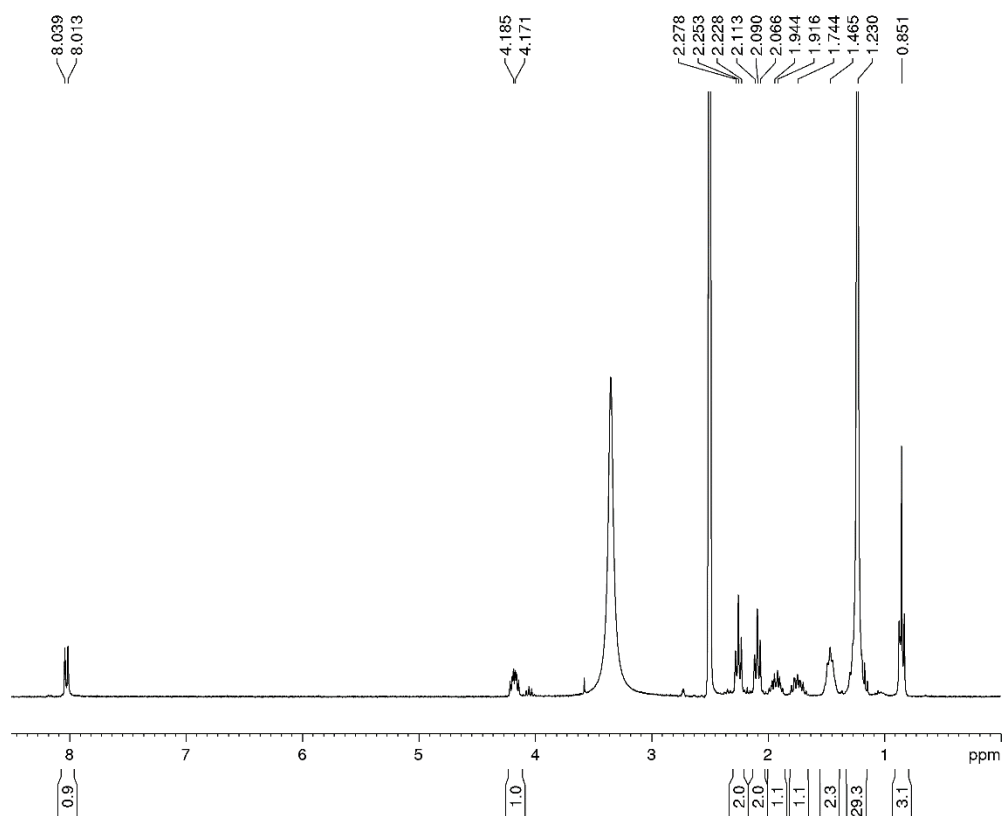


To a suspension of 4-aminopyridine (2.0 g, 21.2 mmol) in DCM (34 mL) and Et₃N (3.3 mL, 23.63 mmol) a solution of 4-chloromethylbenzoylchloride (4.02 g, 21.2 mmol) in DCM (16 mL) was added dropwise over 30 minutes. The reaction mixture was refluxed overnight at 50 °C, until TLC analysis showed full conversion of the starting materials. The mixture was cooled down to RT, filtered, washed with DCM (seven times) and methanol (two times), dried in vacuum. The product was obtained as white powder.

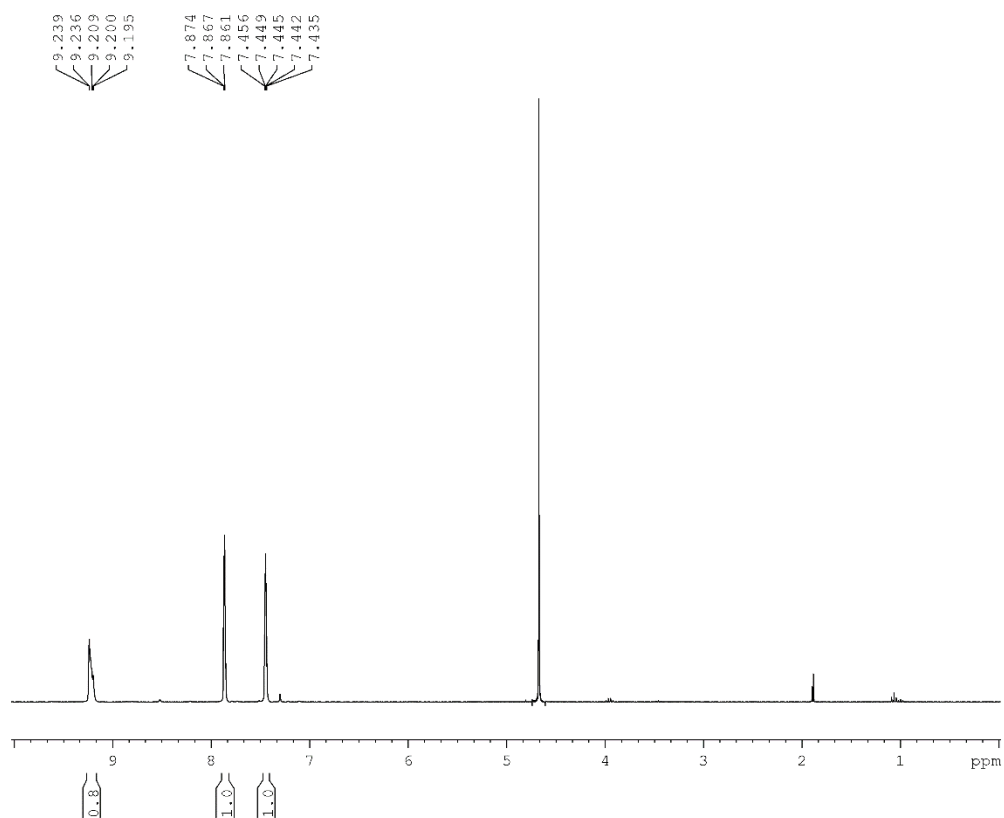
Yield: 4.40g (73%), C₁₃H₁₁N₂OCl

¹H NMR (300 MHz, D₂O) δ (ppm) = 8.58 (d, 2 H), 8.18 (d, 2H), 7.88 (d, 2H), 7.46 (d, 2H), 5.64 (s, 2H).

G NMR Spectra and PXRD

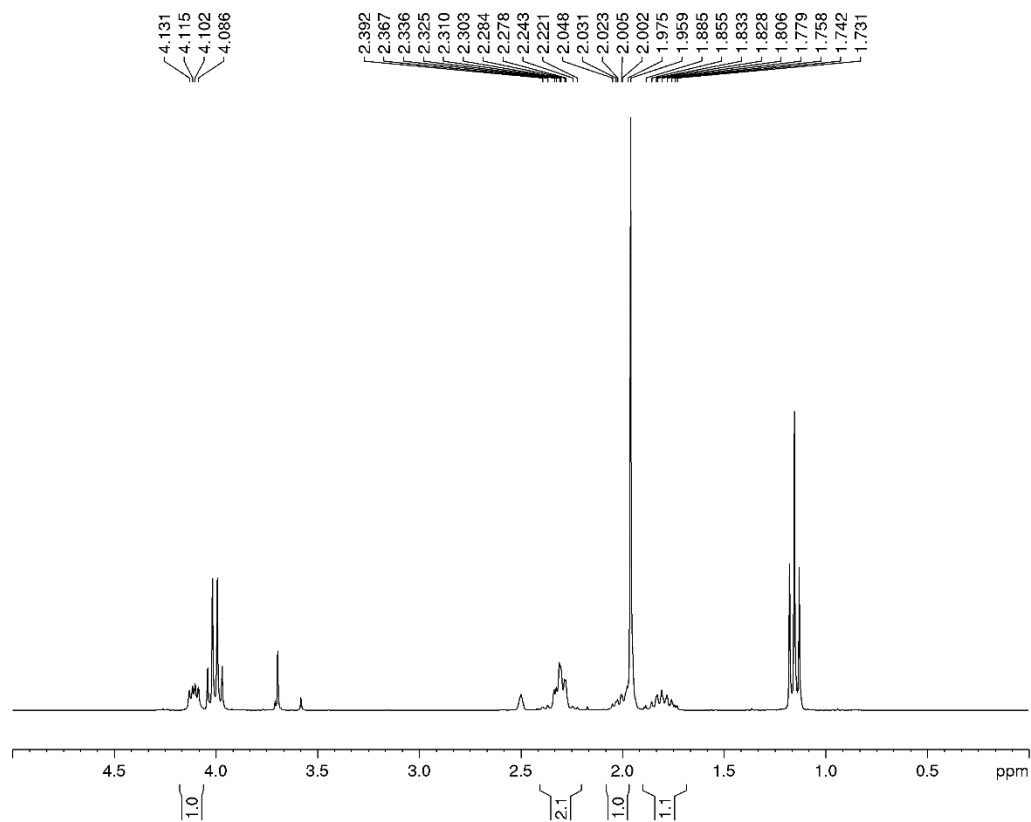


¹H-NMR spectrum (300 MHz, DMSO-d₆) of **C₁₈-Glu**.

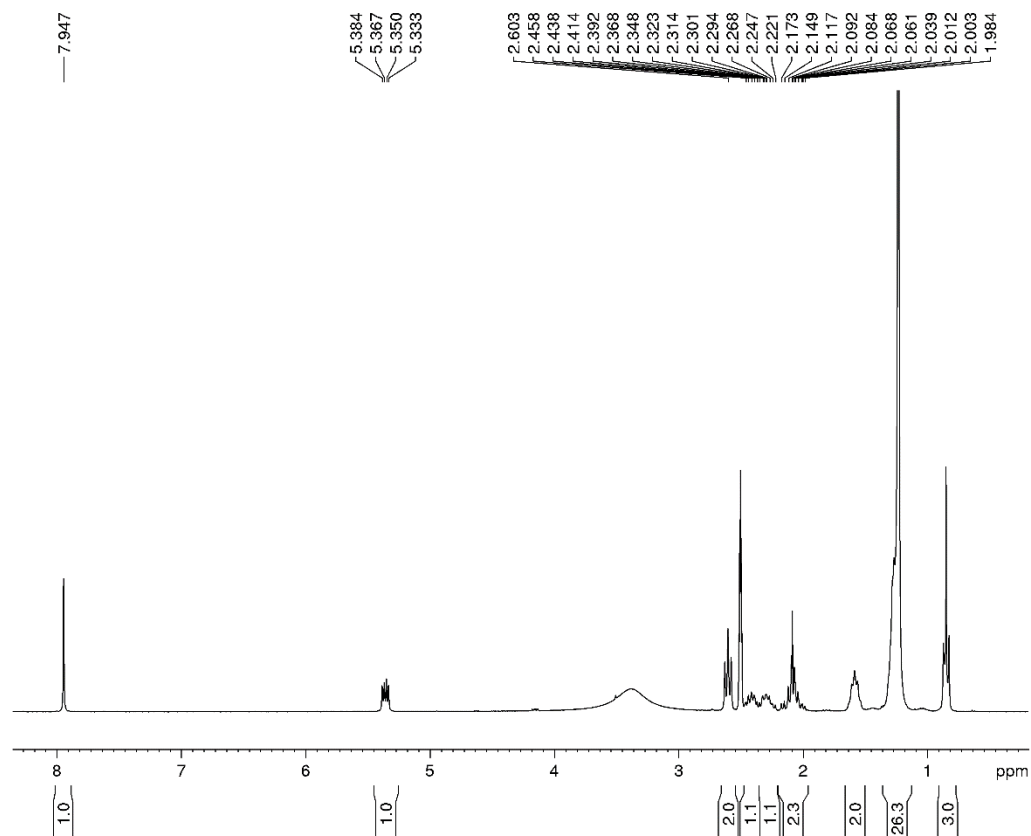


¹H-NMR spectrum (300 MHz, D₂O) of 1H-imidazole-1-sulfonyl azide.

NMR Spectra and PXRD

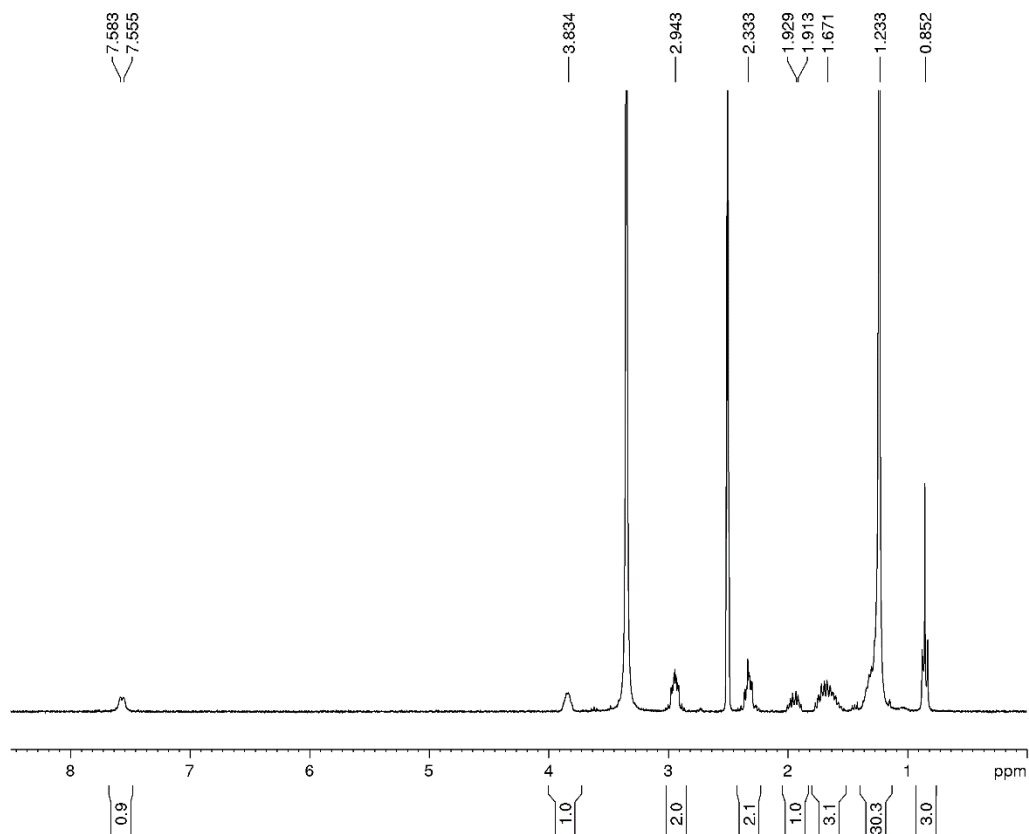


$^1\text{H-NMR}$ spectrum (300 MHz, DMSO-d_6) of (S)-2-azidopentanedioic acid.

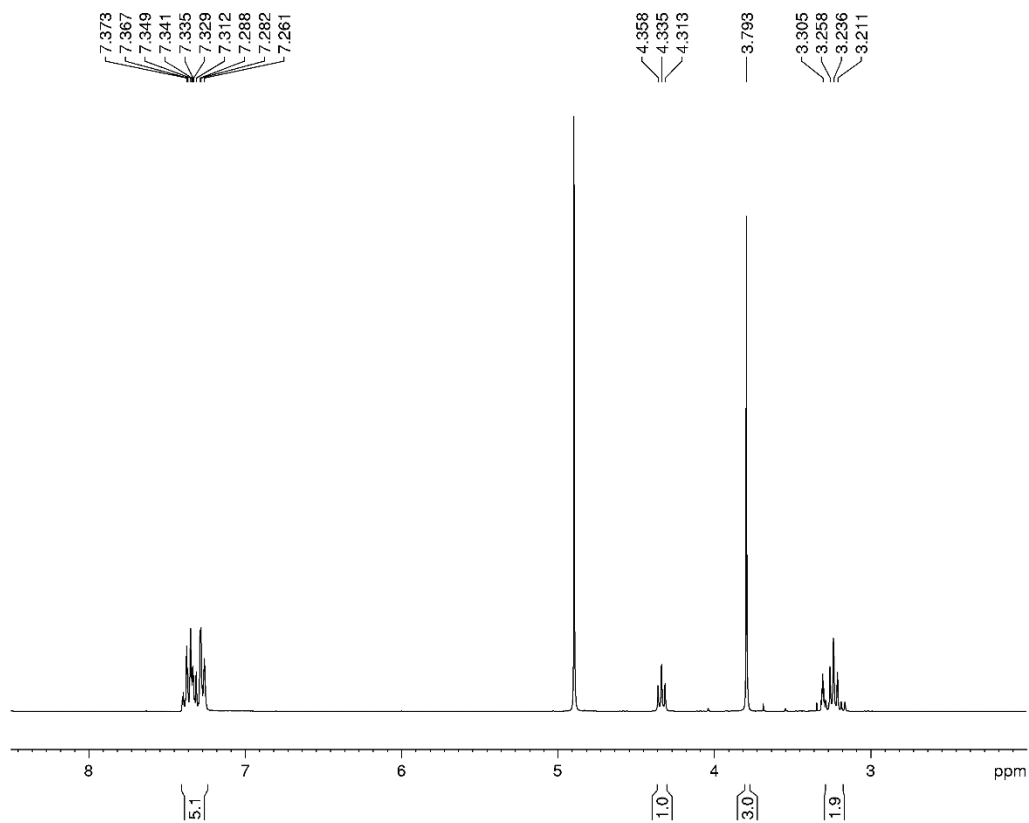


$^1\text{H-NMR}$ spectrum (300 MHz, DMSO-d_6) of **click-Glu**.

NMR Spectra and PXRD

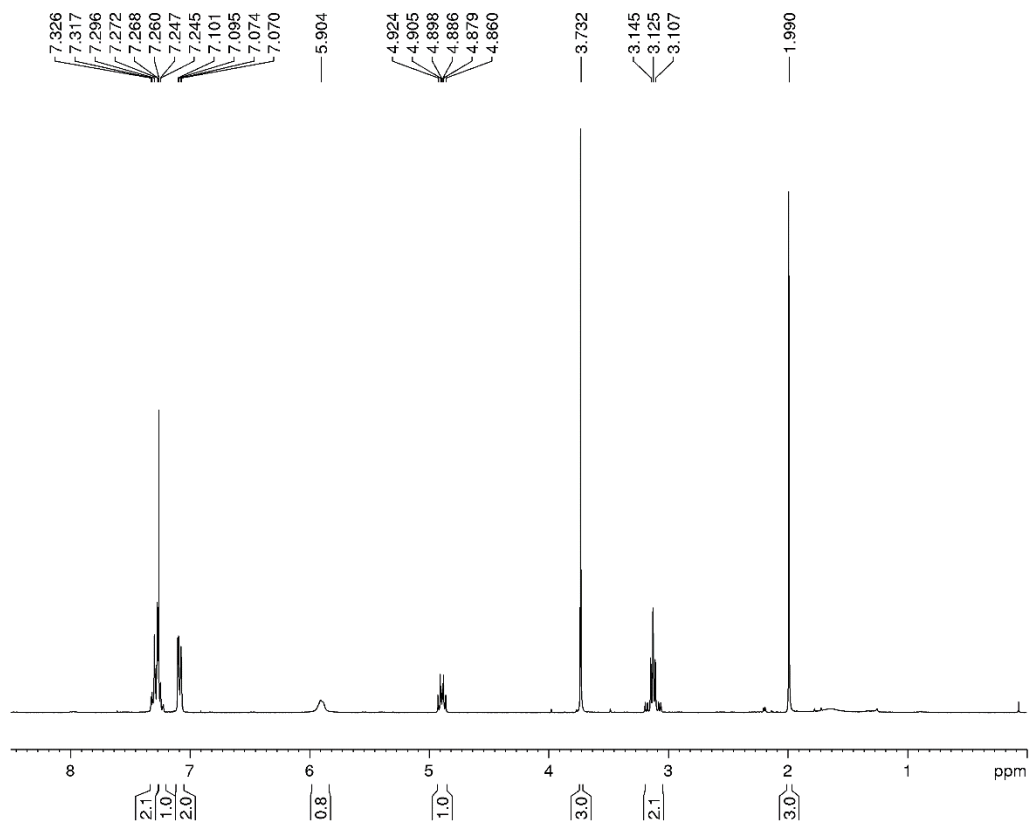


¹H-NMR spectrum (300 MHz, DMSO-d₆) of **sulfo-Glu**.

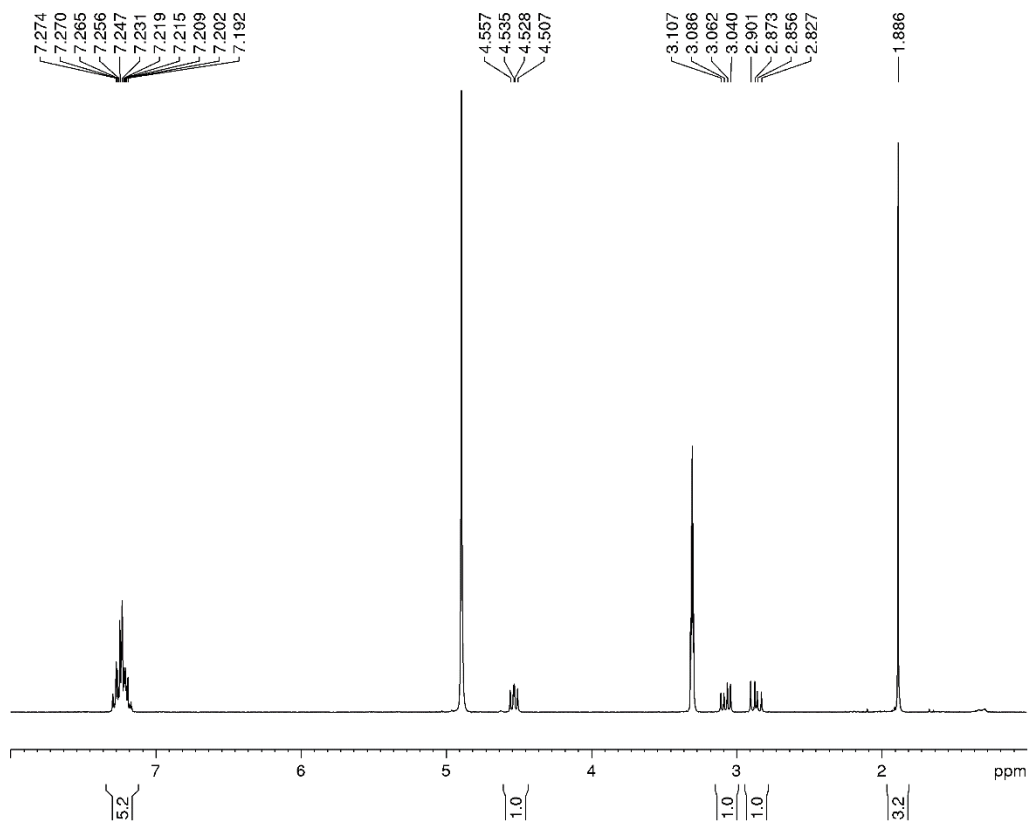


¹H-NMR spectrum (300 MHz, MeOD-d₃) of methyl L-phenylalaninate.

NMR Spectra and PXRD

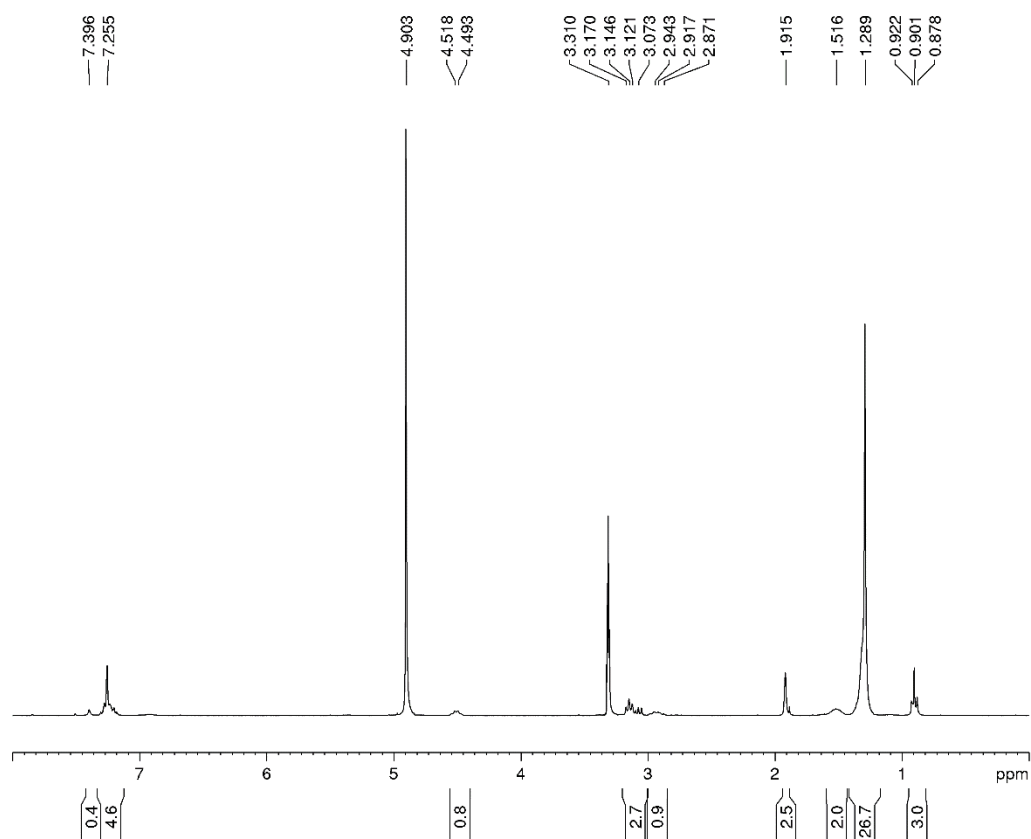


¹H-NMR spectrum (300 MHz, CDCl₃-d₃) of methyl acetyl-L-phenylalaninate.

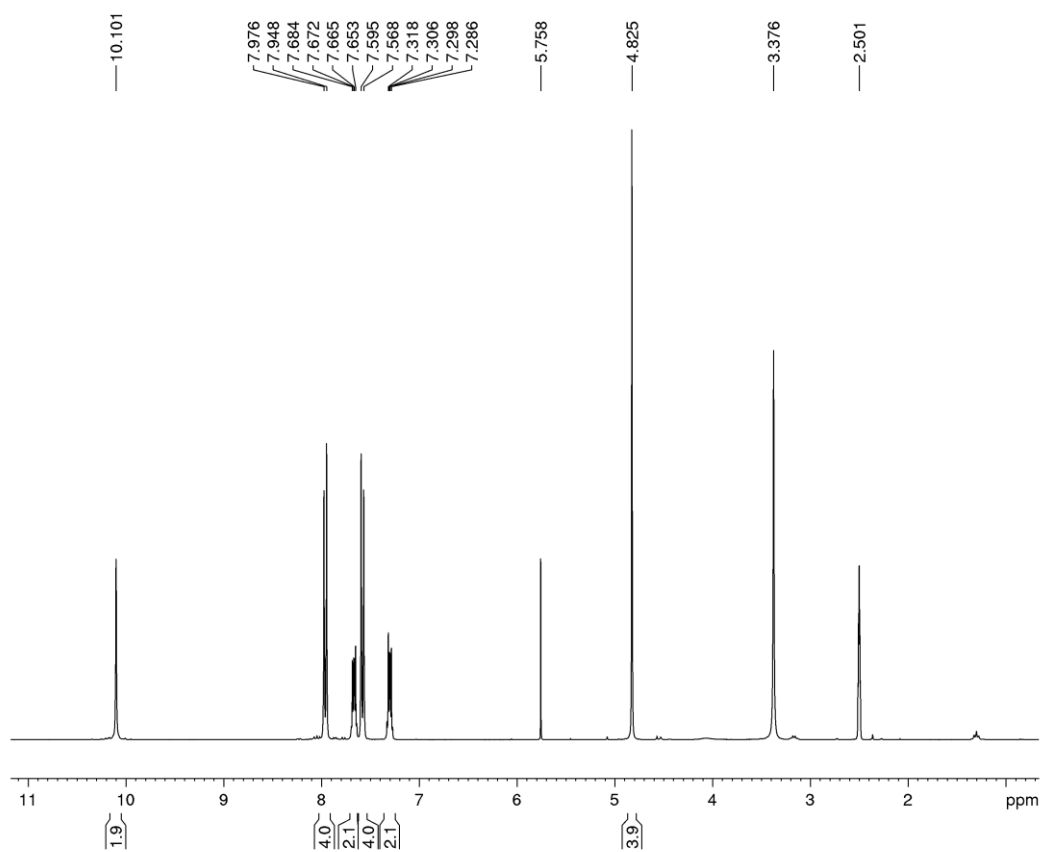


¹H-NMR spectrum (300 MHz, MeOD-d₃) of (S)-N-(1-hydrazineyl-1-oxo-3-phenylpropan-2-yl)acetamide.

NMR Spectra and PXRD

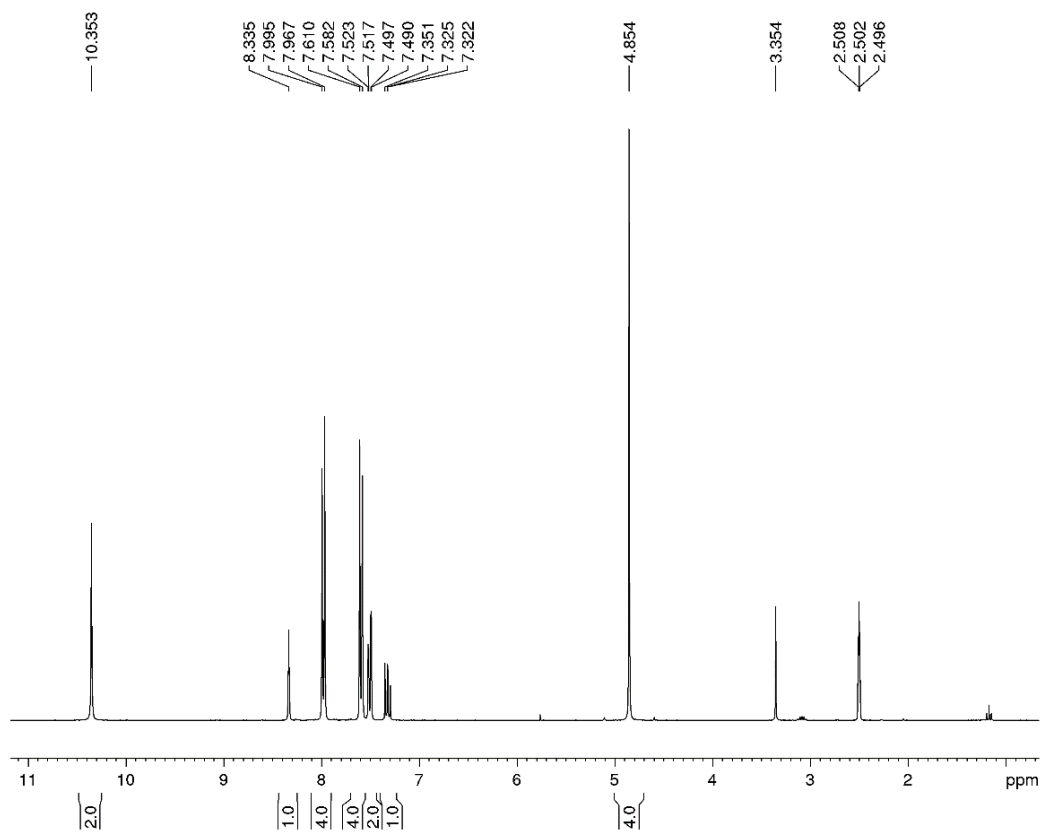


¹H-NMR spectrum (300 MHz, MeOD-d₃) of **FAG**.

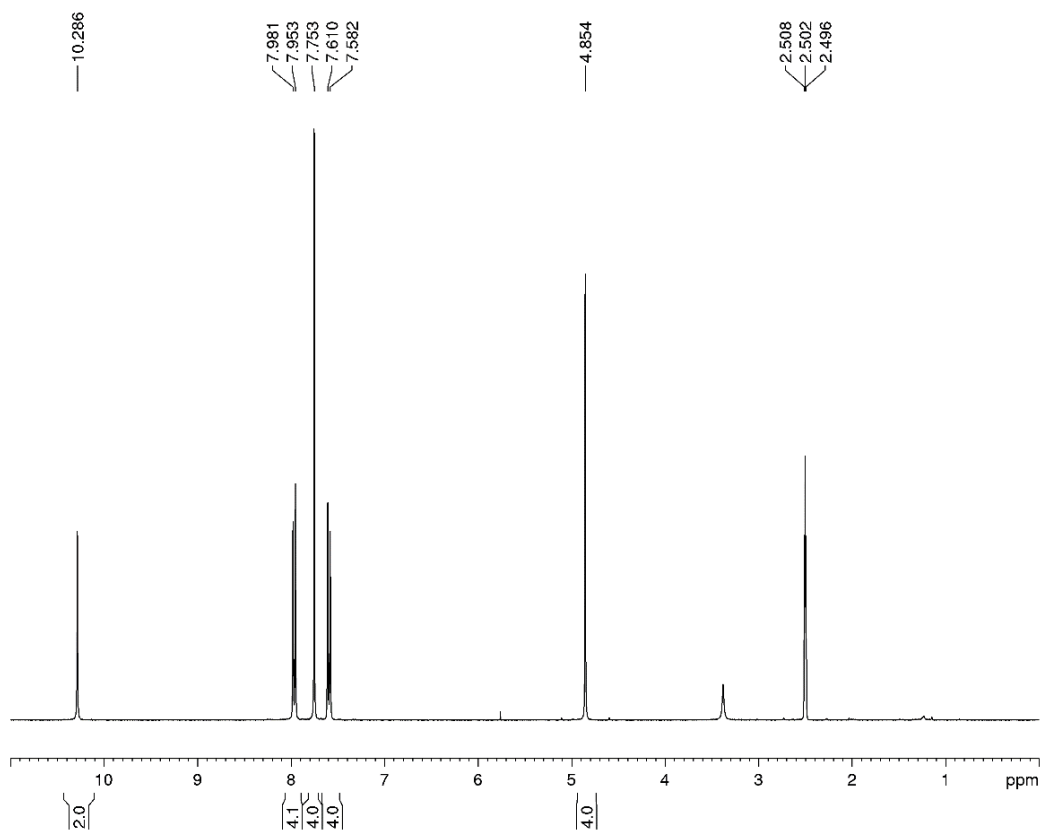


¹H-NMR spectrum (300 MHz, DMSO-d₆) of *ortho*-monomer.

NMR Spectra and PXRD

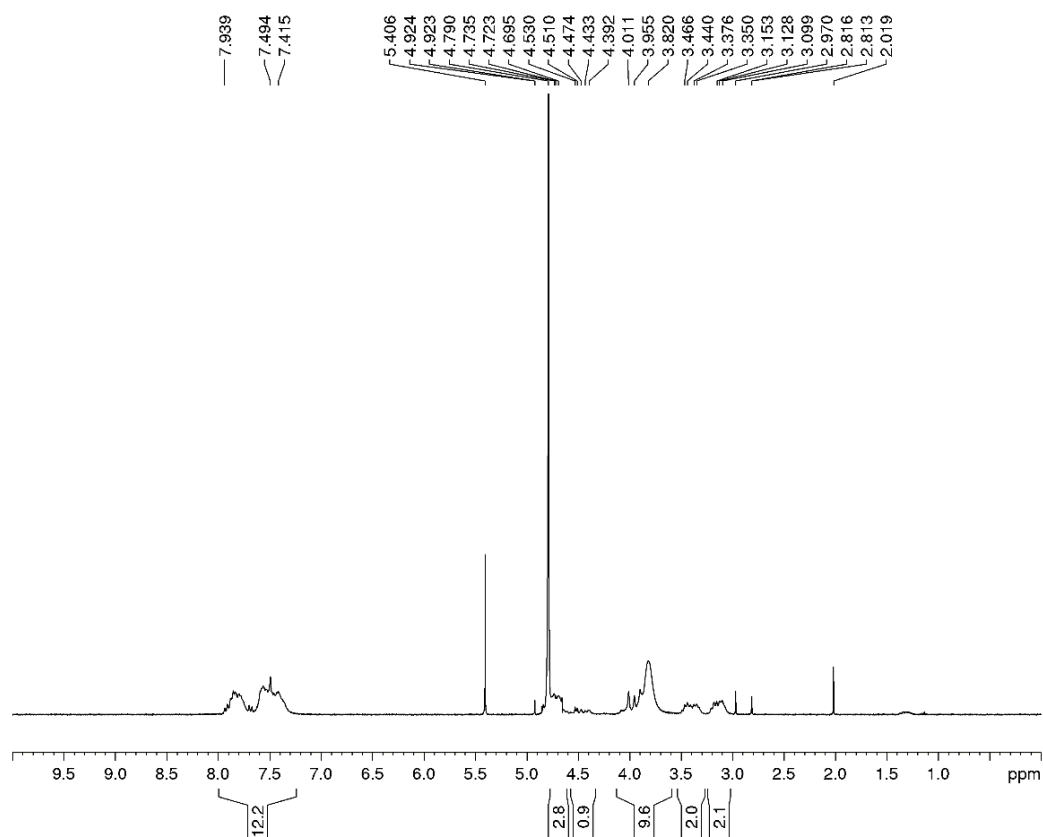


¹H-NMR spectrum (300 MHz, DMSO-d₆) of *meta*-Precursor.

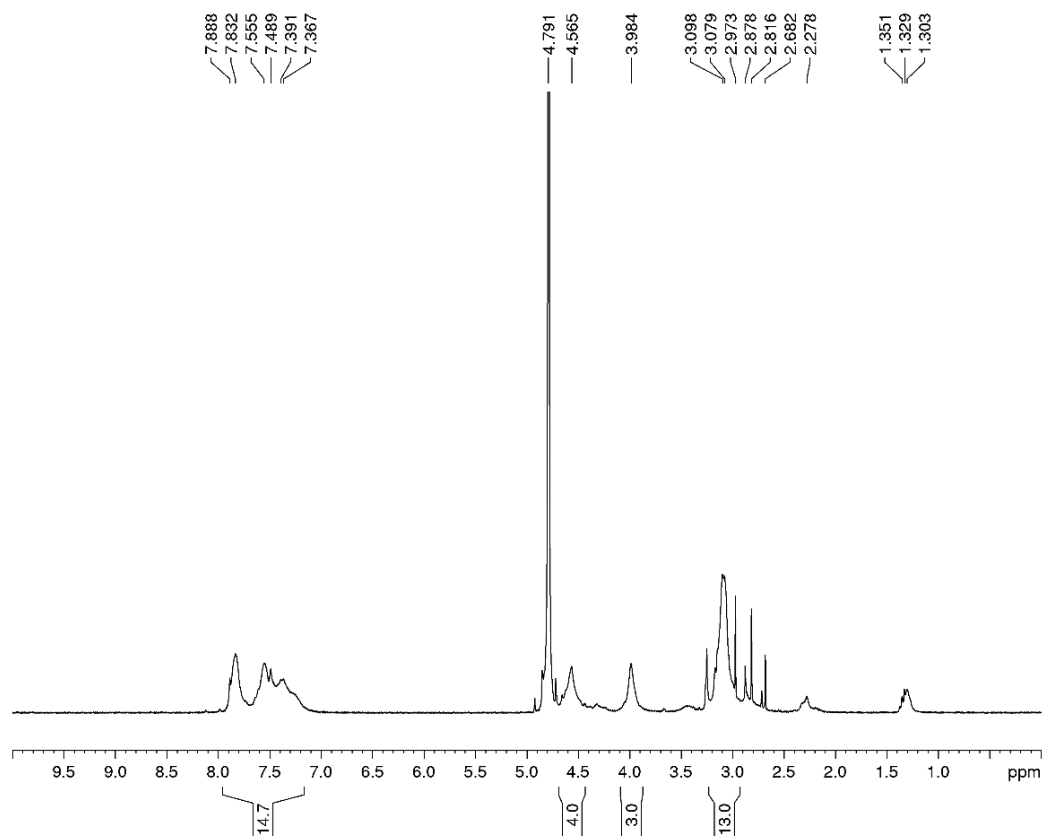


¹H-NMR spectrum (300 MHz, DMSO-d₆) of *para*-Precursor.

NMR Spectra and PXRD



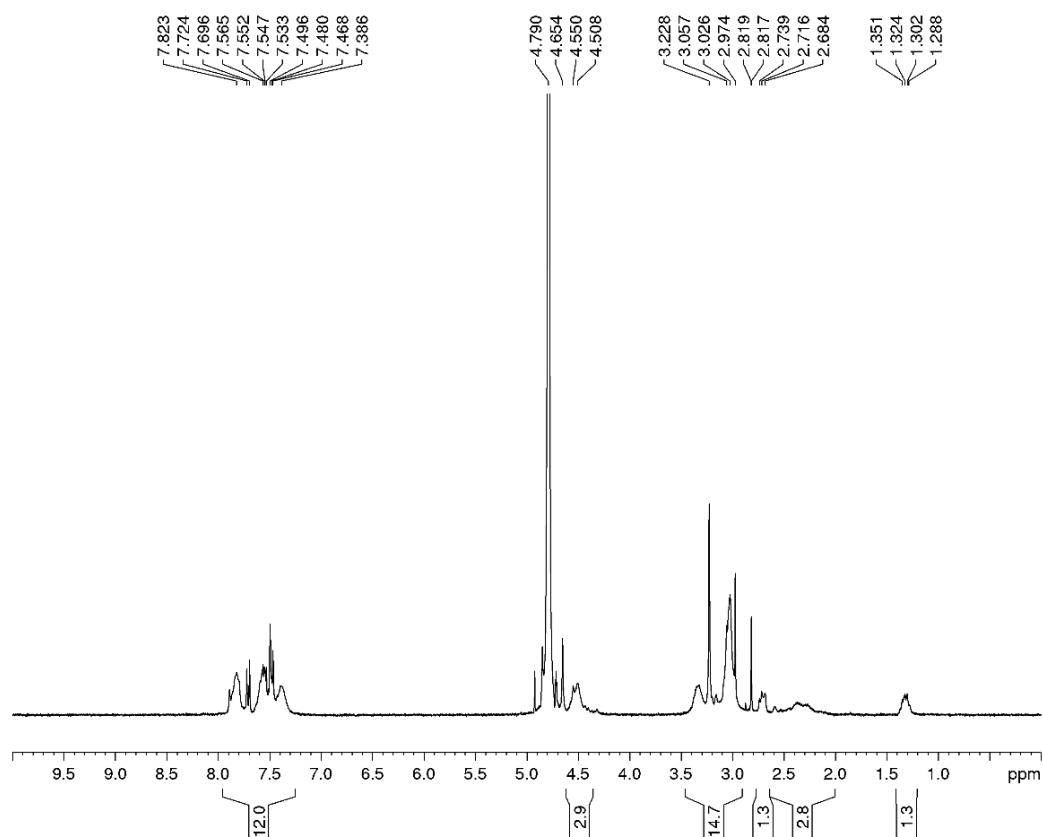
¹H-NMR spectrum (300 MHz, D₂O) of **o-DABCO**.



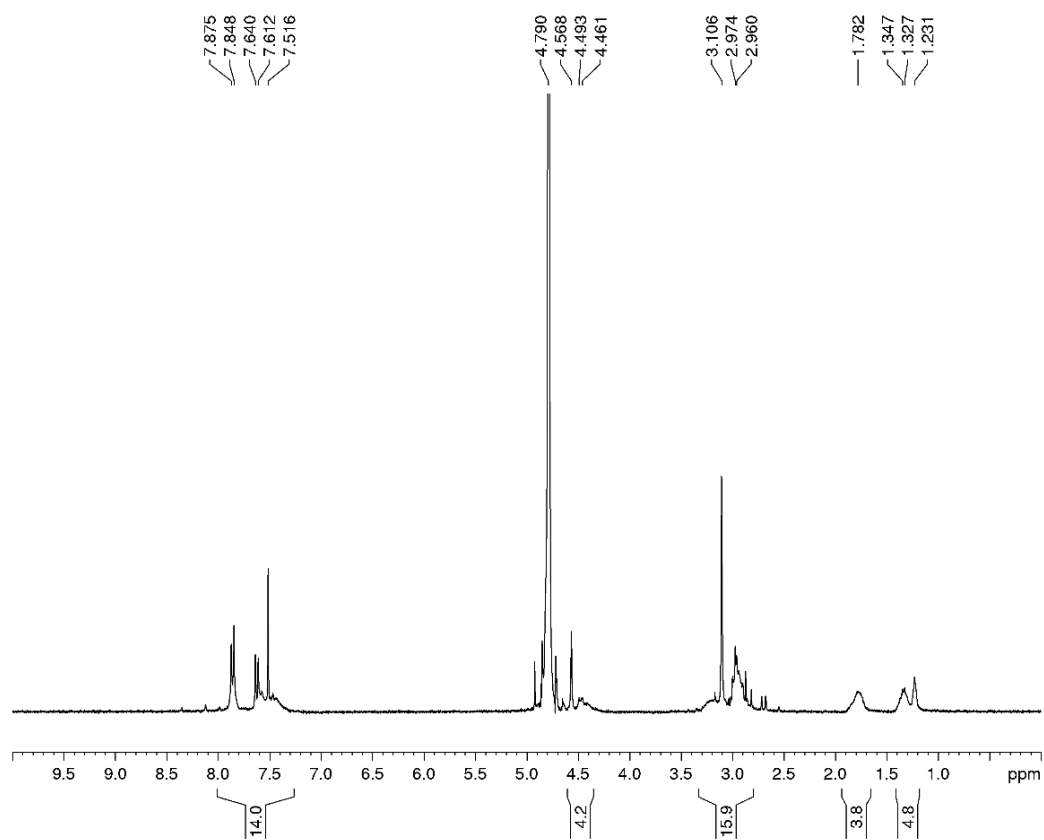
NMR spectrum (300 MHz, D₂O) of **o-C₂**.

¹H-

NMR Spectra and PXRD



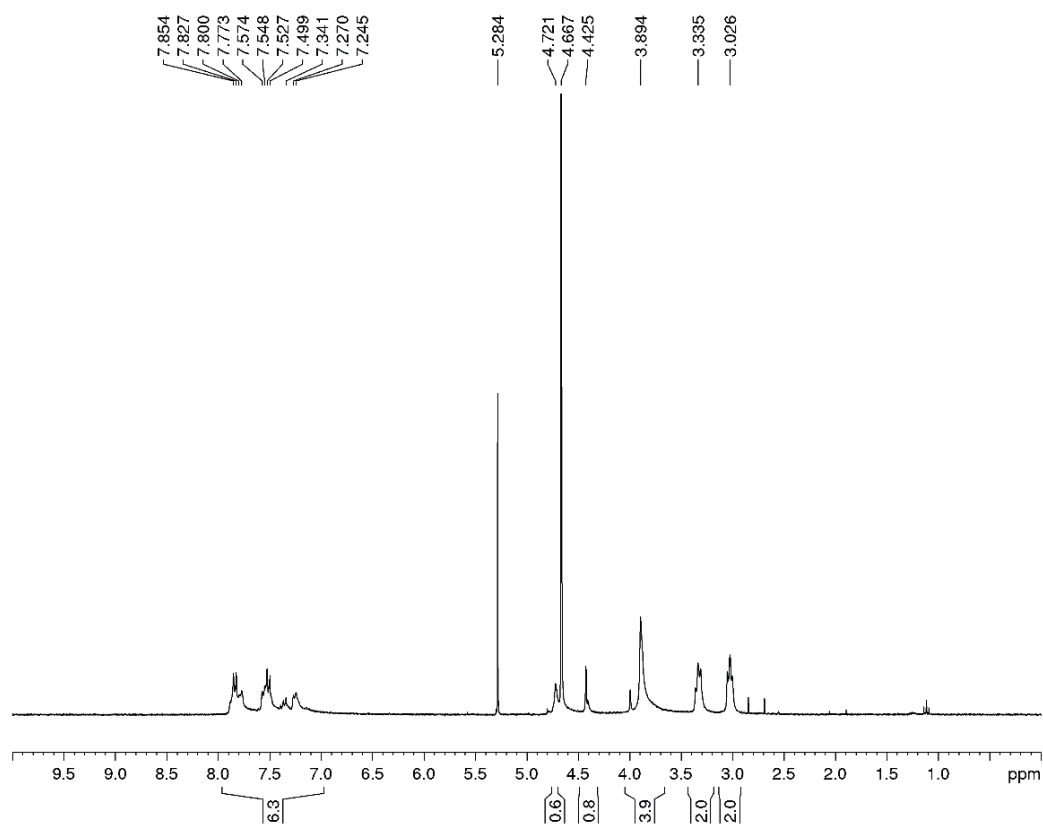
$^1\text{H-NMR}$ spectrum (300 MHz, D_2O) of **o-C₃**.



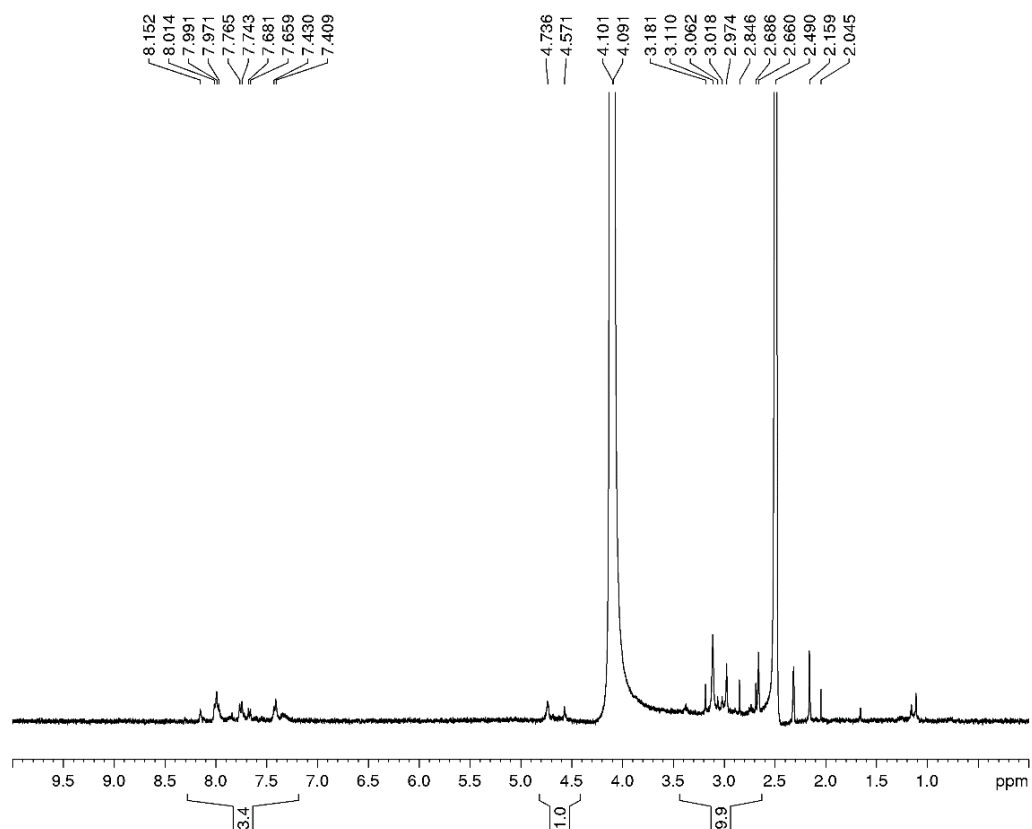
$^1\text{H-NMR}$ spectrum (300 MHz, D_2O) of **o-C₆**.

$^1\text{H-}$

NMR Spectra and PXRD

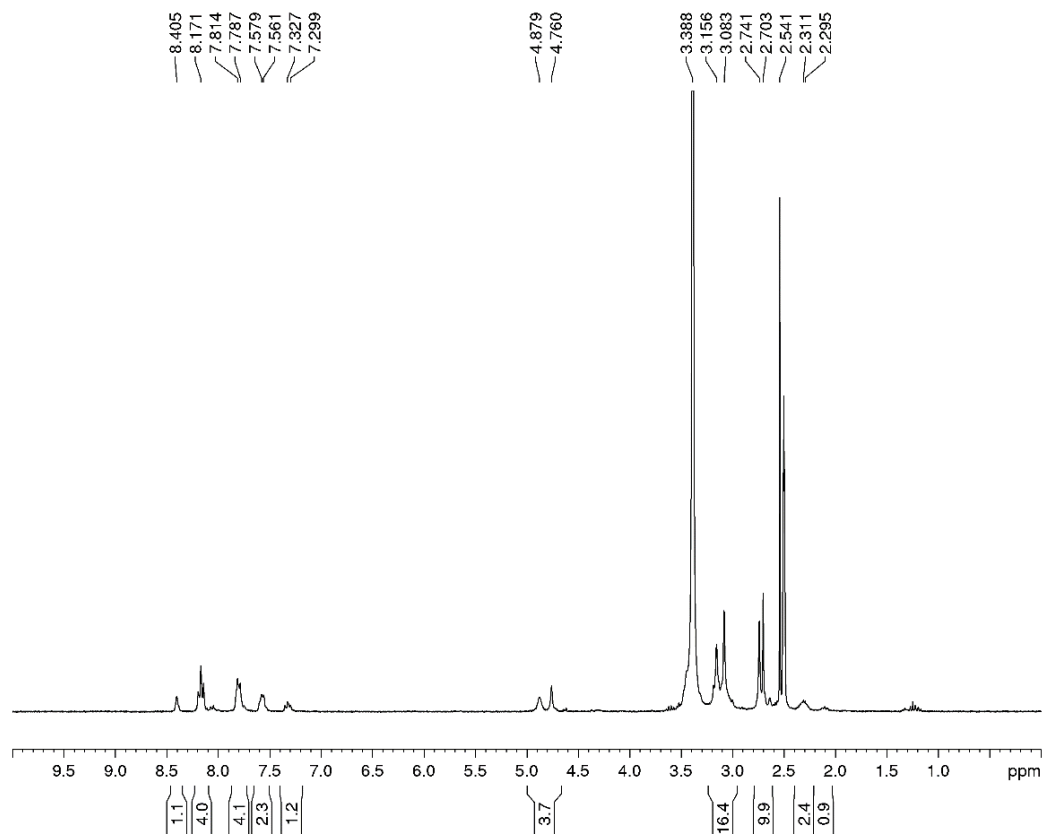


$^1\text{H-NMR}$ spectrum (300 MHz, D_2O) of *m*-DABCO.

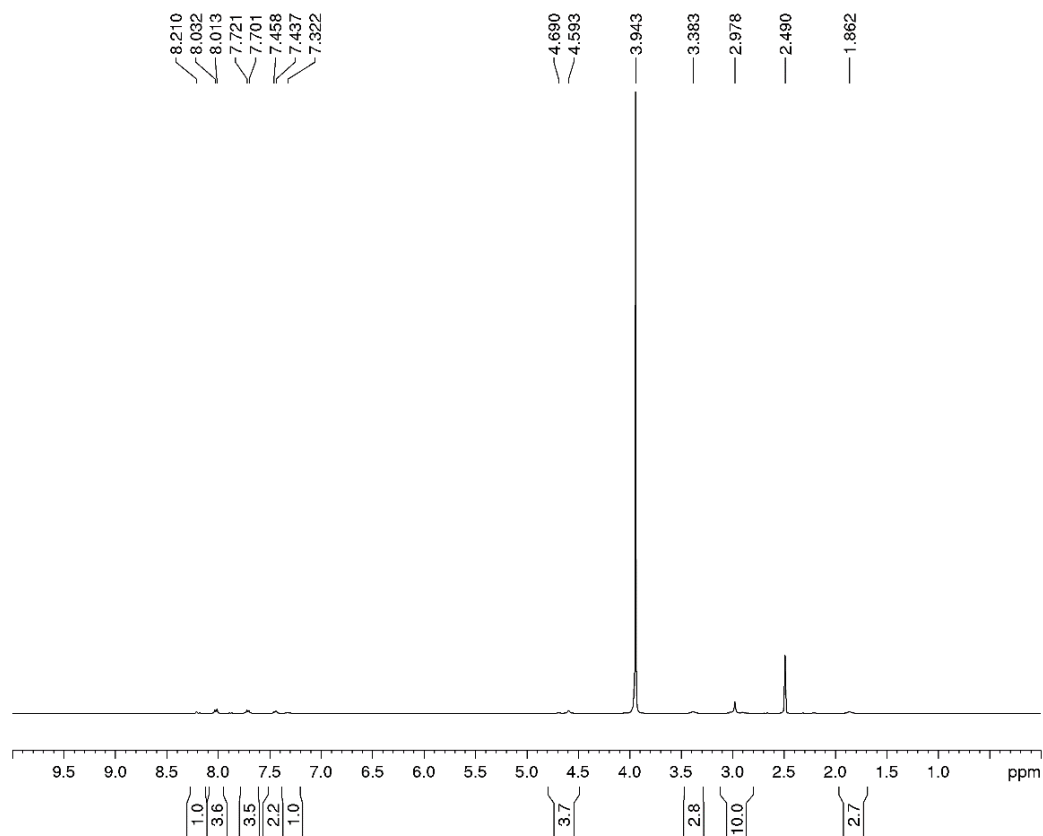


$^1\text{H-NMR}$ spectrum (300 MHz, DMSO-d_6) of *m*-C₂.

NMR Spectra and PXRD

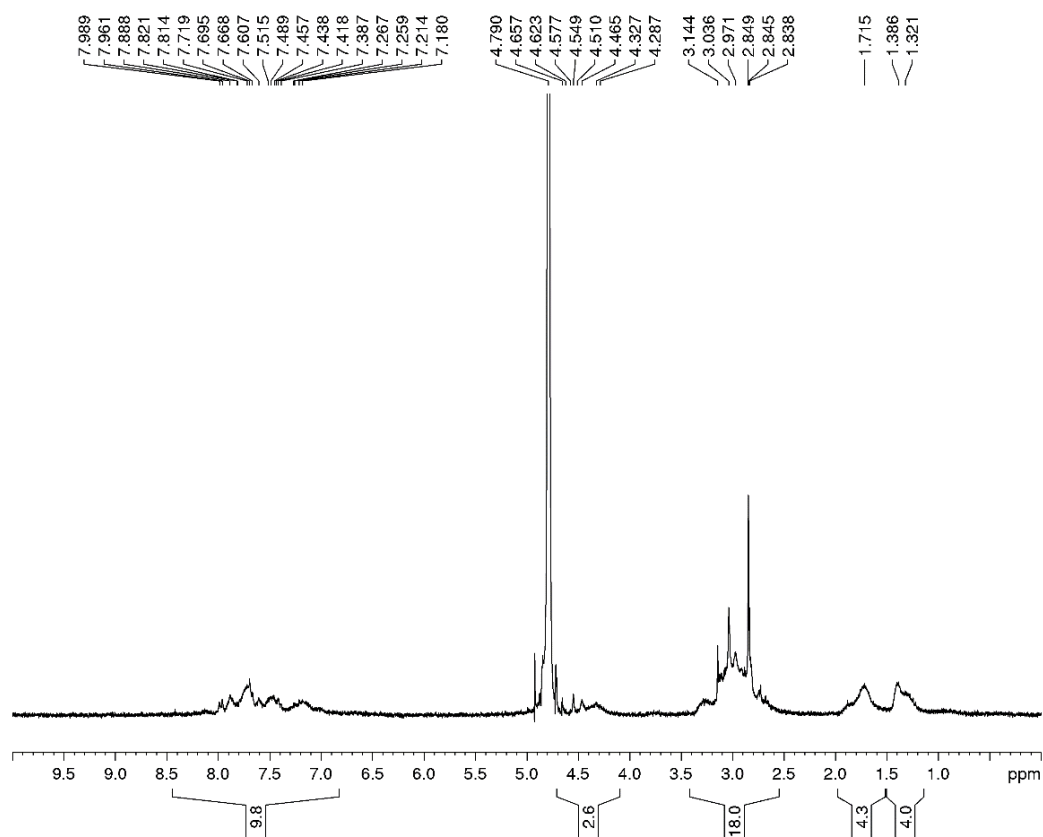


$^1\text{H-NMR}$ spectrum (300 MHz, DMSO-d_6) of *m-C*₃.

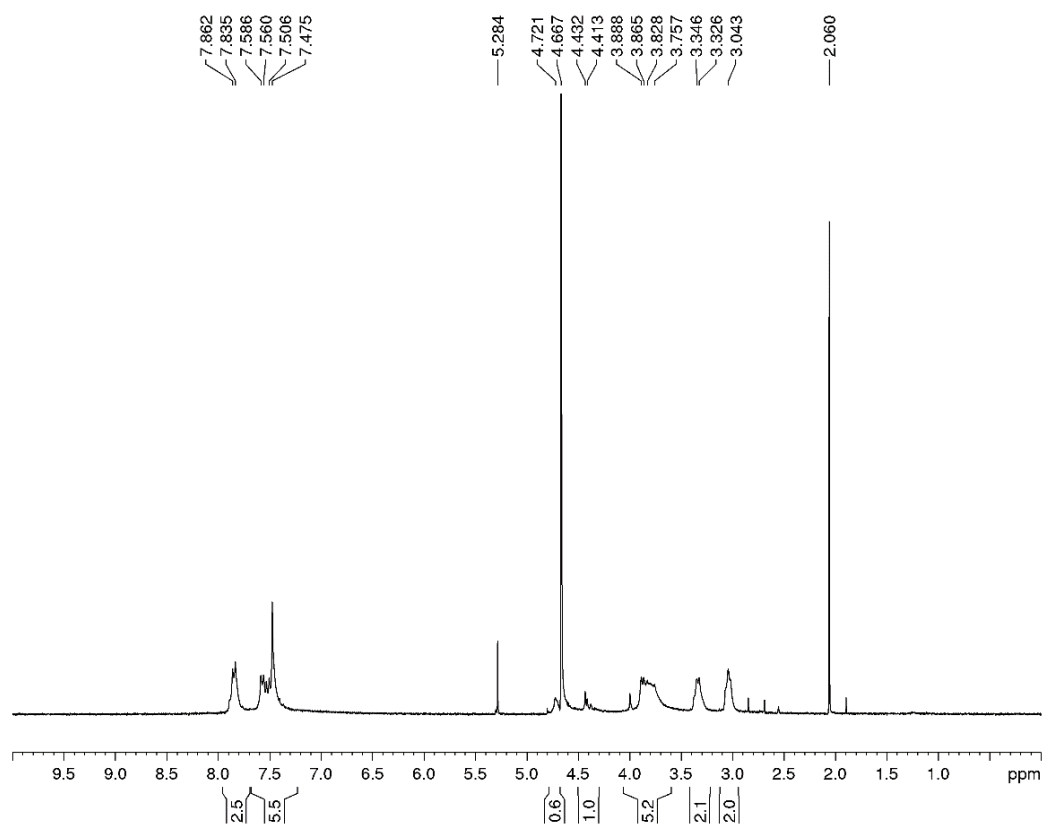


$^1\text{H-NMR}$ spectrum (300 MHz, DMSO-d_6) of *m-C*₄.

NMR Spectra and PXRD

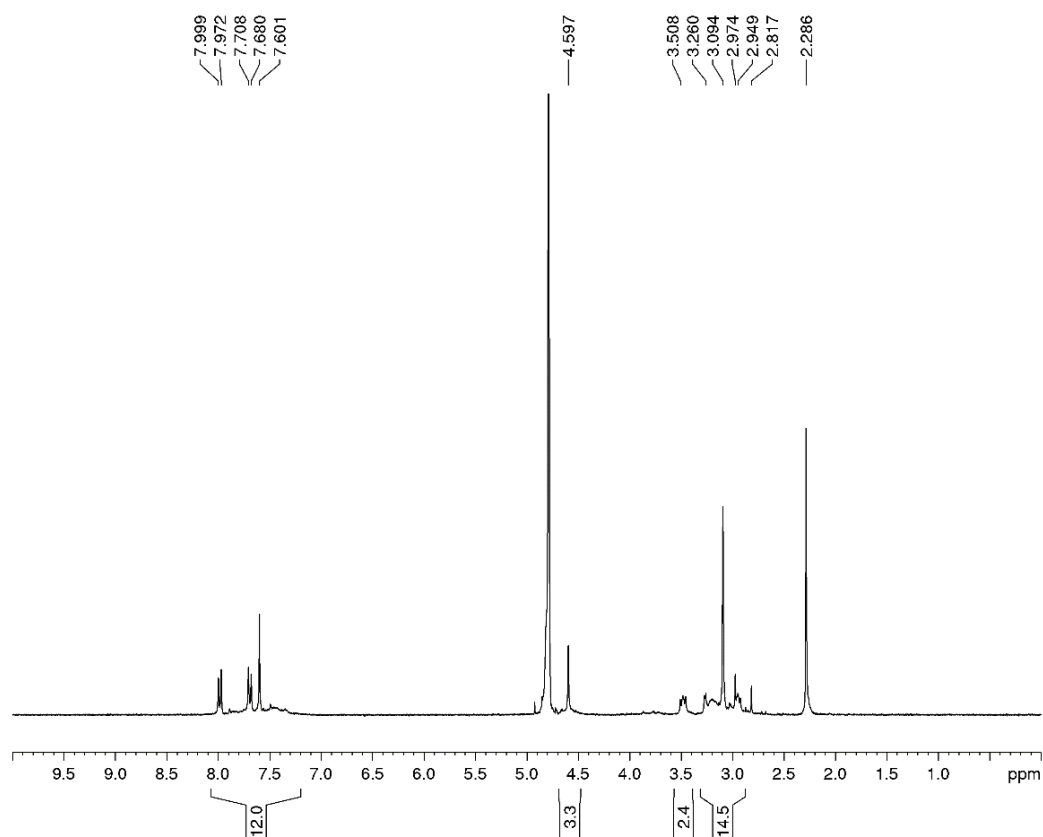


$^1\text{H-NMR}$ spectrum (300 MHz, D_2O) of *m*- C_6 .

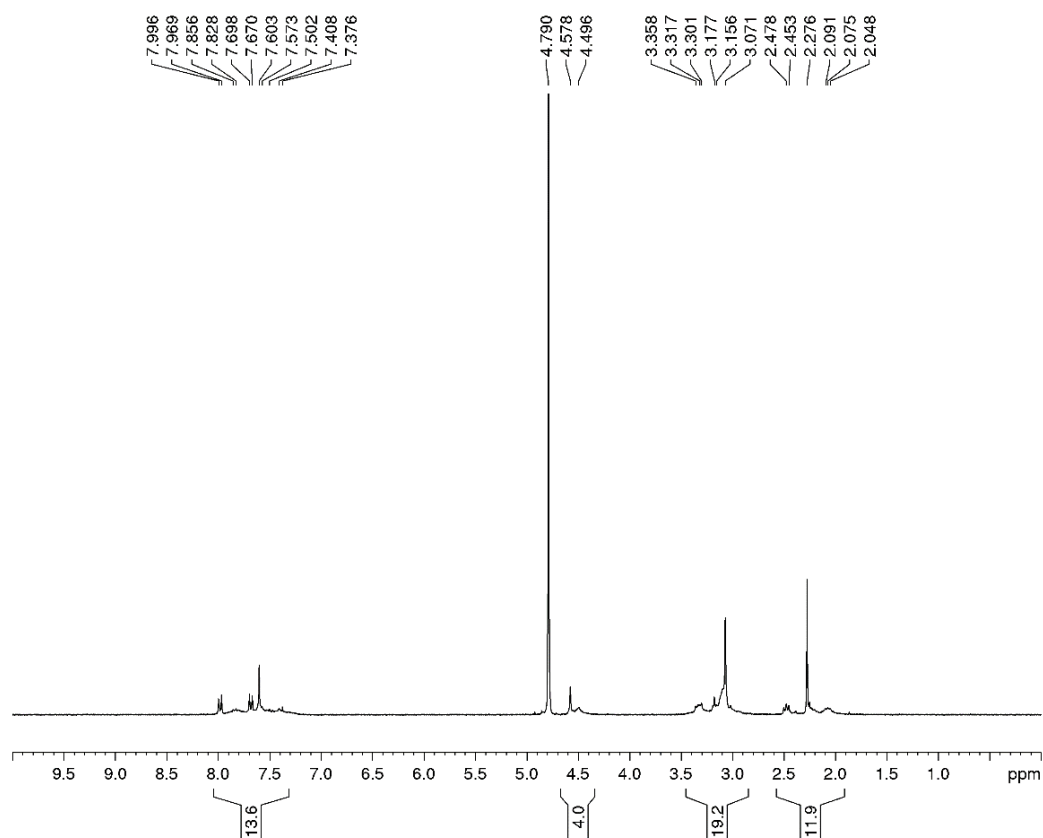


$^1\text{H-NMR}$ spectrum (300 MHz, D_2O) of *p*-DABCO.

NMR Spectra and PXRD

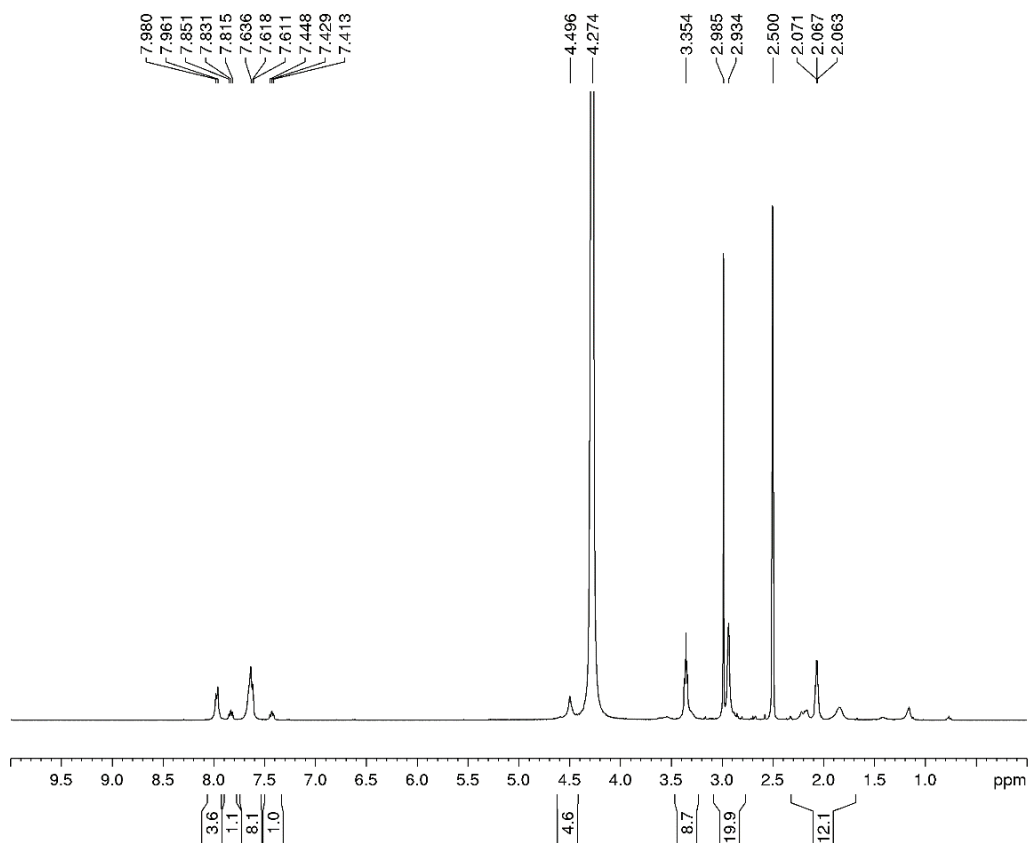


$^1\text{H-NMR}$ spectrum (300 MHz, D_2O) of **p-C₂**.

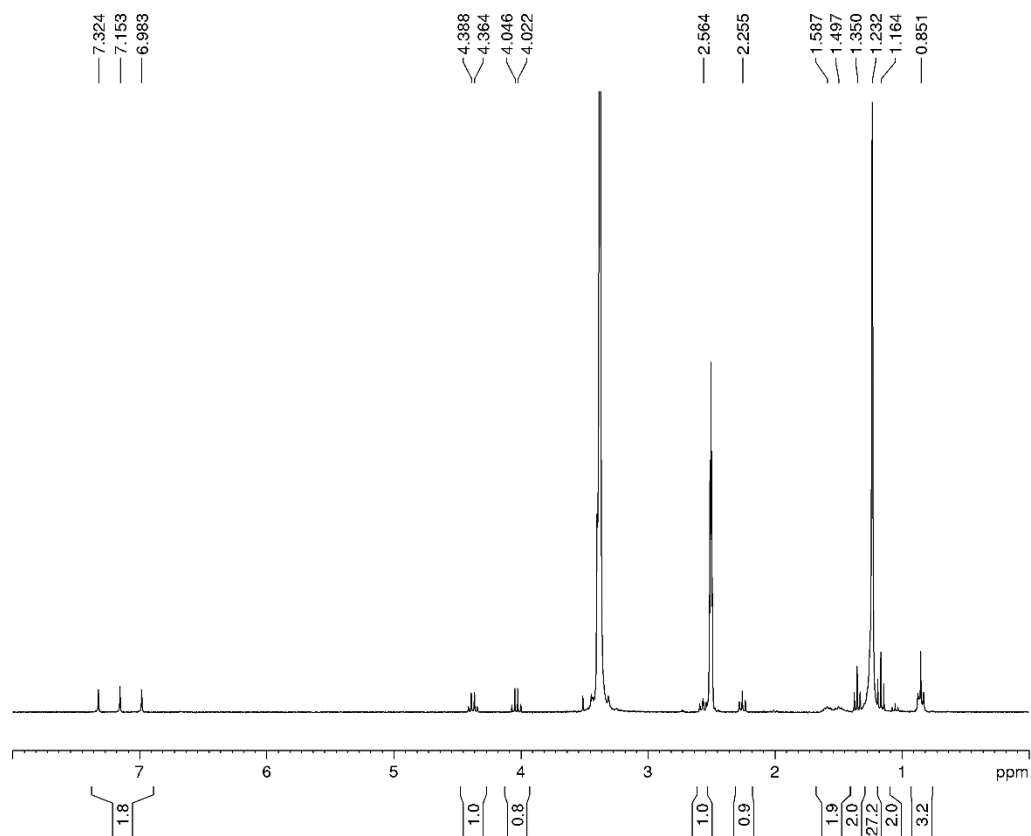


$^1\text{H-NMR}$ spectrum (300 MHz, D_2O) of **p-C₃**.

NMR Spectra and PXRD

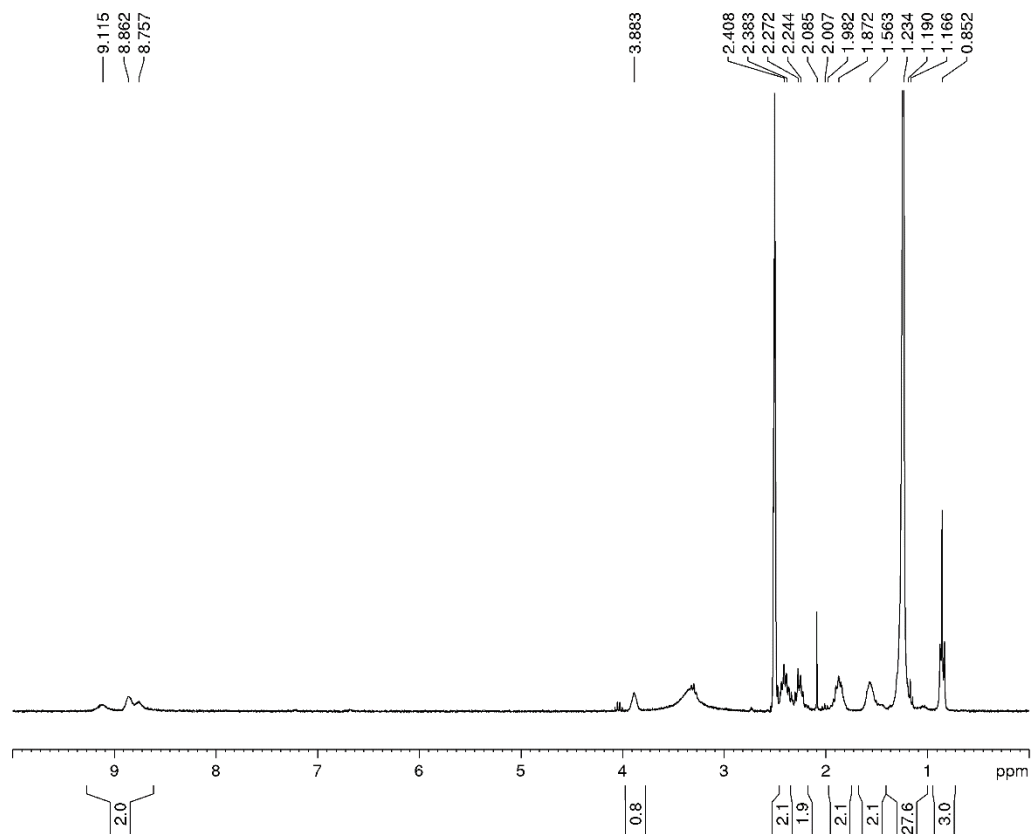


$^1\text{H-NMR}$ spectrum (300 MHz, DMSO-d_6) of ***p*-C₄**.

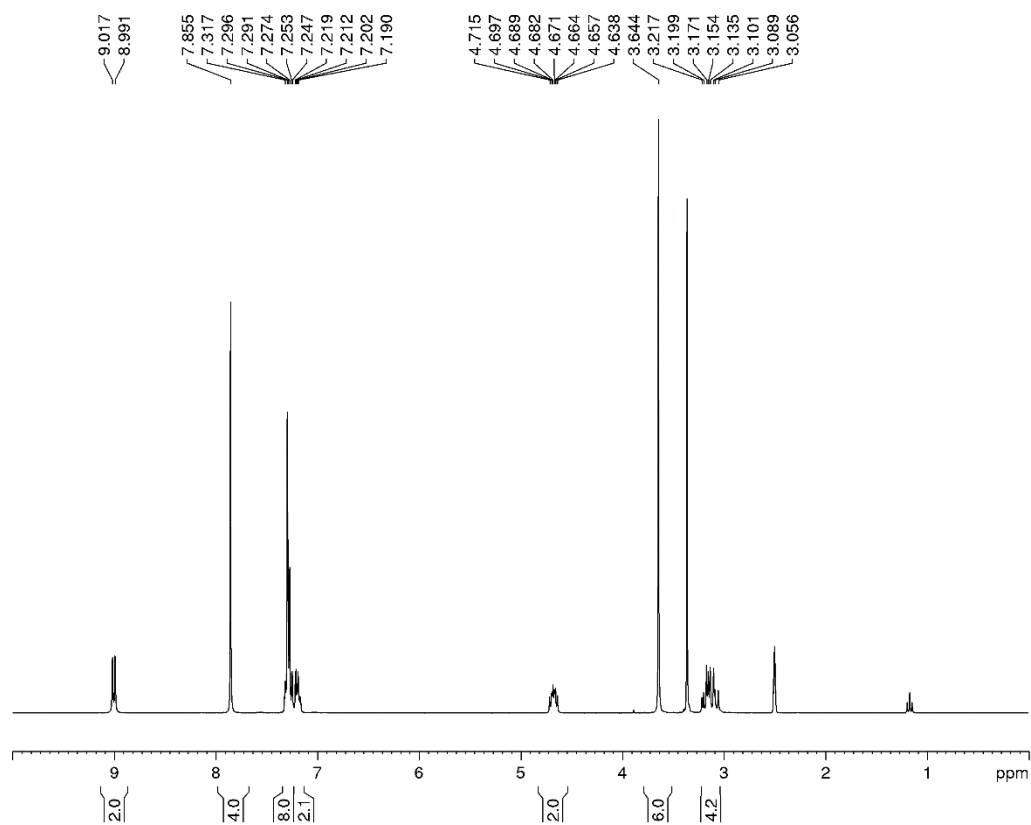


$^1\text{H-NMR}$ spectrum (300 MHz, DMSO-d_6) of ethyl stearimidate.

NMR Spectra and PXRD

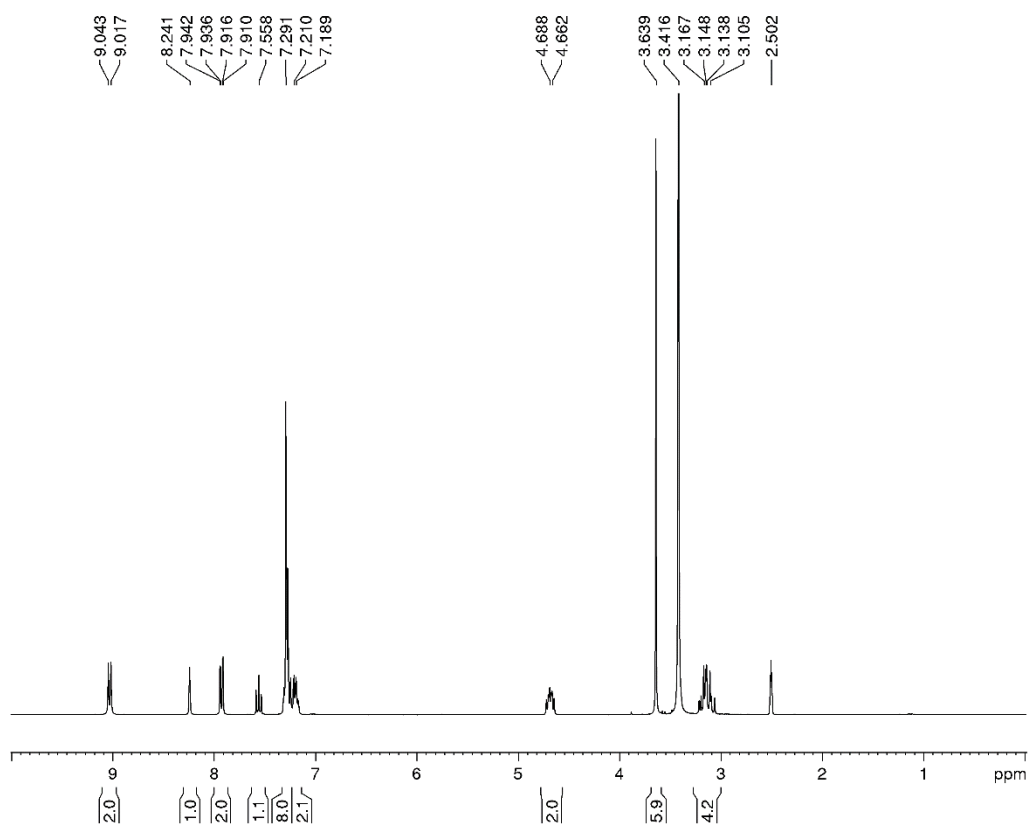


$^1\text{H-NMR}$ spectrum (300 MHz, DMSO-d_6) of amidin-Glu.

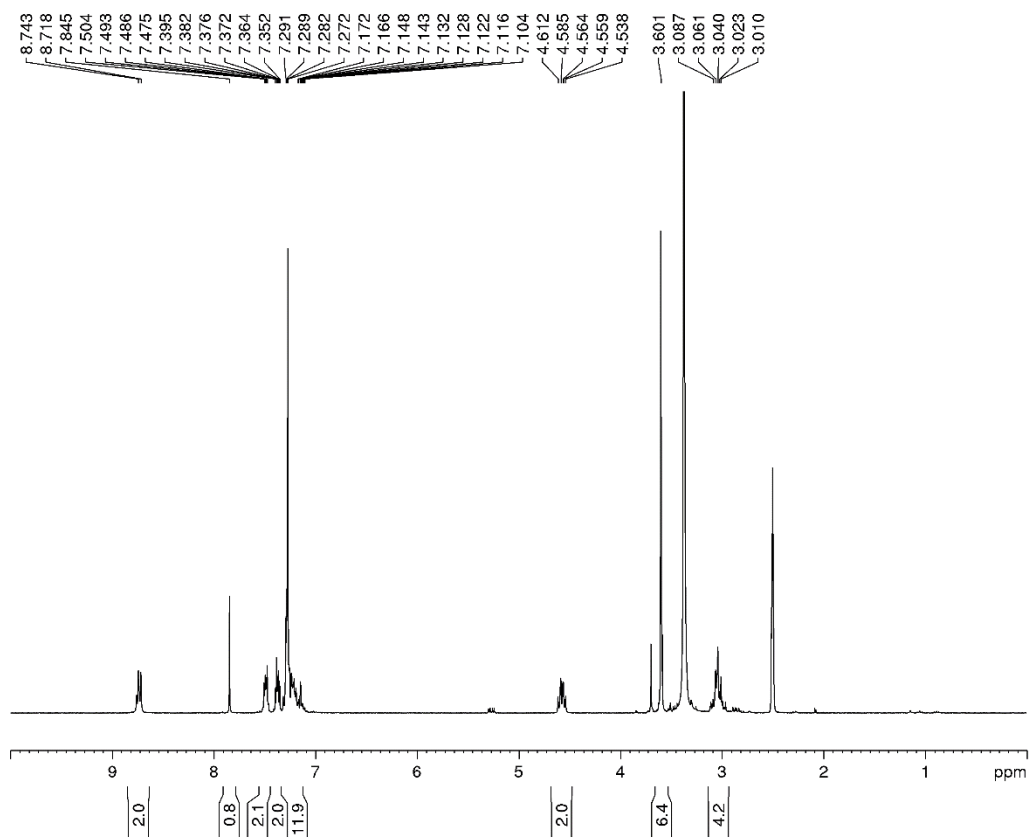


$^1\text{H-NMR}$ spectrum (300 MHz, DMSO-d_6) of **p-precursor 2**.

NMR Spectra and PXRD

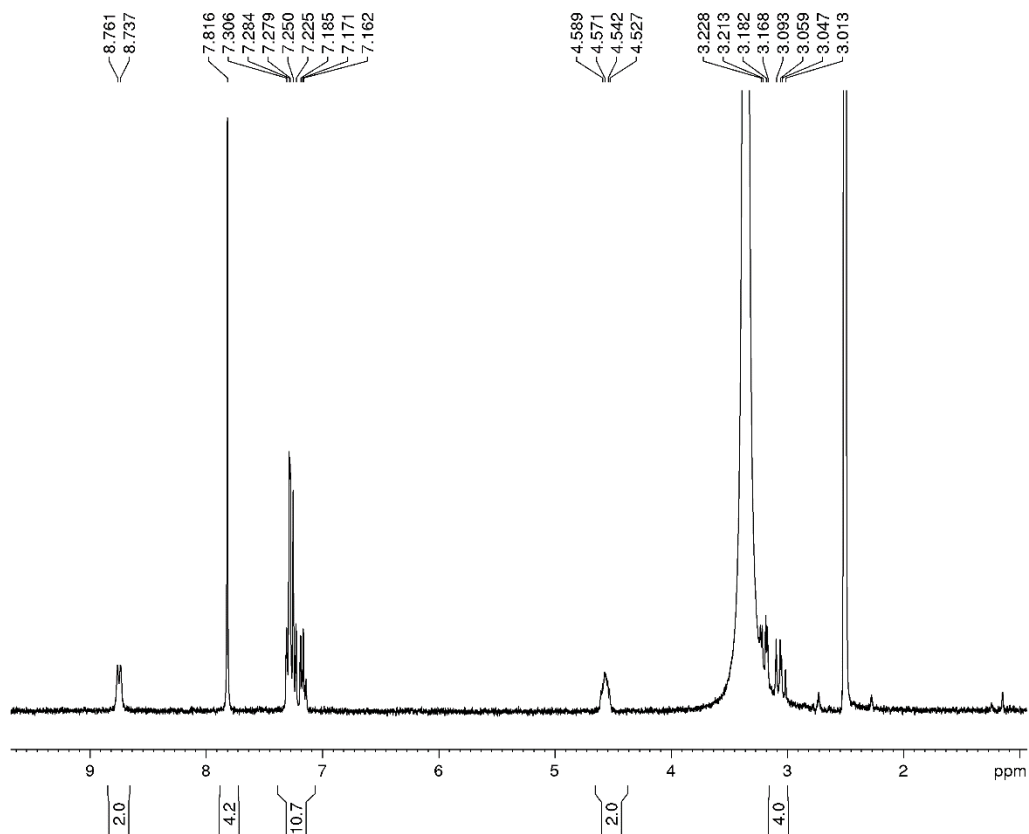


¹H-NMR spectrum (300 MHz, DMSO-d₆) of *m*-precursor 2.

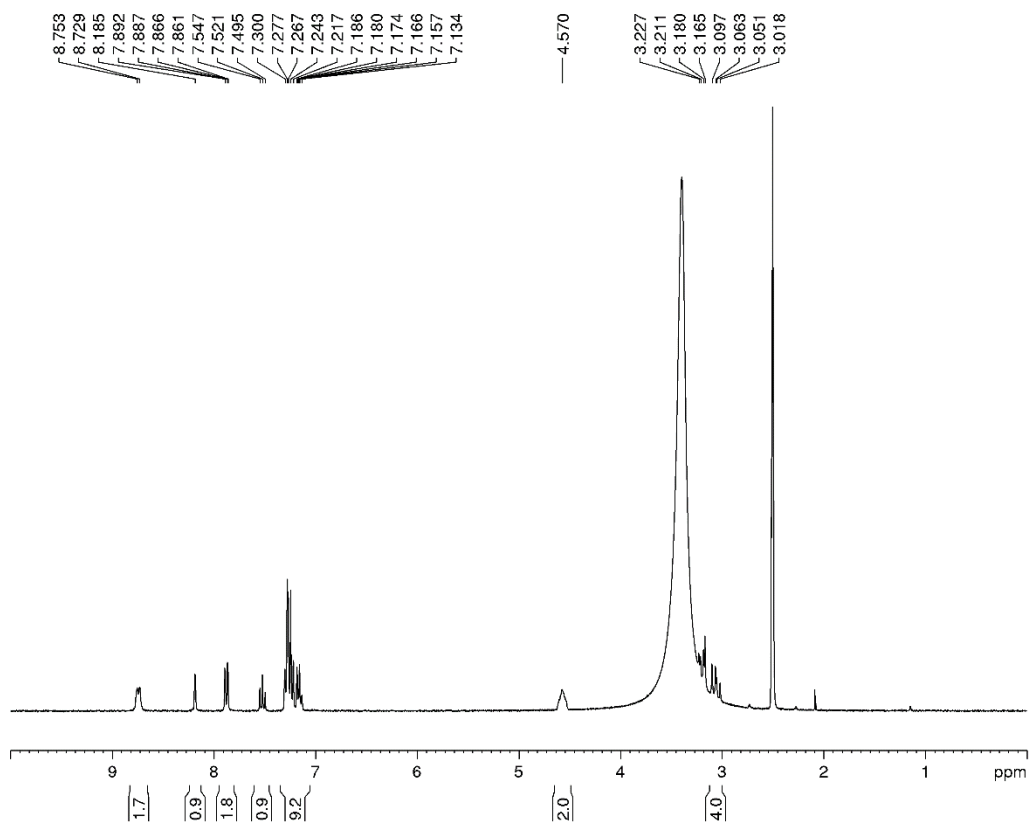


¹H-NMR spectrum (300 MHz, DMSO-d₆) of *p*-precursor 2.

NMR Spectra and PXRD

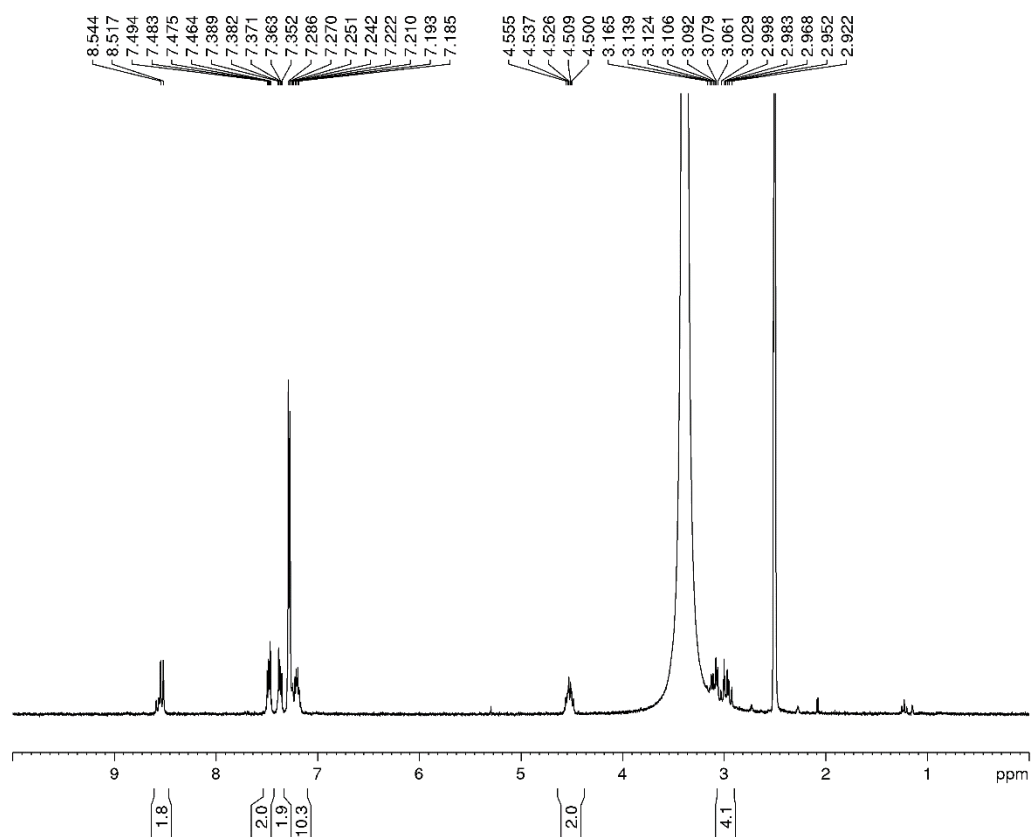


$^1\text{H-NMR}$ spectrum (300 MHz, DMSO-d_6) of ***p*-precursor 1**.

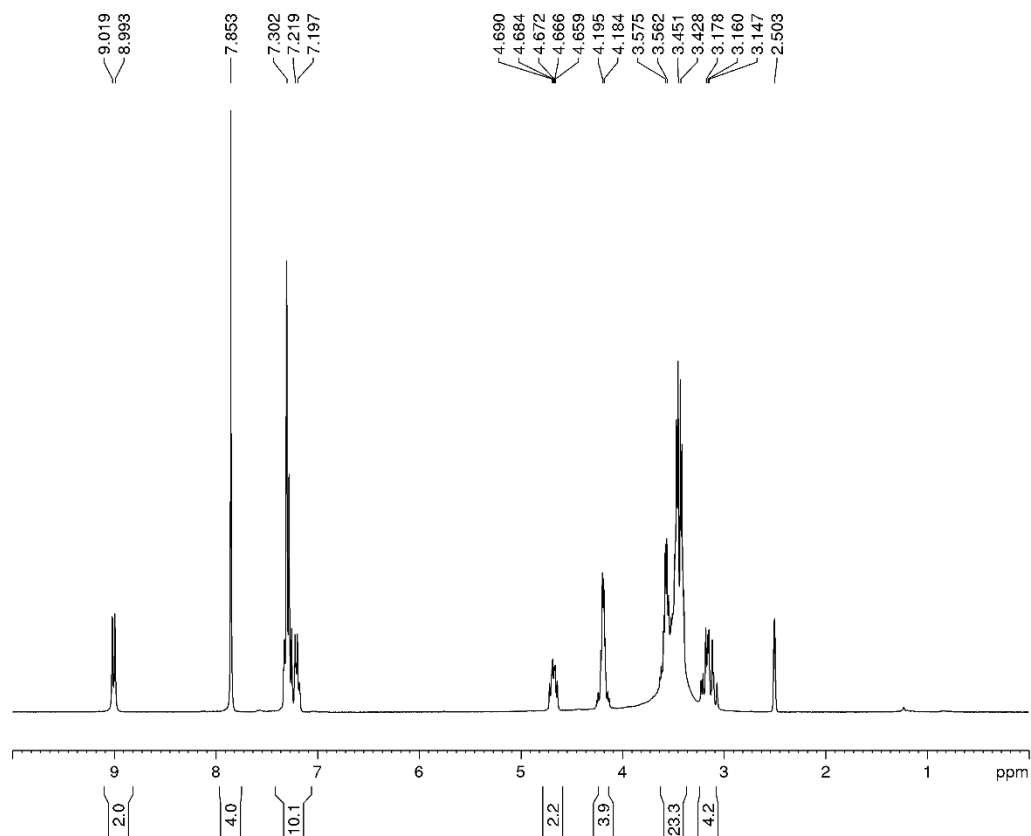


$^1\text{H-NMR}$ spectrum (300 MHz, DMSO-d_6) of ***m*-precursor 1**.

NMR Spectra and PXRD

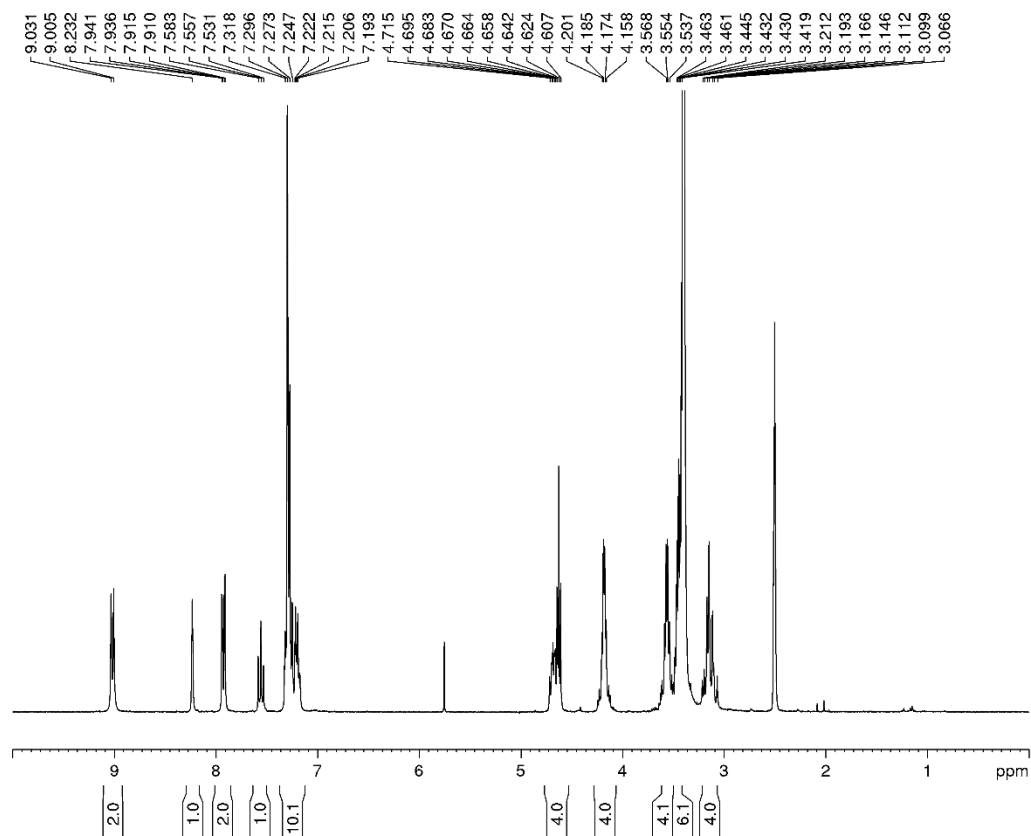


$^1\text{H-NMR}$ spectrum (300 MHz, DMSO-d_6) of **o-precursor 1**.

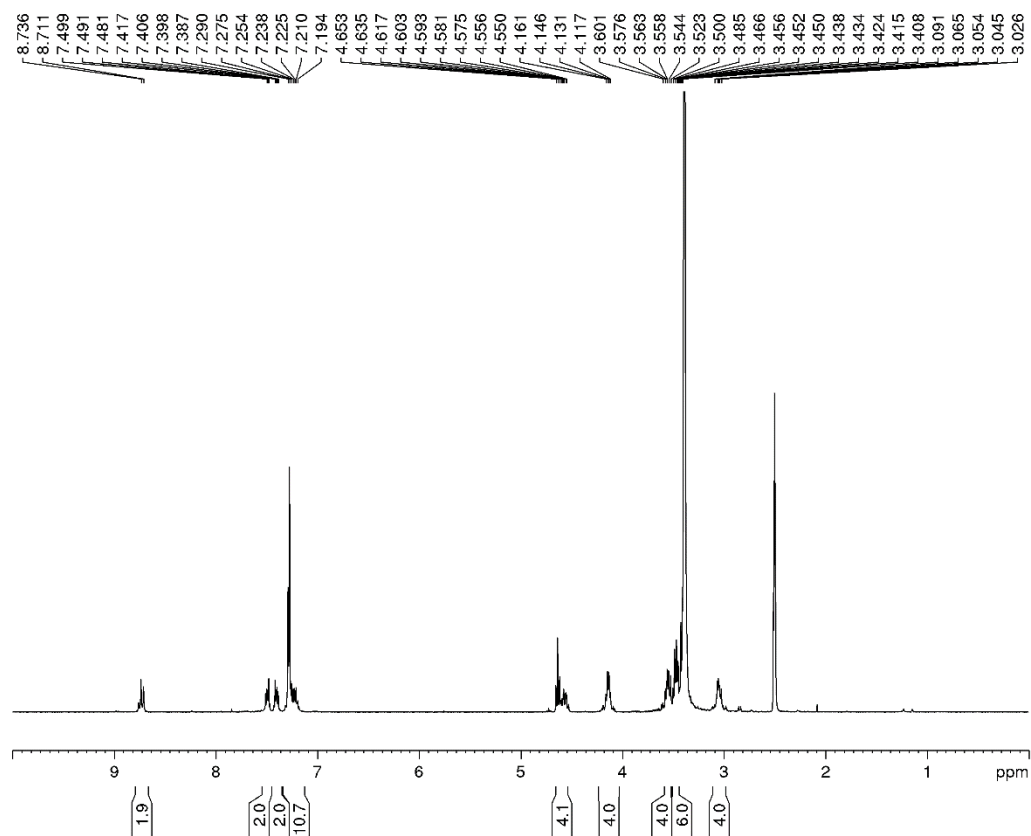


$^1\text{H-NMR}$ spectrum (300 MHz, DMSO-d_6) of **p-PDB**.

NMR Spectra and PXRD

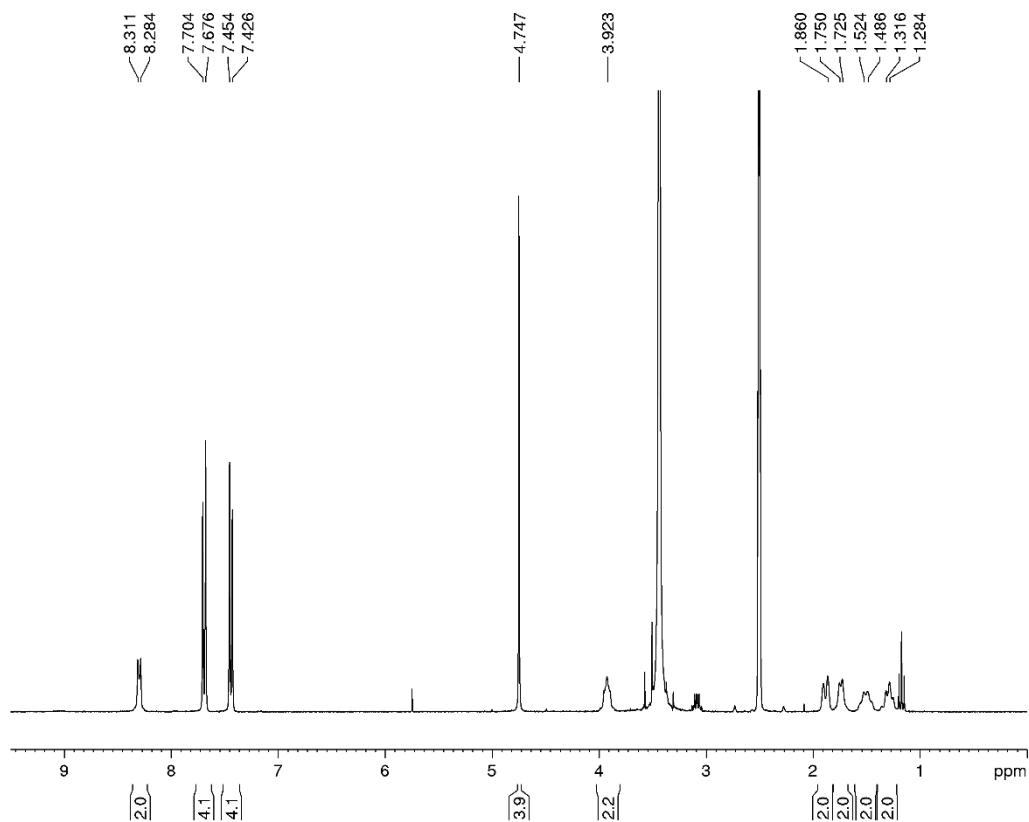


$^1\text{H-NMR}$ spectrum (300 MHz, DMSO-d_6) of *m*-PDB.

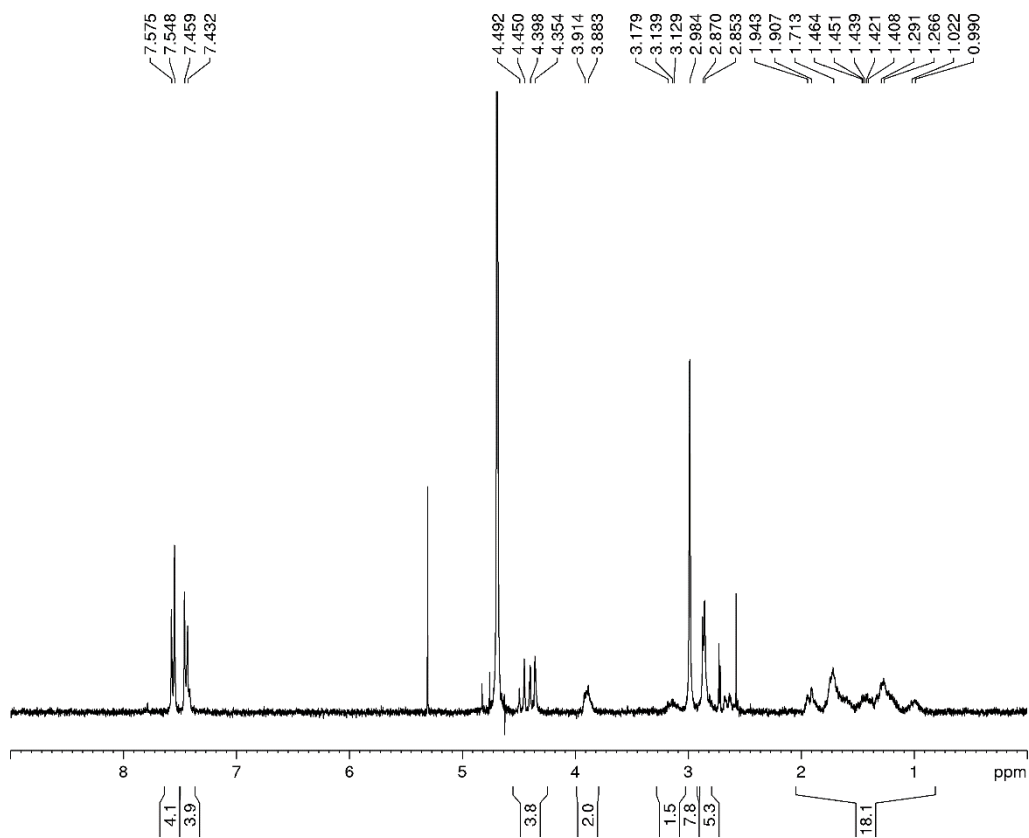


$^1\text{H-NMR}$ spectrum (300 MHz, DMSO-d_6) of *o*-PDB.

NMR Spectra and PXRD

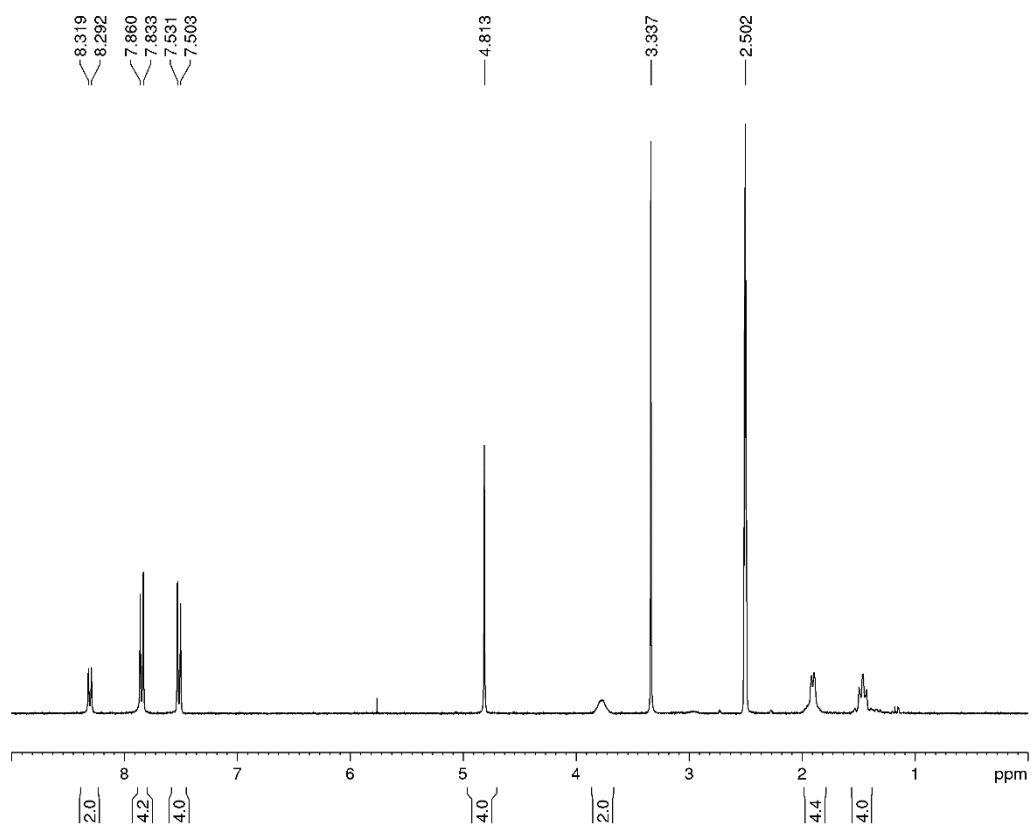


¹H-NMR spectrum (300 MHz, D₂O) of **o-cyclohex-monomer**.

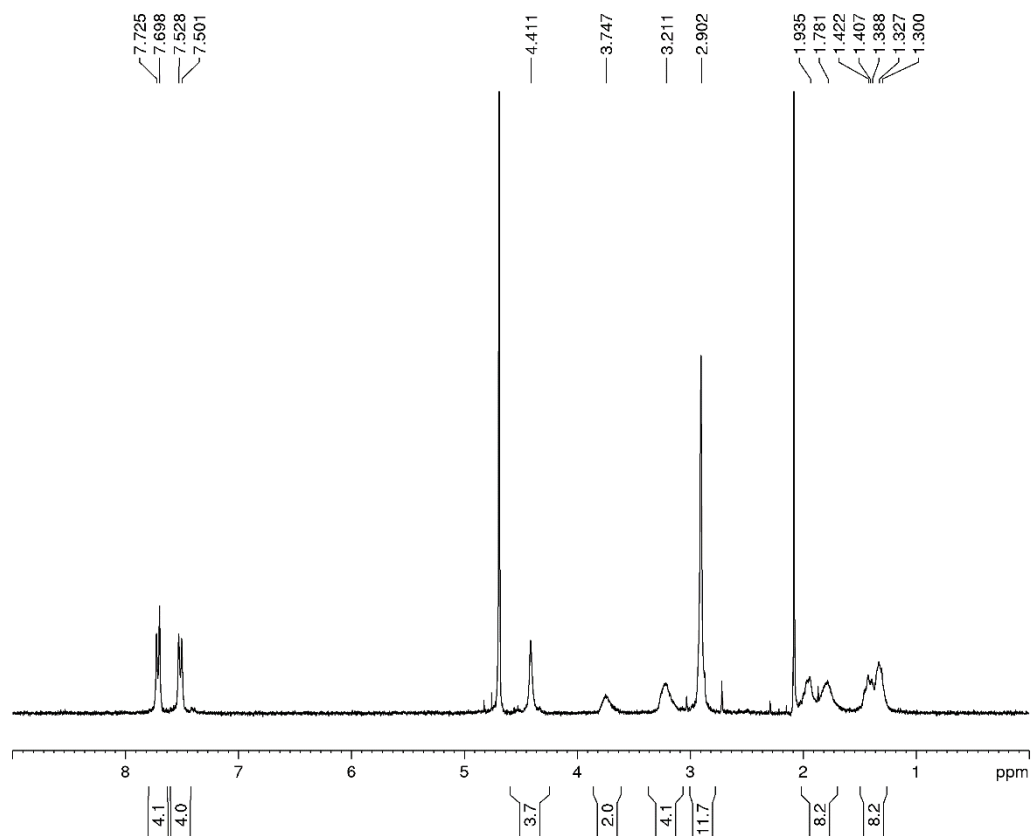


¹H-NMR spectrum (300 MHz, D₂O) of **o-cyclohex**.

NMR Spectra and PXRD

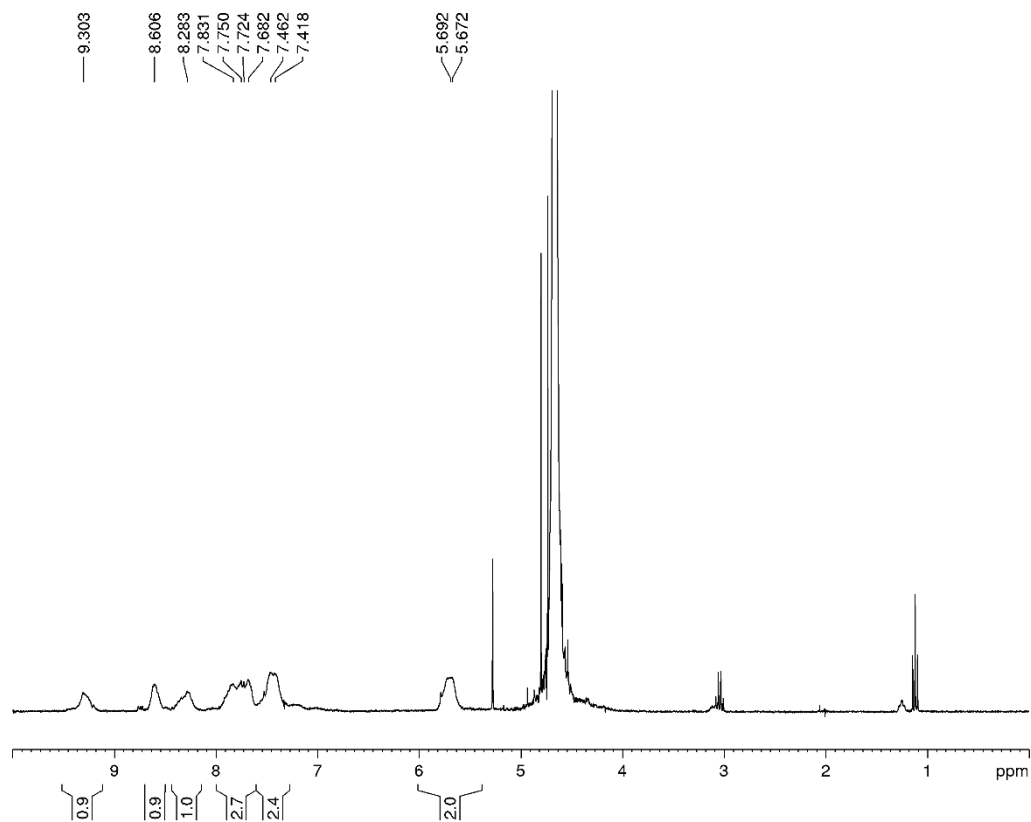


¹H-NMR spectrum (300 MHz, D₂O) of **p-cyclohex-monomer**.

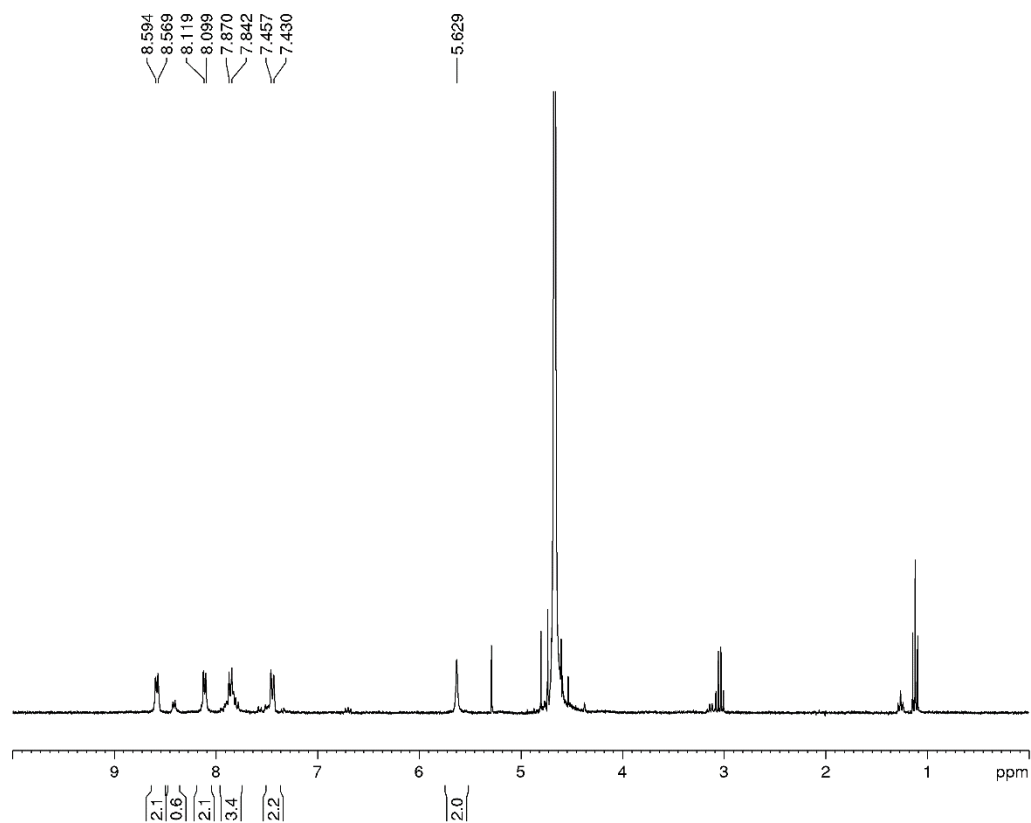


¹H-NMR spectrum (300 MHz, D₂O) of **p-cyclohex**.

NMR Spectra and PXRD

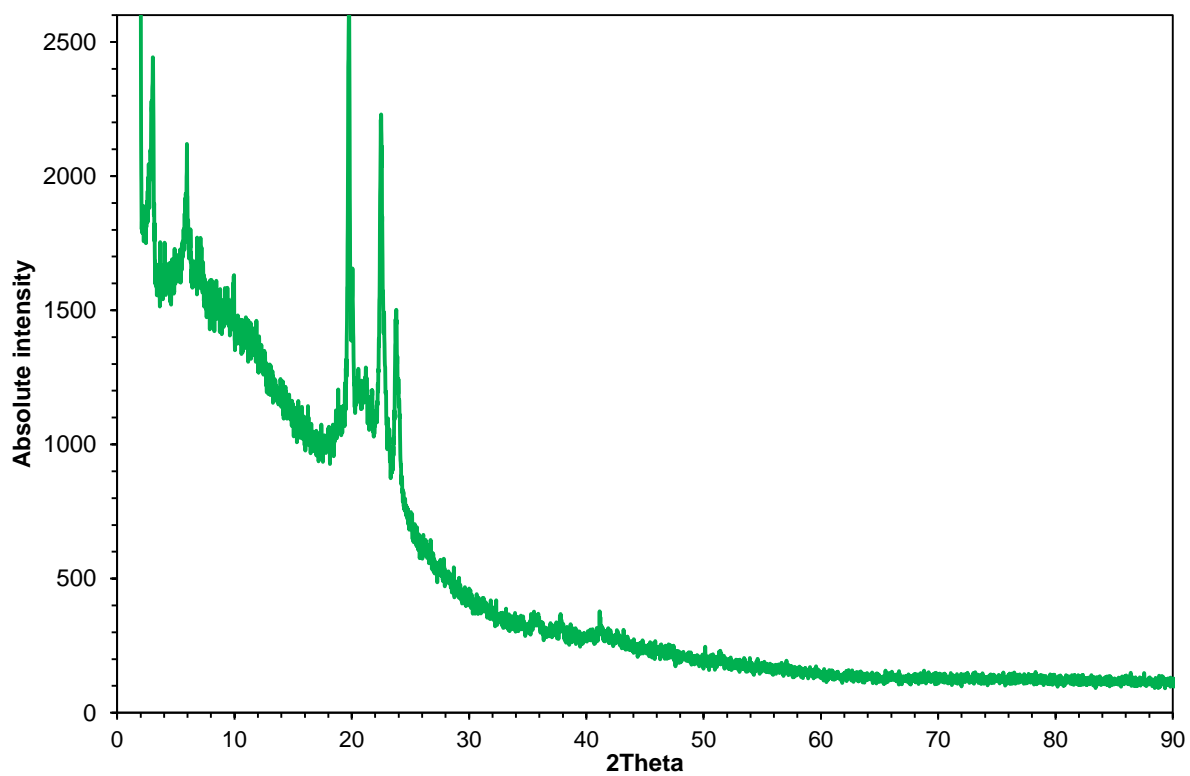


¹H-NMR spectrum (300 MHz, D₂O) of *m*-polypyr.

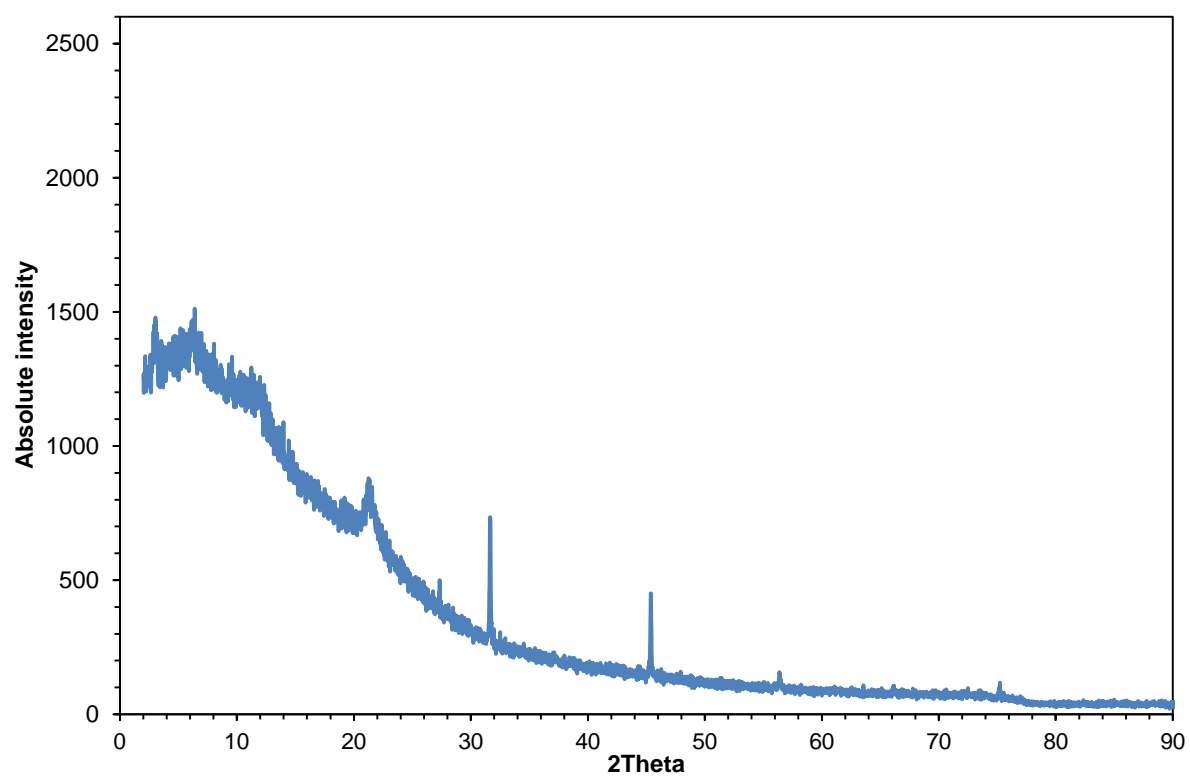


¹H-NMR spectrum (300 MHz, D₂O) of *p*-polypyr.

NMR Spectra and PXRD

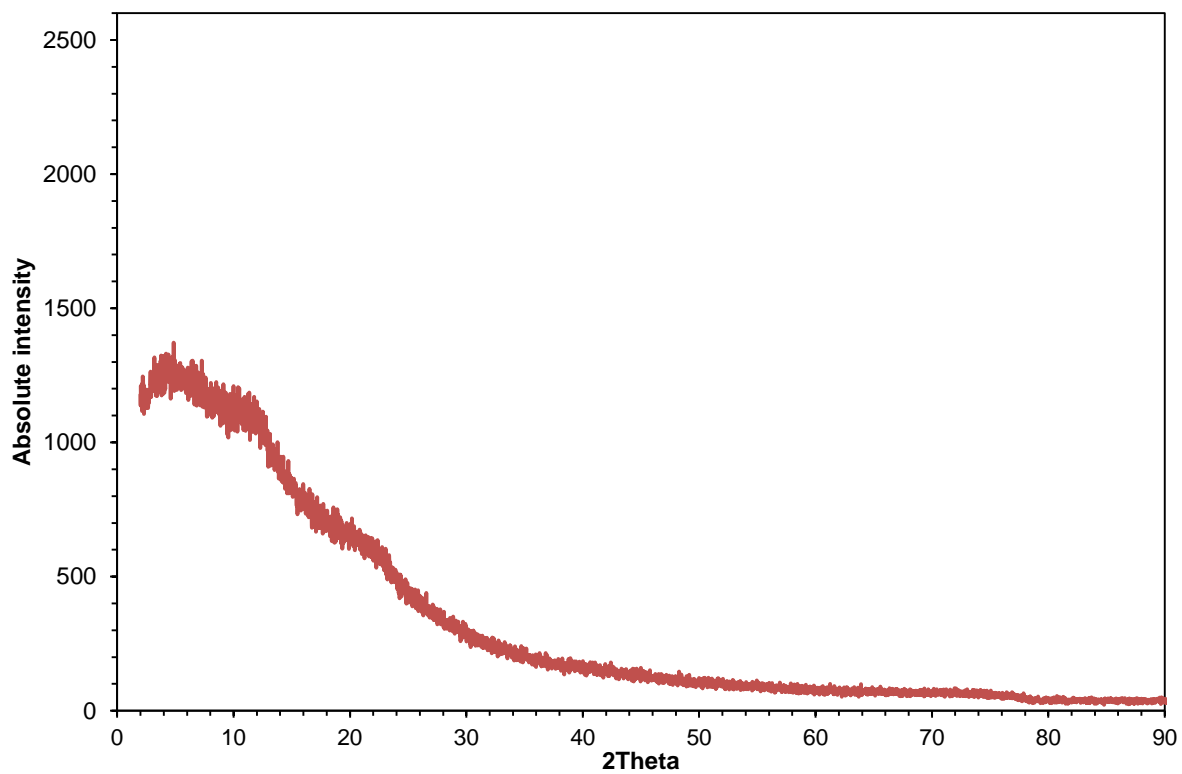


PXRD of FAG powder.



PXRD of a xerogel derived from FAG based hydrogel.

NMR Spectra and PXRD



PXRD of a xerogel derived from FAG based gel in MeCN.

H List of Abbreviations

1D	one-dimensional
3D	three-dimensional
μ	micro
brs	broad singlet
calc.	calculated
CAMP	camptothecin
CGC	critical gelation concentration
DABCO	1,4-diazabicyclo[2.2.2]octane
DCM	dichloromethane (methylene chloride)
DLS	dynamic light scattering
DMF	N,N-dimethylformamide
DMSO	dimethyl sulfoxide
DNA	deoxyribonucleic acid
DSC	differential scanning calorimetry
EDTA	ethylenediaminetetraacetic acid
Et ₂ O	diethyl ether
EtOAc	ethyl acetate
EtOH	ethanol
EI	electron impact ionization
ESI	electron spray ionization
FESEM	field emission scanning electron microscopy
GA	glycyrrhizic acid
h	hours
HEPES	4-(2-hydroxyethyl)-1-piperazineethanesulfonic acid
HPLC	high pressure/performance liquid chromatography
HRMS	high resolution mass spectrometry
i-PrOH	iso-propanol
LMWG	low-molecular-weight gelator
logP	partition coefficient
m	milli
M	mol/liter
MeCN	acetonitrile
MeOH	methanol

List of Abbreviations

MES	2-(<i>N</i> -morpholino)ethanesulfonic acid
min	minutes
MITOX	mitoxantrone hydrate
MS	mass spectrometry
n	nano
NEt ₃	triethylamine
NMR	nuclear magnetic resonance
OXY	oxytetracycline hydrochloride
PBS	phosphate buffered saline
PEE	poly(L-lysine)
PEG	polyethylene glycol
PEI	poly(ethylenimine)
Ph	phenyl
ppm	parts per million
QAS	quaternary ammonium salt
RNA	ribonucleic acid
RT	room temperature
s	singlet
SAXS	small angle X-ray scattering
Scr	scramble
SEM	scanning electron microscopy
t	triplet
TBAF	tetra- <i>n</i> -butylammonium fluoride
T _{gel}	melting temperature of a gel
TGYE	tryptone glucose yeast extract
THF	tetrahydrofuran
TFA	trifluoroacetic acid
UV-Vis	ultraviolet–visible spectroscopy

I Curriculum Vitae

Personal data

Name: Judith Mayr
Date of birth: 07 March 1989
Place of birth: Weilheim, Germany
Nationality: German

Education

01/2014 – 06/2017 **PhD thesis** under the supervision of Prof. Dr. Díaz Díaz at University of Regensburg
„Synthesis, characterization and application of smart materials based on polymers and low-molecular compounds”

10/2011 – 12/2013 **Master studies** of chemistry at University of Regensburg
Master thesis at University of Regensburg
„Synthesis and Pharmacological Characterization of monomeric and dimeric Muscarinic Receptor Ligands derived from 4-DAMP

10/2008 – 09/2011 **Bachelor studies** of chemistry at University of Regensburg
Bachelor thesis at University of Regensburg
„Synthesis, characterization and evaluation of different surfactant free, ionic polymer isomers, forming hydrogels”

07/2008 **Abitur** at Fachoberschule für Technik in Munich

Contribution to scientific meetings an oral presentations

- 12/2016** Christmas colloquium of the Institute for Organic Chemistry at University of Regensburg
“Transfection with DNA-Polycation Hybrids”
- 09/2016** EuCheMS Chemistry Congress in Sevilla, Spain
“Isosteric replacement for fine-tuning the properties of soft gels”
- 12/2014** Christmas colloquium of the Institute for Organic Chemistry at University of Regensburg
„Amide-triazole isosteric substitution for tuning self-assembly and incorporating new functions into soft supramolecular materials”

Languages

German	native
English	fluently
Spanish	basic
French	basic

List of publications

Mayr, J.; Grijalvo, S.; Bachl, J.; Pons, R.; Eritja, R.; Díaz, D. D., Transfection of Antisense Oligonucleotides Mediated by Cationic Vesicles Based on Non-Ionic Surfactant and Polycations Bearing Quaternary Ammonium Moieties, *Int. J. Mol. Sci.*, **2017**, submitted.

Bachl, J.; Bertran, O.; Mayr, J.; Alemán, C.; Díaz, D. D., Aromatic ionene topology and counterion-tuned gelation of acidic aqueous solutions, *Soft Matter*, **2017**, *13*, 3031-3041

Mayr, J.; Bachl, J.; Schlossmann, J.; Díaz, D. D., Antimicrobial and Hemolytic Studies of a Series of Polycations Bearing Quaternary Ammonium Moieties: Structural and Topological Effects, *Int. J. Mol. Sci.*, **2017**, *18*, 303.

Dragan, E. S.; Mayr, J.; Häring, M.; Cocarta, A. I.; Díaz, D. D., Spectroscopic Characterization of Azo Dyes Aggregation Induced by DABCO-Based Ionene Polymers and Dye Removal Efficiency as a Function of Ionene Structure, *ACS Appl. Mater. Interfaces*, **2016**, *8*, 30908–30919.

Tiffner, M.; Zielke, K.; Mayr, J.; Häring, M.; Díaz, D. D.; Waser, M., Phase-Transfer Catalysis with Ionene Polymers, *Org. Supramol. Chem.*, **2016**, *1*, 4030 – 4033.

Grijalvo, S.; Mayr, J.; Eritja, R.; Díaz, D. D., Biodegradable Liposome-encapsulated Hydrogels for Biomedical Applications: A Marriage of Convenience, *Biomater. Sci.*, **2016**, *4*, 555-574.

Häring, M.; Schiller, J.; Mayr, J., Grijalvo, S.; Eritja, R.; Díaz, D. D., Magnetic Gel Composites for Hyperthermia Cancer Therapy, *Gels*, **2015**, *1*, 135-161.

Mayr, J.; Häring, M.; Schiller, J.; Díaz, D. D., Supramolekulare Gele: einfach und funktionell, *Nachr. Chem.*, **2015**, *63*, 899-903.

Bachl, J.; Oehm, S.; Mayr, J.; Cativiela, C.; Marrero-Tellado, J. J.; Díaz, D. D., Supramolecular phase-selective gelation by peptides bearing side-chain azobenzenes: Effect of ultrasound and potential for dye removal and oil spill remediation, *Int. J. Molec. Sci.*, **2015**, *16*, 11766-11784.

Bachl, J.; Mayr, J.; Sayago, F. J.; Cativiela, C.; Díaz, D. D., Amide-triazole isosteric substitution for tuning self-assembly and incorporating new functions into soft supramolecular materials, *Chem. Commun.*, **2015**, *51*, 5294-5297.

Kühbeck, D.; Mayr, J.; Häring, M.; Hofmann, M.; Quignard, F.; Díaz, D. D., Evaluation of the nitroaldol reaction in the presence of metal ion-crosslinked alginates, *New J. Chem.*, **2015**, *39*, 2306-2315.

Carrillo, A.; Bachl, J.; Mayr, J.; Plaza-González, P.; Cátala-Civera, J. M.; Díaz, D. D., Non-invasive and continuous monitoring of the sol-gel transition of supramolecular gels by a fast (open-ended coaxial) microwave sensor, *Phys. Chem. Chem. Phys.*, **2015**, *17*, 6212-6216.

J Acknowledgements

I would like to thank all the people who supported me on my way:

Thanks to Prof. Dr. David Díaz Díaz for giving me the opportunity to carry out my PhD thesis in this group. For always providing me with new ideas and most of all for never letting me give up.

Thanks to Prof. Ramón Eritja for the opportunity of having a research stay in his group. I appreciate this a lot, it was a great time. Also thanks for approving to be my second examiner.

Special thanks go to Dr. Santiago Grijalvo for being a great supervisor during my research stay and for all the work he made for shared projects. You taught me so much in such a short time.

Also thanks to the rest of the group of nucleic acids chemistry at CSIC-IQAC for the warm welcome and great time that I spend with them.

Vielen Dank an Prof. Dr. Jens Schlossmann für die tolle Zusammenarbeit an unserem sehr interessanten gemeinsamen Projekt und für die Bereitwilligkeit als 3. Prüfer zu fungieren.

Auch möchte ich mich recht herzlich bei Astrid Seefeld und Gertraud Wilberg für die tatkräftige Unterstützung bei der Durchführung der antimikrobiellen Tests und der Hämolyse-Experimente bedanken. Vielen Dank auch an Prof. Dr. Frieder Kees, Dr. Andrea Schramm, Michael Majer und Bianca Aichinger für die fachliche Unterstützung.

Mein Dank geht auch an Brigitte Eichenseher, Roxane Harteis und Helena Konkel für die großen und kleinen Hilfen während meiner Arbeit.

Ich möchte mich auch bei meinen lieben Kollegen Marleen, Tobi, Jana, Markus, Ting und Alex für die schöne Atmosphäre innerhalb und außerhalb des Labors bedanken.

Ich danke auch meinen Forschungspraktikanten Johannes Graf, Johannes Mehringer, Andreas Maier, Jakob Asenbauer, Ning Wang und Markus Tautz für die Mitarbeit an meinen Projekten.

Acknowledgements

Vielen lieben Dank an „meine Verrückten“ Dani, Pia, Jeannine und Kati für die gegenseitige Unterstützung vor allem in der schwierigsten Zeit des Studiums und bis heute. Ohne euch hätte ich es nicht geschafft!

Danke natürlich auch an meine anderen Chemiker Frauke, Maria, Moni, Chris, Johanna, Franzi und Sina. Mit euch ist das Leben einfach schöner.

Vielen Dank auch an meine Familie. Ihr habt mich erst zu dem Menschen gemacht, der ich bin. Danke, dass ihr die letzten 28 Jahre immer hinter mir standet und mich immer unterstützt habt.

Lieber Chris, vielen Dank für deine Liebe, dein Verständnis und deine schier unerschöpfliche Geduld mit mir. Ich so dankbar, dass es dich gibt und du an meiner Seite bist.

K Declaration

Herewith I declare that this present dissertation is a presentation of my original work prepared single-handed. Wherever contributions from others are involved, all of them are marked clearly, with reference to the literature and licenses.

Regensburg, 24 May 2017

Judith Mayr